HAL
open science

Tunneling Nanotubes and their role in Glioblastoma Treatment-Resistance

Giulia Pinto

To cite this version:

Giulia Pinto. Tunneling Nanotubes and their role in Glioblastoma Treatment-Resistance. Cellular Biology. Sorbonne Université, 2020. English. NNT : 2020SORUS061 . tel-03228258

HAL Id: tel-03228258

https://theses.hal.science/tel-03228258v1

Submitted on 18 May 2021

HAL is a multi-disciplinary open access archive for the deposit and dissemination of scientific research documents, whether they are published or not. The documents may come from teaching and research institutions in France or abroad, or from public or private research centers.

L'archive ouverte pluridisciplinaire **HAL**, est destinée au dépôt et à la diffusion de documents scientifiques de niveau recherche, publiés ou non, émanant des établissements d'enseignement et de recherche français ou étrangers, des laboratoires publics ou privés.

Sorbonne Université

ED 394 - Physiologie, physiopathologie et thérapeutique

Trafic membranaire et pathogenèse / Institut Pasteur

Tunneling Nanotubes and their role in Glioblastoma Treatment-Resistance

Par Giulia Pinto

Thèse de doctorat de Sorbonne Université

Dirigée par Dr. Christel Brou et Pr. Chiara Zurzolo

Présentée et soutenue publiquement le 16 Novembre 2020

Devant un jury composé de :

Pr. Bertrand FRIGUET, Président

Pr. Philippe CHAVRIER, Rapporteur

Dr. Marie-Luce VIGNAIS, Rapporteur

Dr. Isabelle LEROUX, Examinateur

Pr. Christine TOULAS, Examinateur

Pr. Elizabeth MOYAL-JONATHAN-COHEN, Examinateur

Except where otherwise noted, this work is licensed under
http://creativecommons.org/licenses/by-nc-nd/3.0/

Section I: Preface

Project Information

The presented Ph.D. Thesis Manuscript and Project have been performed by Giulia Pinto under the supervision of Dr. Christel Brou and Pr. Chiara Zurzolo.

This Ph.D. Project was founded for 3 years from the **HTE Program** (Heterogeneity, Tumor & Ecosystem, HTE201502) assigned to Pr. Chiara Zurzolo and Pr. Elizabeth Moyal head of the Equipe 11 in Oncopole Center Toulouse, together with Pr. Christine Toulas. The last year was founded by **Fondation ARC pour la recherche sur le cancer** (DOC20190508549) assigned to Giulia Pinto.

Membrane trafficking and Pathogenesis

Director: Pr. Chiara Zurzolo

Institut Pasteur, Bâtiment Duclaux,

Aile Bertrand, 1ère étage

28 Rue du Dr Roux

75015 Paris

Sorbonne Université

Physiologie, physiopathologie et thérapeutique - ED 394

15-21 Rue de l'École de Médecine

75006 Paris

Acknowledgments

I would like to begin by thanking the members of the jury who have agreed to participate to my Ph.D. defense and review my work, in particular: the President, **Pr. Bertrand FRIGUET**, for his availability and presiding over the committee; the rapporteurs, **Dr. Marie-Luce VIGNAIS**, for her suggestions for the improvement of this manuscript and having made this commitment from Montpellier despite the sanitary crisis, and **Pr. Philippe CHAVRIER**, for his kind comments and for being available *in extremis* in the role of rapporteur, and to the examiners, **Dr. Isabelle LEROUX**, for being available to help me in the last two years and teaching me the preparation of the organoids, **Pr. Christine TOULAS** and **Pr. Elizabeth MOYAL**, for all the collaboration, material and knowledge put at disposal and for welcoming me in Toulouse in several occasions.

I would like to thank **Pr. Chiara ZURZOLO,** our unit head and my thesis director, for allowing me to undertake this path in her unity, for the energetic and determinate thrust provided during the project, for encouraging me to start writing a review of which I ended up feeling very proud of, for having, in general, spurred me on in several occasions and pushed me towards my own improvement.

I want to thanks my thesis director and supervisor, **Dr. Christel Brou**, who has accompanied closely me along this path "putting her hands in the dirt" with me from the very beginning. Thanks for your wise guidance through the project, for encouraging me in front of the negative results and my frustration, for being the person on which I have often pour all my doubts, always finding an available, critical and supportive listener. Thank you for teaching me, for making me grow, for all the conversations from which I came out enriched and all the times you responded to my request for help, I felt lucky to can count on such a support.

A big thanks to **Ines SAENZ DE SANTA MARIA**, first of all for all the practical help, collaboration and teamwork, but especially for your emotional investment in this project, from which I have often drawn inspiration, for being my cheerleader, ally and friend.

My heartfelt thanks to **Patricia CHASTAGNER**, for all the practical collaboration, the participation in those long meetings and the nice time spent in the office holding French lessons, to **Maura SAMARANI**, for the immense support, in all aspects, for being a colleague and friend I could always count on, you will find me ready to do the same for you, and to **Aysegul DILSIZOGLU SENOL**, for having initiated me to research, being my first lab teacher and having brought me to this laboratory, I really wish the best to you and your family in the future.

I immensely thank **all the past and current members of our unit** with whom I shared this path, for their support and help during this journey, for having animated my days in and outside of the lab, for the chats at the coffee corner and the sociable atmosphere that we breath in our unit, a particular thank to **Reine BOUYSSIE**, for the whole organization of the thesis and that fabulous Tarte au Citron.

I thanks my friends **Anna PEPE, Clara GRUDINA, Erica TELFORD and Giulia FRISCO**, for being strong women that I admire, for supporting me in the work life and outside with beautiful evenings together, the liquors and the karaoke.

I thank **all the friends here on the Pasteur campus**, for the shared path and mutual support, in particular thanks to **Marta MASTROGIOVANNI** for poking me to do the "homework" of the Statistics course together allowing our friendship to start, thank you for your presence and support in these years and your ability to relieve me with your naturalness and honesty.

A big thanks to **Franz, Martina and Giorgia** for having long been the heart of my Parisian life, and also a bit of a family, Paris without you it's a completely different thing. Thanks also to **Domenico, Irina, Enrico, Sara and Andrea** for the nice group, the healthy laughter and the abundant meals we had together. To this whole group, thank you deeply for being there.

A particular thanks to **Martina** for all the extraordinary time spent together and all the great little things that have composed our friendship. Thanks for your support and for being there when I needed it, for making my stay in Paris so pleasant and for the feeling of home that I found with you.

A sincere thanks to **Alba and Cariri**, my first bond in Paris that I hope to keep for a long time, wherever our roads will take us. Thank you for being these special friends you are, always available, from a simple beer together to the trips, the moving and the confidences. I am very happy to have shared this path with you.

Thanks to **all my friends in Italy** (and Lyon), in particular **Angela, Silvia, Sara, Daniela and Eleonora**, for being a constant in my life since many years, for being present and supportive despite the distance and always welcoming me back with enthusiasm.

A special thanks to **Emeline**, the most beautiful surprise of my PhD, for being my main source of relief in the past year and a half and have brought immense joy into my life. Thank you for having endured my angry, sad phases and all the times you told me you believe in me, your support and esteem have an immense value to me. You will nail the end of your PhD and all the challenges to come. I bet on your dreams.

A huge thank to my sister **Erika,** which is a bit of a model for me and that is why I always turn to you for advice, thank you for being there during these years, your support has been priceless.

Grazie, infine, a **mamma e papà**, per il vostro infinito supporto durante questi ultimi anni, per aver sopportato la distanza e aver accettato tutte le scelte e novità a cui vi ho messo davanti.

Thanks to you all for making these years so amazing!

Summary

Glioblastoma (GBM) is the most aggressive and deadly of the primary brain tumours, as it is able to relapse despite surgery, chemo and radiotherapy. The mechanism of resistance to treatment is not fully understood, but its recurrence appears to be due to the presence of GBM stem cells (GSCs).

Tunneling Nanotubes (TNTs) are thin open membrane connections that allow the cytoplasmic continuity of two distant cells and the bidirectional transfer of cellular material. TNTs play an important role during development, in the dissemination of viruses and in several neurodegenerative diseases. TNTs are also implicated in cancers where their presence and functionality have been correlated with tumour progression. Recent data have shown that in GBM, GSCs are interconnected in a vast network through thick neurite-like protrusions called Tumor Microtubes (TMs), allowing the propagation of ion flows through GAP-like Junctions. The extent of this network has been correlated with high resistance to treatment as well as cell invasion. One of my main objectives was to determine whether, in addition to the TMs, connections corresponding to the functional definition of TNTs, thus allowing the transfer of cellular material, existed in the GBM models and whether there was a correlation between their presence and the tumour phenotype or its resistance to treatment.

To this aim, in my research project, I studied TNT-mediated communication in three GBM cell lines and in two patient-derived GSCs obtained from distinct areas of the same tumor. GBM cell lines can form TNTs whose functionality has been evaluated by quantifying the transfer of vesicles and mitochondria by imaging and flow cytometry. GSCs also form TNTs when grown in adherent culture but also in three-dimensional tumour organoids, a model that better summarises the characteristics of the tumour. Of interest, the two GSCs showed different TNT communication capabilities, in both control and irradiated conditions, with higher TNT activity (and mitochondrial transfer) in cells from the area with a high potential for relapse, as clinically characterised by functional magnetic resonance imaging. In the organoid model, I observed that the GSCs are interconnected in a network composed of both TMs and TNTs. In conclusion, I propose that TNTs exist in GBM tumour networks, where they allow the transfer of cellular material and that together with TMs they are involved in the resistance to treatment and the relapse of tumours.

Résumé

Le glioblastome (GBM) est la plus agressive et la plus mortelle des tumeurs cérébrales primaires, car il est capable de récidiver malgré la chirurgie, la chimio et la radiothérapie. Le mécanisme de résistance aux traitements n'est pas entièrement compris, mais la récidive semble être due aux cellules souches cancéreuses du GBM (GSCs).

Les Tunneling Nanotubes (TNT) sont de fines connexions membranaires ouvertes qui relient les cytoplasmes de cellules distantes et permettent le transfert bidirectionnel de matériel cellulaire. Les TNTs jouent un rôle important au cours du développement, dans la dissémination des virus et dans plusieurs maladies neurodégénératives. Les TNTs sont aussi mis en jeu dans les cancers où leur présence et leur fonctionnalité ont été corrélées avec la progression des tumeurs. Des données récentes ont montré que dans le GBM, les GSCs sont interconnectés au sein d'un vaste réseau notamment grâce à d'épaisses protubérances semblables à des neurites, appelées Tumor Microtubes (TMs), permettant la propagation de flux ioniques à travers des GAP-like Junctions. La densité de ce réseau a été corrélée à une meilleure résistance aux traitements ainsi qu'à l'invasion cellulaire. L'un de mes principaux objectifs était de déterminer si, en plus des TMs, des connexions correspondant à la définition fonctionnelle des TNTs, et permettant donc le transfert de matériel cellulaire, existaient dans les modèles GBM et s'il y avait une corrélation entre leur présence et le phénotype de la tumeur ou sa résistance au traitement.

J'ai d'abord étudié la communication par TNTs dans trois lignées cellulaires GBM et dans deux GSCs obtenues à partir de zones distinctes d'une même tumeur. Les lignées cellulaires GBM peuvent former des TNTs dont la fonctionnalité a été évaluée en quantifiant le transfert de vésicules et de mitochondries par imagerie et cytométrie de flux. Les GSCs forment aussi des TNTs quand elles sont cultivées classiquement sur boîte mais aussi dans des organoïdes tumoraux tridimensionnels, un modèle qui récapitule mieux les caractéristiques de la tumeur. Il est intéressant de noter que les deux GSCs ont montré des capacités de communication par TNT différentes, dans des conditions contrôle et après irradiation, avec une activité TNT plus élevée (et un transfert mitochondrial) dans les cellules provenant de la zone au potentiel élevé de rechute, caractérisée chez le patient par l'imagerie par résonance magnétique fonctionnelle. Dans le modèle organoïde, j'ai observé que les GSCs sont interconnectées dans un réseau composé à la fois de TMs et de TNTs. En conclusion, je propose que les TNTs existent dans les réseaux tumoraux de GBM, où ils permettent le transfert de matériel cellulaire et qu'avec les TMs, ils sont impliqués ensemble dans la résistance au traitement et la rechute des tumeurs.

Main Index

Section I: Preface ***iii***

Project Information **v**

Acknowledgments **vii**

Summary **xi**

Résumé **xii**

Main Index **xiii**

Other indexes **xvi**

Index of Figures xvi
Index of Tables xvii
Index of Videos Legends xvii
Abbreviations xviii

Section II: Introduction ***2***

Preamble **4**

Chapter 1: Glioblastoma, the most aggressive of the brain tumors **6**

1. Brain tumors, gliomas and their classification 6
2. A general look to Glioblastoma 8
   2.1. Epidemiology 10
   2.2. Risk factors and etiology 10
   2.3. Symptoms 11
   2.4. Imaging 11
   2.5. Prognosis and survival 13
   2.6. Treatments 13
   2.7. Models 14
3. Biological signatures of Glioblastoma 15
   3.1. Cellular origin 15
   3.2. Histological characterization 17
   3.3. Genetic and epigenetic alterations 19
      3.3.1. IDH mutation 19
      3.3.2. Tyrosine-kinase receptors pathways 19
      3.3.3. p53 pathway 20
      3.3.4. Cell cycle regulation pathways 22
      3.3.5. Telomerase regulation genes 22
      3.3.6. Chromosomal loss 22
      3.3.7. C-CIMP 23
      3.3.8. MGMT status 23
4. Glioblastoma heterogeneity 23
   4.1. Genotypic intertumoral variability: four GBM subtypes 24
      4.1.1. Proneural 24
      4.1.2. Neural 26
      4.1.3. Classical 26
      4.1.4. Mesenchymal 26
   4.2. Theories about intratumoral heterogeneity 27

4.2.1. Theory of clonal evolution 27
4.2.2. Cancer stem cells theory 28
4.2.3. Inter-clonal cooperativity and microenvironment 28
5. Glioblastoma microenvironment 30
5.1. Perivascular niche 31
5.2. Hypoxic niche 31
5.3. Invasive niche 32
5.4. Immune response 32
5.5. Neurons 34
5.6. Oligodendrocytes 36
5.7. Reactive astrocytes 36
6. Glioblastoma stem cells 37
6.1. Definition of cancer stem cell 37
6.2. Markers of GSCs 37
6.3. Regulation of GSCs 39
6.4. Metabolism 41
7. Treatment-resistance 42

Chapter 2: Tunneling nanotubes, a highway for intercellular communication 46
1. Introducing intercellular communication 46
2. Tunneling Nanotubes 49
2.1. TNTs, different from other cellular extensions 49
2.2. TNTs identification and structure 51
2.3. TNT formation 54
2.4. Functional study of TNTs 58
3. Roles of TNTs 59
3.1. In development 59
3.2. Pathogens hijacks TNTs to favour their dissemination 60
3.3. Prion-like aggregates spreading 61
4. TNTs in cancer 62
4.1. Evidences of TNTs in cancer 62
4.2. Tumoral context favors TNT connectivity 65
4.3. Roles of TNT in cancer progression 67
4.3.1. TNT-mediated communication promotes invasiveness 67
4.3.2. TNT-mediated communication promotes angiogenesis 69
4.3.3. TNT-mediated communication induces treatment-resistance resistance 70
5. Tumoral networking in Glioblastoma: TNTs and TMs 71

Section III: The Project 76

Aims and objectives 78

TNTs in GBM cell lines 80
Premise 80
Results 81
Discussion 85
Figures 86
Materials and Methods 92

TNTs in GSCs 98
Premise 98
Contribution 99
Abstract 103
Introduction 104
Results 106

Discussion 113
Conclusions 115
Figures 116
Supplementary Figures 129
Supplementary Video Legends 133
Material and Methods 134

Section IV: Discussion and Perspectives 140

Discussion 142
Context 142
Presence of functional TNTs in GBM 144
Transfer of mitochondria 147
Correlation between TNTs and therapy-resistant phenotype 148
Effect of treatments on TNT-mediated communication 150
Coexistence of TNTs and TMs 152

Perspectives 154

BIBLIOGRAPHY 158

Annexe 176

Other indexes

Index of Figures

Figure 1. Distribution of primary Brain cancers and Gliomas. 7
Figure 2. Classification of Gliomas. 9
Figure 3. Magnetic resonance features of Glioblastoma. 12
Figure 4. Cell origin of Glioblastoma 16
Figure 5. Histological features of Glioblastoma 18
Figure 6. Major signaling pathways involved in the pathogenesis of Glioblastoma 21
Figure 7. Glioblastoma subtypes and genetic features 25
Figure 8. Tumoral heterogeneity theories 29
Figure 9. Cellular niches in Glioblastoma 33
Figure 10. Cells composing Glioblastoma microenvironment 35
Figure 11. Glioblastoma Stem Cells features 38
Figure 12. Regulation of GSCs. 40
Figure 13. Therapy and recurrence of Glioblastoma 43
Figure 14. Conventional and proposed therapies for Glioblastoma. 45
Figure 15. Forms of cell signaling 48
Figure 16. Tunneling nanotubes schematic 50
Figure 17. Ultrastructure of TNTs 55
Figure 18. The two models of TNT formation 57
Figure 19. Model of TNT-based communication in cancer 68
Figure 20. Schematic of a Glioblastoma network 74

Figure Cell Lines 1. TNT characterization in GBM cell lines. 86
Figure Cell Lines 2. Establishment of U-251TR and their TNT-mediated communication. 89
Figure Cell Lines 3. TNT-mediated communication between astrocytes and GBM cell lines 90
Figure Cell Lines 4. U-251 GBM cell line can transfer mitochondria. 88

Figure Article 1. GSLCs form TNT-like structures. 116
Figure Article 2. GSLCs transfer mitochondria through TNTs. 118

Figure Article 3. Effect of irradiation on GSLCs on TNT-based communication. 120
Figure Article 4. GSLCs in tumor organoids. 122
Figure Article 5. GAP43 expression and TM characterization in tumor organoids of GSLC cells. 124
Figure Article 6. Effect of irradiation on tumor organoids. 126
Figure Article 7. GSLC network. GSLCs interconnect through different types of cellular extensions..... 128

Supplementary Figure 1. MitoGFP signal in acceptor cells match with TOM20 mitochondrial marker staining. 130
Supplementary Figure 2. Movement of mitochondria by live-imaging in C2-tumor organoids inside TNT-like connections. 131

Index of Tables

Table 1. Types of cellular extensions 52
Table 2. Tumor cell models exploiting *in vitro*..... 63
Table 3. Evidence of TNT-like communication in tissue in cancer 66

Supplementary Table 1. Oligonucleotides used in qPCR 138

Index of Videos Legends

Supplementary Video 1. Movement of mitochondria along TNT-like connections in 2D-conditions. 133
Supplementary Video 2. Transfer of mitochondria via TNT-like connections in tumor organoids. 133
Supplementary Video 3. Motion of mitochondria inside TNT-like connections in tumor organoids. 133

Abbreviations

Acronym(s): full name

A

AEG-1: Astrocyte Elevated Gene-1
Akt/PKB: Protein Kinase B
AMPA: α-Amino-3-Hydroxy-5-Methyl-4-Isoxazolepropionic
APC: Anstrocyte Progenitor Cell
ASCL1: Achaete-Scute Homolog 1
ATP: Adenosine Triphosphate
ATRX: αThalassemia/Mental Retardation Syndrome X-Linked

B

BBB: Blood Brain Barrier
BCRP1: Breast Cancer Resistance Protein
BRN2/POU3F2: POU Domain, Class 3, Transcription Factor 2

C

CAD: Cath.A-Differentiated Cells; 65
CD133/Promin-1
CD15/ SSEA-1: Stage-Specific Embryonic Antigen-1
CDC42: Cell Division Control Protein 42 homolog
CDK4: Cyclin-Dependent Kinase 4
CDKN2B: Cyclin Dependent Kinase Inhibitor 2B
CHI3L1: Chitinase-3-Like Protein 1
Cho: Choline
CIMP: CpG Island Methylator Phenotype
CNS: Central Nervous System
CSCs: Cancer Stem Cells
Cx: Connexin

D

DCX: Doublecortin
DLL3: Delta-Like Ligand 3

E

EBV: Epstein Barr Virus
ECs: Endothelial Cells
EGFR: Epidermal Growth Factor Receptor
ERK1/2: Extracellular Signal-Regulated Kinases 1/2
EVs: Extracellular vesicles
FAK: Focal Adhesion Kinese
FGF: Fibroblast Growth Factor
FLAIR: Fluid Attenuated Inversion Recovery

G

GABRA1: Gamma-Aminobutyric Acid Type A Receptor Subunit Alpha1
GAMs: Glioma-Associated Monocytes/Macrophages
GAP-43: Growth-Associated Protein 43
GBM: Glioblastoma
G-CIMP: Glioma CpG Island Methylator Phenotype
GFAP: Glial Fibrillar Acidic Protein
GJs: Gap-Junctions
GLUT4: Glucose transporter type 4
GO: Gene Ontology
GRP: Glial-Restricted Progenitor
GSCs: Glioblastoma Stem Cells
Gy: Gray

H

HGFR: Hepatocyte Growth Factor Receptor
HIF-1α: Hypoxia-Inducible Factor 1-Alpha
HIV: Human Immunodeficiency Virus
HTLV1: Human T-Lymphotropic Virus

I

IDH1/2: Isocitrate Dehydrogenase
IL-6: Interleukin 6
IL-8: Interleukin 8
iTNTs: individual TNT

J

JAG1: Jagged1

L

L1CAM: L1 Cell Adhesion Molecule
LDH: Lactate Dehydrogenase

M

MDM2: Mouse Double Minute 2 Homolog
MGMT: O-6-Methylguanine-DNA Methyltransferase
MHV-68: Murine Gammaherpesvirus 68
MMPs: Matrix metallopeptidase
MRI: Magnetic Resonance Imaging
MSCs: Mesenchymal Cells

N

NAA: N-Acetylaspartic Acid
NEFL: Neurofilament Light
NES: Nestin
NF1: Neurofibromatosis Type 1
NF-κB: Nuclear Factor Kappa-Light-Chain-Enhancer of Activated B Cells
NG2: Neuron-Glial Antigen 2
Nkx2.2: NK2 Homeobox 2
NMDA: N-Methyl-D-Aspartate Receptor
NO: Nitric Oxide
NSCs: Neural Stem Cells
N-WASP: Wiskott-Aldrich Syndrome Protein

O

OCT4: Octamer-Binding Transcription Factor 4
Olig 1/2: Oligodendrocyte Franscription Factor 1/2
OPCs: Oligodendrocyte Progenitor Cells

P

$p14^{ARF}$: Alternate Reading Frame inkprotein
$p16^{INK4a}$: Cyclin-Dependent Kinase Inhibitor 2A
$p21^{CDKN1A}$: Cyclin Dependent Kinase Inhibitor 1A
p53/TP53: Tumor Protein 53
PC12: Pheochromocytoma Cells
PDGFR: Platelet-Derived Growth Factor Receptor
PDK1: Phosphoinositide-Dependent Kinase-1
PI3K: Phosphoinositide 3-Kinase
PIP_3: Phosphatidylinositol-trisphosphate
PTEN: Phosphatase and Tensin Homolog

R

RB1: Retinoblastoma Protein
ROS: Reactive Oxygen Species
RTEL1: Regulator Of Telomere Elongation Helicase 1

S

SALL2: Spalt Like Transcription Factor 2
SHH: Sonic Hedgehog
SLC12A5: K+/Cl- Cotransporter 2
SNAREs: Soluble N-ethylmaleimide-Sensitive-Fusion Attachment Receptors
SOX: Sex-determining region Y-related high mobility group box proteins
STAT3: Signal Transducer and Activator of Transcription 3
STI1: Stress Induced Phosphoprotein 1
SYT1: Synaptotagmin 1

T

TCF4: Transcription Factor 4
TERT: Telomerase Reverse Transcriptase
TGF-β: Transforming Growth Factor beta
TMs: Tumor Microtubes
TMZ: Temozolomide
TNF-α: Tumor Necrosis Factor Alpha
TNTs: Tunneling Nanotubes
Ttyh1: Tweety Family Member 1

U

US3: Serine/Threonine-Protein Kinase

V

VAMP3: Vesicle Associated Membrane Protein 3
VEGF: Vascular Endothelial Growth Factor

W

WHO: World Health Organization

α

α-SMA: Alpha-Smooth Muscle Actin

Section II: Introduction

Preamble

The introduction will be divided in two Chapters. The first Chapter will give an overview about Glioblastoma from its clinical to molecular aspects, with specific focus on its heterogeneity and the biological mechanisms involved in its treatment-resistance. The second Chapter will be dedicated to Tunneling Nanotubes, their roles in cell-to-cell communication and in particular it will summarize the findings related to the tumoral context. At the end of this part the two topics will converge giving the context where to place the premises of my research project.

Chapter 1: Glioblastoma, the most aggressive of the brain tumors

1. Brain tumors, gliomas and their classification

Brain tumors are a group of intracranial malignancies originating from the abnormal and uncontrollable growth of cells of central nervous system (CNS). The number of new brain cancers for both sexes, at all ages, was estimated to be around 300.000 cases worldwide in 2018, over around 18 millions of all cancer cases (https://gco.iarc.fr). More than 150 different types of brain tumors have been documented: although close in their anatomical location, CNS tumors differ in terms of morphology, site, molecular biology, clinical behaviour and aetiology. They can be divided in **primary tumors**, deriving directly from tissue of the brain or its surrounding, or **metastatic**, evolving from malignancies located elsewhere in the body and migrating to the brain through the bloodstream (https://www.aans.org). Generally, primary brain tumors can be benign or malignant according to their grade of aggressiveness (Figure 1). On the other hand, metastatic brain tumors are always considered as malignant. 78% of all malignant brain tumors are composed of glial cells and are therefore named **glial** tumors (or gliomas), the remaining is defined as **not-glial** (Crocetti et al., 2012), developed from other brain tissues or structures (as nerves, blood vessels and glands). Glial cells are mainly constituted of microglia, astrocytes, and oligodendrocyte lineage cells and they provide the conditions for the appropriate function of neurons and synapses.

Gliomas are a heterogeneous group (Figure 1), they are traditionally ranked accordingly to their histologic type (as astrocytic or oligodedroglial) and malignancy grade (assigned on the base of mitotic activity, nuclear abnormalities, necrosis, microvascular proliferation, level of de-differentiation) by the World Health Organization (WHO):

WHO grade I (low-grade) are low proliferative and well differentiated lesions, with discrete nature unlikely to evolve negatively.

WHO grade II (intermediate-grade) presents atypical cells with infiltrating nature, low mitotic activity, moderately differentiated, it can evolve to higher grade.

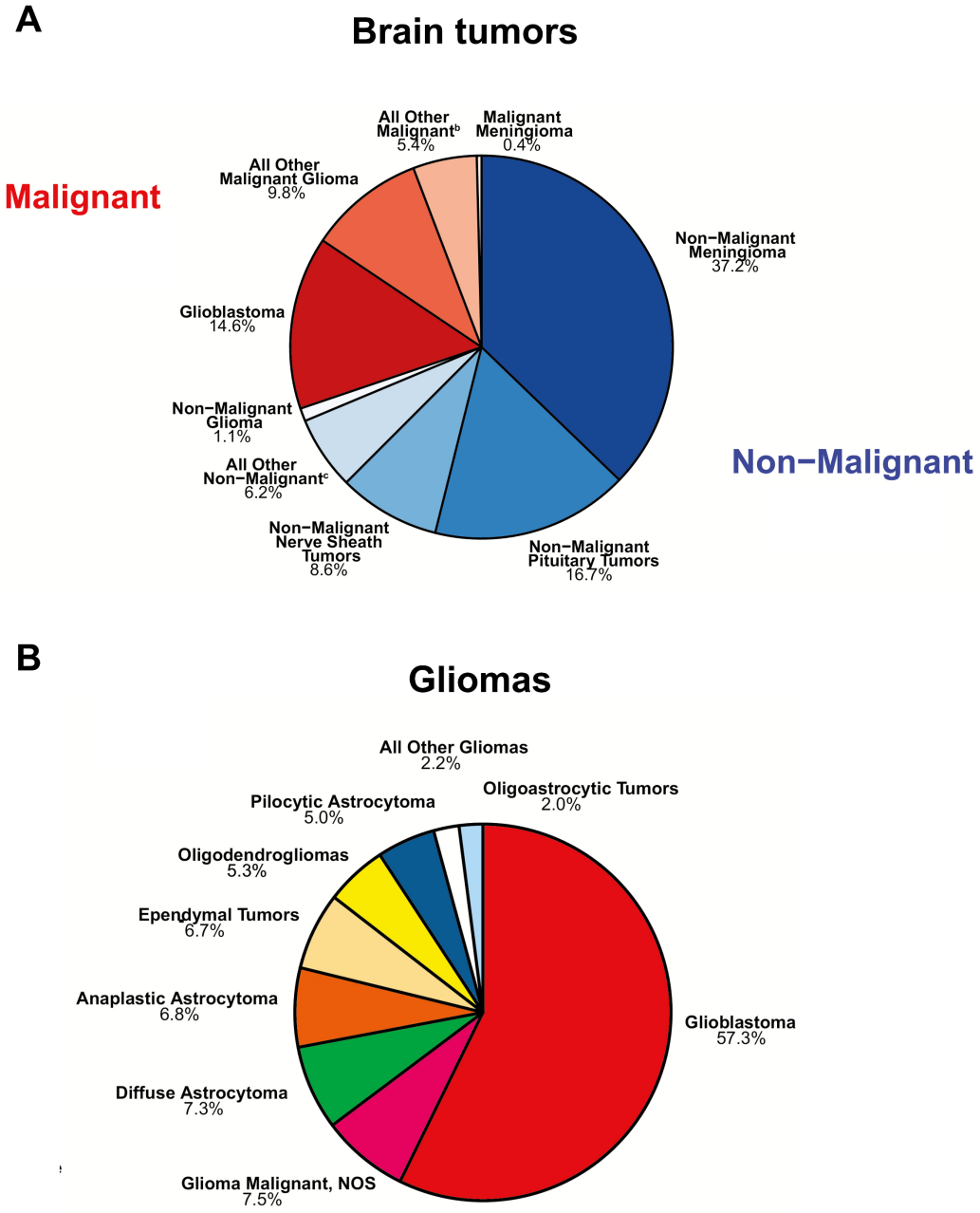

Figure 1. Distribution of primary Brain cancers and Gliomas.

Adapted by Ostrom et al., 2019. (A) Distribution of primary brain and other CNS tumors classified by behavior. (B) Distribution of Gliomas classified by histology subtypes. CBTRUS Statistical Report: US Cancer Statistics - NPCR and SEER, 2012–2016

WHO grade III (high grade) shows histologic evidence of malignancy as infiltrative capacity, anaplastic, increased mitotic activity and poorly-differentiated histology.

WHO grade IV (high grade) are undifferentiated, mitotically-active lesions with a propensity for craniospinal dissemination, necrosis, neovascularization and a rapid post-operative progression with fatal outcome.

The classification and nomenclature of CNS tumors and gliomas was revised in 2016 (Louis et al., 2016; Wesseling & Capper, 2018), including distinctive molecular-genetic criteria on top of histological ones, although the diagnostic use of both approaches also raises the possibility of discordant results (Figure 2). One major observation that has fostered the establishment of a genotype-driven classification was the detection of recurrent point mutations leading to a shared clinical outcome despite divergent histological characterization (Figure 2). Particularly, point mutations in isocitrate dehydrogenase 1 and 2 (IDH1/IDH2), enzymes involved in the Krebs cycle and often dysregulated in carcinogenesis (Olar et al., 2015), occurs at high frequencies in grade II and III. An astrocytic or oligodendroglial type of glioma can be further distinguished according to its histopathological features. Each type also carries specific molecular signatures as the codeletion of the chromosomes 1p and 19q, typical of oligodendrogliomas rather than astrocytomas. Within the astrocytoma histological type, at the IV and highest grade of malignancy, we find Glioblastoma, the most aggressive of the gliomas (Figure 2).

2. A general look to Glioblastoma

Glioblastoma (GBM) is ranked at the grade IV of the WHO classification, it is the most aggressive, invasive, undifferentiated and lethal of the CNS tumors. GBM alone accounts for 14,6% of all primary CNS tumors (including non-malignant ones) and 57.3% of all gliomas (Figure 1) according to the Central Brain Tumor Registry of the United States (incorporating the statistic of the cases between the years 2012-2016). In around 90% of the cases it originates *de novo* (primary GBM), without previous clinical or histological evidence of a less malignant precursor lesion (Ohgaki & Kleihues, 2007).

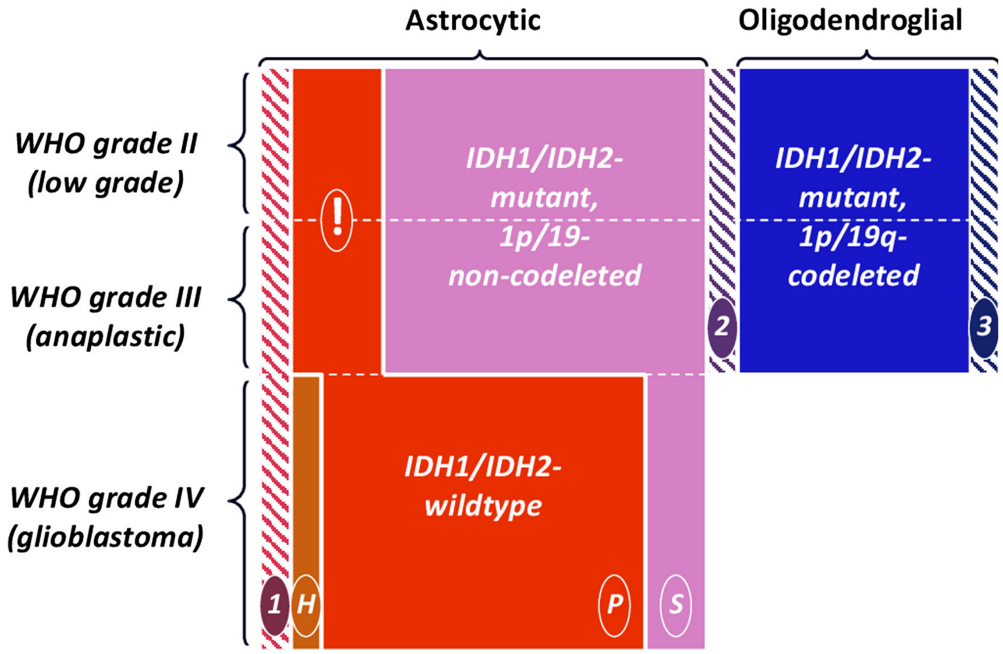

Figure 2. Classification of Gliomas.

Obtained from Wesseling & Capper 2018. WHO 2016 Gliomas are histologically differentiated in Astrocytic and Oligodendroglial subtype and graded from II to IV accordingly to WHO parameters of malignancy. At molecular level, three categories can be defined: IDH-wildtype (red), IDH-mutant but 1p/19q-non-codeleted (pink), or IDH-mutant and 1p/19q-codeleted (blue). In adult patients, lower grade (grade II and III) astrocytic tumours are typically IDH-mutant, and many GBMs with an IDH mutation originate from such a lower grade precursor lesion ('secondary GBM', S). However, IDH-wildtype GBMs are much more frequent, these tumours are generally high-grade malignant from the start ('primary GBM', P). Of note, many histologically grade II and especially grade III IDH-wildtype diffuse gliomas in adults show molecular characteristics of and behave like GBM (!). Differently, lower grade oligodendroglial tumours are typically IDH-mutant and 1p/19q-codeleted. Hatched bar correspond to the tumors were the classification resulted to be inconclusive and are therefore defined 'not otherwise specified' (NOS) as they display various features of those mentioned (types 1, 2 or 3).

Only 10% of the GBM cases derive from lower grades astrocytoma evolving into a secondary GBM (Figure 2) and correspond to a different prognosis.

2.1. Epidemiology

The incidence of GBM is around 3 people every 100.000 and it mainly affects the older population with a mean age of diagnosis at 64 years old. It is very uncommon in children, which account for only the 3% of the cases, while its incidence peak ranges between 75 and 84 years old (Thakkar et al., 2014). The incidence rate can depend on gender or ethnicity as it is higher in male and Caucasian individuals. GBMs are more commonly located in the supratentorial region of the forebrain (in the frontal, temporal, parietal and occipital lobes), although cerebellar location is possible and usually more frequent in younger patients. Also, secondary GBMs, evolving through a different genetic pathway, are more likely to occur in younger age at a mean of diagnosis of 45 years old (Thakkar et al., 2014).

2.2. Risk factors and etiology

The main risk factor associate to with GBM is prior exposure to therapeutic radiation (Hodges et al., 1992). Various life-style characteristics, as smoke, alcohol, drugs consumption, nitrate-containing diet or mobile phone usage, were tested and not substantial evidences of correlation with GBM were found (Thakkar et al., 2014). Curiously, allergies, some atopic diseases (e.g. asthma, eczema, psoriasis) and use of anti-inflammatory medicament were associated to a protective effect against GBM as GBM patients present low level of IgE, a biomarker for allergy (Buerki & Lukas, 2016). At genetic level, some gene variants of cyclin-dependent kinase inhibitor 2B (CDKN2B) and the regulator of telomere elongation helicase 1 (RTEL1) were associated to risk of high-grade glioma (Thakkar et al., 2014).

2.3. Symptoms

GBMs usually evolve rapidly and have a short clinical history before their diagnose (between 3 and 6 months), unless they derive from previous, lower-grade, gliomas. Symptoms are numerous and can vary accordingly to the brain region affected, nevertheless, they can be reconducted to three major mechanisms (Hanif et al., 2017): i) destruction of the brain tissue, as result of the cellular necrosis, that give rise to cognitive impairments and neuronal deficit, ii) increase of the cranial pressure, due to the increase of the tumoral size and edema surrounding the tumor, leading to shift of intracranial content and headaches which can assume progressive severity, iii) depending on the brain region, seizures could be occurring in 20-40% of the cases.

2.4. Imaging

Magnetic resonance imaging (MRI) with or without contrast agent (Gadolinium) is the gold standard for brain tumor visualization and diagnosis (Hanif et al., 2017). T1- and T2-weighted MRI, based on different atomic spin echos, allow together the complete visualization of the tumoral architecture. T1 gives high contrast to the areas higher in fat content corresponding the dense cellularity of the tumor and necrosis, while T2 gives higher signal of area rich in water, representative of the surrounding edema. T2 can be implemented with fluid-attenuated inversion recovery (FLAIR) sequence to suppress the signal of the cerebrospinal liquid allowing a better definition of the tumoral borders (Figure 3). Beyond diagnosis, spectroscopy MRI can be implemented to monitor the levels of cellular metabolites such as choline (Cho), creatine, N-acetylaspartate (NAA), lactate, and lipids to determine tumor activity (Bush et al., 2017). These parameters are relevant to determine the metabolic activities of the tumor areas (Figure 3) and retain a prognostic value (Horská & Barker, 2010). For example, increase of lactate or Cho and decrease of NAA have been associated with a poorer outcome (Deviers et al., 2014). For these reasons, the spectroscopic characterizations of the tumor has been recently incorporated into the treatment-planning process.

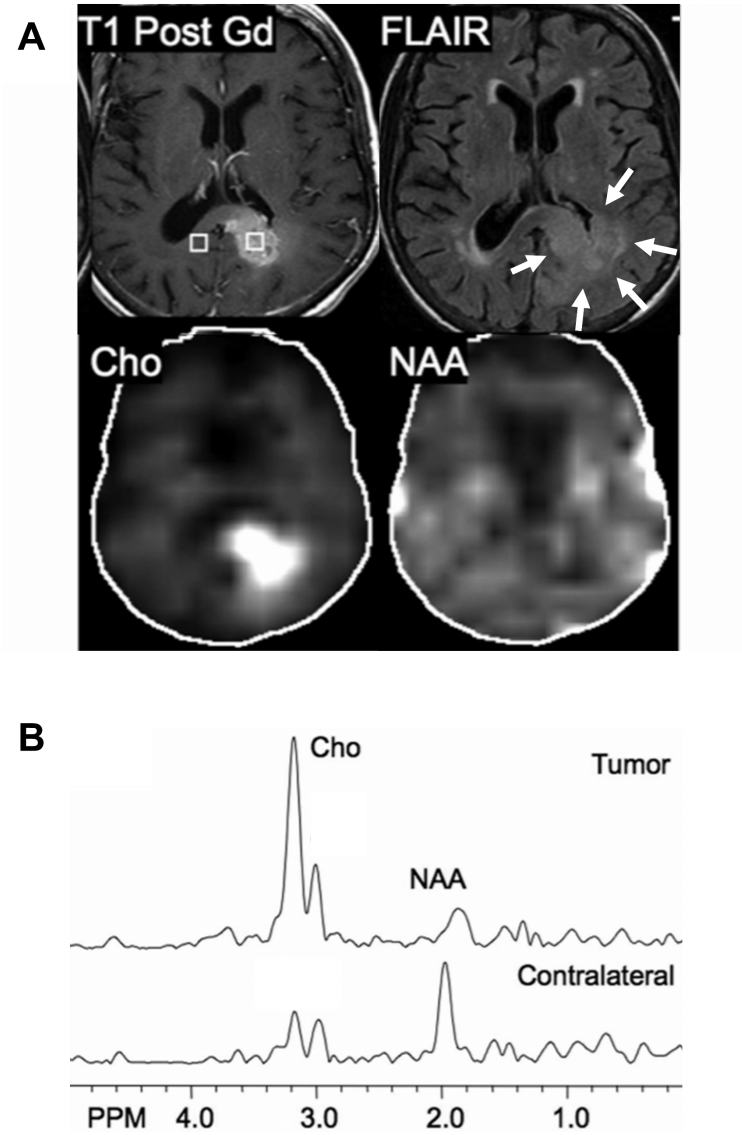

Figure 3. Magnetic resonance features of Glioblastoma.

Adapted from Horská & Barker, 2010. (A) In the upper side, contrasted T1-weighted MRI (left) allow in white the visualization of the tumoral core while FLAIR-T2-weighted (right) shows area of the surrounding edema (white arrows). In the lower side, spectroscopy MRI shows the spatial signal of two metabolites: Cho and NAA. (B) Spectrograms of tumoral and contralateral area (acquired in the frames indicated in the T1 upper image). Cho signal is enhanced in the tumor while NAA is reduced compared to the contralateral area. The ratio between the two is thought to retain a prognostic value.

2.5. Prognosis and survival

GBM has very poor prognosis as the median survival is around 14.6 months from the diagnosis. In most cases, a diagnosis of GBM is a death sentence within a short period of time. Despite the adverse survival and mortality rate, patients surviving 2.5 years from diagnosis have a relatively favourable conditional probability of future survival compared to newly diagnosed patients, with 5% of the cases surviving beyond 5 years (Thakkar et al., 2014). Age and tumor location can also affect the prognosis of GBM patients. Secondary GBM, deriving from lower grade gliomas and corresponding to only 10% of the cases, has a more positive prognosis with an overall median of survival of 31 months.

2.6. Treatments

GBM is still nowadays an incurable form of cancer and little progress has been made in its therapy. Despite the treatments, which improves patients' survival, GBM relapse is almost inevitable. GBM is treated with a multimodal approach that requires, first, its maximal surgical resection, and then, external beam radiations (radiotherapy) and concomitant chemotherapy (Stupp et al., 2005). GBM is an infiltrative tumor with jagged edges and, even with the support of functional MRI, it remains impossible to completely eradicate with surgery. Interestingly, some novel intra-operative techniques are trying to improve the limitation of the operation including the use of fluorescent marker 5-amuionlevulinic acid, a dye preferentially taken up by tumor cells and enhancing the visualization of tumor to aid maximal resection (Bush et al., 2017; de Boer et al., 2015). Surgery is followed by radio and chemotherapy; this double approach aims to target remaining highly proliferative cells as both methods induce errors in DNA replication which overwhelm cellular repair mechanisms and triggers apoptosis. Ionizing radiation generates reactive oxygen species (ROS) that directly damage DNA. The standard dose of radiation is 60 Grays (Gy) and it is usually delivered in 30 to 33 fractions of 1.8–2 Gy in a localized brain field and its surrounding (2-3 cm). Interestingly, previous radiotherapy is one of the few risk factor correlating with GBM (Hodges et al., 1992) and evidences suggest that ionizing radiations activate survivin pathway in GBM cells and possibly favor a fast tumor recurrence (Dahan et al., 2014).

GBM treatment also includes the use of Temozolomide (TMZ), an oral cytotoxic DNA-alkylating agent introducing methylation of guanine bases, consequent mismatch in the double-strand which cause DNA damages. The addition of this drug, has improved the median overall survival compared to radiation alone (14.6 months compared to 12.1 months), with a two-fold increase in 2-year survival from 10.4 to 26.1% (Stupp et al., 2009; Stupp et al., 2005). TMZ is one of the few drugs able to cross the Blood Brain Barrier (BBB); nevertheless, it has a short half-life and it is administrated in high dose to result effective of in the specific site of the tumor. Prolonged systemic administration might lead to significant side effects on the rest of the body. To overcome this limitation, a developing research area is exploring the use of nanoparticles, specifically functionalized, to direct drug delivery in the interested area (C. Y. Lee, 2017; Ung & Yang, 2015). Some alternative therapeutic strategies have been tested with few successes. Immunotherapy with Bevacizumab, a humanized monoclonal antibody targeting the Vascular Endothelial Growth Factor (VEGF) with the aim to inhibit GBM neovascularization, has so far demonstrated no particular benefit as GBM displayed adaptive upregulation of alternative angiogenic pathways (Y. Li et al., 2017). Everolimus, an inhibitor of mTOR (mammalian Target Of Rapamycin), has also been tested and led to an increased toxicity and no clinical benefit in patients (Chinnaiyan et al., 2018). Moreover, intratumoral gene therapy is an alternative strategy under exploration. The rational is to provide specific genes to the cancer cells, through retroviral vectors, inducing their apoptosis or directing an adverse immune response (Bush et al., 2017). Finallythe use of vaccines has been considered with the aim to sensitize the immune system against specific antigens involved in GBM pathogenesis (Schumacher et al., 2014).

2.7. Models

One of the reasons that contributed to proceed slowly in the advancement of GBM care, is the lack of valid models that can authentically reproduce the genetic and phenotypic properties of human GBM. Immortalized serum-cultured cell models have been demonstrated to fail in recreating the original tumor in their biological and transcriptomic features (J. Lee et al., 2006). Research moved toward models more recapitulative of

tumoral environment and heterogeneity. One strategy is to isolate from patient tumor cells and maintained them as neurospheres or organoids in serum-free medium as they retain their genetic heterogeneity and tumorigenic ability (Hubert et al., 2016; Kim et al., 2015). These cells can also be implanted in immune-suppressed mice, as xenograft murine model, and initiate tumor formation (Osswald et al., 2015). Alternatively, spontaneous tumors can be triggered in genetically-engineered mice by induction of driver mutations, however they do not represent the complexity of GBM genetic alterations. Syngeneic murine model allows to reproduce immune system response as the tumor is allografted from an immune-suppressed mouse to an immune-competent one (Broekman et al., 2018b). Although murine models allow the study of the tumors in an adequate microenvironment, none of these is a perfect representation of the human GBM (Broekman et al., 2018b). More recently, cerebral organoids models have been developed: they consist in the recreation of a "miniature" brain, obtained from neural or embryonic stem cells, that incorporates tumoral components. Specifically, this can occur by introduction of oncogenes expression or target mutation in the neural stem/precursor cells composing the cerebral organoids (Bian et al., 2018) or favouring tumor cells infiltration in pre-formed cerebral organoid (Linkous et al., 2019). Additionally closer to the real tumor, are patient-derived GBM organoids obtained by culturing tumor pieces after an initial microdissection of the original tumor tissue (Jacob et al., 2020).

3. Biological signatures of Glioblastoma

3.1. Cellular origin

The cellular origin of GBM is still nowadays matter of debate. Within the cell population that populates the CNS, various progenitor, stem or differentiated cells might be susceptible to the transformation which leads to the formation of GBM. During ordinary glial development, neural stem cells (NSCs) and multipotent progenitor cells, that reside in proliferative subventricular zone, give rise to neurons or glial progenitor cells (Figure 4). Glial progenitors are heterogeneous and can subsequently originate astrocytes or oligodendrocytes (Zong et al., 2012). NSCs and glial progenitors continue throughout

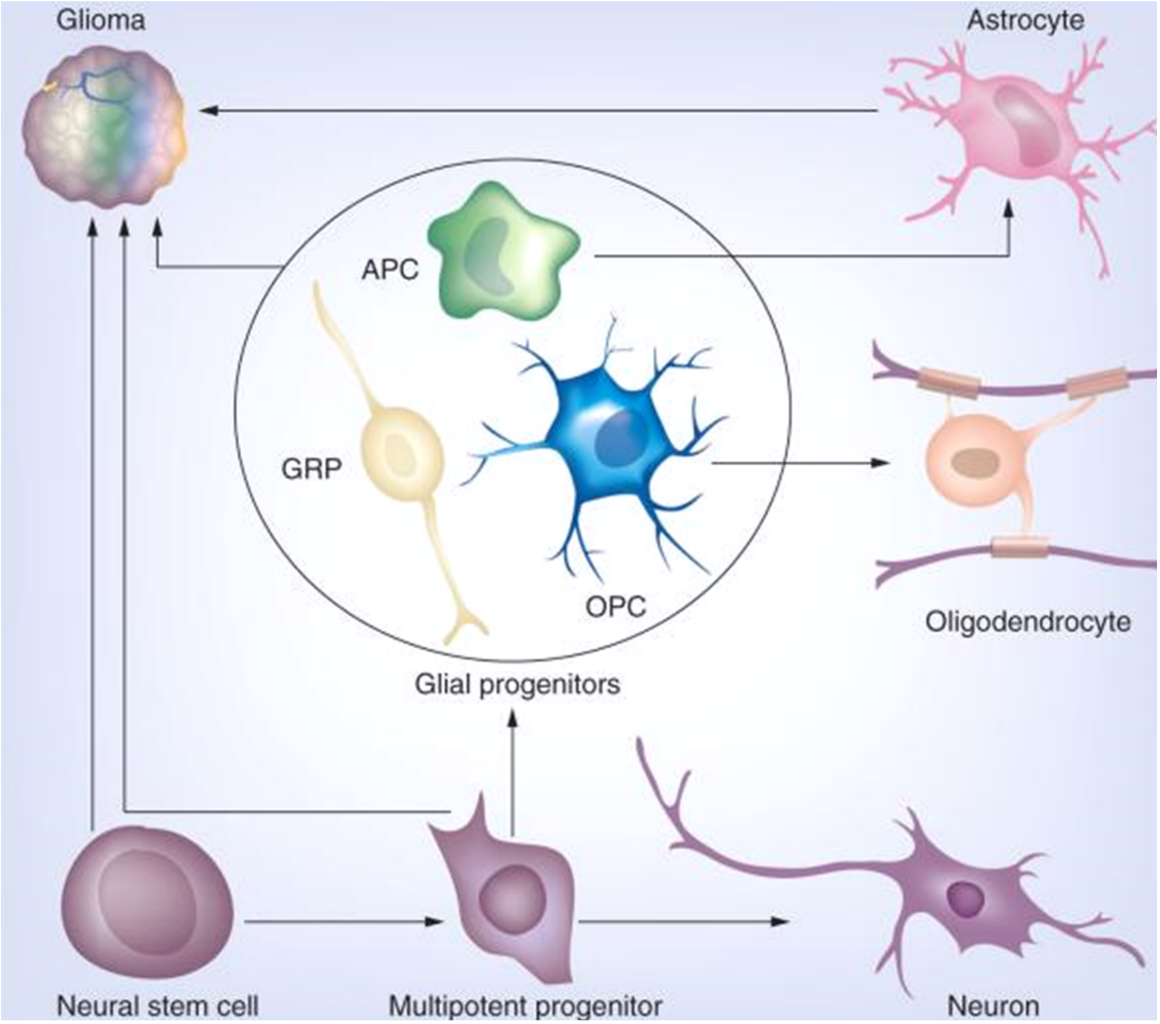

Figure 4. Cell origin of Glioblastoma

Obtained from Zong et al., 2012. At the bottom left, neural stem cells and multipotent progenitors in the subventricular zone can give rise either to neurons or glial progenitors. These later ones can further give rise to Astrocytes Progenitor cells (APC) or Glial-Restricted Progenitor (GRP) or Oligodendrocyte Progenitor Cell (OPC), from which astrocytes and oligodendrocytes can originate. Glioma is a heterogeneous disease and could potentially arise from different cells of this differentiation paths.

adulthood to self-renew and generate progeny cells, and thus are prime suspects as the cell of origin for gliomas. GBM is predominantly composed of cells that resemble immature glia, which display varying degrees of similarity to different glial lineages, suggesting that gliomas arise from cells with a glial-restricted potential. Eventually, different subtype of glioma could derive from a distinct cell of origin: neural stem cells, glial progenitors (including oligodendrocyte progenitor cells) and astrocytes could all serve as cells of origin for gliomas (Zong et al., 2012).

3.2. Histological characterization

GBM is extremely heterogeneous tumor, in fact its remarkable intratumoral histologic and cytologic diversity has made it worthy of the epithet "*multiforme*" in its original name. For gliomas grading, tumoral sections are analysed, after intracranial surgery, in their cellularity by haematoxylin-eosin staining and for the expression of specific cell type marker by immunohistochemistry (Perry & Wesseling, 2016). Haematoxylin-eosin staining allows to determine mitotic activity, and presence of microvascular proliferation and necrosis. Although a specific cut-off for mitotic activity has been not officially defined, the presence of necrosis and/or microvascular proliferation are indicative of a diagnosis of GBM. Dense, irregular and large necrosis, surrounded by pseudopalisading (aligned) cells, can be an explicit feature of GBM as well as prominent microvascular proliferation (Figure 5A and B). By immunohistochemistry, GBMs show similarities to normal and reactive astrocytes, and can express astrocytic lineage markers, such Glial fibrillary acidic protein (GFAP), typical of astrocytic type of glioma (Figure 5C), but also Chitinase-3-like protein 1 (CHI3L1) and Apolipoprotein E (Perry & Wesseling, 2016). Nevertheless, a less frequent subtype of GBM express several genes typical of oligodendrocyte progenitor cells, including Oligodendrocyte transcription factor 2 (Olig2), Neuron-Glial Antigen 2 (NG2) and Platelet-Derived Growth Factor Receptor A (PDGFRα). IDH status can also monitored by immunohistochemistry, allowing the distinction between primary IDH wild-type GBM and secondary IDH-mutated GBM, deriving from previous lower grade IDH-mutated tumors. Additional cellular features can be observed which allow to discriminate some particular variants of GBM as giant cells GBM, characterized by the presence of many large, multinucleated tumor cells (Figure 5D).

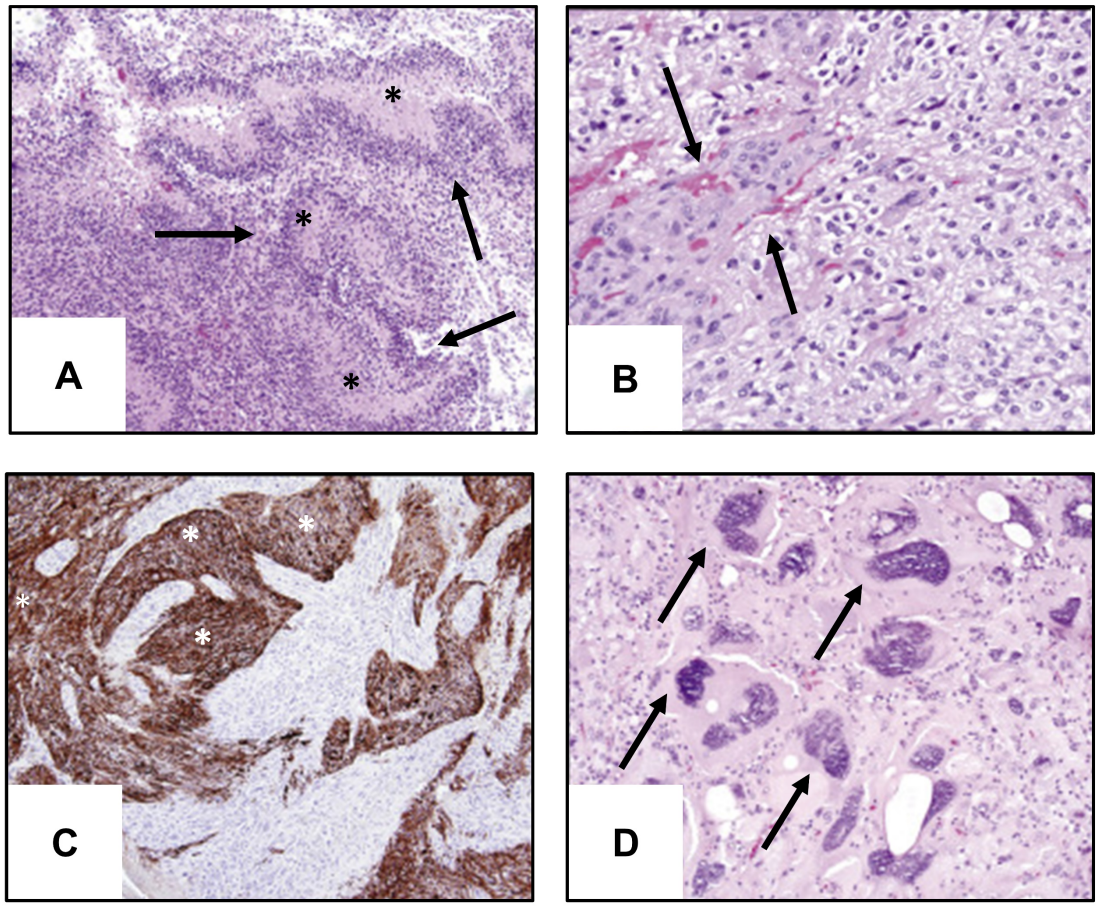

Figure 5. Histological features of Glioblastoma

Adapted from Perry & Wesseling, 2016. (A) Hematoxilin-eosin staining. Pseudopalisading necrosis is a main characteristic of GBM. Black '*' indicate the necrotic areas. Black arrows point at the aligned cells surrounding the necrosis. (B) Microvascular proliferation is also typical of GBM. In this hematoxilin-eosin section arrows point at blood vessels sourronded by proliferative cells. (C) GBM is an astrocytic glioma and it displays GFAP-immunoreactive areas indicated by white '*'. (D) Giant cell GBM is a particular phenotype presenting large, highly pleomorphic, multinucleated giant cells.

3.3. Genetic and epigenetic alterations

Various genotype hallmarks have been identified in GBM, certain have been associated with the different grade of gliomas or even carry prognostic significance. These reasons leaded to the renovation of the WHO classification that occurred in 2016 now based on molecular, on top histological, features here described in the following subchapters.

3.3.1. IDH mutation

IDH1/2 mutations are frequent in II and III grade and are commonly established hallmark for secondary GBMs, as these evolve from pre-existing lower grade tumors. IDH enzymes are involved in the cellular metabolism, specifically in the Krebs cycle, which dysregulation can alter the cellular homoeostasis correlating with the initiating carcinogenic events (Olar et al., 2015). The mutation often occurs in the enzymatic active site, with higher frequency in IDH1 than in IDH2, and introduce a gain-of-function alteration that leads to a 10-100-fold increase of the level of D-2-hydroxyglutarate (Thakkar et al., 2014). Interestingly, D-2-hydroxyglutarate is an oncometabolite which can induce epigenetic programming and disruption of normal stem cell differentiation and also favour the acquisition of additional mutations (Galluzzi & Kroemer, 2018). IDH mutations appear to be inversely related to, or even mutually exclusive, of the alterations of epidermal growth factor receptor pathway, usually related to primary GBM which then rather display a wild-type IDH status (Q.-J. Li et al., 2016).

3.3.2. Tyrosine-kinase receptors pathways

The signaling pathways related to growth factor receptors are majorly impacted in GBM, provoking a dysregulation of the normal cellular proliferation. Epidermal growth factor receptor pathway (EGFR/PTEN/Akt/mTOR) is mostly affected in primary GBM, while alterations of the platelet-derived growth factor receptor (PDGFR) pathway are more typical of the secondary GBM (Agnihotri et al., 2013). **EGFR** pathway can be altered at the receptor level or in downstream elements (Figure 6), with consequences on the proliferation and cell survival (Crespo et al., 2015). Its activity is often enhanced by the amplification and overexpression of EGFR gene (in around 40-60% of the cases of primary GBM (Ohgaki & Kleihues, 2007)). Additionally, 50% of these tumors also express an

aberrant variant named EGF-RvIII, which is constitutively active and cause mitogenic effects and powerful transforming activity (An et al., 2018; Thakkar et al., 2014). In the same pathway, Phosphatase and Tensin homolog gene **PTEN** gene is mutated in 15-40% of primary GBM (Ohgaki & Kleihues, 2007). PTEN is a tumor suppressor act to negatively regulate the intracellular levels of phosphatidylinositol-3,4,5-trisphosphate (PIP_3) modulating Akt/PKB (Protein kinase B) activity and activation of mTOR signaling pathway. On the other hand, secondary GBMs often present overexpression of **PDGFR**, normally involved in the development of normal tissues and acting particularly on neural stem cells and potentially related to their oncogenic transformation (Agnihotri et al., 2013; Crespo et al., 2015).

3.3.3. p53 pathway

p53/MDM2/$p14^{ARF}$ pathway is commonly altered in GBM, particularly in the secondary form. In normal cells, **p53** network is activated in response to a cellular stress to facilitate DNA repair or induce apoptosis in case of excessive damage, but it can also regulate other cellular mechanisms including cell cycle, cell differentiation, and even neovascularization (Crespo et al., 2015; Thakkar et al., 2014). Mutation of TP53 gene (encoding for p53) have been detected already in lower grade gliomas and this has been directly correlated with the malignant transformation that leads to secondary GBM. Around 60% of secondary GBM carry TP53 mutations, while the frequency is lower in primary GBM (<30%) where they likely occur as secondary events contributing to the genomic instability during tumor development (Ohgaki & Kleihues, 2007). Amplification of Mouse Double Minute 2 (**MDM2**) gene, involved with p53 in a feedback loop regulating their activity and the activation of transcription of various genes (Figure 6), is present in <10% of GBM and exclusively in the primary ones that lack a TP53 mutation (Agnihotri et al., 2013). Moreover, the loss of **$p14^{ARF}$** (Alternate Reading Frame protein) expression, inhibitor of p53 and tumor suppressor, has frequently been observed in GBM (76%) with no significant difference between the two subtypes (Agnihotri et al., 2013). Overall, these mutations lead to a dysregulation of this pathway and the loss of its normal function.

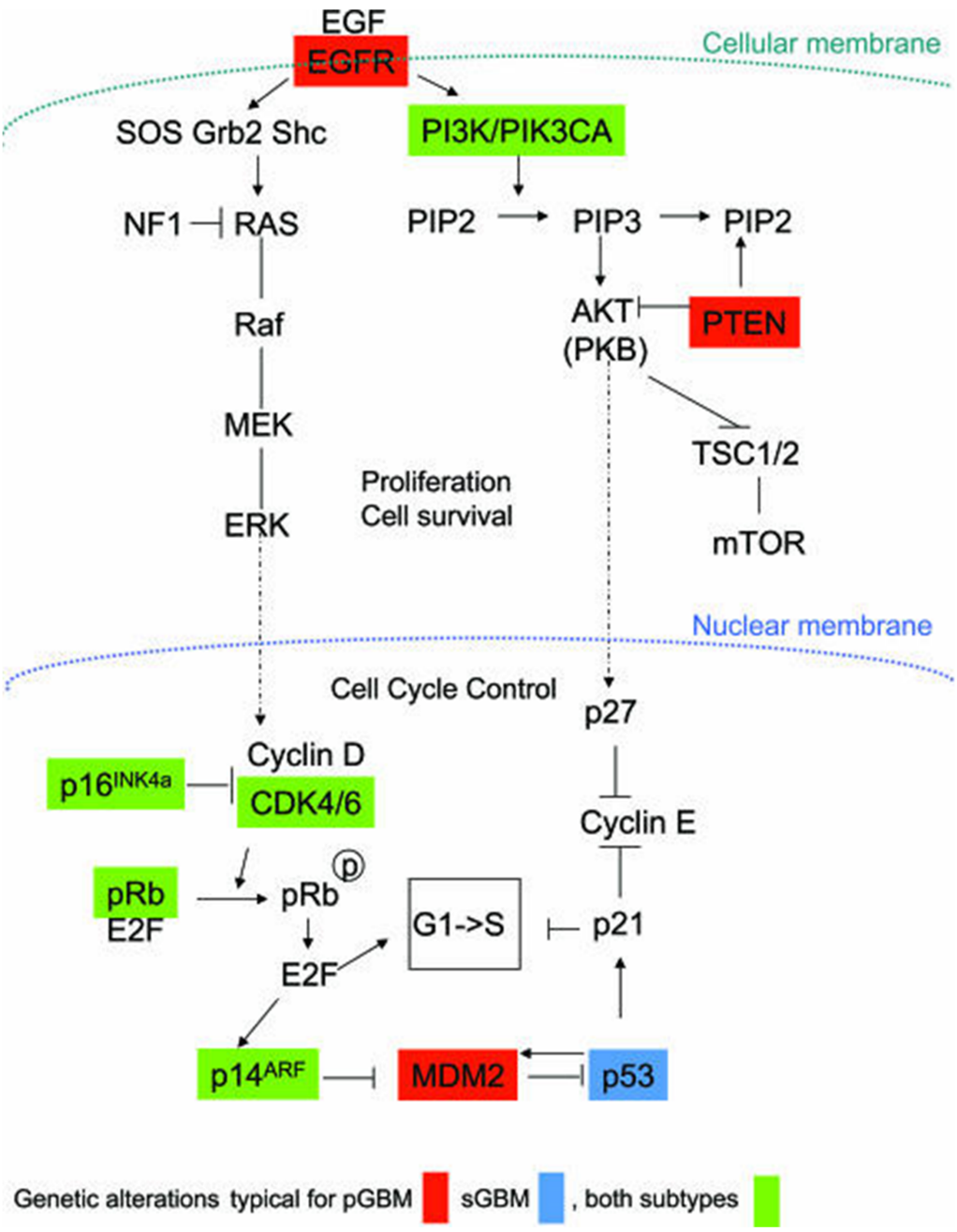

Figure 6. Major signaling pathways involved in the pathogenesis of Glioblastoma

Obtained from Ohgaki & Kleihues, 2007. Typical genetic alterations are highlighted in red, for primary GBM, in blue, for secondary GBM, and in green when frequent in both subtypes.

3.3.4. Cell cycle regulation pathways

$p16^{INK4a}$/RB1 pathway alteration has been observed in both primary and secondary GBM (Figure 6). This pathway coordinates cell cycle and the aberrant activity of its components might lead to the failure of the G_1/S cell cycle checkpoints. In normal cells, the assembly of the cyclin-dependent kinase 4 (CDK4)/cyclin D1 complex, promoting the passage to the S phase by the consequent release of the E2F transcription factor, is regulated by inhibitory functions of **$p16^{INK4a}$** (INhibitor of CDK4) and retinoblastoma-associated protein **RB1** (Crespo et al., 2015). Both $p16^{INK4a}$ and RB1 genes may undergo a loss of their expression due to homozygotic deletion or other epigenetic alterations of the promoter. Alteration of $p16^{INK4a}$ occur with overall similar frequency within primary and secondary GBM, while aberration of RB1 are more frequent in the secondary subtype compared to primary one (43% vs 14% (Ohgaki & Kleihues, 2007)).

3.3.5. Telomerase regulation genes

Alterations of the telomeres is one of the features often altered in GBM, **TERT** (Telomerase reverse transcriptase) and **ATRX** (αthalassemia/mental retardation syndrome X-linked, an ATP-dependent helicase) gene mutations are mutually exclusive and correspond to primary and secondary GBM, respectively (Thakkar et al., 2014). TERT encodes for the enzyme telomerase, involved in telomere maintenance and essential for actively growing cells, and it is frequently mutated in the promoter region. Alternatively, ATRX mutations can cause alternative lengthening of telomeres, associated to genomic instability (Q.-J. Li et al., 2016).

3.3.6. Chromosomal loss

Another common GBM aberration is the depletion of one or several chromosome causing loss of heterozygosity and expression of a single allele increasing the vulnerability of essential genes (Nichols et al., 2020). **Chromosome 10** is lost in 80-90% of the cases causing the loss-of-function of important oncosuppressor genes here located as PTEN (Ohgaki & Kleihues, 2007; Thakkar et al., 2014). Also, **chromosome 22** can be deleted, with a significant higher frequency in secondary GBM (82%) than primary one (41%).

While loss of **chromosome 13 and 19**, is also frequent but relatively uncommon (Ohgaki & Kleihues, 2007).

3.3.7. C-CIMP

Epigenetic analysis of GBM identified the presence of genome-wide hypermethylation of CpG Islands, defined as **CpG Islands Methylator Profile** (CIMP). CIMP has been described in several tumors, including gliomas (G-CIMP) and exhibit distinct epidemiological, clinicopathological, and molecular features, in fact G-CIMP is strongly associated with IDH1 mutation and secondary GBM (Malta et al., 2018; Thakkar et al., 2014).

3.3.8. MGMT status

O6-methylguanine DNA methyltransferase (also known as **MGMT**) status has an important role in the prognosis of GBM and specifically to the response to treatments (Butler et al., 2020). Chemotherapy for GBM consists in the administration of TMZ, an alkylating agent that functions by transferring alkyl groups to guanine bases causing DNA mismatch and double-strand breaks followed by cellular death. MGMT is a DNA repair protein that removes alkyl groups and its activity can reverse the efficacity of TMZ. Approximately 50% of GBM cases present methylation of MGMT promoter, silencing its expression and, therefore, impairing its repair ability (Thakkar et al., 2014). For these reasons, methylation of MGMT promoter is a positive prognostic factor as it allows the therapy to work more effectively. MGMT methylation is associated with IDH1/2 mutant tumors therefore more common in secondary as compared to primary GBM.

4. Glioblastoma heterogeneity

GBM heterogeneity is notorious, its initial name included in fact the epithet "*Multiforme*". In general, tumors can be heterogeneous on an **intertumoral** level, meaning that they can differ from individual to individual even sharing the same diagnosis, or on an **intratumor** level, when the heterogeneity is within the same tumor. Intratumoral heterogeneity can manifest itself at both **cellular** and **molecular** level with diverse cell surface markers, cellular lineage, degree of differentiation, (epi)genetic abnormality, transcriptional

programs, growth rate, etc. Moreover, tumoral cells coexist with various cells of the tumoral microenvironment (pericytes, endothelial, immune cells, etc.). Also, the distribution of hypoxic or necrotic areas leads to what can be defined as a **spatial** heterogeneity, and it impacts on biological mechanisms of each individual region. We can even talk about a **temporal** heterogeneity as the genomic alterations driving the cancer relapse are distinct from those in the initial tumor (Johnson et al., 2014).

4.1. Genotypic intertumoral variability: four GBM subtypes

In 2008, The Cancer Genome Atlas generated a comprehensive catalogue of genomic abnormalities driving tumorigenesis and provided a detailed view of the genomic changes in a vast cohort of GBM patients. This large-scale genomic analysis was a leverage by Verhaak and colleagues few years later to portrait a coherent subgrouping of GBM. Four molecular subtypes, featuring distinct genetic, epigenetic, and transcriptional alterations were identified (Verhaak et al., 2010). The expression of 840 genes was evaluated and the samples were clustered accordingly identifying four subgroups named **Proneural, Neural, Classic** and **Masenchymal** (Figure 7). The subtypes were further validated in an independent dataset to ensure subtype reproducibility and the genetic signature of the GBM subtypes were compared with a brain transcriptome database to define gene sets associated with neurons, oligodendrocytes, astrocytes, and cultured astroglial cells. Finally, the response to aggressive therapy differs by subtype underline the importance to delineate a valid subtype modelling helping in the prediction of the therapeutic response.

4.1.1. Proneural

This group correlate with secondary GBM and significantly younger GBM patients. Alterations of PDGFR, as amplification and mutations, and IDH1 point mutations are the main features of the Proneural class. TP53 mutations and loss of heterozygosity are also typical in this subtype, while chromosome 7 amplification, paired with chromosome 10 loss is more frequent in the other classes compare to this one.

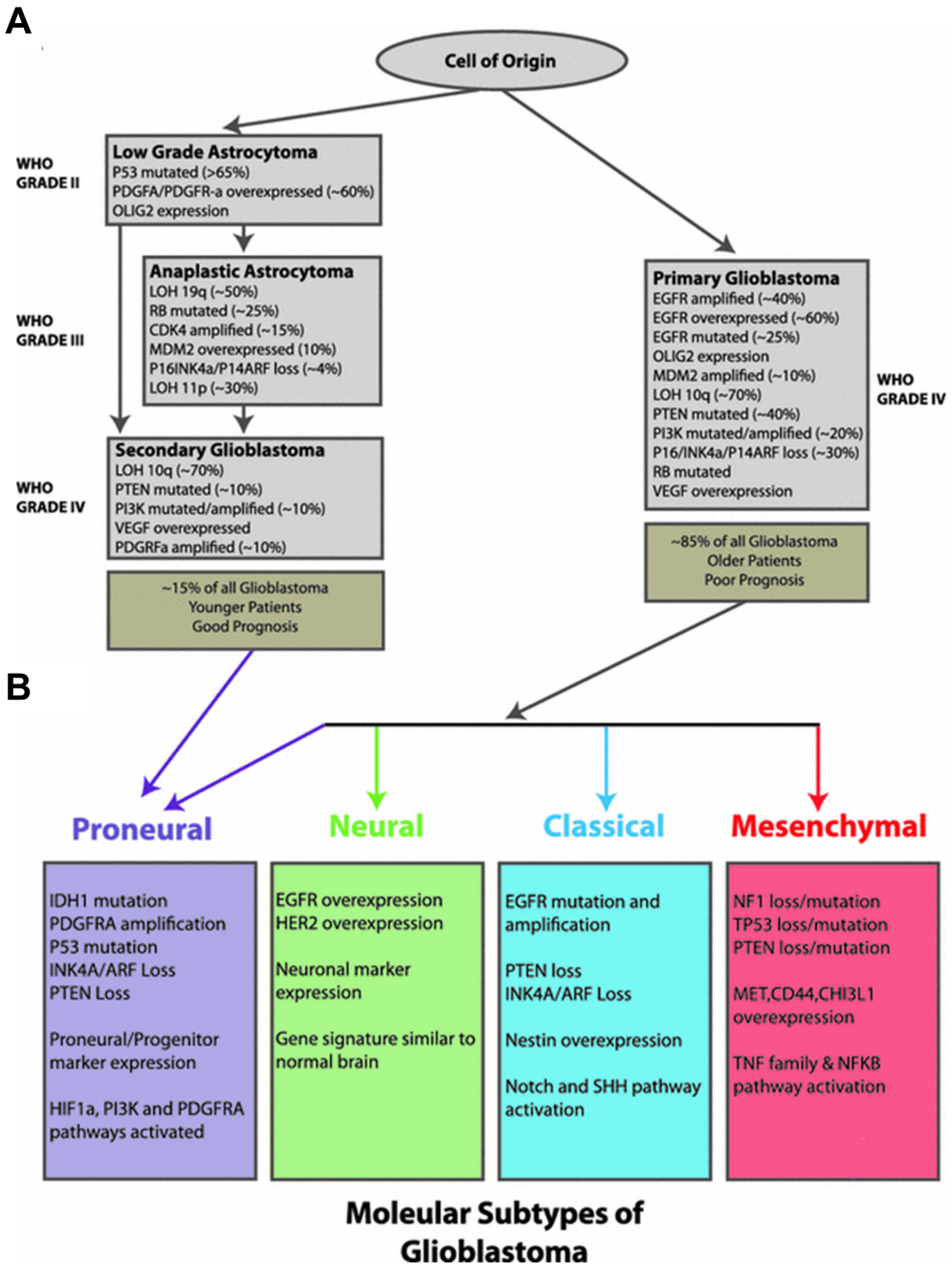

Figure 7. Glioblastoma subtypes and genetic features

Obtained from Agnihotri et al., 2013. (A) Primary GBM originate de novo, whereas secondary evolve from lower-grade astrocytomas. Both present similar aberrations, although certain aberrations are more prevalent in one subtype over the other. (B) Primary and secondary GBMs can be further distinguished in four subtypes characterized by specific molecular alterations. Secondary GBM mainly display proneural phenotype.

It presents high expression of PDGFRA, a marker of oligodendrocytic development, together with expression of the homeobox protein Nkx2.2 and OLIG2. OLIG2 can downregulate the tumor suppressor p21CDKN1A (Cyclin Dependent Kinase 1A), increasing proliferation, in fact p21CDKN1A expression is indeed lower in this class. Proneural development genes such as SOX (Sex-determining region Y-related high mobility group bOX) genes, doublecortin (DCX), Delta-like ligand 3 (DLL3), Achaete-scute homolog 1 (ASCL1), and Transcription Factor 4 (TCF4). Altogether Proneural class is highly enriched in oligodendrocytic, but not astrocytic, signature.

4.1.2. Neural

This class present expression of neuron markers such as Neurofilament Light (NEFL), GABA Type A Receptor Subunit Alpha1 (GABRA1), Synaptotagmin 1 (SYT1) and K+/Cl- cotransporter 2 (SLC12A5). According to Gene Ontology (GO), neural subtype often displays neuronal projection, axons and synaptic transmission. Neural class shows association with oligodendrocytic and astrocytic differentiation but additionally had a strong enrichment for genes differentially expressed by neurons.

4.1.3. Classical

Exclusive feature of the Classical GBM subtype is high EGFR pathway activity due either to its gene amplification or EGFRvIII point mutation. At chromosomic level, it is characterized by the amplification of chromosome 7 paired with chromosome 10 loss, associated with the loss of PTEN. TP53 mutations distinctively lack in this class, while $p16^{INK4a}$ and $p14^{ARF}$ loss is another frequent genomic sign. Neural precursor and stem cell marker Nestin (NES), as well as Notch and Sonic hedgehog (SHH) signaling pathways are highly expressed in this subgroup. When compared to different brain lineage expression pattern, this group result to be strongly associated with an astrocytic signature. Clinically, these patients displayed a reduced mortality upon aggressive treatment.

4.1.4. Mesenchymal

This phenotype is characterized by Neurofibromatosis type 1 (NF1) loss or mutations, commonly intersecting with the loss or mutations of PTEN as well. Mesenchymal, and sometimes astrocytic, markers as CHI3L1, CD44 and hepatocyte growth factor receptor

(HGFR) display an enhanced activity in this subtype, potentially reminiscent of an epithelial-to-mesenchymal transition. Finally, NF-κB (nuclear factor k-light-chain-enhancer of activated B cells) pathway is highly activated in this subtype, as a consequence of higher overall necrosis and associated inflammatory infiltrates. Mesenchymal class exhibit the genomic signature typical of cultured astroglia. Similarly to the Classical group, aggressive treatments result to be more effective on this subclass.

4.2. Theories about intratumoral heterogeneity

A tumour can be considered as an aberrant organ initiated by a tumorigenic cancer cell that acquired the capacity for indefinite proliferation through accumulated mutations (Reya et al., 2001). As any other organ and tissue of the body, tumors are composed of heterogeneous combinations of cells, with different phenotypic characteristics and proliferative potentials. Intratumor heterogeneity confers an evolutionary advantage facing microenvironmental fluctuations or selective pressure imposed by therapies. Thus, the pre-existence of resistant clones can determine therapy outcome and constitute the main cause of therapeutic failure and consequent tumor relapse (Inda et al., 2014).

4.2.1. Theory of clonal evolution

Cancer has been considered for long time as an evolutionary process where natural selection occurs upon successive waves of genetic changes occurring in tumor cells (Figure 8A), some of these convey to a proliferative advantage and, as for Darwinian selection, the better adapted clones expand becoming responsible for the tumor growth. During cancer progression, tumoral cells inherit the expression of diverse oncogenic transcriptional programs favouring their expansion and following acquisition of new mutations which promote genetic variability and an increase in tumor heterogeneity (Inda et al., 2014). In this theory, “driver mutations” allow the progression of a cancer, whereas “passenger mutations” are neutral or only slightly deleterious but contribute to its heterogeneity (Greaves & Maley, 2012). This branched evolution underlines the importance of targeting ubiquitous alterations in the trunk of the phylogenetic tree but also of attenuating the genomic instability which fuel the unpredictable clonal

heterogeneity (McGranahan & Swanton, 2017) . Although the coexistence of different clones within the same tumor could be due to stochastic events, their maintenance is specifically due to the selective pressure applied by the interaction with internal or external factors that can favour or disfavour them. Serial sampling to tumoral genomes has been implemented in the clinical research to predict the trajectories of tumor evolution (McGranahan & Swanton, 2017). In GBM, single cell RNA-sequencing analysis have shown that individual tumors contain a spectrum of cells with inherently variable expression of diverse transcriptional programs related to oncogenic signaling, proliferation and even features of multiple of the four GBM subtypes, drawing into question the utility of targeting therapeutically specific subtype (Patel et al., 2014).

4.2.2. Cancer stem cells theory

In the wide cellular heterogeneity of the tumor environment, most of the cancer cells actually have only limited proliferative potential, only a subset of cells displays extensive proliferative ability and self-renewal potential. These were defined Cancer stem cells (CSCs) and their identification dates back to the 1990s, when, in human leukemia, the tumor clones were found to be organized as a hierarchy originating from rare leukemic stem cells (Bonnet & Dick, 1997). By asymmetric division, CSCs maintain their population and, at the same time, generate more differentiated daughter cells with limited proliferation properties that constitute the bulk of the tumor, while CSCs will remain as a small subpopulation (Figure 8B). According to this theory, intratumoral heterogeneity is organized in a hierarchical organization at the apex of which are CSCs (Inda et al., 2014). It should be noted, that this hierarchy is not a one-way route, but can be reversible or plastic whereby even terminally differentiated cells can dedifferentiate and gain CSCs properties under specific conditions (Prasetyanti & Medema, 2017). GBM stem cells, or GSCs, have been identified in human brain tumors (Singh et al., 2003) and will be described in a dedicated chapter.

4.2.3. Inter-clonal cooperativity and microenvironment

Each tumor area can vary in terms of cell content, both in cells of the microenvironment or different tumor clones. The presence of a specific cell composition may retain a greater or minor tumor thrust. The theory of interclonal cooperativity suggests that tumor

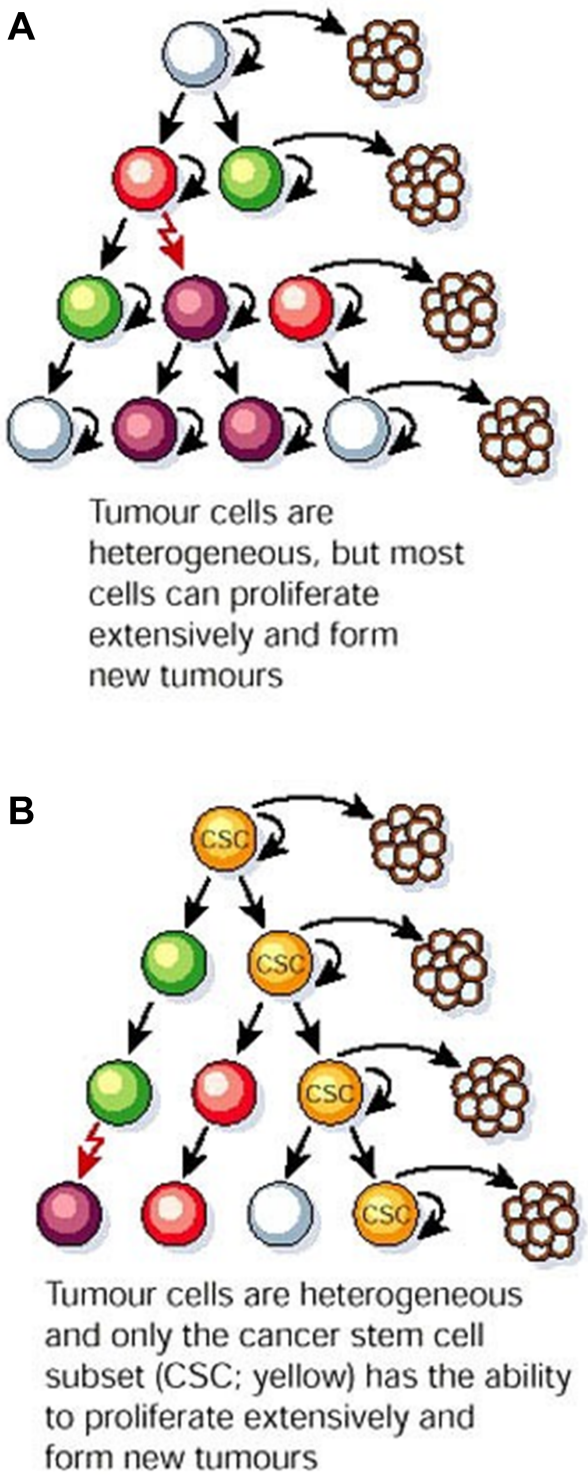

Figure 8. Tumoral heterogeneity theories

Obtained from (Reya et al., 2001). (A) Clonal evolution model. From one initiating cell different phenotypes and subclones can form giving rise to tumoral heterogeneity. Cancer cells of many different phenotypes have the potential to proliferate extensively. (B) Most cancer cells have only limited proliferative potential, but a subset of cancer cells consistently proliferates extensively in clonogenic assays and can form new tumours on transplantation.

evolution and heterogeneity is promoted by interactions between tumor cell clones and their microenvironment influencing its malignant progression (Parker et al., 2015). One clone could display oncogenic mutations leading to the production of factors that promote the establishment of a pro-oncogenic environment confering an advantage to other nearby clones. Even a small minority of phenotypically distinct cells can have a profound impact on the behaviour of the rest of the population (Bonavia et al., 2011). For example, in GBM, a deleted form of EGFR, common pathogenetic signature, has a potent ability to enhance tumorigenicity. Despite this, its expression is typically observed in a subpopulation of cells and almost never in the entire tumor (Inda et al., 2010). Potentially this minority does not only enhance intrinsic tumorigenic abilities, but can promote the proliferation of the neighbouring cells for the majority expressing the amplified wild-type form of EGFR. The tumoral microenvironment is also not homogeneous as oxygen pressure, blood vessel density, growth factors, composition of extracellular matrix and immune infiltration can differ in different tumoral areas. These differences affect tumor cells and might be the cause of phenotypic and genetic differences, resulting in different cell growth, invasiveness, cell death/therapy resistance and immune escape (Inda et al., 2014). For example, some area could select “hypoxia-fit” clones and other, more nutrient dense regions, may select for fast-growing clones. According to this heterogeneity model the interactions between immune/stromal factors and different genetic subpopulation of tumor cell clones collaborate to drive disease progression and a malignant phenotype.

5. Glioblastoma microenvironment

The tumoral microenvironment represents the non-cancerous cells inside the tumor. In GBM this is constituted by normal and reactive astrocytes, neurons, fibroblasts, immune cells, microglia/macrophages, endothelial cells (ECs) and vascular pericytes. The cross-talk between these cells and GBM occurs through various mechanisms of direct or indirect communication, and often favour tumor progression.

5.1. Perivascular niche

Perivascular niches are represented by small capillaries or arterioles, typical of the micro-vascularization and composed by ECs, GSCs, pericytes, and other specific tissue components. Tumor-initiating cells are notably detected in this location (Broekman et al., 2018b) that acts as a hub for generation of multiple cellular phenotypes and has important functions in the maintenance of the oncogenic thrust (Figure 9A). Particularly, ECs were found to closely interact with GSCs and maintain their stem cell-like state (Calabrese et al., 2007). Larger vessels with defined layers, cannot function as niches as they prevent the direct contact between GSCs and ECs. Notch stemness pathway is activated in GSCs through the interaction of Notch1/2 receptors, expressed by GSCs, and their ligands JAG1 (Jagged-1) and DLL4 present on the ECs (Schiffer et al., 2018). Alternatively, Notch signaling pathway can also be activated by the paracrine secretion of Nitric Oxide (NO) on behalf of ECs (A. Sharma & Shiras, 2016).

It has been reported that GSCs can undergo mesenchymal differentiation and transdifferentiate into ECs or pericytes, another functional component of the perivascular niche. The activation of the Notch signaling pathway in GSCs can direct these cells toward the expression of pericytes markers as α-smooth muscle actin (α-SMA), NG2 and PDGFR (Aderetti et al., 2018; Jhaveri et al., 2016). Stimulation of pericytes activity can turn into formation of new blood vessels. GSCs act on pericytes and ECs proliferation secreting pro-angiogenic growth factors, as VEGF (Broekman et al., 2018b). Therefore, GSCs have the capability to generate the cell types required to construct their niches and simulate cancer progression (Aderetti et al., 2018).

5.2. Hypoxic niche

In GBM, the high density of tumoral cells, the presence of pseudopalisading necrotic areas and the vasculature morphology, tortuous and often leading to dead ends, drive to the establishment to hypoxic regions. Hypoxia is, in fact, another hallmark of GBM and occurs in the whole tumor, distributed with variable intensity. Hypoxic niches are typically hyperproliferative, they can support and maintain GSCs self-renewal and even induce

non-stem cells to acquire GSC characteristics increasing the tumorigenic potential (Aderetti et al., 2018). The hypoxic environment induces expression of stem cell markers as SOX2, OCT4 (octamer-binding transcription factor 4) and CD133 (Promine-1) in GBM cells, indicating their dedifferentiation to GSCs. Hypoxia also causes acidification of the microenvironment and stimulation of Hypoxia-inducible factor 1α (HIF-1α), transcription factor which triggers the production of VEGF, promoting tumoral angiogenesis (Aderetti et al., 2018), and induces the expansion of GSCs through the phosphatidylinositol 3-kinase (PI3K)/Akt and ERK1/2 (Extracellular signal-regulated kinases) pathways (Schiffer et al., 2015).

5.3. Invasive niche

GBM, as other gliomas, has the propensity to invade normal tissue, although it is rarely observed forming metastasis. GBM cells preferentially invade as single cells along vascular basement membranes or on myelinated axons, suggesting that some microenvironmental features is involved in this invasion (Bonavia et al., 2011). Major cell types that constitute the microenvironment at the invasive edge of GBM include ECs, pericytes, activated microglia, reactive astrocytes and neurons. Invading GBM cells make surgical resection incomplete and are responsible for tumor recurrence. Invasive edges also occur at perivascular locations, where ECs expressed chemotactic molecules capable of attracting GSCs (Diksin et al., 2017). Various inflammatory mediator causes blood vessels dilatation allowing extravasion of the tumoral cells. Additionally, GSCs release extracellular vesicles stimulating the disruption of tumour vasculature and BBB integrity allowing tumor cells to infiltrate normal tissue (Diksin et al., 2017). Microglia, fibroblast and GSCs themselves actively remodel and degrade extracellular matrix acting through metalloproteases (MMPs).

5.4. Immune response

Compelling evidences show that this immune response contributes significantly to the creation and maintenance of immunosuppression and tumor progression.

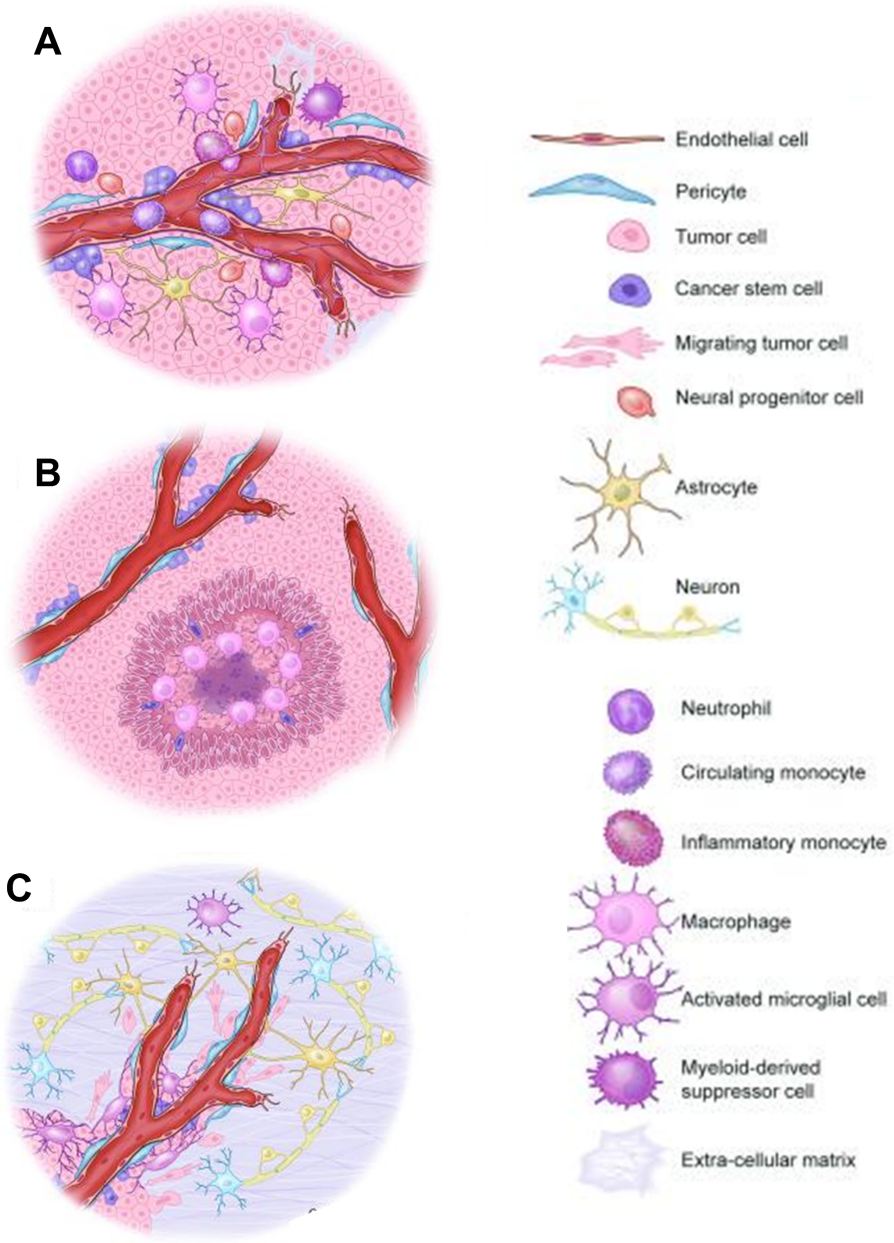

Figure 9. Cellular niches in Glioblastoma

Adapted from Hambardzumyan & Bergers, 2015. (A) ECs, pericytes, astrocytes and various immune infiltrate interact with GSCs in a specialized perivascular niche which provides a supportive environment for growth, maintenance, and survival. (B) Pseudopalisading necrotic areas contain a hypoxic core that recruits innate immune cells and promotes the expansion of GSCs through activation of HIF-1α. (C) GBM cells migrate along blood vessels and reach the invasive edge where ECs, pericytes, activated microglia, reactive astrocytes, and neurons create a permissive environment for their invasion.

GBM microenvironment contains brain-resident microglia and infiltrating monocytes, activated into macrophages, which acquire the name of GAMs (Glioma-Associated Microglia/Macrophages). GAMs release TGF-β (Transforming Growth Factor beta) which triggers the release of pro-MMP2 from GBM cells promoting cell invasion, or other factors, as stress-inducible protein 1 (STI1) and EGF, which stimulates GBM proliferation (Hambardzumyan et al., 2016). Similarly, neutrophils and mast cells, are also recruited into the tumour microenvironment and redirected toward pro-tumoral functions: upon activation by GBM cells, mast cells produce soluble factors (IL-6, IL-8, VEGF, etc) that can facilitate tumour growth and angiogenesis (Broekman et al., 2018b). T-cells recalled into the tumoral area are exposed to a network of immune-regulatory mechanisms that promote their differentiation into a dysfunctional state (Broekman et al., 2018b).

5.5. Neurons

Neurons certainly belong to GBM microenvironment and can also participate in tumor progression. The intercommunication between neurons and GBM cells appear to have relevant outcome on both sides. GBM cells can release glutamate, causing excessive activation of N-methyl-D-aspartate receptor (NMDA) receptors on neuronal cells which can manifest symptomatically as seizures. In the other direction, neuronal activity appears to support GBM growth. The firing activity of cortical projection neurons promotes the secretion of a postsynaptic molecule (synaptic protein neuroligin 3) that activates, in glioma cells, the downstream signaling of the focal adhesion kinase (FAK), PI3K, growth factor receptors and oncogenic proteins promoting glioma proliferation and growth (Venkatesh et al., 2015, 2017). In addition to secreted factors, neurons can interconnect through long neuritic extensions, named Tumor microtubes (TMs), with GBM cells forming functional neuro-gliomal synapses enriched in glutamatergic AMPA (α-amino-3-hydroxy-5-methyl-4-isoxazole propionic acid) receptor. This intercommunication coordinates calcium transients in GBM cells and their networks regulating tumour invasion and growth (Venkataramani et al., 2019).

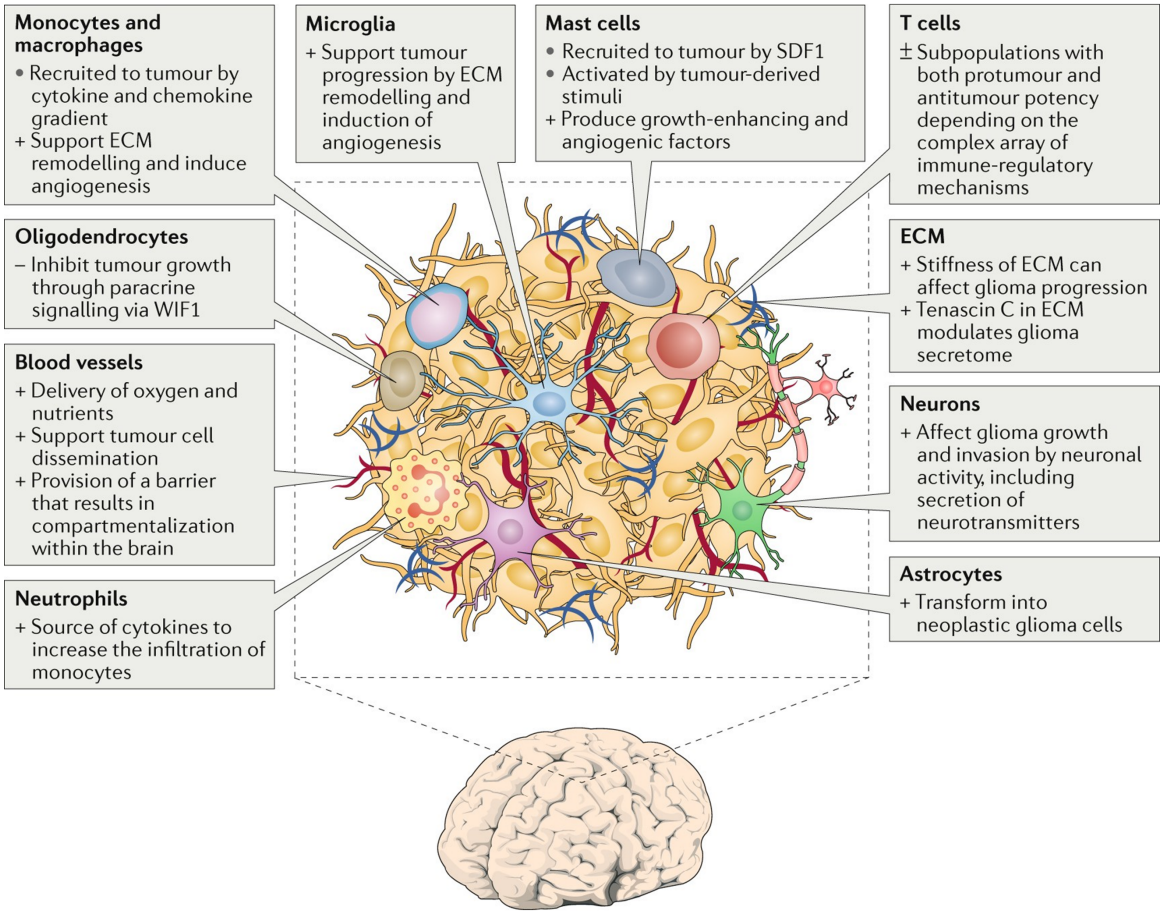

Figure 10. Cells composing Glioblastoma microenvironment

Obtained from Broekman et al., 2018. GBM microenvironment is composed of various non-neoplastic cells that display pro-tumoral (+) or anti-tumoral (-) or mixed (±) functions.

5.6. Oligodendrocytes

Oligodendrocytes establish a complex relationship with GBM cells that can include both tumour-promoting and tumour-suppressing signals. Less is known about their interaction although some evidences suggest that oligodendrocytes activity inhibit GBM growth and proliferation by paracrine signaling via WNT inhibitory factor 1 (Broekman et al., 2018b).

5.7. Reactive astrocytes

Astrocytes comprise nearly half of the total number of cells in mammalian brains and are an important component of the BBB. Reactive astrocytes are a constant phenomenon associated with gliomas. The transformation into reactive astrocytes, led by NF-κB signaling pathway, is characterized by hypertrophy, upregulation of intermediate filaments composed of nestin, vimentin, and GFAP, as well as activation of cell proliferation. When this state is achieved, reactive astrocytes release cytokines, chemokines, interleukins or NO exacerbating the neuroinflammatory responses and promoting tumor cell invasion and migration, proliferation, and growth (Guan et al., 2018). For example, through the activation of the IL-6/p-STAT3 (Signal transducer and activator of transcription 3) mechanistic pathway, IL-6 increases MMP2 expression enhancing GBM invasiveness. Another factor, astrocyte elevated gene-1 (AEG-1), is associated with poor survival in GBM and induced GBM proliferation through the activation of PI3K/Akt pathway. Beyond secretion, reactive astrocytes can communicate directly with GBM cells via gap junction channel and tunneling nanotubes (TNTs), long and thin tubular structures connecting the two cell population and participating in cell communication and influencing GBM proliferation and invasion (Civita et al., 2019; Formicola et al., 2019; Zhang & Zhang, 2015). Finally, the interaction between GBM cells and astrocytes is further facilitated further by ion channels and ion transporters (Guan et al., 2018).

6. Glioblastoma stem cells

6.1. Definition of cancer stem cell

As previously described, CSCs are a population at the apex of the cellular hierarchy within the tumoral heterogeneity. The term 'stem' does not imply a derivation from transformed stem cell, as multiple cell types are amenable to invert the differentiation process due to their oncogenic transformation. CSCs are defined accordingly to their functional abilities (Lathia et al., 2015), rather than origins, particularly the ability to self-renew and give rise to differentiated progeny (as the classical stem cells) but also the generation of a secondary tumor upon re-implantation that contains progeny at various degrees of differentiation and self-renewal capacity (typical instead of tumor-initiating or tumor-propagating cells) (Figure 11). CSCs also share other features with somatic stem cells as the expression of stem cell marker, for this reason their isolation through the identification of these marker remains controversial. The gold standard for CSC determination remains the ability of a limiting dilution of cells to recapitulate the complexity of the original patient tumor when transplanted orthotopically (Lathia et al., 2015).

6.2. Markers of GSCs

Single-cell analysis also revealed that a surprisingly large subpopulation of cells (~40%) had a stemness signature (Patel et al., 2014). GSCs exhibit activation of early growth signaling pathways, particularly common embryologic pathways of the CNS, as Notch, Wnt, and Sonic Hedgehog, governing their self-renewal (Rajakulendran et al., 2019). Many of the transcription factors or structural proteins essential for normal NSCs function also mark GSCs, as for example SOX2, Homeobox protein NANOG, OLIG2, MYC and NES (Lathia et al., 2015). However, a multitude of potential cell surface markers have been suggested, and particularly CD133, a glycoprotein expressed on neural stem cells, was initially elected as putative cell surface marker (Singh et al., 2003).

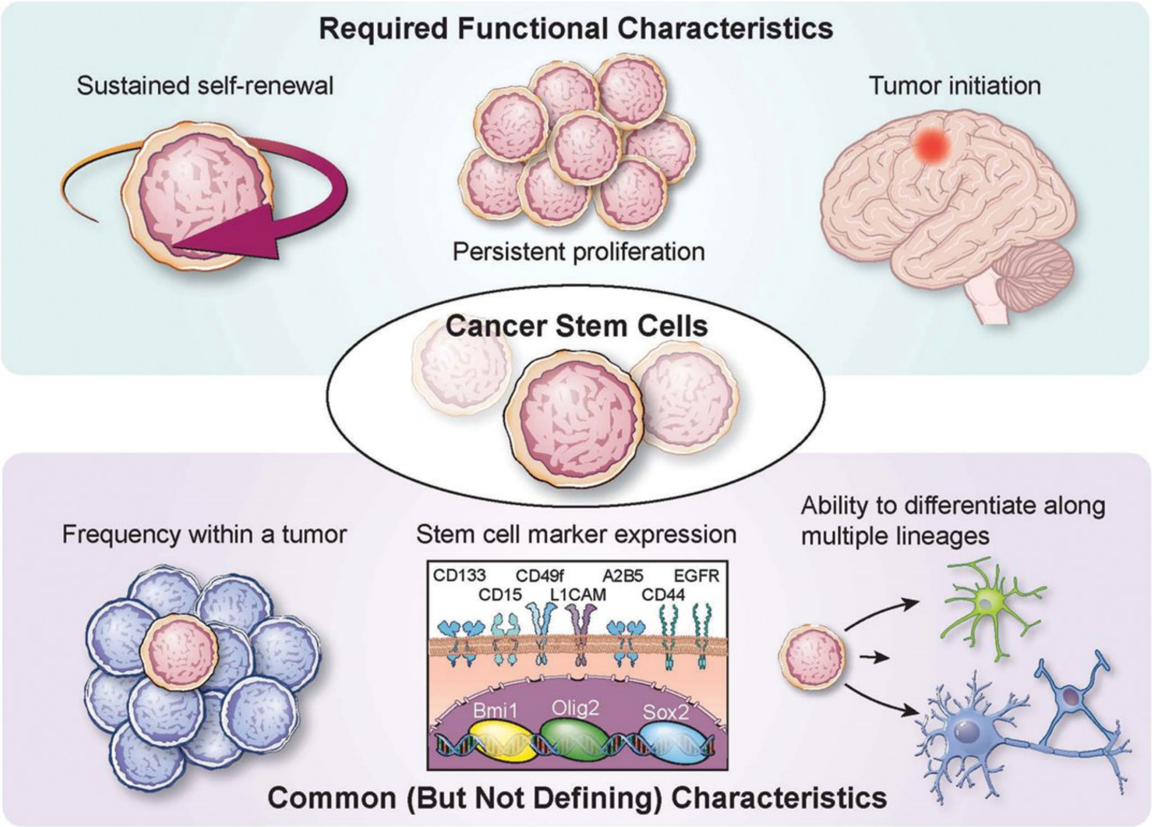

Figure 11. Glioblastoma Stem Cells features

Obtained from Lathia et al., 2015. CSCs are defined accordingly to their functional abilities as sustained self-renewal, persistent proliferation and initiation and propagation of a tumor, upon re-implantation, representative of original heterogeneity. Other common feature of CSCs, shared with classical stem cells but not defining CSCs state, are frequency in the tumor, expression of specific stem surface markers and ability to originate multiple differentiation lineages.

Although, the surface expression of CD133 marks stem cells and decreases with differentiation, CD133-negative cells were found to be clonogenic and multipotent (Bhaduri et al., 2020; Sun et al., 2009), discarding CD133 to be an exclusive GSC marker. Other proteins often found expressed in GBM-initiating cells are CD15/ SSEA-1 (Stage-Specific Embryonic Antigen-1) (Son et al., 2009), integrin α 6 (Lathia et al., 2010), CD44 (Anido et al., 2010; Bhaduri et al., 2020) and Sox2 (Bhaduri et al., 2020; Prager et al., 2020). These GSC-associated cell membrane markers do not represent a clonal entity and have high utility as GSC enrichment methods, rather than isolation, as each can mark a large percentage of cells, consistent with a high false-positive rate. Additionally, single cell RNA-sequencing of various GBM has shown that tumor cells display a spectrum of stemness and differentiation states, variable proliferative capacity, and variable expression of quiescence markers, enabling the identification putative regulators of stemness in vivo and confounding therapeutic strategies (Patel et al., 2014).

6.3. Regulation of GSCs

GSCs, and CSCs in general, are regulated by various intrinsic and extrinsic factors. Key intrinsic (self-autonomous) regulators include genetic, epigenetic, and metabolic regulation, while extrinsic (external) regulators include interaction with the microenvironment, including niche factors and the immune system (Lathia et al., 2015) (Figure 12A), as we previously described. The heterogeneity and chaotic fluctuations in which GSCs are immersed lead tumors for their adaptation and evolution. Their stemness is maintained by a permissive epigenetic landscape and oscillating expression of a large number of genes but GSCs are ready to respond to a wide variety of stimuli. Changes of state can be driven by non-stochastic forces or events – defined as attractors – generated by the microenvironment, therapeutic intervention, or cell–cell interactions (Prager et al., 2020). Stem cells differentiate and get locked into a more stringent and regulated genetic programs with fewer degrees of freedom compared to the original state (Figure 12B). In fact, single-cell RNA-sequencing analysis revealed that malignant GBM cells exist in a limited set of cellular states (neural-progenitor-like, oligodendrocyte-progenitor-like, astrocyte-like and mesenchymal-like).

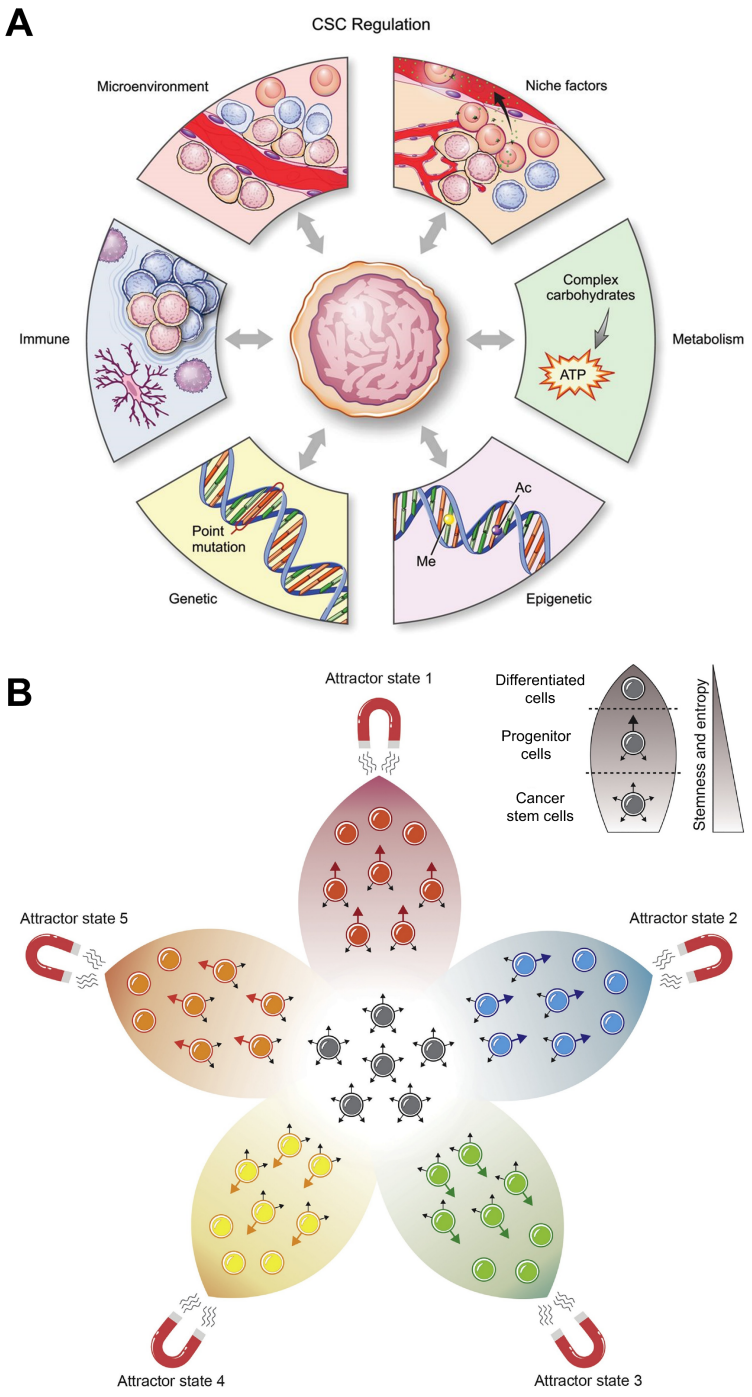

Figure 12. Regulation of GSCs.

Adapted from Lathia et al., 2015 and Prager et al., 2020. (A) CSCs regulation depends on various intrinsic and extrinsic factors. (B) Attractor state model. CSCs are in the centre and have the highest degree of freedom. Their differentiation can be driven by attractors, or environmental forces, that direct them toward different possible evolutions.

These states co-exist in the same tumor and are plastic between each other, moreover a single cell has the potential to generate all four states (Neftel et al., 2019). Differentiated cells can also be directed toward a stem-like state capable of *in vivo* tumor propagation, as it has been demonstrated that inducing the expression of four transcriptional factors - BRN2/POU3F2 (POU domain, class 3, transcription factor 2), SOX2, SALL2 (Sal-like protein 2), and OLIG2 – was sufficient to induce the reprogramming (Suvà et al., 2014).

6.4. Metabolism

In 1924, Otto Warburg discovered that tumor cells metabolism is strongly based on the anaerobic production of energy via conversion of glucose to lactate into of the glycolytic process, even in the presence of oxygen. In GBM, some oncogenic alteration converge toward an enhanced glycolysis: p53 mutations besides inducing genetic instability, triggers glycolysis, loss of PTEN leads to the constitutive activation of Akt1, which stimulates glucose uptake by enhancing GLUT4 (Glucose transporter type 4), and the activation of c-MYC induces Lactate dehydrogenase (LDH-A) and Phosphoinositide-dependent kinase-1 (PDK1) expression facilitating the production of lactate (Garnier et al., 2019). Interestingly, by infusions of (13)C-labelled nutrients into mice bearing GBM cells with a distinct set of mutations, it was shown that, beyond the typical glycolytic metabolism, GBM cells were as well directing the energy sources toward mitochondrial glucose oxidation (Marin-Valencia et al., 2012). GSCs appear to rely even more on mitochondrial-based metabolism. In contrast to the proliferating tumor mass, GSCs are rather quiescent and slowly proliferating cells: they display less glycolysis, less glucose consumption and lactate production, whereas they contain higher ATP levels than their differentiated cancer counterparts (Vlashi et al., 2011). Of note, slow-cycling GSCs display invasive capacity and treatment-resistance to ionizing radiation and TMZ treatment (Hoang-Minh et al., 2018; Sabelström et al., 2019). Glucose is not the only energetic source for GSCs, lipid catabolism and glutamate-dependency have also been described in GBM, with predilections for the mesenchymal subtype (Garnier et al., 2019). GSCs appear to behold a remarkable metabolic plasticity, which allows them to adapt to transient bioenergetic crisis caused by hypoxia or nutrients deprivation. Moreover, GSCs

metabolism have been shown to deeply influence their maintenance and survival as demonstrated by HIF1a activation in the hypoxic niches.

7. Treatment-resistance

GBM relapse occurs despite surgery, chemo and radiotherapy. Surgery is insufficient to eradicate the invasive borders of GBM as tumoral cells invade and diffuse in the normal surrounding tissue. Single-cell RNA-sequencing analysis demonstrated that infiltrating GBM cells share a consistent gene signature distinct from those of the tumoral core, as upregulation of the genes involved in the invasion of the interstitial matrix, cell survival signaling via the Fibroblast Growth Factor (FGF) receptor 3 or inhibition of TP53-mediated apoptosis (Darmanis et al., 2017). Chemo and radiotherapy aim to the elimination of these remaining cells, but due to the complex tumoral heterogeneity, previously described, a small fraction of tumor cells survive and initiate the formation of the recurrent tumor (Figure 13). The vast cellular heterogeneity in GBM contributes to therapy-resistance by preventing adequate control of the entire tumor mass by a single drug and by facilitating escape mechanisms from targeted agents. The molecular mechanism of treatment-resistance has not been fully elucidated yet and treatments themselves appear to contribute to this phenomenon. Irradiation causes various changes in the tumoral microenvironment, including increased oxidative stress, hypoxia, neuroinflammation, altered cell adhesion and extracellular matrix and changes in stemness markers expression (Gupta & Burns, 2018). These alterations are not always beneficial and they have been shown to possible induced therapeutic resistance. In fact, ionizing radiations induce expression of the anti-apoptotic protein survivin and various stemness marker in differentiated GBM cells, as well as increase their tumorigenicity *in vivo* (Dahan et al., 2014). Similarly, TMZ-chemotherapy promotes the accumulation of HIFs in the GBM cells inducing their dedifferentiation and the formation of therapy-resistant GSCs (G. Lee et al., 2016) and can also facilitate the expansion of pre-existing drug-resistant GSCs (Lan et al., 2017). GSCs, that by definition own the tumor-initiating capability, seem to be the key driver of resistance. Some GBM subpopulation display an intrinsic chemo and radioresistance (Bao et al., 2006; J. Chen et al., 2012) and they are likely responsible for

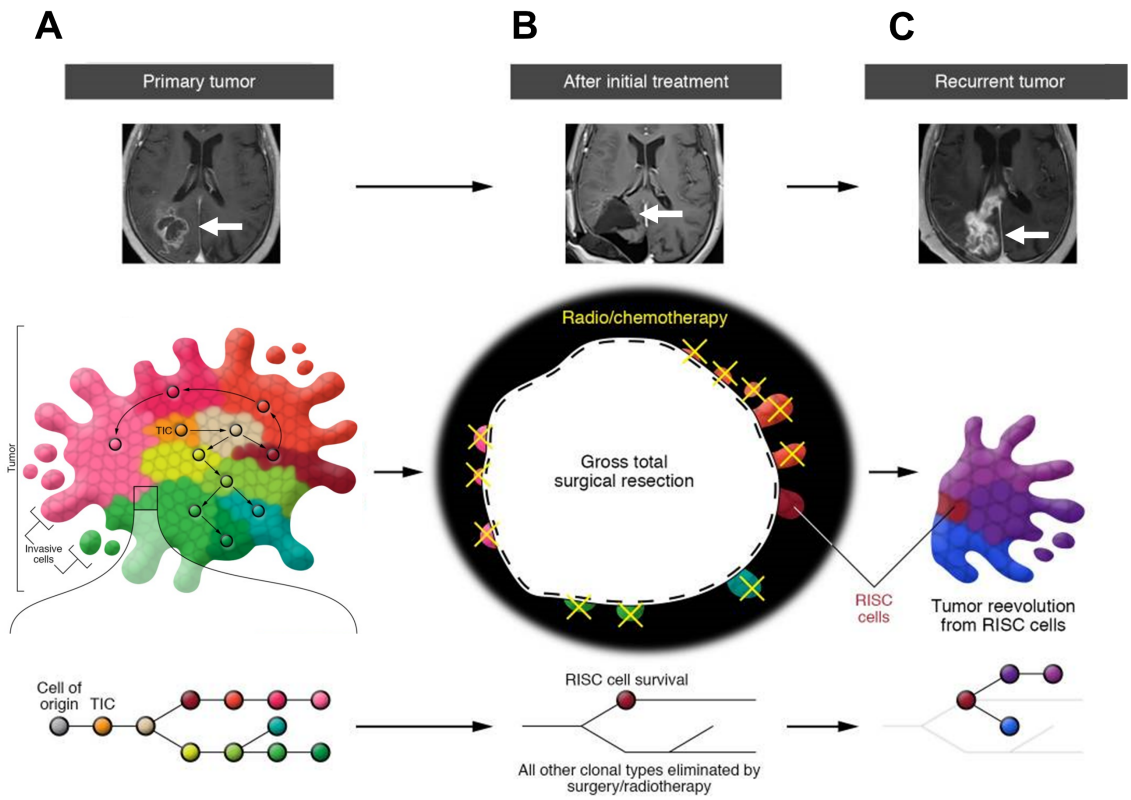

Figure 13. Therapy and recurrence of Glioblastoma

Obtained from Osuka & Van Meir. (A) Primary tumor. A representative MRI image of the tumor (white arrow). In the schematic, the tumor is a mass with irregular borders and few invasive cells separated from the main mass. Primary tumor is highly heterogeneous (different colors) and it originates by evolution of a tumor-initiating cell (TIC) which retain the potential to give rise to several lineages. (B) After initial treatment. Surgical resection removes the main tumoral mass leaving the most invasive areas which are targeted by chemo and radiotherapy. Of the initial heterogeneity of the primary tumor, only the cells displaying particularly resistant phenotype remain and become recurrence-initiating stem-like cancer (RISC) cells. (C) Recurrence of the tumor. RISC cells proliferate and differentiate developing a new heterogeneous tumor.

therapy failure. GSCs display higher expression of drug resistant genes as gene Breast cancer resistance protein (BCRP1) and MGMT, as well as the anti-apoptosis protein (Liu et al., 2006). GSCs also overexpress invasion-associated protein, such as L1 Cell Adhesion Molecule (L1CAM), and therefore retain an elevated invasive potential (Cheng et al., 2011). GSCs also exhibit a peculiar intercellular communication, as they interconnect through long cellular extensions and create a tumoral network which allows the propagation of electrical signals (Osswald et al., 2015). Interestingly, the cellular cooperation sustained by this network protected from cell death inflicted by radiotherapy and promote cell invasion, proliferation (Weil et al., 2017). Tunnelling nanotubes, extensively described in the next part, could participate to this tumoral network and provide a route for the exchange of cellular content, participating to treatment-resistance. On the metabolic point of view, slow-cycling cancer cells are more likely to evade anti-proliferative therapies and they can give rise to a more rapidly cycling progenitor population with extensive self-maintenance capacity (Lan et al., 2017). These cells also display invasive capacity as well as chemo and radioresistance (Hoang-Minh et al., 2018; Sabelström et al., 2019). In this vision, therapies target only populations which evolve from a small core of cells which remain unaffected and are permanently able to give rise to the whole tumor heterogeneity (Figure 14A).

All considered, GSCs are the most relevant target for GBM therapy, and the complete elimination of slow-cycling, resistance-driving, tumor-initiating and -propagating GSCs is crucial in treating GBM. Current therapies resulted to be unsuccessful in impairing tumor recurrence, and a change in the approaches used might be necessary. **GBM remains difficult to treat at various level due to its intertumoral and intratumoral heterogeneity (including genetic, epigenetic, cellular, spatial and temporal variability) mainly driven by GSCs that additionally bring multiple therapy-resistance features and remarkable plasticity and/or adaptability to a changing environment and to the therapeutic treatments.** A possible solution, proposed by Pranger and colleagues, would be to direct a complete differentiation of GSCs, in order to empty the core of recurrence-driving cells, toward a uni-lateral cellular fate that can be targeted by specific, directed therapy (Figure 14B).

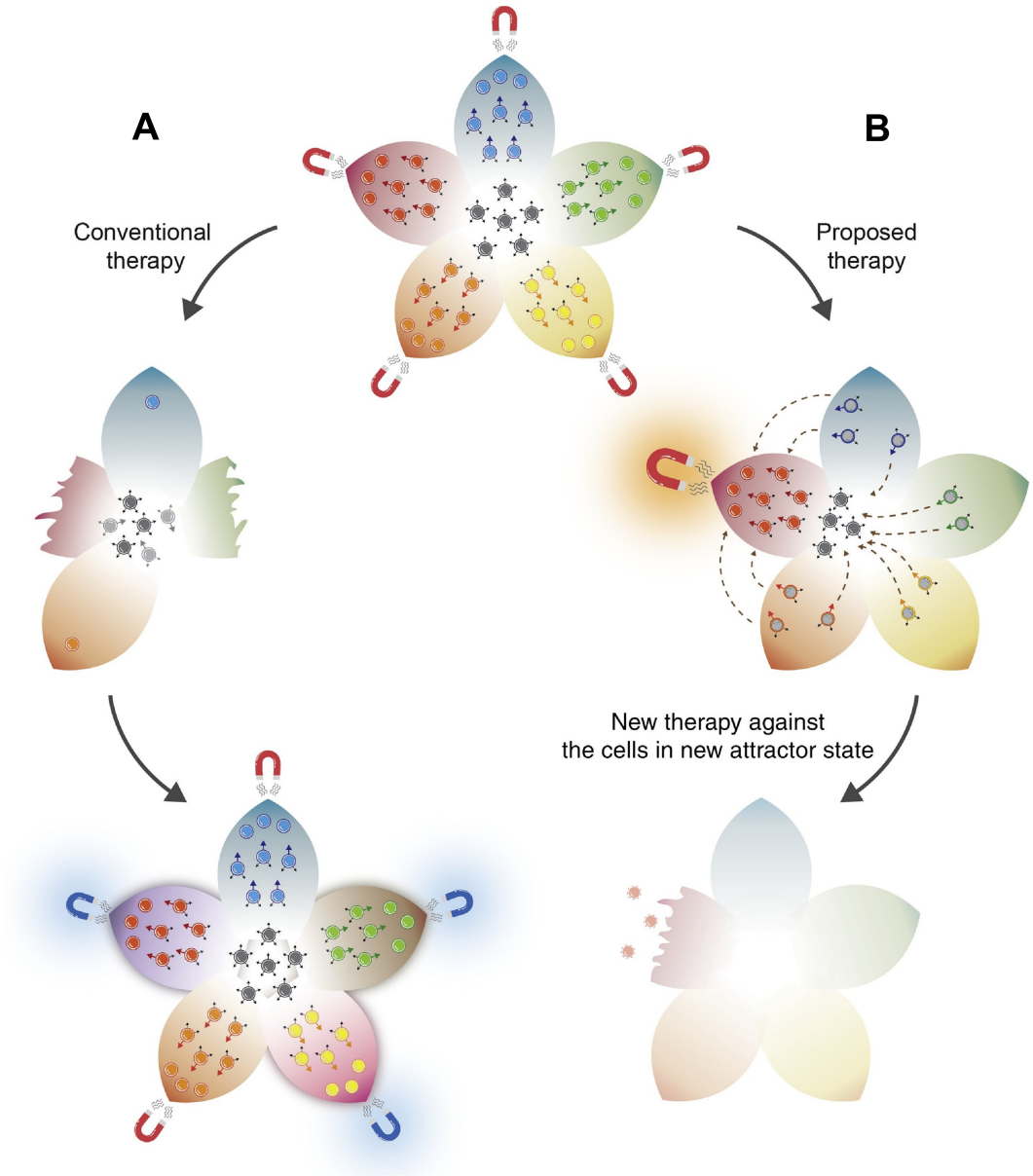

Figure 14. Conventional and proposed therapies for Glioblastoma.

Obtained from Prager et al., 2020. Conventional therapies approach often target individual components of the tumor landscape (petals) sparing the GSC population (at the center). This generates new attractors that drive the differentiation of the GSCs repopulating the tumor. An effective therapy would be to direct tumoral adaptation toward one state, applying an initial stimulus. The secondary would be targeting specifically the resulting cellular state.

Chapter 2: Tunneling nanotubes, a highway for intercellular communication

1. Introducing intercellular communication

As in a social community, cells are able to communicate and exchange messages between them. Since the origin of life, cells, either as unicellular or multicellular organisms exchange information, either from between individual unicellular organisms or within cells forming the same tissue or from tissue to tissue. Intercellular communication permits to coordinate cellular activity in order to execute sophisticated tasks that would not be possible otherwise.

Diverse long- and short-range mechanisms of communication are displayed by various cell types to coordinate their activities ensuring the proper functioning of that tissue, organ or organ system. Specific chemical and biological signals can be delivered as paracrine, endocrine, autocrine or direct signaling (Figure 15). The main difference between these categories of signaling is the distance that the signal travels through the organism to reach the target cell. **Autocrine** signaling implies the production of an extracellular mediator by a cell followed by the binding of that mediator to receptors on the same cell initiating the signal transduction. This type of signaling is important to re-enforce some self-autonomous mechanisms in development, to direct cell differentiation toward the correct identity, or in the immune response of macrophages, in which secreting IL-6 activates their own receptors triggering the release of additional cytokines, including IL-1 (King, 2007). In cancer, autocrine signaling can be exploited to self-induce proliferation by release of growth factors (Walsh et al., 1991). More common is **paracrine** signaling that also involves secreted factors targeting this time neighbouring cells. The secreted signal can be a chemical, like NO that regulates vasodilatation (Laurindo et al., 2018), but also extracellular vesicles (EVs), including exosomes, microvesicles and apoptotic bodies. EVs expose numerous signaling proteins and lipids on their surface act to stimulate target cells directly, alternatively EVs can also allow the transfer of cellular material as receptors (on the surface) or protein, lipids, mRNA and miRNA through membrane fusion (Ståhl et al., 2019). EVs-mediated communication take place in a variety of in various physiological mechanisms (from neurite growth to angiogenesis or immune modulation) as well as in

pathologies as in cancer and various inflammatory disorders (Ståhl et al., 2019). Synapses are also considered a form of paracrine signal specific of neuronal cells, as synaptic vesicle are released from the axon extremity in order to activate the depolarization of the post-synaptic cell. **Endocrine** signals travel instead along long distances, they are released by glands (pituitary, thyroid, hypothalamus, pancreas, etc.) into the bloodstream and target organs or tissues regulating their functions. Some examples are the Growth Hormone, peptide secreted by the hypothalamus and targeting multiple tissues to stimulate their growth, or cortisol, that have instead a lipidic nature and is produce from adrenal glands, it can regulate the cell metabolism and immune response. Due to the dilution to which they undergo during the transport, hormones are able to be effective even at low concentration, differently from autocrine and paracrine pathways where the local concentration of the ligand is often very high.

Cells can also interact and communicate by **direct cell-to-cell contact**. Gap-junctions (GJs) are one of the most frequent means of direct interaction. These junctions act as small pores through the cell membranes and allow passage of molecules from the cytoplasm of one cell to the one of the adjacent cell. GJs are channels constituted by two hemichannels, named connexons, each exposed on membrane of the two cells in contact. Connexons are composed by hexamers of connexin (Cx) subunits. Over 20 Cx exist in the human genome permitting various compositions of the GJs which correspond to distinct physiological processes and are often not interchangeable (Weber et al., 2004). GJs has a cut-off of 1 kDa (Weber et al., 2004), granting the transfer of inorganic salts, sugars, amino acids, nucleotides or vitamins but not large molecules such as proteins or nucleic acids. Interestingly, GJ are one of the principal mediators of tissue homeostasis as they allow a sort of intercellular network propagated by adjacent cells. This homeostasis is disrupted in the case of cancer, in fact a general decrease in GJs/Cxs expression is frequent in tumors and correlate with their progression and increased cell proliferation (Asencio-Barría et al., 2019). Another form of direct signaling is mediated by direct binding of complementary (ligand-receptor) proteins expressed on the membrane surface of two distinct cells. This interaction generates an intracellular signaling cascade in the receiving cells and the consequent activation of the cellular response. For example, the activation of Notch

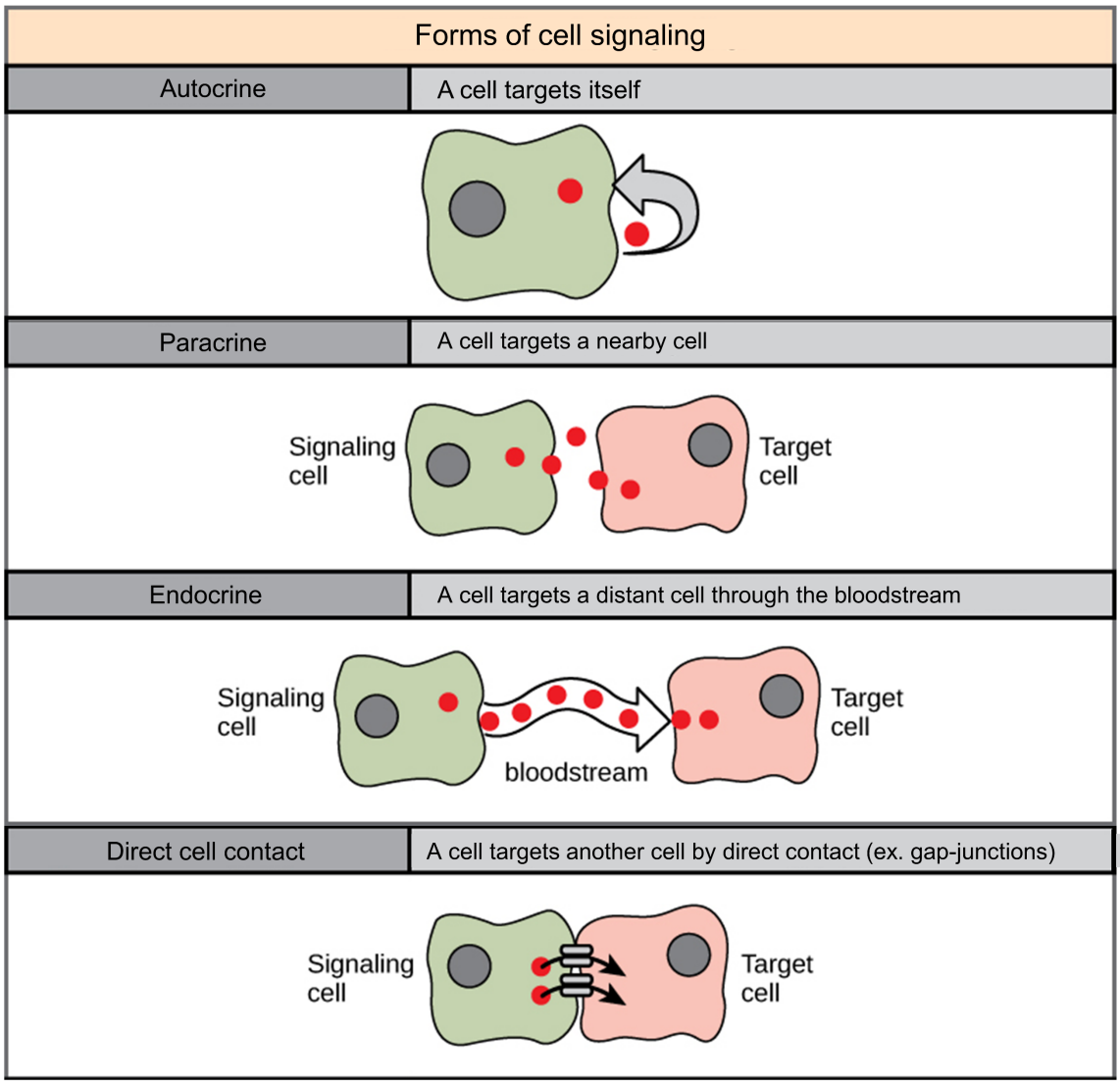

Figure 15. Forms of cell signaling

Adapted from "Signaling molecules and cellular receptor" by OpenStax College, Biology. There are different form of cell signaling: in the autocrine signaling the cell realising the signals targets itself, in the paracrine signaling it targets a nearby cell, in the endocrine signaling it targets a distant cells releasing the factor in the bloodstream and in the direct cell contact the interaction between the two cells is mediated by short or long range channel of communication (ex. Gap-junction).

receptors on behalf of one of its ligands (jagged or delta) plays a major role in the CNS development where it promotes NSC survival, self-renewal, and cell fate specification, neuronal or glial (Lathia et al., 2008). An additional example, is the contact between cadherins on opposite membranes that regulates the contact inhibition of cell proliferation (Klezovitch & Vasioukhin, 2015). Another, more recently discovered, mechanism for direct cell communication are Tunneling Nanotubes.

2. Tunneling Nanotubes

Tunneling Nanotubes, or TNTs, are physical bridges of communication providing cytoplasmic continuity between distant cells (Figure 16). TNTs are thin, actin-rich membrane tubes that, differently from other cellular protrusions, are open-ended at their extremities (Rustom et al., 2004; Sartori-Rupp et al., 2019). They allow the transfer of various-sized cellular cargoes (Figure 16), such as small molecules (e.g. calcium ions), macromolecules (nucleic acids, proteins etc.) and even organelles (vesicles, lysosomes, mitochondria, autophagosomes, etc.) (Abounit & Zurzolo, 2012). Multiple cells can be connected by TNTs, possibly leading to the formation of a functional cellular network (Ariazi et al., 2017).

2.1. TNTs, different from other cellular extensions

TNTs are unique compared to other cellular protrusions in the cytoplasmic continuity they provide between communicating cells (Rustom et al., 2004; Sartori-Rupp et al., 2019). Mammalian cells can form a variety of cellular extensions, of different morphology, size and function (Table 1). For example, **cilia**, **stereocilia** and **filopodia** act to sense the environment and modulate cellular behavior accordingly (Gallop, 2019; Hua & Ferland, 2018; Tilney et al., 1992). Particularly, cilia and stereocilia, also play a major role in cell polarity, creating a specialized domain to receive and transduce stimuli from the environment at one specific cell side. Also involved in polarity, but rather for leading cell migration, is the role of

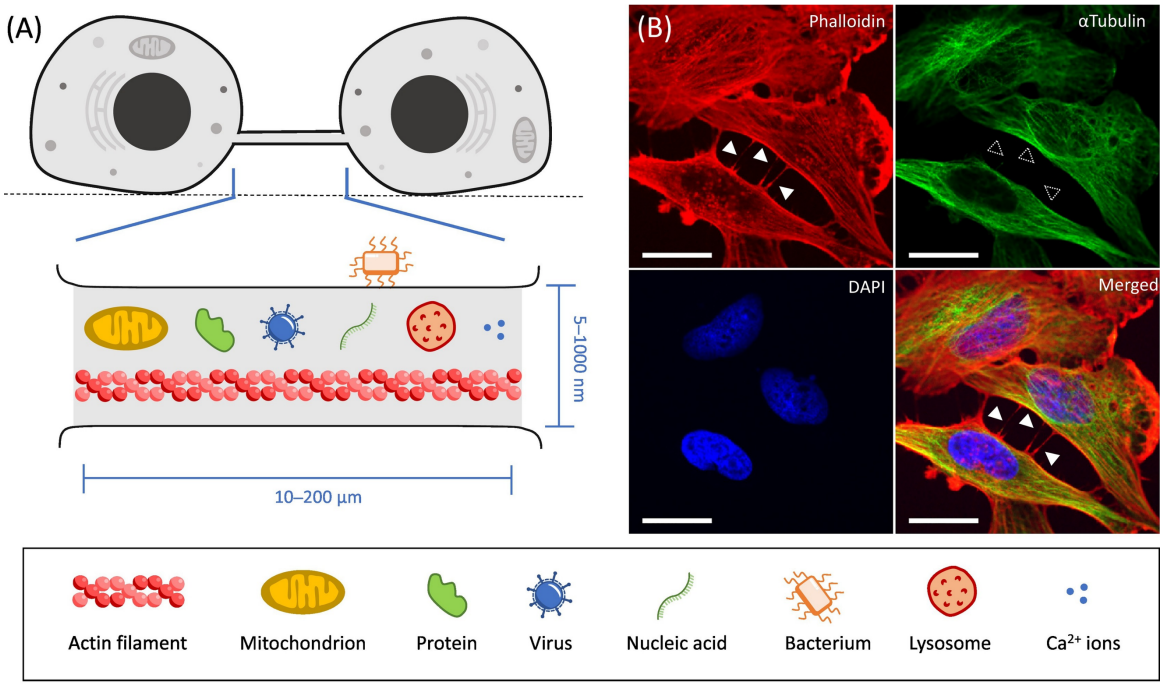

Figure 16. Tunneling nanotubes schematic

Obtained from Pinto et al. 2020. Tunneling Nanotubes (TNTs) in cell culture. (A) Schematic of two cells connected by a TNT in cell culture. The connection floats above the adhesion surface (dashed line). The lower part shows a magnification of the TNT and possible cargoes traveling along it. The range of TNT diameters and lengths is indicated. (B) Representative fluorescence images of TNTs between cells in culture. U-251 glioblastoma cells were plated at a density of 20 k cells/cm2 for 24 h, fixed with PFA 4%, and permeabilized in 0.2% Triton-X100. Actin filaments (in red), microtubules (in green), and nuclei (in blue) were stained with phalloidin-rhodamine (1/500 Invitrogen R415), anti-αTubulin (1/1000 Sigma-Aldrich T9026), and DAPI (Sigma-Aldrich D9542), respectively. White-filled arrowheads point to TNTs positive for actin staining. Dashed arrowheads indicate the absence of tubulin staining. Confocal images acquired with Spinning Disk Yokogawa CSU-X1. Scale bars 20 µm.

lamellipodia, **cellular ruffles** and **podosomes** (Innocenti, 2018; Schachtner et al., 2013; Veillat et al., 2015). Alternatively, podosomes and filopodia are adherent membrane extremities that can also anchor the cell body to the adhesion surface. In the case of cancer, podosomes or **invadopodia** act as dynamic, extracellular matrix-degrading membrane domains and facilitate cell invasion and metastasis through the action of metalloproteases (Castro-Castro et al., 2016; Ferrari et al., 2019). While in development, specialized filopodia, named **cytonemes**, specifically deliver ligands/morphogens on the membrane of the target cells, activating the intracellular transduction of the signal (González-Méndez et al., 2019; Korenkova et al., 2020; Kornberg & Roy, 2014). **Axons** and **neurites** are also specific cell membrane protrusions typical of the CNS and responsible for neurotransmitter release/reception and propagation of the action potential (Flynn, 2013). Similar to these last in their function are **tumor microtubes** (TMs), although they are thought to propagate the ion flux through Cx43-positive GJs (Osswald et al., 2015). TMs can also appear as finger-like extensions leading cell invasion and the tumoral repopulation of a surgically resected areas (Weil et al., 2017). Finally, a membrane thread between daughter cells can remain as reminiscence of the cell division, through which eventually some material can be exchange; these structures have been defined **mitotic bridges** (Fykerud et al., 2016).

Of all these types of cellular extensions, only TNTs, mitotic bridges, and potentially TMs (as it remains unclear the presence of GJs along their length (Osswald et al., 2016)), display cytoplasmic continuity between two cells. TNTs are, although, unique in their being open-ended and provide a direct route for the intracellular exchange of cellular content by their lumen (Rustom et al., 2004; Sartori-Rupp et al., 2019).

2.2. TNTs identification and structure

Rustom and colleagues were the first, in 2004, to identify and define TNTs in pheochromocytoma of the rat adrenal medulla PC12 cells (Rustom et al., 2004). In this study, electron-microscopy images show thin membranous connections between cells with open-extremities that allow the selective transfer of membrane vesicles and organelles. Subsequently, several publications reported the presence of “TNT-like

Table 1. Types of cellular extensions

Adapted from Pinto et al. 2020.

NAME	DESCRIPTION	ACTIN / MICROTUBULES CONTENT	MEMBRANE FUSION WITH A TARGET CELL	FUNCTION
Cilia	Large protuberance emerging from the cell body	Actin and microtubules	No	Environment sensing, coordination of signaling pathways
Stereocilia	Thin specialized cell protrusion on the apical surface	Actin	No	Cellular polarity, transduction of mechanic stimuli
Lamellipodia and ruffles	Dynamic veil-shaped cell protrusions	Actin	No	Leading edge in cell migration
Filopodia	Finger-like dynamic, thin membrane protrusions	Actin	No	Cell adhesion, environment sensing
Cytonemes/specialized filopodia	Finger-like dynamic, thin membrane protrusions extending to a target cell	Actin	No	Morphogens-delivery by direct contact to the target cells
Mitotic bridges	Thin bridges between daughter cells after mitosis	Actin	Yes	Reminescence of cellular division, can share material
Neurites	Large extensions from the cell body of neurons	Actin and microtubules	No	Neurotransmitter release/reception and propagation of the action potential
Tumor microtubes	Thick membrane extensions containing GAP-junctions, either connecting cells either finger-like	Actin and microtubules	Yes/No	Transmission of intercellular ion fluxes, cell invasion, formation of neuron-glioma synapses
Tunneling nanotubes	Thin membrane connections, open-ended	Actin, sometimes microtubules	Yes	Exchange of cellular cargoes between cells
Invadopodia	Finger-like membrane protrusions	Actin	No	Matrix degradation
Podosomes	Dynamic membrane-bound microdomain	Actin	No	Adhesion, mechanosensing and matrix degradation

structures", rather based on their nanotubular morphology, in many other cell types in *in vitro* cultures, including astrocytes (D. Zhu et al., 2005), immune cells (Onfelt et al., 2006), human embryonic kidney HEK cells (Sherer et al., 2007), Hela (Hase et al., 2009) as well as in several tumor cancer cell lines (further described). TNTs can be identified in cell culture by fluorescent labelling of the plasma membrane and cytoskeleton components and observed by the use of light microscopy, (Figure 16B), while their identification in a more complex context such as animal models or tumor resections is still very challenging. In fact, no specific marker for these structures has been identified yet, and the optical resolution of classical microscopy doesn't allow for the morphological characterization of these connections in complex environment, as tissues and *in vivo* models (Korenkova et al., 2020; Sartori-Rupp et al., 2019). Also, specific fixation protocols are needed to preserve their fragile and delicate nature in cell culture (Abounit et al., 2015), and their observation needs to be supported by functional assays to fulfill the definition of TNTs as channels for cell material passage.

TNTs exhibit high variability in their morphology, in terms of length, thickness and cytoskeleton content, specifically regarding the presence/absence of microtubules (Abounit et al., 2015). Some cell lines can even present both types of connections: those containing only actin and those with actin and microtubules (Connor et al., 2015; Sáenz-de-Santa-María et al., 2017). Nevertheless, their functionality seems to be rather disrupted by the inhibition of actin polymerization (with latrunculin, cytochalasin) rather than the one of tubulin, as tested by Nocodazole treatment (J. Wang et al., 2018) (see Table 2). TNTs can range from tens to several hundreds of microns in length (Ady et al., 2014; Connor et al., 2015; Sáenz-de-Santa-María et al., 2017), whereas, the diameter of the connections is inferior to 1 µm, hence the term "nanotubes". In some particular cases, long (>500 µm) and thick (>1 µm) extensions were observed (Antanavičiūtė et al., 2014; Latario et al., 2020), however these structures are fitting best with the definition of tumor microtubes rather than TNTs (Table 1) (Osswald et al., 2016). At present, we do not know whether TNTs display different morphologies *in vitro* or *in vivo* or whether nanoscale connections are detectable in the complexity of the tissue. The thickness of TNTs also correlates with their cytoskeleton content, as microtubule-containing connections were displaying larger diameters (Onfelt et al., 2006).

Few studies have addressed the ultrastructure of TNTs in cancer models using electron microscopy (Kolba et al., 2019a; J. Lu et al., 2017; Rustom et al., 2004). A deeper structural analysis of TNTs, using a combination of cryo-fluorescence microscopy with cryo-electron microscopy, was recently conducted in our laboratory. Two types of neuronal cell lines were used, such as Catecholaminergic-a-differentiated (CAD) cell line, established from a brain tumor in a transgenic mouse, and SH-SY5Y cells, isolated from a neuroblastoma patient (Sartori-Rupp et al., 2019). By using experimental conditions set up to better preserve TNT structure, this study has shown that TNTs can be composed of multiple individual tubes (named iTNTs) held together by N-cadherin-positive structures and often open-ended at their tips (Figure 17). Nonetheless, whether iTNTs exist in different cell types and/or *in vivo* remains an open question.

The limitations, the heterogeneity and, sometimes, the poor molecular and structural characterization of TNT-like connections represent a major problem for their investigation. To lend the confusion in the field was also a variable nomenclature across the publications which named the intercellular connections observed differently as nanoscale conduit (Connor et al., 2015), tunneling nanotubes (Lou et al., 2012, p. 201), intercellular bridges (Korenkova et al., 2020) or membranous tunneling tubes (Antanavičiūtė et al., 2014). This raised confusion and skepticism in the field (Gurke et al., 2008), and calls out for both more rigorous definition and more accurate technical approaches to study them. Given the current knowledge about TNT and other intercellular structures, TNTs could be defined the connections that fulfill the following characteristics: i) continuous membrane connections with the plasma membrane of the connected cells, ii) non-adherent to substratum, iii) containing actin, iv) proven cargo transport, and v) open-ended (see Table 1).

2.3. TNT formation

The full molecular mechanism driving TNT formation has not been fully elucidated yet, but according to time-lapse imaging studies two possible models have been drawn: 1) **actin-driven outgrowth** and 2) **cell dislodgement**.

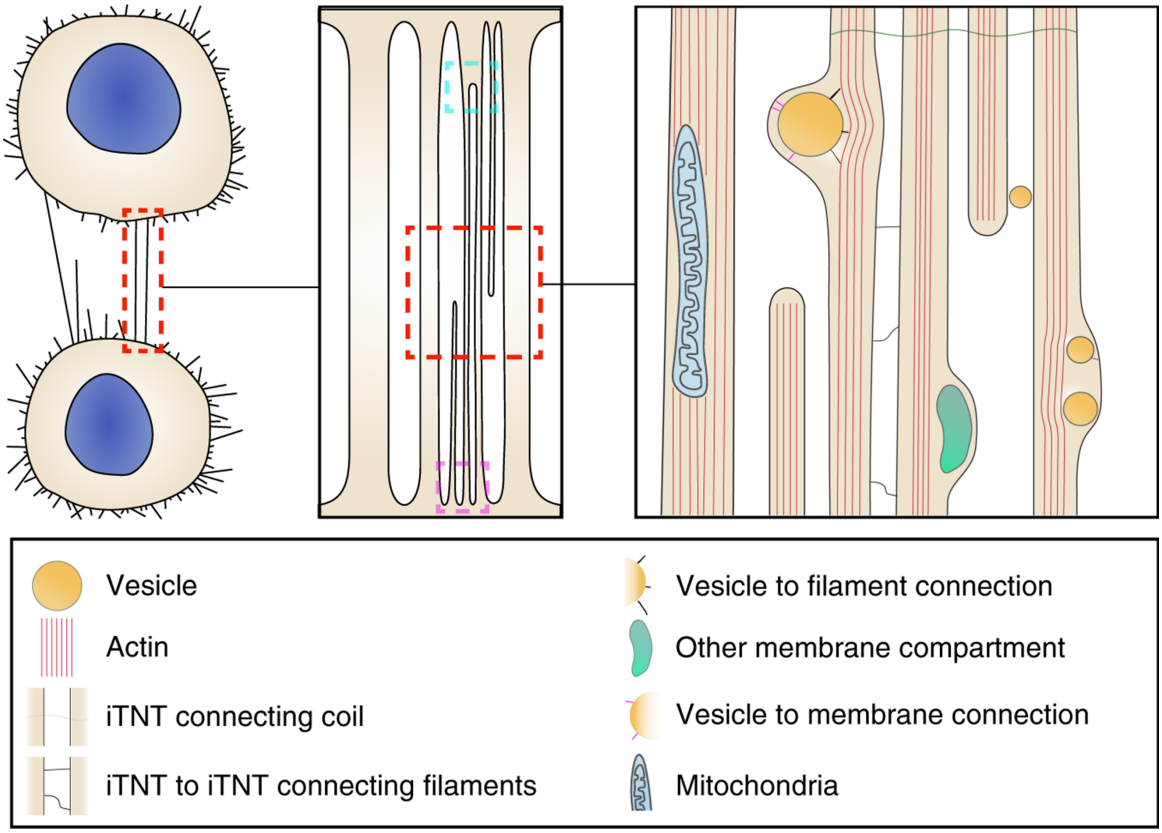

Figure 17. Ultrastructure of TNTs.

Obtained from Sartori, Cordero, Pepe at al., 2019. TNTs can either appear as a single thick connection or a bundle of thin individual TNTs, named iTNTs. iTNTs can contain vesicles and mitochondria. iTNTs appear to be held together by thin filaments. Contact site between the cell body and the connections are indicated by cyan and magenta dashed squares.

According to the first model, an actin-rich filopodia-like protrusion is originated from one cell and directed toward another target cell (Figure 18). The forming extension might have a precise orientation that could be directed by a chemical gradient as for the case of cytonemes (Kornberg & Roy, 2014). Once reached the target cells, membrane fusion occurs, either spontaneously or by the help of fusion proteins that lead to the establishment of an open connection (Abounit & Zurzolo, 2012; S. Zhu et al., 2018). The fusion phenomenon is highly dynamic and could be transient, as the half-life of TNT is relatively short, between 15 minutes to one hour (Gerdes et al., 2013; Rustom et al., 2004; Vargas, Loria, et al., 2019). The actin-driven mechanism has been proven in CAD and PC12 cells (Abounit & Zurzolo, 2012; Rustom et al., 2004). On the other hand, TNTs formation have been observed in consequence of the second type of mechanisms, defined as cell dislodgment, in immune, hematopoietic and leukemic cells (Davis & Sowinski, 2008; Gerdes et al., 2013; Kolba et al., 2019a; Reichert et al., 2016, p. 133). According to this second model, two cells come in contact so that the membrane fusion can occur and the consequent migration in opposite directions leave an open-ended nanotube that could entirely belong to one of the two cells or both (Figure 17). In the particular case of immune cells, this formation could go through an intermediate step where the two cells connect by an immune synapse, mediated by connexins oligomers (Abounit & Zurzolo, 2012). These two models for TNT formation described here are not mutually exclusive as they could both occur in the same type of cells.

The molecular machinery at the basis of TNT formation remains unclear, although several actin regulators and vesicle trafficking components seem to provide the material required by the elongation process. M-Sec, aka TNFaip2, is one of the major positive regulator of TNT in various cell types (Hanna et al., 2019; Hase et al., 2009; Ohno et al., 2010). It can recruit the exocyst complex and activate downstream proteins as small GTPase Ral-A and the cell division control protein 42 homolog (CDC42) to contribute to the remodelling of the actin cytoskeleton or to the delivery of membrane at the site of TNT formation. Rab

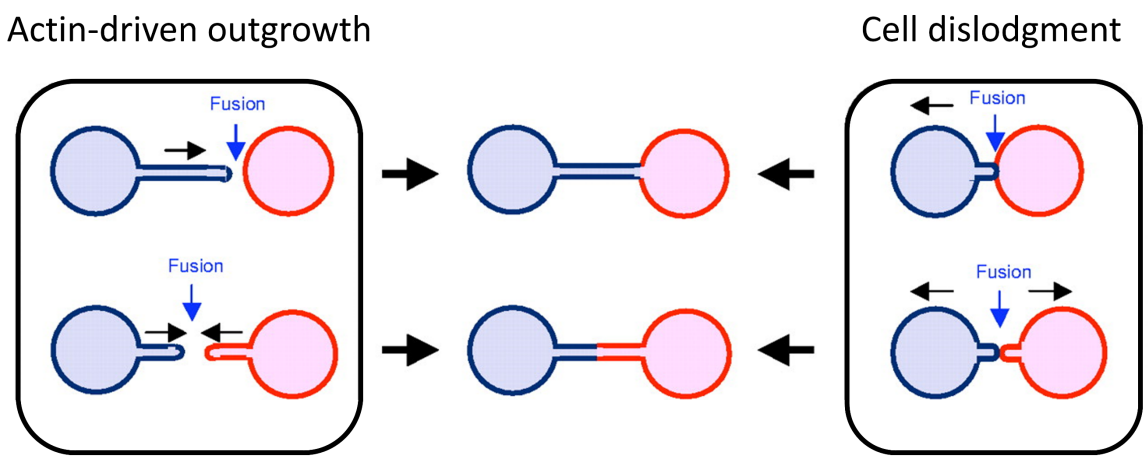

Figure 18. The two models of TNT formation

Adapted from Abounit et al., 2012. On the left, the actin-driven outgrowth: one or both cells extend a protrusion that will eventually fuse with the neighboring cell, forming an open connection (in the center). On the right, the cell dislodgment model starts with an event of membrane fusion between two adjacent cells that subsequently move apart leaving an open connection (in the center). The TNTs could contain membrane element derivate from one or both cells.

GTPases are considered to be master regulators of intracellular membrane trafficking and, within these, Rab8a and Rab11a positively regulate TNT formation and transfer function through downstream v-SNARE and Vesicle-associated membrane protein 3 (VAMP3) that provide membranous component for their outgrowth (S. Zhu et al., 2018). On the other hand, CDC42, protein part of Ras superfamily, controls actin polymerization through direct binding to the neural Wiskott–Aldrich syndrome protein (N-WASP), which subsequently activates Arp2/3, a protein complex that promotes actin branching. Interestingly, filopodia-promoting CDC42/IRSp53/VASP network negatively regulates TNT formation in CAD cells while elevation of Eps8, an actin regulatory protein that inhibit the extension of filopodia in neurons, increases TNT formation, suggesting that these two actin modifiers might have opposite actions on filopodia and TNT formation (Delage et al., 2016).

2.4. Functional study of TNTs

The unique feature of TNTs compared to other cellular extensions previously mentioned, is their ability to transfer cellular material. Therefore, it is insufficient to provide exclusively qualitative evidence of cargoes inside of TNT-like structures without proving that actual transfer had occurred and excluding cell division as the possible mechanism to share material. This latter possibility can be excluded performing a co-culture assays between differently labelled cell populations. Membrane vesicles or organelles, such as mitochondria or lysosomes, can be labelled in a population of cells defined as donors, subsequently culture together with an acceptor population (differently labelled) to further detect and quantify the cargoes transferred from donors to the acceptors of the labelled cargo. The detection of the transfer in the acceptor cells can be performed by fluorescence microscopy (in fixed or live condition) or flow cytometry (Abounit et al., 2015). The co-culture has to be performed allowing direct physical contact between the two populations and at an appropriate cell density that favors the formation and detection of TNTs. In order to evaluate secretion as a possible mechanism of transfer, the two populations can be separated by a filter which allows the transfer of secreted material, or they can be grown in different dishes and the acceptor population challenged with the conditioned medium from donor cells (Abounit et al., 2015). The weakness

of this approach is that it only allows the direct transfer (cell contact-mediated) of the labelled cargo to be determined. Other materials that could be transported through the same connections, including the ones that could be shared in the opposite direction, and remain undetected. To overcome this limit, other approaches such as mass spectrometry (Kolba et al., 2019a) and transcriptomic analysis (Connor et al., 2015) have been recently applied to detect alterations at the proteome and transcriptome levels. Few approaches have studied the dynamics and transfer ability of these structures *in vivo*. Using multiphoton microscopy, thick connections between tumor cells, such as tumor microtubes, were detected in mouse xenografts (Osswald et al., 2015), but the resolution was not sufficient to detect thinner structures (Table 3). Still *in vivo*, the transfer between human and murine cells can be monitored and quantified by amplification of species-specific DNA sequences (Connor et al., 2015; Marlein et al., 2017, 2019). Although powerful and of great interest, these approaches have made possible to monitor the transfer without specifically identifying its mechanism, in particular without excluding the secretion mechanism. The fields need to pursues the study of these fragile structures in cellular models as much as possible representative of the tumoral tissue (e.g, patient-derived cells) and additional efforts are needed to overcome the technical limitations of the *in vivo* study.

3. Roles of TNTs

TNTs appeared to be involved in stress-related conditions or in development, rather than in homeostatic condition. Oxidative stress, viral, bacterial or prion-like pathogens presence and even tumorigenic environment seem to favor and exploit this route for cell-to-cell communication, as it will be deepened in a separated chapter.

3.1. In development

Intercellular communication is a fundamental property to orchestrate the fine coordination required during embryonic development. Intercellular connections have

been identified in various developing organisms, although it turns out to be difficult to definitely categorize the observed protrusion. In 1995 and 2004, the first observations of long cell connections, in sea urchin gastrula and chick embryos respectively, were rather suggesting a signaling function of these structures, more typical of cytonemes (Miller et al., 1995; Teddy & Kulesa, 2004). Further evidences, in chick embryo, suggested that also an active transfer mechanism was present (McKinney et al., 2011). Similar cellular extensions were also identified in the early phases of zebrafish gastrulation (Caneparo et al., 2011) and in Xenopus Laevis early blastulas (Danilchik et al., 2013). In developing mouse embryo, the use of whole embryo culture systems in combination with live imaging of a genetically-encoded reporter allowed to visualize neural tube formation where membrane bridges containing inclusions likely of vesicle nature were identified (Pyrgaki et al., 2010). Several of these observations highlight that the structures observed could hold a transfer ability typical of TNTs rather than other cellular protrusions, although further studies applying transfer-detecting techniques need to be perform.

3.2. Pathogens hijacks TNTs to favour their dissemination

TNTs can be used as a route for the dissemination of pathogens as various types of viruses and some bacteria. The first TNT-transmissible virus identified was the human immunodeficiency virus (HIV), of the family of retroviruses (Sherer et al., 2007; Sowinski et al., 2008), the transfer was followed by infection in the receiving cell. This route of HIV dissemination was validated in numerous studies and in different cells if the immune system as macrophages, B- and T-cells (Eugenin et al., 2009; Hashimoto et al., 2016, 2016; Kolba et al., 2019a; Souriant et al., 2019; Sowinski et al., 2008; Xu et al., 2009). The virus was either transferred in endocytic vesicles in the lumen of the connection, or surfing on the outer membrane surface (Sherer et al., 2007). Interestingly, the presence of the HIV could also induce TNT formation, favoring its transmission, in T-cell via Nef-dependent pathway (Hashimoto et al., 2016). Another retrovirus, Human T-cell leukemia virus type 1 (HTLV1) can also be transferred by TNTs and trigger their formation via its p8 protein (Omsland et al., 2018). Alphaherpesvirus induces TNT growth by the activity of Serine/threonine-protein kinase (US3) protein, although electron microscopy analysis

revealed that US3-induced TNTs were closed-ended and viral spread was occurring through the exit of enveloped viral particles at the contact site, at the extremity of the extension (Jansens et al., 2017). Other viruses have been described to be transmitted by TNTs, as Epstein-Barr virus (EBV), murine 243 gamma-herpesvirus-68 (MHV-68), influenza, etc. (Jansens et al., 2020). Finally, also bacteria can spread through TNTs, as demonstrated by Onfelt et al. (2006) which showed that *Mycobacterium bovis* can surf on thin TNT-like connections between macrophages before being internalized by receptor-mediated endocytosis.

3.3. Prion-like aggregates spreading

TNTs appear to play a relevant role in the spreading of prion-like aggregates causing neurodegenerative diseases as Parkinson's, Alzheimer's and Creutzfeldt-Jakob's diseases. According to Braak's staging of neurodegenerative diseases progression (Braak et al., 2006), the pathology evolves with a specific and predictable pattern, moving between adjacent brain areas triggering the fibrillation of endogenous protein (as αSynuclein, β-amyloid, Tau protein, etc.) in a prion-like manner. This propagation along adjacent areas is compatible with a direct, cell-to-cell, transmission of the protein aggregates. Various amyloid aggregates originated from Prion Protein (PrP) scrapie, αSynuclein, β-amyloid, Disrupted In Schizophrenia 1 (DISC1) protein, Tau or mutant Huntingtin have been shown to exploit and hijack TNTs, increasing their number, as route for their spreading and consequent seeding (Abounit et al., 2016; Abounit et al., 2016; Costanzo et al., 2013; Damodaran et al., 2020; Gousset et al., 2009; Gousset & Zurzolo, 2009; Loria et al., 2017; Vargas, Grudina, et al., 2019; Victoria et al., 2016; Victoria & Zurzolo, 2017; Y. Wang et al., 2011; S. Zhu et al., 2017). It has been proposed that prion-like proteins, when aggregated, are capable of inducing TNT formation via a common mechanism, that is possibly linked to oxidative stress pathways, as H_2O_2 was shown to induce TNT formation in neuronal cells and primary neurons (D. Zhu et al., 2005) and oxidative stress is associated with the presence of aggregated proteins in neurodegeneration (X. Chen et al., 2012). Increased number of TNTs would in turn favor the transfer of prion-like aggregate from one cell to another and contribute to the spreading of the pathogenic aggregates. Protein aggregates

can travel along TNTs alone or embedded in endocytic or lysosomal vesicles and seed the aggregation of the soluble protein of the recipient cell.

4. TNTs in cancer

4.1. Evidences of TNTs in cancer

After the first observation of TNTs in PC12 cells, derived from a rare rat tumor of adrenal gland tissue (Rustom et al., 2004). TNTs have been identified in a wide variety of cancer cell lines (listed on Table 2). Cancer cells can share material in between themselves as, as well, form heterotypic connections with cells of the tumor microenvironment, including mesenchymal (Pasquier et al., 2013), endothelial (Connor et al., 2015) and immune cells (Hanna et al., 2019). This cross-talk with the tumor microenvironment plays a significant role in sustaining cancer progression, providing nutrients or buffering metabolic stress (Yuan et al., 2016), and interaction with immune cells can contribute to overcoming immunosurveillance (P. Sharma et al., 2017). Beyond cell lines, TNT-like structures were also observed in primary cells directly obtained from patients, for example in squamous cell carcinoma (Antanavičiūtė et al., 2014; Sáenz-de-Santa-María et al., 2017), mesothelioma (Ady et al., 2014; Lou et al., 2012) and different forms of leukemia (Marlein et al., 2017, 2019; J. Wang et al., 2018). Additionally, TNT-like connections were identified in resections of solid tumors, the first time occurred thanks to the laboratory of Emil Lou in 2012, which described mitochondria-containing connections in tissue sections of a mesothelioma resected from a patient (Lou et al., 2012). These observations were followed by others, showing various intercellular connections in squamous cells carcinoma (Antanavičiūtė et al., 2014; Sáenz-de-Santa-María et al., 2017), in ovarian (Thayanithy et al., 2014) and pancreatic cancer (Desir et al., 2018) (see Table 3). Little is known about the structural and functional features of these connections *in vivo*. In some cases, however, the presence of cellular cargoes inside them supports the hypothesis that these structures may be open-ended as canonical TNTs and may allow the transfer of cellular content.

Table 2. Tumor cell models exploiting TNTs *in vitro*.

Adapted from Pinto et al., 2020.

TUMOR MODEL	CARGO	TNT FUNCTION	TNT REGULATORS[a]	YEAR
Rat pheochromocytoma cell lines	Lysosomes, soluble and membrane marker	n.d.	n.d.	2004
HeLa (cervical cancer)	Calcium	n.d.	M-Sec	2009
Mesothelioma cell lines and primary human mesothelioma cells	Golgi vesicles, Mitochondria, fluorescent proteins	n.d.	Low-serum (+), hyperglycemic (+), acidic medium (+), EMT inducing cytokines (+), Metformin (-), Everolimus (-), Latrunculin A (-)	2012
Ovarian and breast cancer cell lines	Cytoplasmic content, Mitochondria	Mitochondria transfer from stromal cells promotes chemoresistance	n.d.	2013
Osteosarcoma and ovarian cancer cell lines	miRNA	Spreading of genetic and oncogenic material between tumoral-tumoral and tumoral-stromal cells	Low-serum and hyperglycemic medium (+)	2014
Mesothelioma cell lines	n.d.	TNT correlates with more aggressive phenotype and the expression genes related to invasion and metastasis	Low-serum and hyperglycemic medium (+), Migrastatin (-)	2014
Head and neck squamous cell carcinoma primary cells	Mitochondria and nucleic acids	Electrical coupling	n.d.	2014
Primary rat astrocytes and glioma cell line	Mitochondria	Support in glioma cell proliferation	H_2O_2 (+), Latrunculin A (-)	2015
Metastatic breast cancer cell lines	miRNA	Transfer of miRNA and alter the phenotype of the receiving endothelial cells. TNT correlates with more aggressive phenotype	Docetaxel (-), LatrunculinA (-), Cytochalasin D (-)	2015
Pancreatic adenocarcinoma cell lines	Electron-dense particles	n.d.	Radiofrequency treatment (+)	2015
Rat pheochromocytoma cell lines	Mitochondria	Rescued of UV-treated apoptotic cells	Cytochalasin B (-)	2015

Ovarian cancer cell lines (different chemoresistances)	Mitochondria	Adaptation mechanism to hypoxia in chemoresistant cells	Hypoxia (+)	2016
Head and neck squamous cell carcinoma cell lines	Lysosomes, mitochondria, autophagosomes	n.d.	MMP2, FAK	2017
Bladder cancer cell lines	Mitochondria	Mitochondria transfer promotes invasiveness	n.d.	2017
Acute myeloid leukemia (AML) primary cells	Mitochondria	Mitochondria transfer from the bone marrow supports cancer cell metabolism and promotes stress-adaptative response	NOX2	2017
Pancreatic adenocarcinoma and ovarian cancer cell lines	Doxorubicin	Redistribution of the drug	Doxorubicin (+)	2018
Acute lymphoblastic leukemia cell lines and human primary T-leukemic cells	Mitochondria	Mitochondria transfer promotion of chemoresistance	Cytochalasin D (-), MTX (-)	2018
Colon cancer cell lines	n.d.	Transfer of oncogenic protein (mutated KRAS) and activation of Erk pathway in acceptor cells	KRAS	2019
Breast cancer cell lines	Membrane and/or vesicles	Transfer between macrophages and tumor cells inducing invasiveness	M-Sec	2019
Prostate cancer cell lines	Lysosomes, mitochondria, stress-induced chaperones	Adaptation mechanism therapeutic stress	Chemotherapy by androgen receptor blockade (+), Low-serum, hyperglycemic, acidic medium (+), hypoxia (+), Cytochalasin D (-)	2019
Chronic myeloid leukemia cell lines	Protein-containing vesicles	Protein transfer from stromal cells provides protection to leukemic cells	n.d.	2019
Patient bone marrow cells and multiple myeloma-derived cell lines	Mitochondria	Mitochondria transfer from the bone marrow supports cancer cell metabolism and promotes stress-adaptative response	CD38, Chemotherapy by Bortezomid (+), Cytochalasin B (-)	2019
Bladder cancer cell lines	miRNA	Induction of invasive and proliferative phenotype	n.d.	2019
Glioblastoma cancer cell line	Functionalized liposomes	Delivery of nanoparticles	n.d.	2019

[a](+), induced; (-), inhibited; “n.d.” stands for “not described”

4.2. Tumoral context favors TNT connectivity

Since their discovery, TNTs have been often described as a mechanism of adaptive response to cellular stress. Cancer presents several environmental conditions have been shown to stimulate their formation. For instance, ROS, intensively produced by cancer cells (Sosa et al., 2013), stimulated TNT formation in different contexts, including cancer (Marlein et al., 2019; Victoria & Zurzolo, 2017; Y. Wang et al., 2011; Zhang & Zhang, 2015; D. Zhu et al., 2005) (Table 1). Some treatments, as chemo and radiotherapy are known to increase ROS production in the tumoral context (Matejka & Reindl, 2019). Also hypoxia, typical microenvironmental feature of several cancer, in their denser regions, has been observed to stimulate TNT-mediated communication in ovarian (Desir et al., 2016) and prostate cancers (Kretschmer et al., 2019). Other conditions mimicking the tumor microenvironment *in vitro* can also stimulate TNT formation, such as acidic pH, hyperglycemia, serum deprivation (Kretschmer et al., 2019; Lou et al., 2012) and exposure to TNF-α (Tumor necrosis factor) often produced in cancer-related inflammation (Ranzinger et al., 2011). Finally, different signaling pathways, often dysregulated in cancer, have been shown to be involved in TNT formation, as PI3K/Akt/mTor (Desir et al., 2016; Kretschmer et al., 2019; J. Lu et al., 2017; Y. Wang et al., 2011), K-RAS (Desir et al., 2019) and p53 (Y. Wang et al., 2011; Zhang & Zhang, 2015). These signaling cascades could activate downstream proteins, such as M-Sec in the case of immune cells (Hase et al., 2009), which are involved in actin remodeling and polymerization and have been shown to induce TNT formation (Ohno et al., 2010). Altogether, these findings suggest that the tumor context, globally experienced as a stress by cells, provides the conditions that favor TNT formation and communication.

Table 3. Evidence of TNT-like communication in tissue in cancer

Adapted from Pinto et al., 2020.

CANCER	MODEL	LABELLING	YEAR
Malignant pleural mesothelioma and lung adenocarcinoma	Patient tissue	Mitochondria	2012
Ovarian cancer	Patient tissue	Mitochondria	2014
Osteosarcoma	Murine orthotopic model of osteosarcoma	Mitochondria	2014
Head and neck squamous cell carcinoma	Patient tissue	F-actin, mitochondria	2014
Glioma	Mouse tumor xenograft from primary stem cells	Cytosolic GFP expression	2015
Head and neck squamous cell carcinoma	Patient tissue	Actin, tubulin	2017
Head and neck squamous cell carcinoma	Mouse tumor xenograft from cell line	Actin, tubulin	2017
Acute myeloid leukemia	Mouse tumor xenograft from human leukemic cells	Mitochondria	2017
Glioma	Mouse tumor xenograft from primary stem cells	Cytosolic GFP expression	2017
Pancreatic adenocarcinoma	Patient tissue	Mitochondria	2018
Developing human telencephalon and human GBM	Patient tissue	Collagen IV	2018
Multiple myeloma	Mouse tumor xenograft from cell line	Mitochondria	2019

4.3. Roles of TNT in cancer progression

Cancer cells can interconnect among them and this ability could be possible correlate with their degree of aggressiveness. In fact, in both ovarian and breast cancers, highly malignant and metastatic cells are more prone to interconnect in tumor networks than their less aggressive counterparts (Ady et al., 2014; Connor et al., 2015). The mechanism by which TNTs might be beneficial for cancer progression are several and will be deepened int the following paragraphs, although a global vision of their role has not been fully elucidated yet. In fact, different strategies could be displayed in different tumoral forms and eventually a unique or multiple mechanism may be determined. As we will see TNTs can drive the acquisition of various pro-tumoral features in the receiving cells through the transfer of different cellular materials. TNTs can be exploited as route to get rid of dangerous material (Figure 19A, C) or to deliver cellular material such as miRNA, mitochondria or other sets of proteins might drive phenotypic modifications of the recipient cells (Figure 19A, B).

Of the possible cargoes transferable by TNT, mitochondria appear to be one of the most frequent and has been shown to induce pro-tumoral changes in the receiving cells (Antanavičiūtė et al., 2014; Hekmatshoar et al., 2018; Pasquier et al., 2013; Sáenz-de-Santa-María et al., 2017). For example, transfer of mitochondria from healthy cells was recovering UV-damages PC12 from apoptosis (X. Wang & Gerdes, 2015) or it can restore tumorigenic potential in cells devoid of mitochondrial DNA (Dong et al., 2017; Tan et al., 2015). Nevertheless, TNTs are not the unique mechanism that allow mitochondria transfer as astrocytes were found to release mitochondria subsequently taken up by neuronal neighboring cells (Hayakawa et al., 2016).

4.3.1. TNT-mediated communication promotes invasiveness

TNT-dependent transfer appears to stimulate invasiveness in various tumors. In bladder cancer, different cancer cell lines in co-culture could exchange functional mitochondria with each other stimulating invasiveness and migratory capacity in the acceptor cells, as assessed by *in vitro* assays (J. Lu et al., 2017). Interestingly, cells receiving mitochondria

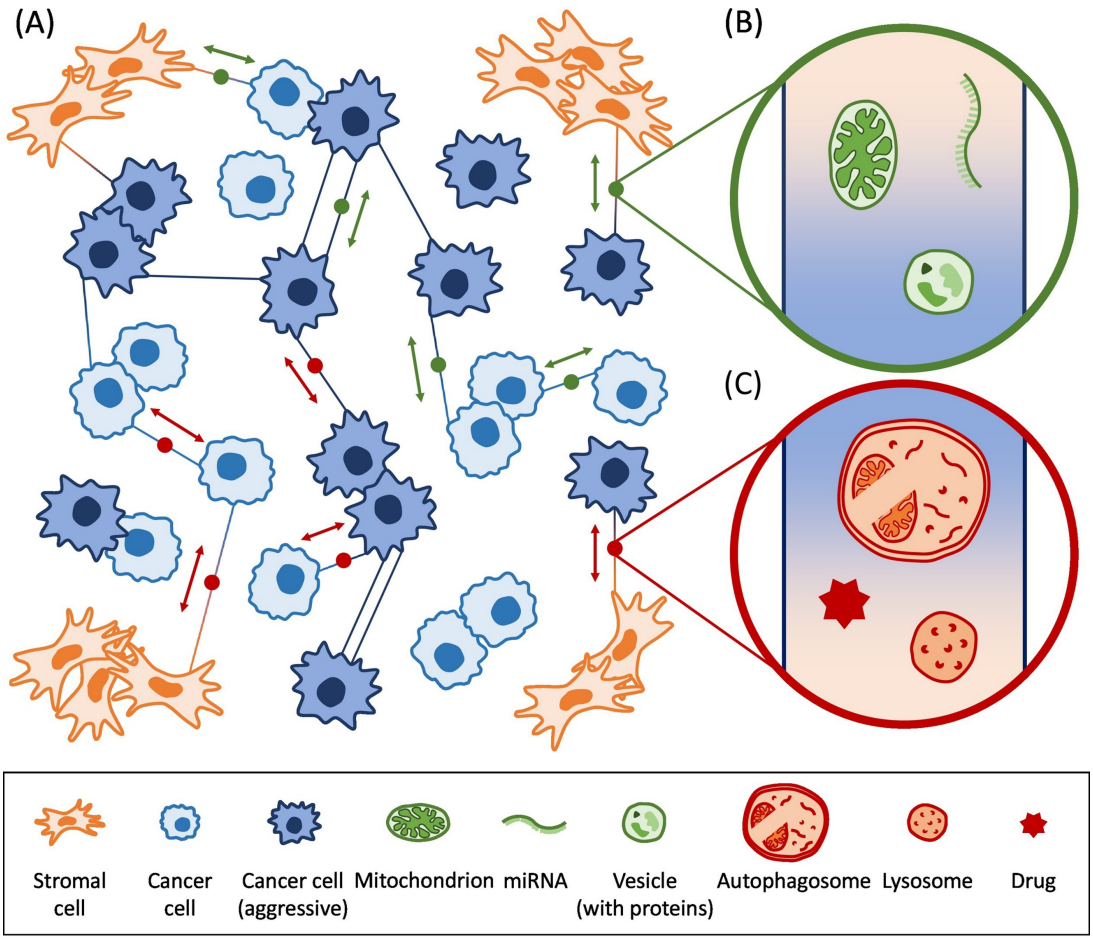

Figure 19. Model of TNT-based communication in cancer

Obtained from Pinto et al., 2020. (A) Cancer cells with different states of aggressiveness coexist and interact via TNTs. Aggressive cancer cells (dark blue) display higher interconnection rates than their less aggressive counterparts (light blue). Cancer cells are surrounded by stromal cells (red) to which they also communicate through TNTs. The homotypic or heterotypic connections between these cell types can be used to share oncogenic content (green circle) or to remove material to degrade (red circle). (B) Magnification of oncogenic cargoes traveling along the connection providing pro-tumoral features in the receiving cell and healthy lysosomes. Acquisition of mitochondria can promote chemoresistance and invasiveness and provide metabolic help in stress-induced conditions. Transfer of miRNA can drive modifications in the phenotype of recipient cells, leading to a more aggressive phenotype. Moreover, cellular vesicle content can impact the proteomic profile of the receiving cells and change their ability to respond to treatments. (C) Different materials discarded by a cell through TNTs. Organelles used for degradation, such as autophagosomes and lysosomes, might be transferred via TNTs as a clearing mechanism. TNTs could also be used as a route for the redistribution of drugs, which would otherwise be toxic in high concentration.

transfer also increased their ability to form larger tumors with a higher vascularization index when implanted in nude mice (J. Lu et al., 2017). Later, it was demonstrated that the acquisition of this pro-tumor properties could be due to TNT-mediated transfer of miRNA from the most aggressive to the least aggressive cells leading to the activation of the Deptor-mTor signaling pathway, an important downstream mediator of cancer cell proliferation and motility (J. J. Lu et al., 2019). In the case of breast cancer, TNT-mediated contact between macrophages and breast cancer cell line could drive the acquisition of an invasive phenotype in these latter ones (Hanna et al., 2019). Although the mechanism through which this contact was stimulating invasiveness was not defined, other studies demonstrated that breast cancer cells could receive mitochondria from mesenchymal cells (MSCs) through TNT-like structures (Pasquier et al., 2013) and MSCs-derived isolated mitochondria could be uptaken by a protocol defined as MitoCeption and induce migratory ability and cellular proliferation (Caicedo et al., 2015).

4.3.2. TNT-mediated communication promotes angiogenesis

TNT-mediated communication could also potentially induce vascularization, especially when they connect to endothelial cells (ECs). ECs have a critical role in physiological and tumoral angiogenesis and TNT-like sprouting from ECs or pericytes, constituent of the Blood Brain Barrier, have been identified in tissue sections of developing cerebral cortex and human glioblastoma, both conditions where the vascularization process is strongly active (Errede et al., 2018). Interestingly, ECs exposed to chemotherapeutic stress have been shown to be able to receive mitochondria from MSCs through TNTS, and this transfer could recover cells from the cellular stress and induce proliferation, invasive ability and angiogenesis potential (Feng et al., 2019). Metastatic tumor cells of various origin have also been found contacting ECs via TNTs and being able to induce the transformation from healthy to tumoral endothelium through the transfer of miRNA. The transcriptomic profile of the acceptor cells resulted to be altered and reprogrammed toward a angiogenic phenotype (Connor et al., 2015).

4.3.3. TNT-mediated communication induces treatment-resistance resistance

Therapy-resistance and TNTs also have demonstrated a possible correlation, the mechanisms described are multiple and a unique pattern did not appear yet. As previously mentioned, TNTs can be differently exploited by tumoral cells either to discard harmful material (as drugs or ROS-injured components) or to receive/deliver specific factor enhancing the possibility of cells to defend from the therapeutic damage, as miRNA but also mitochondria that can provide metabolic help (Figure 19). In both pancreatic and ovarian cancer cellular models, TNTs were exploited are route for the outflow of soluble doxorubicin (Desir et al., 2018). Interestingly, the drug was redistributed from chemo-resistant toward chemo-sensitive cells, leading to cell death of the latter and enrichment of the therapy-resistant population. In addition, therapies induce a cellular stress and often free radicals production, as in the case of irradiation and chemotherapy (Marlein et al., 2017; Matejka & Reindl, 2019) which typically induce TNT formation (D. Zhu et al., 2005). For example, radiofrequency treatment was found to promote TNT networking (Ware et al., 2015) as well as the chemotherapeutical inhibition of the androgen receptor, in prostatic cancer (Kretschmer et al., 2019). In this study, TNTs could deliver lysosomes, mitochondria and stress-induced chaperones and the disruption of this TNT-based network, by actin polymerization inhibitor (cytochalasin D), sensitized tumoral cells to the treatment promoting their cell death. The transfer of mitochondria seems to be highly relevant in treatment-resistance (Hekmatshoar et al., 2018; Vignais et al., 2017) as it can provide metabolic support against the therapeutic stress and rescue the aerobic respiration (Caicedo et al., 2015; Moschoi et al., 2016; Spees et al., 2006). Transfer of mitochondria from healthy cells was recovering UV-damages PC12 from apoptosis (X. Wang & Gerdes, 2015) and it can restore tumorigenic potential in cells devoid of mitochondrial DNA (Dong et al., 2017; Tan et al., 2015). Nevertheless, TNTs are not the unique mechanism that allow mitochondria transfer as astrocytes were found to released mitochondria subsequently taken up by neuronal neighboring cells (Hayakawa et al., 2016). Tumoral microenvironment could play a protective role toward tumoral cells providing healthy mitochondria. MSCs and ECs were observed to deliver mitochondria to ovarian and breast cancer cells improving their resistance to doxorubicin (Pasquier et al., 2013). In leukemia, human tumoral cells implanted into mice bone marrow could obtain

murine mitochondria from the stromal cells and stimulate aerobic cellular metabolism, cell proliferation and chemoresistance (Griessinger et al., 2017; Marlein et al., 2017; Moschoi et al., 2016; J. Wang et al., 2018). Alternatively, MSCs can receive and eliminate damaged mitochondria from tumoral cells stabilizing the homeostasis of the cancer population (J. Wang et al., 2018). Mitochondrial transfer could be an adaptive response to treatment, in fact chemotherapy-induced ROS production enhances mitochondria transfer (Marlein et al., 2017) and targeting this organelle exchange promote apoptosis in leukemic cells and improved mice survival (Marlein et al., 2019). Beyond mitochondria, other factors could be responsible of providing pro-resistant features. With the use of mass spectrometry, Kolba and colleagues identified that the transfer of a specific set of proteins, including stress-induced chaperons, that could promote cell survival in leukemic cells (Kolba et al., 2019a). miR-19 and miR-199a, miRNA highly expressed in chemo-resistant cells but not in chemo-sensitive ones, can also be transferred by TNTs in osteosarcoma and ovarian cancer (Thayanithy et al., 2014), suggesting that their transfer could drive treatment-resistant features in the receiving cells.

5. Tumoral networking in Glioblastoma: TNTs and TMs

TNTs might possibly have a relevance in GBM too. TNT-like connections were observed in two cellular models of GBM such as U-251 and U-87 cell lines. In these studies, GBM cell lines were exploited to study the transfer of protein aggregates related to Amyotrophic lateral sclerosis (Ding et al., 2015) or their potential role in cocaine addition (Carone et al., 2015), but their involvement in the tumoral context was not addressed. Moreover, astrocytes, abundant in the brain, were described forming TNTs toward C6 glioma cells in cell culture and their formation induced by ROS presence (Zhang & Zhang, 2015). Later in time, other publications reinforced the observation of a TNT-dependent communication between GBM cell lines and astrocytes (Civita et al., 2019; Formicola et al., 2019) describing a protective role on behalf of the astrocytes by the transfer of mitochondria (Civita et al., 2019). Only recently, some evidences have shown that TNTs might be modulated by TMZ and irradiation in two cell line models and that MGMT, marker of chemoresistance, could be transferred by these structures (Valdebenito et al., 2020). Nevertheless, serum-cultured cell lines and primary cells were demonstrated to be poorly

representative of the genotypic, transcriptomic and biologic features of parental GBM tumor, differently from basic FGF and EGF cultured primary cells (J. Lee et al., 2006). In this interesting work, serum-free Neurobasal media supplemented with basic FGF and EGF primary cells displayed constant features (proliferation, clonogenicity/tumorigenicity, differentiation potential and telomerase activity) across the cellular passages, extensive migration, genotype and gene expression of the original tumor, including stemness makers expression (NES, Sox2, CD133, Musashi-1 and Bmi polycomb complex protein). In 2015, Winkler and collaborators implanted GSCs, coming from patients with different grades of glioma, in nude murine brain and followed the tumor progression with the use of *in vivo* multi-photon microscopy (Osswald et al., 2015). What they observed was the progressive formation of a multicellular and communicative network between tumoral cells composed by long and thick (1.7 µm on average) membrane protrusions, containing both actin and microtubules, which the authors termed tumor microtubes (TMs, see Table 1). They demonstrated that more interconnected tumors were derived from higher glioma grades and were more resistant to irradiation than the lowest grades (Osswald et al., 2015). Cancer cells were using these communications to propagate calcium fluxes, which intracellular homeostasis is critical to induce radiotherapy-induced cytotoxicity (Tombal et al., 2002). TMs connections were found to be positive for connexin 43 (Cx43), a monomeric component of GAP-junctions and known regulator of the intracellular concentration of calcium (Lurtz & Louis, 2007). Interestingly, it has been previously reported that a subset of TNTs observed in kidney-derived cells contained Cx43 forming a hemi-connexon or a GAP-junction at their tip (Xiang Wang et al., 2010). It was, in fact, proposed that GAP-junctions could mediate the transfer of electrical signals in electrically-coupled TNTs (Abounit & Zurzolo, 2012). Given the similarities, it was initially unclear whether TNTs and TMs were two distinct structures or a variant of each other. Nonetheless, the presence of GAP-junctions along TNT-connections would not allow the transfer of cellular cargo larger than 1 kDa, like organelles or macromolecules, in respect of their pore size (Weber et al., 2004). On the other hand, in the TMs studies, the authors did not report transfer of conventional TNT-cargoes, such as mitochondria or vesicles, within TM lumen (Osswald et al., 2015), suggesting that the connection might be closed by GAP-juctions. TMs nature seems to diverge from the one of TNTs as their main drivers in the formations are growth-

associated protein 43 (GAP-43), crucial for neurite formation, regeneration, and plasticity (Osswald et al., 2015), and tweety-homolog 1 (Ttyh1), a membrane protein also linked to neuronal development (Jung et al., 2017). Indeed, GAP-43 knocked down decreased TMs number and promote the sensitivity to radiotherapy (Osswald et al., 2015). In addition, TMs display features typical of neurites, as they have been described to be post-synaptic targets for the surrounding neurons. Axons can dock onto TMs, forming chemical synapses, and generate synchronized calcium transients in glioma networks via AMPA receptors (Venkataramani et al., 2019; Venkatesh et al., 2019). The depolarization of the post-synaptic glioma cells was stimulating TM formation (Venkatesh et al., 2019) and invasion (Venkataramani et al., 2019). Finally, TMs also appear as finger-like protrusions and play a role in cell invasion (Jung et al., 2017) and in the repopulation of a surgically resected area in GBM mouse models (Weil et al., 2017). Interestingly, GBM cells were able to form a TM-based network in mice xenografts, but failed in forming connections when cultured *in vitro* (Weil et al., 2017) suggesting that TMs may exist only in the *in vivo* condition, although, protrusions resembling TMs have been recently observed also in pancreatic cancer (Latario et al., 2020). Importantly, the complexity of the tumoral tissue and the resolution of the multiphoton *in vivo* imaging are an obstacle for TNT identification, therefore their presence in the tumoral network remains an open question. GBM could possibly be an exception among the tumors and its intercellular communication might be orchestrated by TMs alone or, as we propose, GBM network is composed of both types of connections where TNTs provide a route for the direct transfer of cellular material and together, they cooperate in creating a resistant tumoral network (Figure 20).

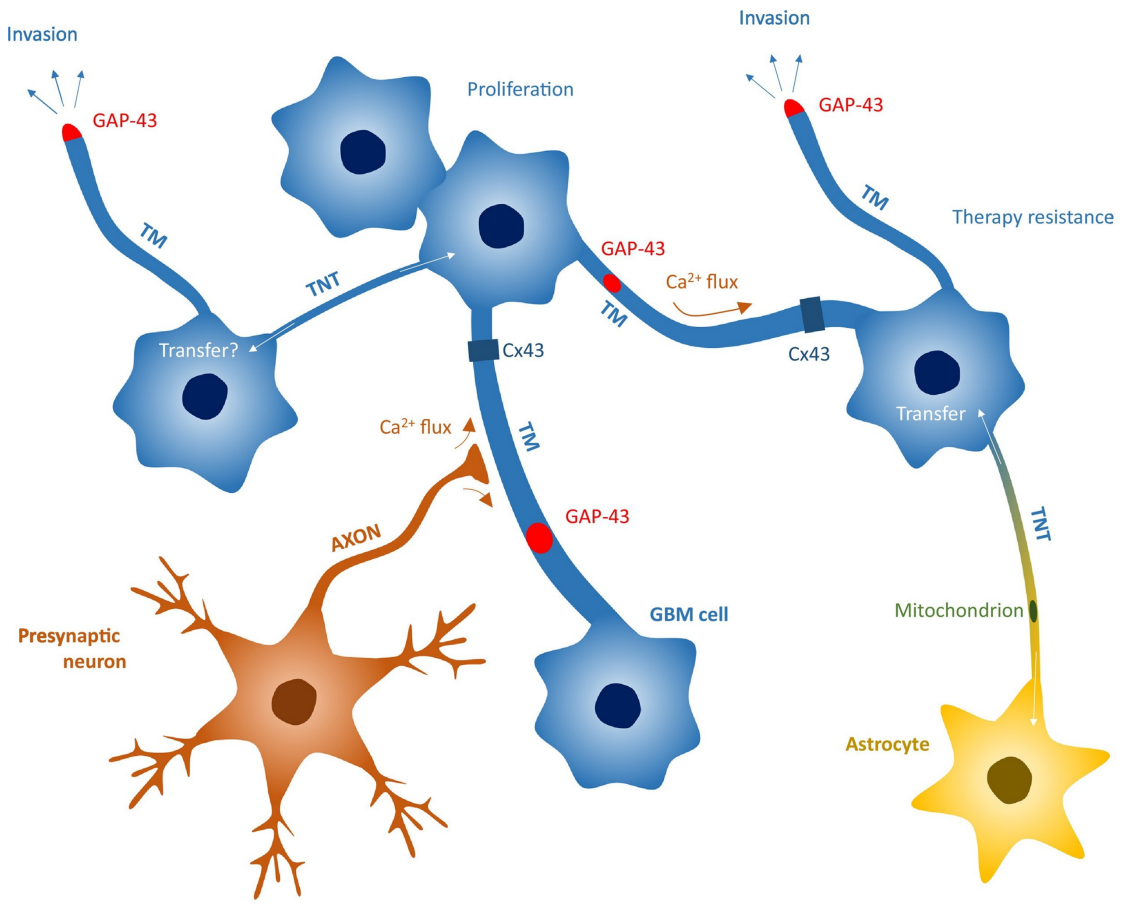

Figure 20. Schematic of a Glioblastoma network

Obtained from Pinto et al., 2020. GBM cells (blue) interconnect forming a functional network comprising different types of connection. Thick (>1 µm) protrusions (tumor microtubes; TMs) connect GBM cells and contain both Connexin 43 (Cx43) and growth-associated protein 43 (GAP-43), which regulate Ca^{2+} flux along the network. Thinner (<1 µm) TNT-like connections are present between GBM cells and may allow the transfer of material. GBM cells also form TMs that do not contact other cells and are able to drive cell invasion in a GAP-43-dependent manner. Presynaptic neurons (orange) extend axons that appose onto TMs and regulate the Ca2+ flux along the GBM network, promoting cell invasion and cell proliferation. Astrocytes (yellow) of the tumoral brain environment can communicate with GBM cells through TNT-like connections and transfer mitochondria to the tumoral cells, eventually affecting the behavior (e.g., proliferation and response to treatments) of the receiving cells.

Section III: The Project

Aims and objectives

My thesis project has been outlined in the context of GBM and TNTs that I have described above. The general goal of my research was to study TNTs in GBM and their involvement in its treatment-resistance. The points that I specifically aimed to address were: 1) determining the presence of TNT-connections, owning the transfer ability of cellular cargos that distinguish them from TMs, in different GBM models, from immortalized cell lines to more physiologically relevant ones, such as GSCs-derived tumor organoids; and 2) assessing whether therapeutic treatments (specifically irradiation) induced a response at TNT level, and if this would correlate with a more aggressive phenotype of cancer cells.

TMs were described to play a major role in the intercommunication and treatment-resistance of GSCs in murine xenograft model (Osswald et al., 2015) and, due to their similarity with TNTs (Osswald et al., 2016) and the extensive literature describing TNTs in cancer models (that I reviewed in Pinto et al., 2020), it was initially not clear whether these two entities were distinct or one the variant of the other. In addition, the tissue complexity of the *in vivo* condition and the limited magnification of the applicable imaging techniques prevented the visualization of nanoscale connections, such as TNTs, leaving open the possibility that these structures could co-exist with TMs. Further studies on TMs recently revealed that TMs and TNTs, owe a different nature and physiological roles as the TMs rather resemble neuritic extensions and allow the transmission of an electrical/synaptic signal (Jung et al., 2019; Venkataramani et al., 2019; Venkatesh et al., 2019), likely mediated by GAP-junctions (Osswald et al., 2015). **Our aim was to determine whether connections fitting the functional definition of TNTs, therefore allowing the transfer of cellular cargos (Abounit & Zurzolo, 2012; Pinto et al., 2020), could exist in GBM models.**

In addition to this, **we aimed to investigate whether the presence of TNTs could be correlated with a response to treatments or with a more aggressive and resistant phenotype of cells**. TNTs are often described as a stress-induced response, and various treatments has been found to promote their formation (Desir et al., 2018; Matejka & Reindl, 2019; Ware et al., 2015; D. Zhu et al., 2005). Particularly, in cancer, TNTs have been correlated with cells displaying more aggressive features and even they have been

described to be the route for the transfer of oncogenic materials (as I reviewed in Pinto et al., 2020). Also, the observations relative to TMs, orchestrating therapy-resistant network, corroborate the hypothesis that direct communication between GSCs is an important player acting in resistance to treatments typical of GBM.

In this frame, our laboratory has undertaken the study of TNTs in the context of GBM. The project has been initiated as part of a large collaboration, funded by Inserm, between different teams across France aimed to improve our understanding of GBM treatment-resistance from different point of view, predict the circumstances of the relapse, ameliorate the effect of the therapies and patients' quality-life. Ours is a multidisciplinary network, named MoGlimaging, in which different expertise has converged: from experimental biologist and clinicians to mathematicians and statistician. This allowed us to work on common material, and, in the specific case of this project, on GSCs cells obtained from real human tumor areas, previously characterized by magnetic resonance and cultured through the techniques aimed to the isolation (or enrichment) of GSCs. 16 couples of GSCs were obtained from as much patients that were participants of the STEMRI clinical trial (Identifier: NCT01872221). Due to the quantity of experiments to be performed with these cells and their duration, I had to restrict my thesis work to two patients.

TNTs in GBM cell lines

Premise

As the GBM was a new field of exploration in our laboratory, I started to set up the conditions for the study of TNTs in GBM cell lines. Few evidences were showing the existence of a TNT-based communication in U-87 and U-251 GBM cell lines (Carone et al., 2015; Ding et al., 2015), but its role in the context of GBM was not addressed (rather the transfer of ALS-related aggregates and the effect of Cocaine treatment). We aimed to characterize TNT-mediated communication in U-87, U-251 and LN-18 GBM cell lines, according to the well-established techniques in use in the lab (Abounit et al., 2015), quantifying TNT presence and transfer ability. This would allowed to set up the condition for the study of TNTs in a more relevant model, as the GSCs provided by our MoGlimaging network. Additionally, we aimed to compare the TNT phenotype displayed by the three cell lines as LN-18 cell line as it was providing an example of GBM cells expressing MGMT, known chemoresistant marker. In fact, our focus was also to study whether a correlation between TNTs functionality and treatment-resistance was present, as TNTs are often described as a stress-induced response, and various treatments has been found to promote their formation (Desir et al., 2018; Matejka & Reindl, 2019; Ware et al., 2015; D. Zhu et al., 2005). I aimed to exploit the GBM cell lines to set up the treatment conditions and determine their effect on TNT-based communication in the cell lines. Moreover, we aimed to investigate the presence and functionality of a heterotypic TNT-based astrocytes-GBM interaction, using the cell lines in study and to test whether this communication was altered by the treatments. Astrocytes are, in fact, the major component of the tumoral microenvironment in GBM and their cross-talk with GBM cells appear to facilitate tumor progression (Guan et al., 2018). Tumoral microenvironment has been shown to support tumor progression also by TNT-based communication (Feng et al., 2019; Marlein et al., 2017; J. Wang et al., 2018) and astrocytes can form TNTs with glioma cells (Zhang & Zhang, 2015).

Results

1) **Characterization of TNT in GBM-derived cell lines**

To characterize TNT in GBM cell lines models, I used three well-described GBM cell lines: LN18, U-251, and U-87, the two latter already described to form TNT-like connections (Carone et al., 2015; Ding et al., 2015; Formicola et al., 2019). I used these cell lines to validate the methodology for morphological and functional characterization of TNT, previously set up and used in the lab in the context of neurodegenerative diseases (Abounit et al., 2015), in the context of GBM. In order to identify these membranous channels, the cell's plasma membrane was labelled with fluorescent-Wheat Germ Agglutinin (WGA) and thin, continuous, non-attached to the substratum protrusions (Abounit et al., 2015) connecting distant cells were identified as TNTs (Figure Cell Lines 1A and B). Vinculin staining further confirmed the difference between TNTs and attached filopodia, as shown before (S. Zhu et al., 2018) (Figure Cell Lines 1C). All the three GBM lines were showing similar frequency of TNT-connected cells, around 40% (Figure Cell Lines 1D). In order to assess whether the connections observed were functional for the passage of cellular cargoes, an essential property of TNTs, I performed co-culture assays (Abounit et al., 2015) and assessed the transfer of intracellular vesicles from a donor cell population, labelled with the lipophilic dye DiD, to acceptor cells stained with Cell-Tracker Green. I quantified the percentage of acceptor cells positive for DiD after 24 hours of co-culture by flow cytometry. As control transfer by secretion was also monitored by challenging acceptor cells with conditioned media derived from donor cells (Abounit et al., 2015) grown in separate dishes. This portion of the transfer was removed from the total transfer obtained from the direct co-culture condition and referrers as cell contact-mediated transfer. The contact-mediated transfer was similar in all three cell lines, with 5-10% of acceptor cells receiving donor-derived DiD vesicles (Figure Cell Lines 1E), consistent with the similar percentage of TNT-connected cells observed. Furthermore, I found TNT connections containing DiD labelled vesicles (Figure Cell Lines 1F), supporting that contact-dependent transfer between cells was likely mediated by TNTs, as shown previously in other cell types (Delage et al., 2016).

2) **U-251 can transfer mitochondria through contact-dependent mechanism**

Mitochondria transfer appears to be particularly relevant in cancer (Hekmatshoar et al., 2018; Vignais et al., 2017). We aimed to verify that this transfer could occur in our cellular model. I co-cultured Mito-dsRed expressing U-251 cells, as donor population, with acceptor nls-GFP expressing U-251 cells, and the corresponding secretion control. After 24h of direct co-culture, but not in secretion control, I could detect by confocal imaging acceptor cells receiving Mito-dsRed puncta in their cytoplasm (Figure Cell Line 2), consistently with the transfer of mitochondria via contact-mediated mechanism. The percentage of acceptor cells receiving the transfer was inferior to 2% (data not shown). For all the tuning experiments that will follow, we decided to pursue with the vesicle transfer assay as it was allowing to work with an elevated percentage of transfer.

3) **TMZ-resistant U-251 form TNTs with similar frequency compared to parental U-251**

Since 2005, GBM treatment includes the use of TMZ as adjuvant chemotherapy in support of radiotherapy. TMZ is an alkylating agent inducing methylation of DNA, replication errors and consequent apoptosis. We were interested setting up the treatment conditions in these cell lines and studying the response to TMZ at the level of TNT formation and contact-mediated transfer. I treated U-251 and U-87 with various concentration of TMZ (25-50-100-250-500 µM) and counted TNT-frequency after 6 and 24 hours from the TMZ administration. After 24h, in both cell lines, I observed a tendency to an increased TNT-connectivity, although not statistically significant, using 50 µM of TMZ (data not shown). Since, U-251 cells have been shown to acquire resistance under prolonged exposure to TMZ treatment (Q. Pan et al., 2012; Rabé et al., 2020; Stritzelberger et al., 2018), we decided to study whether this resistant phenotype was displaying different TNT communication ability. I established a U-251TR (TMZ-Resistant) cell line culturing the parental U-251 cells in presence of 25 µM TMZ over 3 weeks (Figure Cell Lines 3A). TMZ-resistance is associated with the expression of DNA repair enzymes, specifically MGMT which is able to remove the methyl group imported by TMZ on the DNA. MGMT is expressed in 50% of GBM and it is a negative prognostic factor (Thakkar et al., 2014). I

evaluated the expression of MGMT by western-blot analysis in parental U-251 and derived U-251TR and I observed enhanced expression in the U-251TR cell lines (Figure Cell Lines 3B), suggesting that the cell line had acquired TMZ resistance as also it could normally proliferate after transient slow-proliferative phase (Rabé et al., 2020). Next, I plated U-251 and U-251TR in the same condition and counted the percentage of cells connected by TNTs. U-251TR did not show variation in TNT number compared to the parental cell line (Figure Cell Lines 3C) and a light, not significant, decrease in its contact-mediated vesicle transfer (Figure Cell Lines 3D). These results suggested that neither short- not long-term TMZ treatment, correlated with the development of TMZ-resistance, affect the ability of U-251 GBM cell line to interconnect and communicate through TNTs.

4) **Chemotherapy does not affect TNT-based communication between U-251 and astrocytes**

The cross-talk between tumoral cells and their microenvironment is known to influence cancer progression. In the case of GBM, astrocytes have been shown to interact and facilitate the glioma progression, aggression, and survival (Guan et al., 2018) also *via* TNT-like connections (Zhang & Zhang, 2015). I co-cultured both U-251 and U-251TR cells with primary murine astrocytes. Tomato-expressing astrocytes were obtained from the post-natal (P0-P2) dissection of tomato-expressing mice pups' brains. Heterotypic connections were observed between the two cell types (Figure Cell Lines 4A). As tumoral microenvironment has been shown to be supportive toward cancer cells providing pro-tumoral transfer of mitochondria, miRNA and protein-containing vesicles (Connor et al., 2015; Hekmatshoar et al., 2018; Kolba et al., 2019a), I assessed the transfer of DiD from astrocytes to U-251. I observed that the transfer was occurring mainly by secretion process (data not shown). Alternatively, I tested the directionality U-251-to-astrocytes, as TNTs have been shown to be as well a route to discard cellular waste as autophagosomes, lysosomes or even drugs (Desir et al., 2018; Sáenz-de-Santa-María et al., 2017) resulting in a beneficial outcome for tumor progression (Pinto et al., 2020). U-251TR did not show a significant variation of the vesicle transfer compared to the parental cell line toward primary astrocytes (Figure Cell Lines 4B), consistently with what previously observed in

homotypic culture. In order to assess the effect of radiotherapy, the other typical treatment administrated to GBM patients on TNT-mediated transfer, I also treated parental U-251 cells with irradiation before co-culture with astrocytes. U-251 cells were irradiated with 2 fractionated doses of 5 Gy before the co-culture, not significant variation in the vesicle transfer mediated by cell contact to astrocytes was observed (Figure Cell Lines 4C).

Discussion

In this part of the project I exploited three different cellular models of GBM to set up the study of TNTs in the GBM context. Using protocols previously established in neuronal cell lines (Abounit et al., 2015), I confirm the presence of functional TNTs in the three cellular models that displayed similar TNT-based communicative abilities, in terms of frequency of connections and contact-mediated transfer (Figure Cell Lines 1). Moreover, the observation that mitochondria transfer, mediated by direct cellular contact, may occur opens the door to further study of the pro-tumoral effect that this might bring in the real tumoral context, as observed in other cancers (Hekmatshoar et al., 2018; Vignais et al., 2017). Interestingly, I have found that neither LN-18 nor U-251TR cells, both expressing MGMT, drug-resistance marker, presented variation in their TNT-connectivity compared to MGMT-negative cells as U-87 and the parental U-251 cells (Figure Cell Lines 1 and 2), suggesting that the expression of this DNA-repairing enzyme may not influence the ability of cells to interconnect *via* TNTs. Although I validated the presence of intercommunication based on TNTs between U-251 cells and astrocytes (Figure Cell Lines 3), this interplay did not result to be affected neither by the acquisition of a chemo-resistant state in U-251, nor their previous irradiation. Generally, the ability of GBM cell lines to interconnect and communicate through TNTs did not show to be drastically altered by the treatments, particularly TMZ, that we decided to abandon for the following on the project. Nevertheless, we cannot extrapolate general conclusions regarding GBM from this model, as it has little relevance for disease (J. Lee et al., 2006), this part of the project laid the foundation for the study of TNTs in GSCs that were not available at that time.

Figures

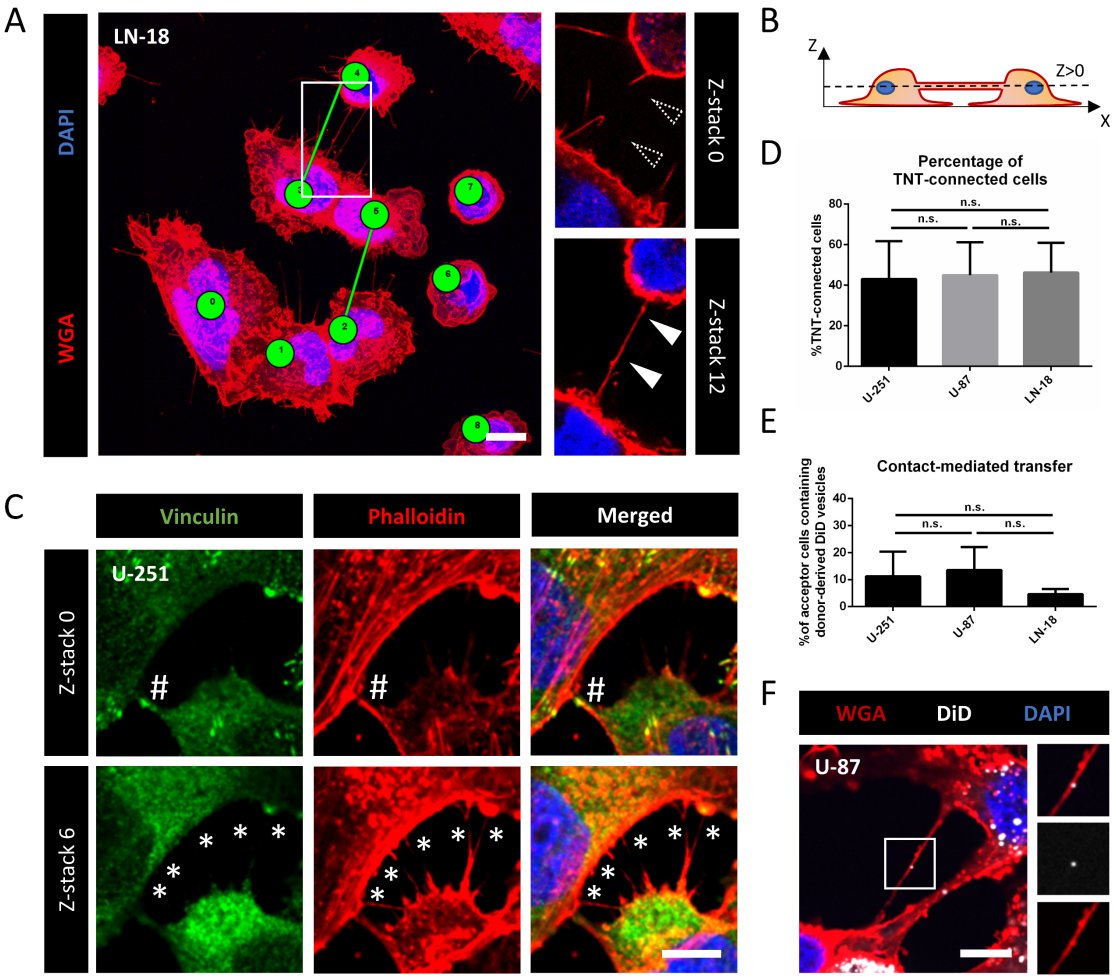

Figure Cell Lines 1. TNT characterization in GBM cell lines.

(A) Representative image of TNT counting by Icy software. LN-18 cells were plated and plasma membrane was labelled with WGA (in red), nuclei are stained with DAPI (in blue). The image is the result of a max intensity projection of 30 slices (0.33 µm step size). Each cell is indicated with a numbered green circle which can be connected by a line in presence of TNTs. On the right, a magnification of one of the TNT at two different z-section (z=0 and z=12). Dashed arrowhead indicated absence of the TNT on the dish surface, while-filled arrowheads indicate the appearance of the TNT in an upper stack. (B) Schematics of a TNT between two cells in a XZ perspective. TNTs connect cells at a Z-slice >0. (C) Quantification of TNT-connected cells in each cell line. GBM cell lines were plated at the described density, fixed after 24h and stained with WGA. Confocal images were acquired with 40x objective and analysed by Icy software. The percentage of TNT-connected cells calculated was 43,0 ± 18 % for U-251 (n=16, n cells=1989), 44,9 ± 16 % for U-87 (n=10, n

cells=990) and 46,2 ± 14 % for LN-18 (n=5, n cells=1472). P-values were deduced from contrast comparing the three cell lines in a logistic regression model. (D) Representative image of difference between TNT and filopodia. U-251 cells were plated, fixed with 4% PFA and actin cytoskeleton was stained with phalloidin (in red), nuclei with DAPI (in blue), filopodia tips were stained with vinculin (in green). In the lowest z-stack (z=0), filopodium tips is indicated with '#', moving up through the sections (z=6) several TNTs appear, indicated with '*'. Step size 0.26 µm. (E) Quantification of DiD labelled vesicle transfer by contact-dependent mechanism in the three cell lines. Co-culture between donor and acceptor cells was established according to the mentioned protocol and at least 10000 events were acquired by flow cytometry. The total transfer was obtained from the direct co-culture of acceptor and donor cells and subtracted of the percentage of transfer obtained by the secretion control to obtained the contact-mediated percentage of transfer. The percentage of acceptor cells receiving the transfer was 11,2 ± 9 % for U-251 (n=7), 12,9 ± 9 % in U-87 (n=7) and 4,6 ± 2 % in LN-18 (n=3). ANOVA one-way test was performed and no statistically significant difference was observed. (F) Representative image of DiD labelled vesicle into TNTs formed by U-87 cells. U-87 were stained for DiD and fixed after 24 hours. Cell membrane was labelled with WGA (in red) and nuclei were stained with DAPI (in blue). Error bar = SD.

A

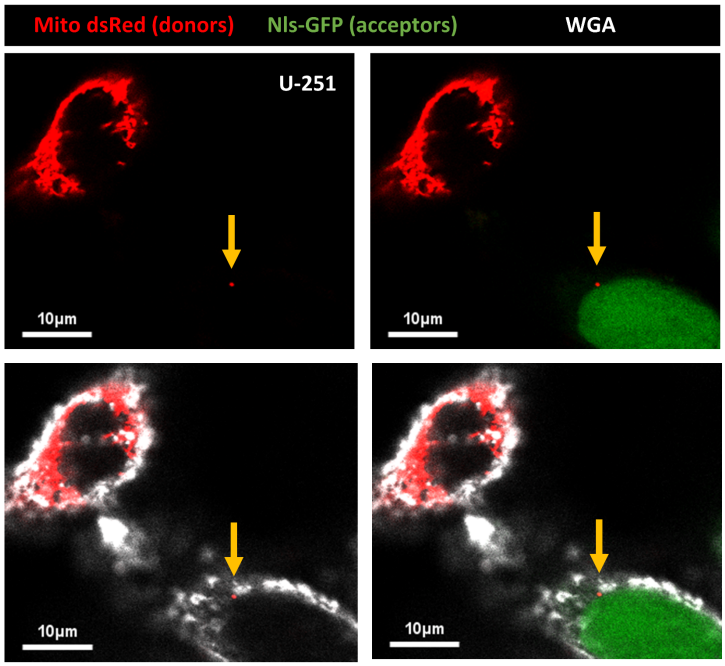

Figure Cell Lines 2. U-251 GBM cell line can transfer mitochondria.

(A) Representative image of the acceptor cell receiving donor-derived mitochondria. Mito-dsRed expression was induced in U-251 cells (in red) and used as donor cells in co-culture 1:1 with nls-GFP expressing U-251 (nucleus, in green) as acceptors. Cells were fixed after 24h and stained with WGA (in white). Confocal images were acquired with 40x objective.

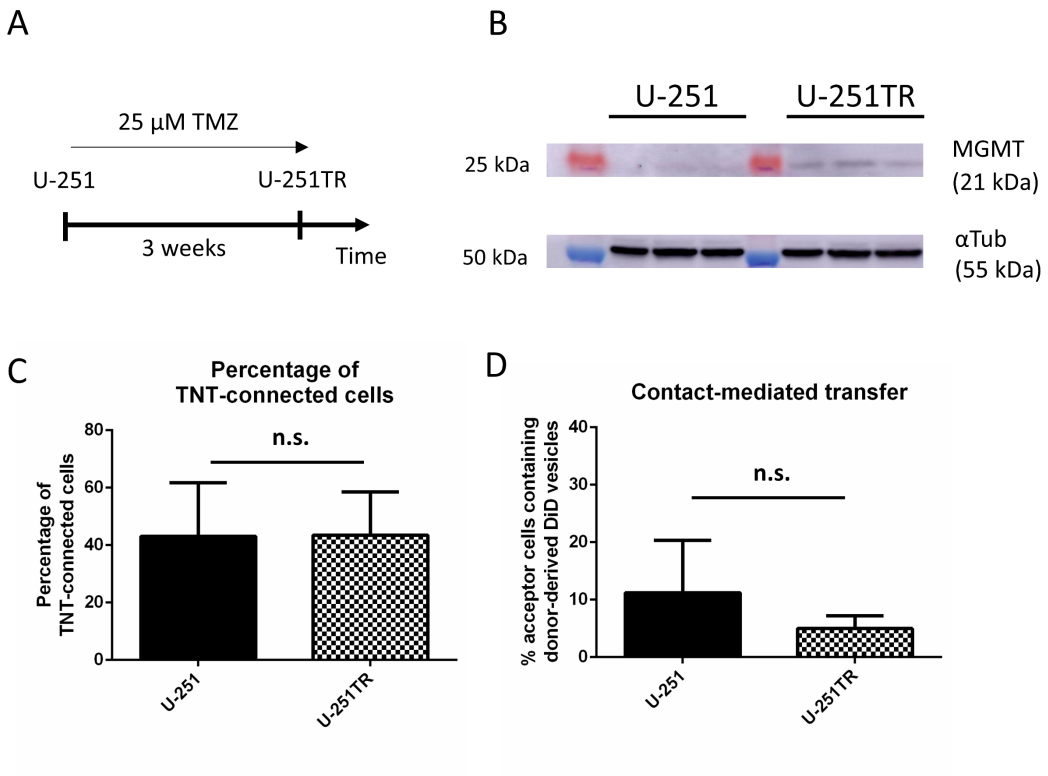

Figure Cell Lines 3. Establishment of U-251TR and their TNT-mediated communication.

(A) Protocol for U-251TR preparation. 25 µM of TMZ was added in the culture medium of U-251 for three weeks, which was changed every 2-3 days, at the end of which the U-251TR (TMZ-resistant) population was established. (B) U-251TR cells express MGMT differently from parental U-251. 20 µg of protein extract from U-251 and U-251TR cells was loaded on SDS-polyacrylamide gel. MGMT (21 kDa) expression was revealed with the specific antibody, anti-αTubulin (55 kDa) was used as loading control. (C) Quantification of U-251 and U-251TR TNT-connected cells. Both cell lines were plated at the same density (20.000 cells/cm^2), fixed after 24h and stained with WGA. Confocal images were acquired with 40x objective and analysed by Icy software. U-251 were forming 43,0 ± 18 % of connecting-cells (n=16, n cells=1989), similar to U-251TR that were forming 43.5±14% of TNT-connected cells (n=7, n cells=1167). Mann-Whitney not-parametric statistical test was performed. (D) Quantification of contact-mediated DiD labelled vesicle transfer in U-251 and U-251TR. Co-culture between donor and acceptor cells was established according to the mentioned protocol and at least 10000 events were acquired by flow cytometry. The total transfer was obtained from the direct co-culture of acceptor and donor cells and subtracted of the percentage of transfer obtained by the secretion control to obtained the contact-mediated percentage of transfer. The percentage of acceptor cells receiving the transfer was 11.2±9% in U-251 (n=7) and 4.9±2% in U-251TR (n=3). No significative statistical difference was calculated by Mann-Whitney not-parametric statistical test.

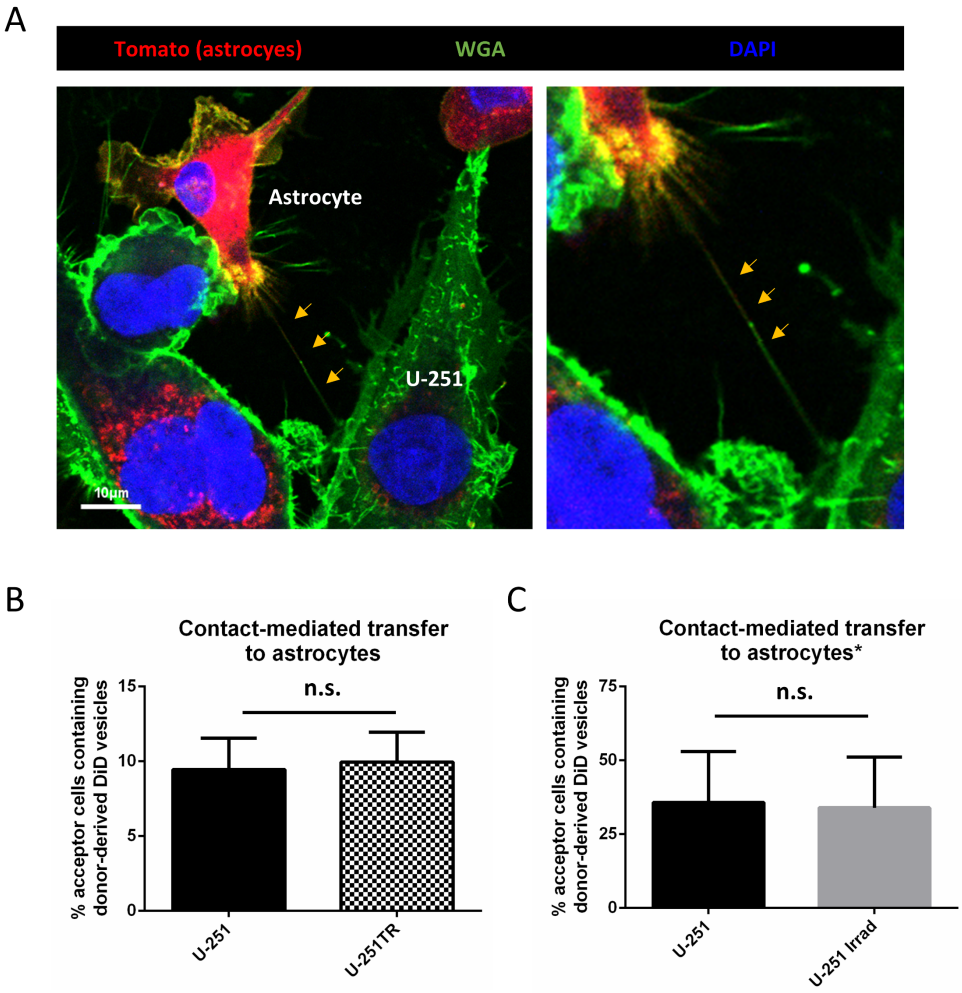

Figure Cell Lines 4. TNT-mediated communication between astrocytes and GBM cell lines.

(A) Representative image of a heterotypic connection between U-251 and astrocytes. Primary tomato-expressing astrocytes (in red) were obtained from the dissection of tomato-expressing post-natal mice pups and co-cultured at 1:1 ratio with U-251. After 24 hours the co-culture was fixed and the plasma membrane was stained with WGA (in green) and nuclei with DAPI (in blue). Confocal image was acquired with 40x objective. (B) Quantification of DiD labelled vesicle contact-mediated transfer from U-251 or U-251TR toward primary murine astrocytes. Co-culture between donor and acceptor cells was established according to the mentioned protocol and at least 10000 events were acquired by flow cytometry. The total transfer was obtained from the direct co-culture of acceptor and donor cells and subtracted of the percentage of transfer obtained by the secretion control to obtained the contact-mediated percentage of transfer. The percentage of primary astrocytes receiving the transfer was 9.5±6% in co-culture with U-251 (n=8) and 9.9±5.6% in co-culture with U-251TR (n=8). Mann-Whitney not-parametric statistical test was performed. (C) Quantification of contact-mediated DiD labelled vesicle transfer from U-251 or irradiated U-

251 toward primary murine astrocytes. Treated U-251 donor cells received a two irradiation of 5 Gy each the two days antecedent to the co-culture. Co-culture between donor and acceptor cells was established according to the mentioned protocol and at least 10000 events were acquired by flow cytometry. The total transfer was obtained from the direct co-culture of acceptor and donor cells and subtracted of the percentage of transfer obtained by the secretion control to obtained the contact-mediated percentage of transfer. The '*' is referent to the fact that in these set of experiments the secretions was monitored through a co-culture by filter, rather than conditioned medium, explaining the difference in percentage between U-251 % of transfer in the panel B and C. The percentage of primary astrocytes receiving the transfer was 35.8±17% in co-culture with U-251 (n=3) and 33.9±17% in co-culture with irradiated U-251 (n=3). Mann-Whitney not-parametric statistical test was performed.

Materials and Methods

Cell culture

U-251 MG (Sigma-Aldrich 09063001), U-87 (Sigma-Aldrich 89081402) and LN-18 (ATCC® CRL-2610™) cell lines were cultured in Dulbecco's Modified Eagle's Medium (ThermoFisher 31966-021), supplemented with 10% Fetal Bovine Serum (EuroBio CVFSVF00-01) and 1% Pen/Strep (100x Gibco 10378016) at 37°C in 5% CO_2 humidified incubators. Cells were passed with a frequency of 2-3 times per week and kept at less than 20 passages. Absence of mycoplasma contamination was verified with MycoAlert™ Mycoplasma Detection Kit (Lonza LT07-118).

TNT identification and counting

Tunneling nanotubes were identified accordingly to the protocol of Abounit et al., 2015. We experimentally assessed the ideal cell density for the observation of TNTs (20000 cells/cm^2 for U-251, 30000 cells/cm^2 for LN-18 and 40000 cells/cm^2 for U-87). U-251, U-87 and LN-18 were fixed after 24 hours. 15 minutes fixation in solution 1 (2% PFA, 0.05% glutaraldehyde and 0.2 M HEPES in PBS) followed other 15 minutes in solution 2 (4% PFA and 0.2 M HEPES in PBS) were performed at 37°C in order to preserve TNTs integrity. Cells were washed with PBS and plasma membrane was labelled with fluorescent Wheat Germ Agglutinin (1:500 in PBS, Life Technologie W21405, W849, W11261) for 20 min at RT. Nuclei ware stained with DAPI (1:5000 Sigma-Aldrich D9542) before mounting with home-made Mowiol.

Tiles confocal images of the whole volume of the cells were acquired with a Zeiss LSM 700 controlled by ZEN software. Optimal image stack was applied. Images were processed using ICY software to manually count the number of TNT-connected cells. Cells connected through thin, continuous, phalloidin-positive connections were counted as TNT-connected cells.

Immunofluorescence

Cell were seeded on glass coverslips at the TNT-density previously mentioned. Cells were fixed with a solution of 4% PFA for 20 minutes at RT. After PBS washes, quenching and permeabilization steps were performed using 50 nM NH4Cl solution and 0.1-0.2% Triton-X100, respectively. 30 minutes of blocking was performed with a solution of 10% FBS. Primary antibodies were incubated diluted in the blocking solution for 1 hours. Anti-vinculin (1:1000 Sigma-Aldrich V9264) was used. Cells were washed in PBS and incubated for 45 minutes with secondary antibody anti-mouse and anti-rabbit Invitrogen Alexa 488, 564 or 647 antibodies (1:1000) or phalloidin-rhodamine to stain F-actin (1:500 R415 Invitrogen) diluted in blocking solution. DAPI (1:5000 Sigma-Aldrich D9542) in PBS solution was applied for 5 minutes before washes and mounting with Mowiol.

Immunofluorescence staining were analysed on a Zeiss LSM 700 inverted confocal microscope (Carl Zeiss, Germany), with a Pln-Apo 10X/0.45 to image the entire organoid, 40X : EC Pln-Neo 40X/1.3 (NA = 1.3, working distance = 0.21mm) or Pln-Apo 63X/1.4 (NA = 1.4, working distance = 0.19mm) oil lens objective and a camera (AxioCam MRm; Carl Zeiss).

Lentivirus preparation and transduction

Lentiviral particles have been produced using the cell line 293T cultured in Dulbecco's Modified Medium (ThermoFisher 31966-021) supplemented with 10% Fetal Bovine Serum (EuroBio CVFSVF00-01) and 1% Pen/Strep (100x Gibco 10378016) at 37°C in 5% CO_2 humidified incubators. Cells were plated at a 50-70% confluency the day before the transfection. Transfection mix was prepared in serum-free OptiMEM (ThermoFisher 51985-026) medium, using FuGENE HD Trasfection reagent protocol (Promega E2311). Plasmids coding for lentiviral components, pCMVR8,74 (Gag-Pol-Hiv1) and pMDG2 (VSV-G) vectors, and plasmid of interest were added in the transfection mix at a ratio of 4:1:4 µg, respectively. Mito-dsRed (pLV-CMV-pDsRed2-mito) and nls-GFP (pLV-CMV-nls-GFP), plasmids encode respectively for a fragment of the subunit VIII of human cytochrome C oxidase fused with RFP, and for nuclear-localization-sequence tagged to GFP, both under the Cytomegalovirus (CMV) promoter. After 48 hours the culture medium was collected

for the concentration of the lentiviral particles using LentiX-Concentrator (TakaraBio 631231).

Quantification of TNT-mediated transfer by flow cytometry

Transfer assays were performed accordingly to the protocol of Abounit et al., 2015. In the cell lines U-251, U-87 and LN-18, donor and acceptor cells were respectively stained with a solution of 333 nM Vybrant DiD (Life Technologie V22887) and 10 µM Cell Tracker Green (Thermofisher C2925) both diluted in complete medium, for 30 minutes at 37°C. Cells were detached with a solution of 0.05% Trypsin (Thermofisher 25300054) and counted with TC20 Automated Cell Counter (Bio-Rad). For the 2D co-culture, cells were plated at the density previously mentioned (see TNT identification and counting). Cells were detached after one overnight of co-culture. To monitor the transfer by secretion in 2D co-culture, acceptor cells were plated alone and cultured overnight with donor cells conditioned medium. Acceptor cells were similarly detached as previously mentioned and fixed for the flow cytometry analysis.

Flow cytometry data were acquired with a BD Symphony A5 flow cytometer. GFP and CellTracker green, dsRed and DiD fluorescence were analysed at 488 nm, 561 nm and 640 nm excitation wavelength, respectively. 10,000 events were acquired for each condition and data were analysed using FlowJo analysis software.

TMZ treatment

TMZ was purchased from Sigma-Aldrich (T2577) and prepared in DMSO according to the datasheet instructions. TMZ was added directly in the culture medium of the GBM cell lines, control cells were treated with equal volume of DMSO. For the establishment of U-251TR, cells were cultured in their classical complemented medium in which TMZ was diluted at a concentration of 25 µM. Fresh medium was changed every 2-3 days to keep the cells under constant chemotherapeutic pressure.

Western blot

Cells were lysed in lysis buffer (50 mM Tris, pH 7.4, 300 mM NaCl, 1% Triton X-100, 5 Mm MGgCl). Protein samples were incubated at 100°C for 5 min and electrophoresed on Criterion XT Precast Gel 4-12% (BioRad 3450123). Proteins were transferred to PVDF membranes (GE Healthcare Life Sciences). Running (XT MOPS, BioRad) and transfer (Tris/Glycin). Membranes were blocked in 5% milk in Tris-buffered saline with 0.2% Tween 20 (Sigma) (TBS-T) for 1 h. Membranes were then incubated at 4°C with a primary antibody, rabbit anti-MGMT (1:1000 2739S Cell Signaling), mouse anti-αTubulin (1:1000 Sigma-Aldrich T9026) then washed several times with TBS-T. After 1 h incubation with horseradish peroxidase conjugated with the respective IgG secondary antibody (1:10,000) (GE Healthcare Life Sciences), membranes were washed with TBS-T and protein bands on the membrane were detected using an ECL-Plus immunoblotting chemiluminescence system (GE Healthcare Life Sciences). Membranes were imaged using ImageQuant LAS 500TM camera (GE Healthcare Life Sciences).

Astrocytes preparation

Gt(ROSA)26Sor$^{tm4(ACTB\text{-}dtTomato,\text{-}EGFP)Luo}$ mice from Institut Pasteur (Paris, France) in-house colony were used for primary astrocytes experiments. Handling of animals was performed in compliance with the guidelines of animal care set by the European Union and approved by the Ethics Committees of Institut Pasteur and Erasmus Medical Center. Pups were sacrificed between 0 to 2 days after their birth. The forebrain was isolated, meninges, hypothalamus, cerebellum were discarded. The tissue was mechanically dissociated by trituration with two fire-polished Pasteur pipettes and the resulting cellular suspension plated on Poly D-Lysin-coated (5 mg/mL for 1 hour at 37°C) surface. The cell suspension was cultured in DMEM F12 medium (Gibco) supplemented 10% Fetal Bovine Serum (EuroBio CVFSVF00-01) and 1% Pen/Strep (100x Gibco 10378016) at 37°C in 5% CO_2 humidified incubators. After one week, fluorodeoxyuridine (FdU) and Uridine were added to the medium and changed every 2-4 days in order to establish a pure-astrocyte culture.

Irradiation

Irradiation was performed with X-Ray machine (Xstrahl LTD). 5 Gy irradiation were performed exposing the cells to X-rays for 3 minutes and 33 seconds (250 kV, 12 mA).

Statistical analysis

Mann-Whitney not-parametric statistical test was performed to compare the percentages of TNT-connected cells and vesicle transfer in the co-culture experiments. ANOVA two-way test was performed to compare TNT counting and contact-mediated transfer of U-251, U-87 and LN-18 in Figure Cell Lines 1.

TNTs in GSCs

Premise

GBM cell lines have been described to be poorly representative of tumoral context (J. Lee et al., 2006) and the study of GSCs and their features is becoming of increasing interest as their role in GBM relapse has become evident (Bao et al., 2006; Prager et al., 2020). We intended to contribute to the field investigating the communicative ability of GSCs, in light of the observations of the laboratory of F. Winkler reporting the presence of TMs in a GBM murine xenograft model, and addressing the question of the presence and role of TNTs in a GBM representative and relevant model. Thanks to our collaboration with Elizabeth Moyal and Christine Toulas leading the Equipe 11 at the Oncopole Center of Toulouse, I had the possibility to work with two different patient-derived GSCs obtained from different regions at infiltrative border of the same tumor, representative of the heterogeneous cancer cell populations remaining in the brain even after surgery. The area of origin of both GSCs were previously characterized by functional MRI and found to display different metabolic activity, correlated to a different relapse-initiating potential (Deviers et al., 2014; Laprie et al., 2008). These cells were found to be tumorigenic in mice (Dahan et al., 2014) and to display different radio-resistance, more elevated in the GSC population owning more relapse-initiating potential (data not shown, article in preparation in Toulouse). Using these GSCs, we could investigate the role of TNTs in a relevant model of GBM relapse, also taking into account the intra-tumoral heterogeneity typical of this tumor and confronting the two different phenotypes. Exploiting the experience gained with the work on the cell lines, we aimed to identify, characterize and assess the TNT-mediated communication ability of these two GSCs populations, using both in adherent cell culture as well as in tumor organoids, a tridimensional and tumor-representative model (Hubert et al., 2016) in which GSCs retain their tumorigenic potential and TNTs presence and functionality have never been investigated. Further, we aimed to address the effect of irradiation to determine whether an heterogenous response was present at TNT level and how this was correlated with the most aggressive phenotype in both adherent and tumor organoid model. Beyond this comparison, we

aimed to finally unravel the confusion between TNTs and TMs and assess whether communicative structures that directly allow the transfer of cellular material, as TNTs, are present in a relevant model of GBM, such as tumor organoids, and whether they could coexist with TMs.

Contribution

As the GBM project was initiated at the time of my arrival in the lab, I took care of setting up of the GBM cell line cell culture and all the experiments in the GBM cell line model, adapting the protocols for the study of the TNTs in the use in the lab (Abounit et al., 2015) to the GBM context. Once obtained the GSCs from the Oncopole Center of Toulouse, I established the methodology for their maintenance and culture which I imported in our lab. Similarly, I established tumor organoids preparation thanks to the suggestions of Dr. Isabelle Leroux (Institut Cerveau Moelle Epinière, Paris), who thought me the methodology. I used these knowledges to obtain most of the results in GSCs presented in the "Result" section. During the last 20 months Inés Saenz De Santa Maria has joined the project as post-doc and she helped me carrying on the project, by adding the study of a second couple of GSCs obtained from a different patient. She also contributed to the work described in the "Result" section, bringing her experience in microscopy, particularly in live-cell imaging. In this last year, due to the little time left for my PhD project and the restrictions caused by the recent pandemic, we decided to put all results concerning the one pair of patient cell together for an article that is currently under revision. The data on the GBM cell lines are not published, as well as the data on the 2nd patient as they are still incomplete.

In this article I took care of the draft writing of Abstract, Introduction, Results, Material and Methods (except Time-lapse microscopy, RT-qPCR and Statistical analysis) and Discussion, although this last part was greatly expanded by my supervisors. I prepared all the graphs and composed all the figures. In the results section, I performed the TNT counting and immunofluorescence of Figure Article 1E and F. I performed the co-culture assay by FACS and confocal imaging, and corresponding growth curves presented in Figure

Article 2C, D, E, F. I performed the irradiation and all the experiment of TNT counting, transfer assays and curves upon irradiation present in Figure Article 3. I took care of the organoids imaging shown in Figure Article 4B and the transfer assays and proliferation graph presented in Figure Article 4D and E. I acquired the confocal images presented in Figure Article 5B (only the Day 6), C and D. I performed the irradiation and all the experiment of transfer assays and curves upon irradiation present in Figure Article 6. I prepared the schematics presented in Figure Article 1A, 2B and 7. I acquired, deconvolved and prepared Supplementary Figure 1.

Patient-derived Glioblastoma Stem cells transfer mitochondria through Tunneling Nanotubes in Tumor Organoids

Giulia Pinto*[1,2], Inés Saenz-de-Santa-Maria *[1], Patricia Chastagner [1], Emeline Perthame [3], Caroline Delmas [4], Christine Toulas [4], Elizabeth Moyal-Jonathan-Cohen[4], Christel Brou [1$], Chiara Zurzolo [1$].

[1]Unité de Trafic Membranaire et Pathogenèse, Institut Pasteur, UMR3691 CNRS, 28 rue du Docteur Roux, F-75015 Paris, France

[2]Sorbonne Université, ED394 - Physiologie, Physiopathologie et Thérapeutique, F-75005 Paris, France

[3]Hub de Bioinformatique et Biostatistique – Département Biologie Computationnelle, Institut Pasteur, USR 3756 CNRS, F-75015 Paris, France

[4]Institut National de la Santé et de la Recherche Médicale (INSERM) UMR 1037, Cancer Research Center of Toulouse (CRCT); Institut Claudius Regaud; Université Toulouse III Paul Sabatier, Toulouse F-31000, France.

*These authors equally contributed to this work

[$]These authors equally contributed to this work

Corresponding authors: chiara.zurzolo@pasteur.fr (+33 (0)1 45 68 82 77)

Keywords: tunneling nanotubes, cancer, glioblastoma, cell communication, stem cells

Abstract

Glioblastoma (GBM) is the most aggressive brain cancer and its relapse after surgery, chemo and radiotherapy appears to be led by GBM stem cells (GSLCs). Also, tumor networking and intercellular communication play a major role in driving GBM therapy-resistance. Tunneling Nanotubes (TNTs), thin membranous open-ended channels connecting distant cells, have been observed in several types of cancer, where they emerge to drive a more malignant phenotype. Here, we investigated whether GBM cells are capable to intercommunicate by TNTs. Two GBM stem-like cells (GSLCs) were obtained from two tumoral areas of the same patient. We show, for the first time, that patient-derived GSLCs, grown in both classical 2D culture and in 3D-tumor organoids, form functional TNTs which allow mitochondria transfer. In the organoid model, which better recapitulate tumor's features we observed the formation of a network between cells composed of both tumor microtubes (TMs), previously observed *in vivo*, and TNTs. We also show that the two GSLCs responded differently to irradiation in terms of TNT induction and mitochondria transfer, with the higher response in cells derived from most the metabolic active area. Thus, TNT-based communication could be an additional feature of tumor cell networking that might favour tumor progression.

Introduction

Glioblastoma (GBM) is the most common and aggressive brain cancer which nowadays lacks understanding and resolutive therapeutic strategies. After surgery, patients undergo a mixture of chemo and radiotherapy (Stupp, et al., 2005), aiming to kill the remaining cancer cells at the edges of the resected region. Although these treatments have been proven to be effective in extending patients survival (Batash et al., 2017), lethal relapse from these peripheral regions occurs in 100% the cases. The elevated intra-tumoral heterogeneity seems to be at the origin of the relapse and particularly due to the presence of GBM stem cells (GSCs) that have been found to be the most resistant to treatments (Bao et al., 2006; Lathia et al., 2015; Prager et al., 2020; Suvà et al., 2014). Moreover, it has been shown that post-surgical treatments can induce cellular plasticity and trans-differentiation resulting in more aggressive phenotypes (Dahan et al., 2014). How this occurs is still not clear, however it appears that intercellular communication in the tumoral context has a major role in the plasticity, survival and progression of many different types of cancer (Asencio-Barría et al., 2019; Broekman et al., 2018a). In particular, in the case of GBM, Winkler and colleagues have shown that patient-derived GSCs, xenografted into murine brains, are able to grow tumors where cells interconnect through membranous extensions and form a unique communicating network (Osswald et al., 2015). These finger-like protrusions called Tumor Microtubes (TMs) range in the microscale for their diameter (>1µm) and could extend for over 500 µm in length, creating a complex tumor cell network. TMs allow the propagation of ion fluxes, providing a fast, neurite-like, communication between cancer cells, and could also drive the repopulation of surgically-injured areas (Weil et al., 2017). TM-connected cells resulted to be protected by chemo and radiotherapy, and the protection could be suppressed in by the inhibition of TM-inducers such as Cx43, GAP43 and TTYH (Jung et al., 2017; Osswald et al., 2015; Weil et al., 2017).

Another mechanism of intercellular communication that has been recently proposed to facilitate tumor progression is represented by Tunneling Nanotubes (TNTs) (Hekmatshoar et al., 2018; Pinto et al., 2020). TNTs are thin cellular extensions connecting distant cells observed in a wide variety of cellular and murine models as well as in *ex vivo* resections

from human tumoral tissue (Pinto et al., 2020). They are membranous structures supported by an actin-based cytoskeleton and, differently from other cellular protrusions, including TMs (assumed to provide communication through GAP-junction), are open at both extremities, thus allowing cytoplasmic continuity between connected cells (Rustom et al., 2004; Sartori-Rupp et al., 2019). TNTs allow the transfer of various-sized cargos, such as small molecules (e.g. Ca^{2+} ions), macromolecules (e.g. proteins, nucleic acids) and even organelles (vesicles, mitochondria, lysosomes, autophagosomes, etc.) (Abounit & Zurzolo, 2012). They appear to play a critical role in several physiopathological contexts, as in the spreading of protein aggregates in various neurodegenerative diseases (Abounit et al., 2016; Abounit et al., 2016; Victoria & Zurzolo, 2015, 2017; S. Zhu et al., 2015) or in the transmission of bacteria (Onfelt et al., 2006) and viruses (Eugenin et al., 2009; Souriant et al., 2019) or, finally, during development (Korenkova et al., 2020). Specifically, it was shown that in many cancer types, TNTs are exploited as route for the exchange of material between cancer cells or with the tumoral microenvironment. As consequence of this transfer, cells can acquire new abilities as enhanced metabolic plasticity, migratory phenotype, angiogenic ability and therapy-resistance. In particular, the transfer of mitochondria has been related to all the previously mentioned features since they can provide energy and metabolic support to the cancer cells in displaying their aggressive features as observed in various cancers (Hekmatshoar et al., 2018; Vignais et al., 2017).

Few studies have reported TNT-like communication in GBM cells lines (Carone et al., 2015; Ding et al., 2015; Formicola et al., 2019; Valdebenito et al., 2020; Zhang & Zhang, 2015), however, no data on the presence and role of TNTs are available in the context of a whole GBM tumor or in primary GSCs. This is likely due to the fragility of these connections and to the low-resolution images that can be obtained in the *in vivo* studies (Osswald et al., 2015). Functional TNTs have been shown in a variety of cancers using *in vitro* and *ex vivo* tissue cultures (Pinto et al., 2020); whether in GBM the intercellular communication is orchestrated exclusively by tumor microtubes or TNTs are also present and functional is still not known. Specifically, whether TNTs can be formed between patient-derived GSLCs and cargo exchange occurs through these structures, as well as if their presence and/or functionality could be induced/affected by the treatments contributing to the tumoral progression and treatment-resistance remain outstanding questions. In order to address

these issues, we cultured different patient-derived GBM stem-like cells both in 2D and in tumor organoids, where we assessed the presence of TNTs and their possible role in intercellular communication and cancer progression.

Results

1) Patient-derived GBM cells with stem-like features form TNT-like connections

We obtained GBM cells from one patient in the frame of the clinical trial STEMRI (Identifier: NCT01872221). This trial was aimed at studying the tumoral cells remaining in the vicinity of the core tumor after the latter has been surgically removed, and better understanding and possibly anticipating which of them are at the origin of the relapse. Bulks of tissue were resected from the infiltrative tumor area defined by the Fluid-attenuated inversion recovery (FLAIR) sequence on MRI (Figure Article 1A) (Shukla et al., 2017). The tumors were also characterized by multimodal MRI spectroscopy, in particular by the Choline/N-AcetylAspartate Index (CNI), indicative of the metabolism of the area. Inside the FLAIR area, the more metabolically active zones (CNI>2, named CNI+) were found to be predictive of the site of the relapse (Laprie et al., 2008) in contrast to the less metabolically active (CNI<2, named CNI-) (Deviers et al., 2014; Guo et al., 2012). The tissue samples were desegregated and cultured in stem cell medium (Dahan et al., 2014) to enrich in GBM stem cells rather than differentiated ones (Avril et al., 2012). If implanted orthotopically in mice, these kinds of cells were shown to be able to generate tumors (Dahan et al., 2014). Two populations of cells were obtained from the same patient respectively corresponding to the CNI- area, named C1 cells, and to the CNI+ area, named C2 cells that both grow in suspension in neurosphere-like aggregates (Figure Article 1B). To further characterize the two populations, we monitored the expression of genes related to different cell types, from differentiated to progenitor/stem cells (Neftel et al., 2019; Prager et al., 2020; Singh et al., 2003; Suvà et al., 2014; Verhaak et al., 2010). GFAP and CHI3L1 (respectively astrocytic and mesenchymal markers) were found not to be expressed, low expression was observed for the neural markers Tubβ3 and GAP43. On the other hand, expression of the progenitor and stem cell markers Olig1, Olig2, Sox11 and

Sox2 was significant (Figure Article 1C). Also, this pattern of gene expression was maintained over culture passages indicating maintenance of the stemness properties. Altogether, these two primary cell lines fulfilled the criteria of GBM stem-like cells (GSLCs).

Different GBM-derived cell lines have been described to form TNT-like connections and to be able to transfer cellular content including mitochondria (Carone et al., 2015; Ding et al., 2015; Formicola et al., 2019; Zhang & Zhang, 2015). Because such cell lines are only partially recapitulative of the original tumoral features (J. Lee et al., 2006), here we aimed to address whether patient-derived GSLCs can form functional TNTs. Thus, C1 and C2 cells were plated for 6h on laminin-coated surface in 2D culture to make them adhere to the support for ease of TNT recognition. Thin cell connections were detected after 6 hours of culture by live imaging (Figure Article 1D). After fixation, we assessed the presence of actin-containing connections floating above the laminin coated surface, which is a the distinguishing characteristics of TNTs, that hoover above the substrate, as exemplified in Fig.1E, where both attached-to-the-substrate (z-stack=0) and above (z-stack>3) stacks are shown (Abounit et al., 2015; S. Zhu et al., 2018, p. 8). GSLC TNTs resulted to be always positive for actin and negative for microtubules markers, consistent with the description of classical TNTs(Sartori-Rupp et al., 2019) (Figure Article 1F). For quantification of TNTs, we labelled the cell's plasma membrane with fluorescent-Wheat Germ Agglutinin (WGA) and counted thin, continuous, non-attached to the substratum protrusions (Abounit et al., 2015) connecting distant cells. Both C1 and C2 populations formed TNT-like connections with a significantly different frequency: about 10% of TNT-connected cells in C1 and 15% in C2 (Figure Article 1F). These data showed for the first time that GSLCs can interconnect through TNT-like structures, with a significant higher incidence in CNI+ cells.

2) **TNT-like structures of GSLCs can transfer mitochondria**

TNTs are described to be open-ended connections allowing the passage of cellular cargoes. To determine whether the connections observed were apt to this purpose, we decided to assess the transfer of mitochondria, shown to occur in several types of cancer cells (mesothelioma, leukemias, ovarian, etc.) (Hekmatshoar et al., 2018; Pinto et al., 2020; Vignais et al., 2017) and GSCs were described to be able to uptake isolated

mitochondria (Nzigou Mombo et al., 2017). To observe mitochondria in living samples, we introduced a GFP-tagged fragment of the subunit VIII of human cytochrome C oxidase located in the inner mitochondrial membrane (MitoGFP) in both GSLCs by lentiviral transduction. We then performed live-imaging on GSLCs and found mitochondria moving inside TNT-like structures and entering into a connected cell (Figure Article 2A, Supplementary video 1), supporting an open-ended TNT relying the two cells. To quantify this transfer, we performed co-culture assays (Abounit et al., 2015) between a donor population, expressing MitoGFP, and an acceptor cell population transduced with lentivirus governing the expression of cytosolic mCherry (Figure Article 2B). More than 80% of each cell population was stably expressing the constructs, allowing a 1:1 co-culture ratio between the two populations. Cells were plated on laminin-coated surface and the percentage of mitochondria transfer was assessed after 2 or 5 days of co-culture by flow cytometry (Abounit et al., 2015). Between 1 and 3% of acceptor cells received donor-derived mitochondria, exclusively due to contact-dependent mechanisms since negligible transfer was observed when the two cell populations were separated by filter (Figure Article 2C). Furthermore, the percentage of acceptor cells receiving mitochondria was increasing over time in both GSLCs (Figure Article 2D). It is worth noting that C2 had higher mitochondria transfer compared to C1, in accordance with the higher percentage of TNT-connected cells in this population (Figure Article 1E). Also, the different transfer abilities of the two cell types was independent from cell proliferation as both GSLCs had a similar proliferation rate in this condition (Figure Article 2E). To confirm that the fluorescence signal detected by flow cytometry corresponded to true mitochondria inside acceptor cells, confocal microscopy was performed in the same co-culture conditions used for the flow cytometry experiments. By this mean, MitoGFP puncta (Figure Article 2F) which overlapped with TOM20 (Translocase of the Outer Membrane, Supplementary Fig.1) were observed in acceptor cells. These data indicate that both C1 and C2 GSLCs are able to form functional TNTs when cultured in 2D. However, C1 and C2 transfer mitochondria with distinct efficiencies, consistent with their distinct abilities to form TNTs (Figure Article 1F).

3) **Effect of irradiation on TNT-based communication in GSLCs in 2D culture**

Next, we aimed to assess the effect of irradiation on the TNT-based communication in GSLCs. We irradiated cells at a dose of 2 Gray (Gy). This dose, daily administrated to GBM patients for six weeks during radiotherapy, was applied only once on our cells in order to be effective but subtoxic (Dahan et al., 2014) and preserve cell viability for all the duration of the experiment, independently of their actual and possibly different resistance to irradiation. Cells were plated on laminin-coated coverslips for 6 hours at 1, 3 and 6 days after the irradiation, and next were fixed and analyzed for their TNT content. While C1 cells showed a slight decrease, not statistically significant, in their TNT number after irradiation, TNT frequency was significantly increased in C2 cells the day following the irradiation (Figure Article 3A), suggesting an acute effect induced by the irradiation in this CNI+ -derived population. To assess the effect of irradiation on the transfer of mitochondria, 2 Gy irradiation was applied on the donor cells the day before the co-culture and transfer was quantified after 2 or 5 days of co-culture. The percentage of C1 acceptor cells containing donor-derived mitochondria was not affected by irradiation, whereas a tendency to an increased transfer upon irradiation was observed in C2 (Figure Article 3B), although not statistically significant. Potentially, the acute effect of irradiation on the induction of TNT in C2 resulted in an increased transfer of mitochondria, the result of which remained visible in the days following the irradiation. Of note, the growth curve showed significantly less C1 cells at 5 days after irradiation, compared to control cells, differently from C2 which were not affected in their proliferation upon the treatment (Figure Article 3C). Interestingly enough, C2, potentially more resistant to treatment because CNI+, responded by inducing TNT after irradiation, while C1 did not. These data showed that different GSLCs of the same patient are intrinsically different and have diverse response to irradiation regarding the effect on TNT formation and likely transfer function. This consistent with the wide heterogeneity present in GBM tumors where distinct molecular profiles coexist and exhibit differential therapeutic responses (Lathia et al., 2015).

4) **TNT-like structures exist in GSLC tumor organoids**

In order to study whether TNTs participate to GBM networking in a context more representative of the tumor, we cultured the GSLCs in tumor organoids according to the protocol published by J. Rich and colleagues (Hubert et al., 2016). Tumor organoid in culture are a relevant, 3-dimensional culture method, which allows long-term growth which has been shown to efficiently reconstitute the morphological and transcriptomic heterogeneity of the original tumor (Hubert et al., 2016). We were able to grow such tumor organoids using our GSLCs up more than 23 days of culture (Figure Article 4A), further showing that these cells, derived from the infiltrative area of patient tumor, were indeed able to reconstitute tumor's features. To date, TNT visualization in 3D cultures and their quantification had not been reported, as preserving and identifying these fragile thin structures in 3D is extremely challenging. Different types of cell protrusions were observed in these culture conditions (Figure Article 4B), including thin (<1 µm), actin-rich structures resembling TNTs that were found in organoids already within the first week of culture in both GSLCs. However, at this resolution we were not able to assess if these connections were functional TNTs or close-ended protrusions (like filopodia). To address this, we imaged tumor organoids prepared with GSLCs stably expressing MitoGFP construct. Several cell extensions were found to be rich in content of mitochondria. Of note, by using live-imaging we observed thin TNT-like connections containing mitochondria trafficking between two connected cells (Figure Article 4C, Supplementary Video 2, white arrow, and Supplementary Fig.2), in accordance with what was observed in 2D. Next, to quantify mitochondrial transfer, we prepared tumor organoids mixing MitoGFP donor and mCherry acceptor cells in a 1:1 ratio. After 6, 9, 13, 16, 20 and 23 days of co-culture inside the same organoids, organoids were desegregated in a single cell suspension and analyzed by flow cytometry for the presence of MitoGFP into acceptor mCherry-positive population. The percentage of acceptor cells receiving mitochondria was increasing over time, reaching around 3% in C1 and 8% in C2 after 23 days of culture. Higher efficiency of transfer was observed in C2 cells when comparing the general trend of the transfer with the one of C1 (Figure Article 4D), in agreement with the data obtained when cells were cultured in 2D. Mitochondria transfer was not related to cell proliferation as both GSLCs grow similarly in organoids (Figure Article 4E). Overall, these data were

consistent with the results obtained in 2D and suggested that C2 have higher ability to form and use TNTs for transferring cellular content than C1. To verify that mitochondria transfer was not due to secretion, we cocultured organoids composed of only one cell population, donor or acceptor cells, in the same medium. We have not observed any transfer of MitoGFP from donor organoids to acceptor organoids in these conditions over time, strongly suggesting that the mitochondria transfer that we quantified in mixed organoids was dependent on direct cell contacts between donor and acceptor cells. Therefore, our data strongly suggested that GSLCs have the ability to transfer mitochondria through thin TNT-like connections.

Interestingly, when staining actin and αTubulin, we observed that different types of connections were present in organoids (Figure Article 4B): i) thin (<1 µm) connections positive only for actin filaments, as the TNTs that we observed in 2D cultures, and ii) thick (>1 µm) and long protrusions containing both actin and microtubules, rather similar to TMs (previously observed *in vivo* (Osswald et al., 2015), but not in the 2D cultures).

To characterize the transcriptional changes undergone by the cells in tumor organoids over time, we quantified the expression of differentiation and progenitor/stem markers from 23-days-old organoids by RT-qPCR, including GAP43, a neuronal marker driving TMs formation (Osswald et al., 2015). We observed no significant variation in the expression of all tested genes, except of GAP43 in C2 cells (Figure Article 5A), that resulted to be 12-fold more in organoids compared to classical culture. This result showed that although most of the cells still expressed progenitor markers, maintaining therefore their pluripotency, some could also commit to a more differentiated profile, as it happens in real tumors. This was corroborated by immunofluorescence that showed an increase in the number of GAP43-positive C2 cells over time (see days 2, 6 and 13 labelling's in Figure Article 5B, and C), confirming that tumor organoids reproduced to some extent tumoral heterogeneity. In addition, we evaluated GAP43 labelling in TM-like protrusion by immunofluorescence in 6-day organoids. Part, but not all, of TM-like extensions resulted positive for GAP43 (Figure Article 5D) in C2. Of interest also, thick TM-like structures were found to be containing mitochondria in C1 and C2 organoids (Supplementary video 2, red arrow), similarly to the observations of Winkler and colleagues, although mitochondria transfer was not detected through such structures (Osswald et al., 2019). These results

showed that the 3D organoid model using GSLCs is a valid representation of the tumoral complexity *in vivo* (Hubert et al., 2016) and that different types of connections, including TNTs and TMs, could coexist in the network formed by both cell lines, as possibly in the real tumoral environment. However, only TNTs could provide a route for the exchange of cellular material, notably mitochondria.

5) **Effect of irradiation on TNT-based communication in GSLC cells in tumor organoids**

Next, we tested the effect of irradiation on TNT functionality in the tumor organoids derived from the two GSLCs population. 2 Gy irradiation was performed 5 days after tumor organoid preparation. Mitochondria transfer was assessed at different timepoints. In C1, 3% and 1.7% of transfer were observed at 23 days in control and irradiated condition, respectively, showing a significant decrease of transfer in the irradiated condition (Figure Article 6A). In C2, 8% and 7% of transfer were observed at 23 days in control and irradiated condition, respectively, with no significant reduction of their transfer efficiency over time (Figure Article 6A). This phenotype was independent of the effect of irradiation on cell growth as the number of cells into both organoids was not significantly affected by irradiation (Figure Article 6B), as expected with the chosen doses. Importantly, we did not observe either any transfer when co-culturing single population organoids in the same dish to assess secretion mechanisms of transfer. Overall, our data indicated that after irradiation, TNT functionality was preserved in C2 organoids whereas it was reduced in C1 organoids, suggesting that C2 TNT-based communication was more resistant to radiotherapy, again highlighting the different properties of these two GSLCs.

Discussion

Tunneling nanotubes (TNTs) are gaining an increasing relevance in the context of cancer development and progression (Pinto et al., 2020). Their presence and ability to transfer cellular material including organelles, has been correlated with the induction of migratory ability, angiogenesis, cell proliferation ad therapy-resistance (Hekmatshoar et al., 2018; Vignais et al., 2017). Few reports have addressed the presence of TNTs in GBM, where it was shown that GBM-derived cell lines were able to form TNT-like connections (Carone et al., 2015; Ding et al., 2015; Valdebenito et al., 2020) and even exchange mitochondria with the tumoral microenvironment (Civita et al., 2019; Formicola et al., 2019; Zhang & Zhang, 2015). Nevertheless, serum-cultured GBM cells lines appear to be drastically divergent from the original tumor at transcriptomic level (J. Lee et al., 2006). Indeed, TNTs were not observed in patient-derived GSCs, which when xenografted into murine brains, formed a complex tumor cell network based on TMs, thicker neurite-like connections (Osswald et al., 2015). Whether TNTs participate to this networking in a tumoral relevant model therefore remains unknown. To address this question, here we have assessed their presence and functionality in two GSLCs derived from two metabolically different areas of the same tumor (C1 for CNI- area, less metabolically active, and C2 for CNI+ area, more metabolically active). By using live-imaging and quantification of transferred mitochondria within both cell populations, we showed for the first time that GSLCs are able to interconnect and transfer mitochondria *via* TNT-like structures in 2D culture. Importantly, to visualize and characterize these connections and to monitor their ability to transfer mitochondria in a context closer to the tumor, we cultured GSLCs in tumor organoids, where we showed that they maintained their progenitor characters over more than 23 days of culture. This organoid model is very relevant, since it recapitulates at transcriptomic level (Hubert et al., 2016) and cell level (this work) the cell heterogeneity and networking observed in patient tumors. We provided live-imaging showing mitochondria moving along TNTs and entering into the connected cells, therefore demonstrating for the first time that TNTs exist and are functional in tumor organoids and suggesting that TNT-based communication may be relevant in the actual tumor. Interestingly in GSLCs tumor organoids, we also observed thicker connections resembling TMs (Osswald et al., 2015). TMs are neurite-like extensions (Jung et al., 2019), able to

connect to distant cells and propagate action potential (Venkataramani et al., 2019; Venkatesh et al., 2019) and proposed to scaffold the network formed by cancer cells. Although TMs are organelle-rich structures, no cargo transfer through them has been demonstrated (Osswald et al., 2019), while the presence of GAP-junctions along their length (Osswald et al., 2015) support their role in electric signal transmission. Our data confirmed these observations in organoids, since we could follow movements of mitochondria in cell bodies and protrusions, including TM-like structures. However, the effective transfer of mitochondria until entering a connected cell could be observed only through TNT-like connections, and not in TM (Osswald et al., 2015; Venkataramani et al., 2019; Weil et al., 2017). Of note, we observed and quantified mitochondria transfer in both C1 and C2 GSLCs, in 2D conditions where none of them expressed GAP43, which is a typical marker and the major known driver of TMs (Osswald et al., 2015; Weil et al., 2017), and in 3D where only C2 subpopulations began to express GAP43, strongly suggesting that the transfer of mitochondria through TNT-like connections does not occur through GAP43-dependent structures. Notwithstanding, we observed that C2 cells, which can express GAP43, were transferring mitochondria more efficiently compared to C1 cells, even after irradiation. These results are in accordance with the work of F. Winkler (Osswald et al., 2015; Weil et al., 2017) suggesting that GAP43 expression could be correlated to the aggressiveness of the tumor. From our work, we propose that TNTs and TMs coexist and cooperate in GBM networking, carrying on complementary roles that could participate eventually to treatment-resistance. In particular, we hypothesize that in a situation in which a TM tumor network is formed based on signalling exchanges between interconnected cells there will be the possibility to form more TNTs, which will provide the transfer function and material exchange (Fig.7). In our GSLC model we have chosen to specifically look at mitochondria transfer; as mitochondria can provide metabolic support to cancer cells (Hekmatshoar et al., 2018; Vignais et al., 2017), transfer of mitochondria has been shown to modulate the response to treatments in a beneficial manner for the recipient cells impacting on their metabolism, rescuing their aerobic respiration and providing a metabolic support against treatment-related stress (Vignais et al., 2017; Xiaoqing Wang et al., 2016). However the observation of mitochondria transfer between GSLCs does not preclude the possibility that other cellular material (e.g. RNA, proteins, other vesicles) could be additionally transferred through the same connections, as

observed in other cancer types (Connor et al., 2015; Desir et al., 2019; Kretschmer et al., 2019).

Wide cellular heterogeneity is one of the many reasons that make GBM very difficult to treat. We have shown that two GSLCs derived from different tumor areas of the same patient, potentially correlating with different aggressiveness, display different behaviour, including the percentage of TNT-connected cells and transfer of mitochondria over time in response to irradiation. C2 (CNI+) cells, derived from the highest metabolic part of the tumor , previously shown to be predictive of the site of the relapse after irradiation(Laprie et al., 2008), are the cells where TNT functionalities are more active and resistant to irradiation. Overall, our data are consistent with tumor networking being important in GBM progression, resistance to treatment and relapse. In addition to TMs, the ability to grow functional TNTs could participate to the formation of a functional tumor network (Fig.7). In the future, it will be interesting to further investigate the relevance of these data in further cases and to exploit them by considering inhibition of TNT-dependent transfer as a new way for optimization of radiotherapy efficacy in GBM.

Conclusions

Our data suggest that TNT-mediated exchange of cellular material occurs between GSCs and that TNTs participate to GBM tumoral networking providing a route for the transfer of intracellular material and potentially contributing to tumor progression and treatment-resistance.

Figures

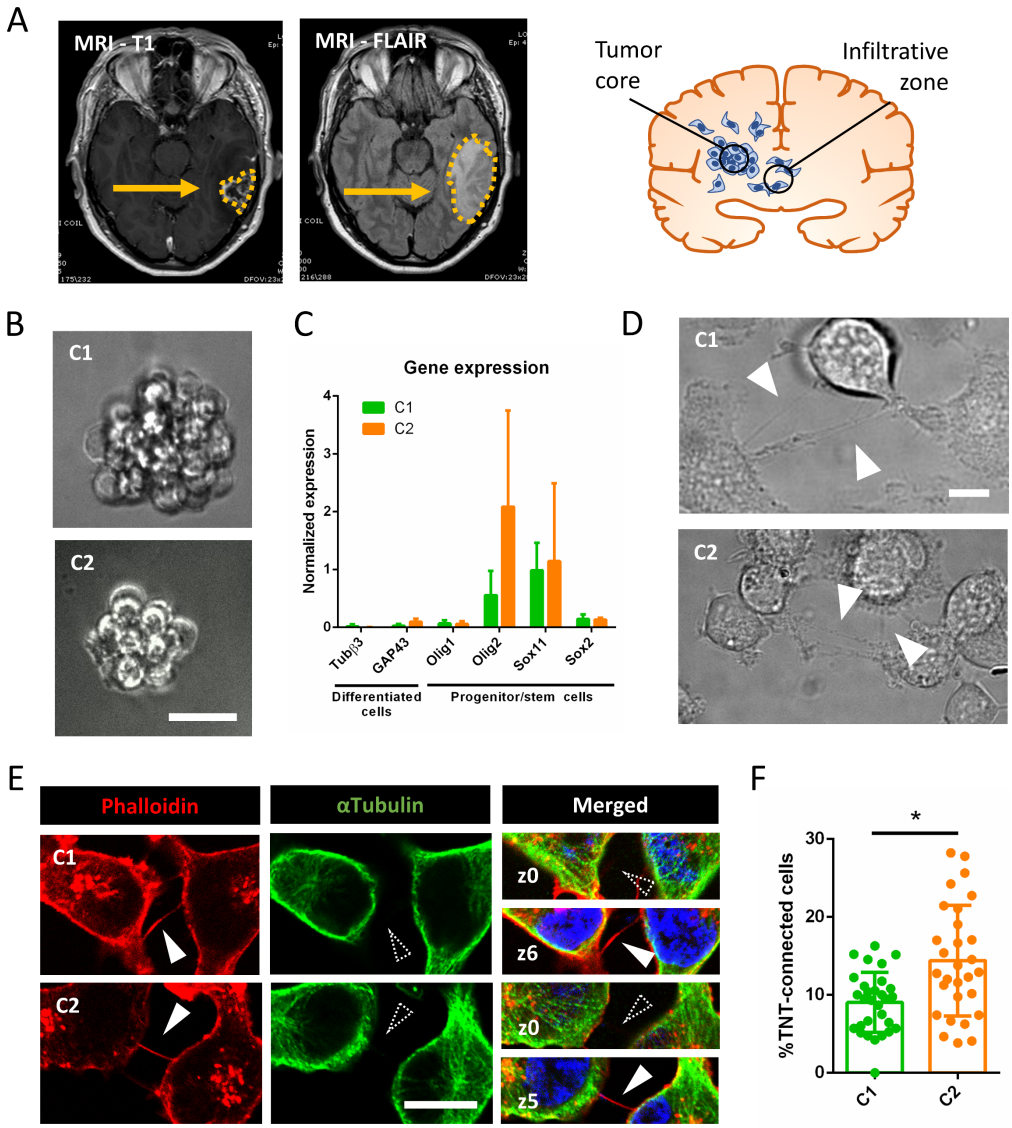

Figure Article 1. GSLCs form TNT-like structures.

(A) MRI analysis of SRC patient glioblastoma. The tumor is composed by a compact cellular part defined 'Tumor core', identified by MRI T1-Gadolinium (on the left). Some tumoral cells infiltrate the normal tissue, forming the 'Infiltrative zone' which is identified by MRI-FLAIR (right picture and schematics). C1 and C2 cells were obtained from different parts of the infiltrative zone. (B) C1 and C2 cell growth, forming neurosphere-like clusters in suspension. The resulting images represents a Z-projection of 30 and 50 slides (step size: 0.5 µm), respectively, acquired in Bright field using 40X magnification. (C) Expression of differentiation and progenitor/stem cells markers in C1 and C2, respectively in green and orange. The relative gene expressions were quantified by RT-qPCR after RNA extraction. Data were normalized over the expression of HPRT, housekeeping

gene. GFAP and CHI3L1 showed no expression in both C1 and C2 and are not represented on the graph. The graph represents the means with SD of 5 independent experiments, each point performed in triplicate. P values > 0.05 are not significant and not indicated on the figure. (D) Representative images of GSLCs connected by TNT in live imaging in 2D culture. Cells were seeded on laminin-coated plates and pictures were taken after 6h of seeding using 60 × 1.4NA CSU oil immersion objective lens using Bright field. Arrowheads point to TNT-like connections. (E) GSLC TNTs containing actin but not microtubules. Cells were plated on laminin-coated surface, stained with phalloidin (actin filaments, red), anti-αTubulin (microtubules, green) and DAPI (nuclei, blue). Representative images were acquired showing TNTs, actin-positive and αTubulin-devoid, floating above the dish surface. White-filled arrowhead indicates presence of TNT labelling, dashed arrowhead indicated absence of TNT staining. (F) Quantification of TNT-connected cells in C1 and C2, respectively in green and orange. GSLC were plated on laminin-coated surface, fixed after 6h and stained with WGA. 2x2 tiles images were acquired with 60x objective and analysed by Icy software. C1 were forming 9.0±4% of connecting cells (n=5, n cells=1239), while C2 were forming 14.4±7% (n=4, n cells=1367), significantly more connected cells than C1 (p=0.0370). Each dot represents an observation. P-values were deduced from contrast comparing the two cell populations in a logistic regression model. Error bar = standard deviation. P value < 0.05 (*). Scale bar = 10 µm.

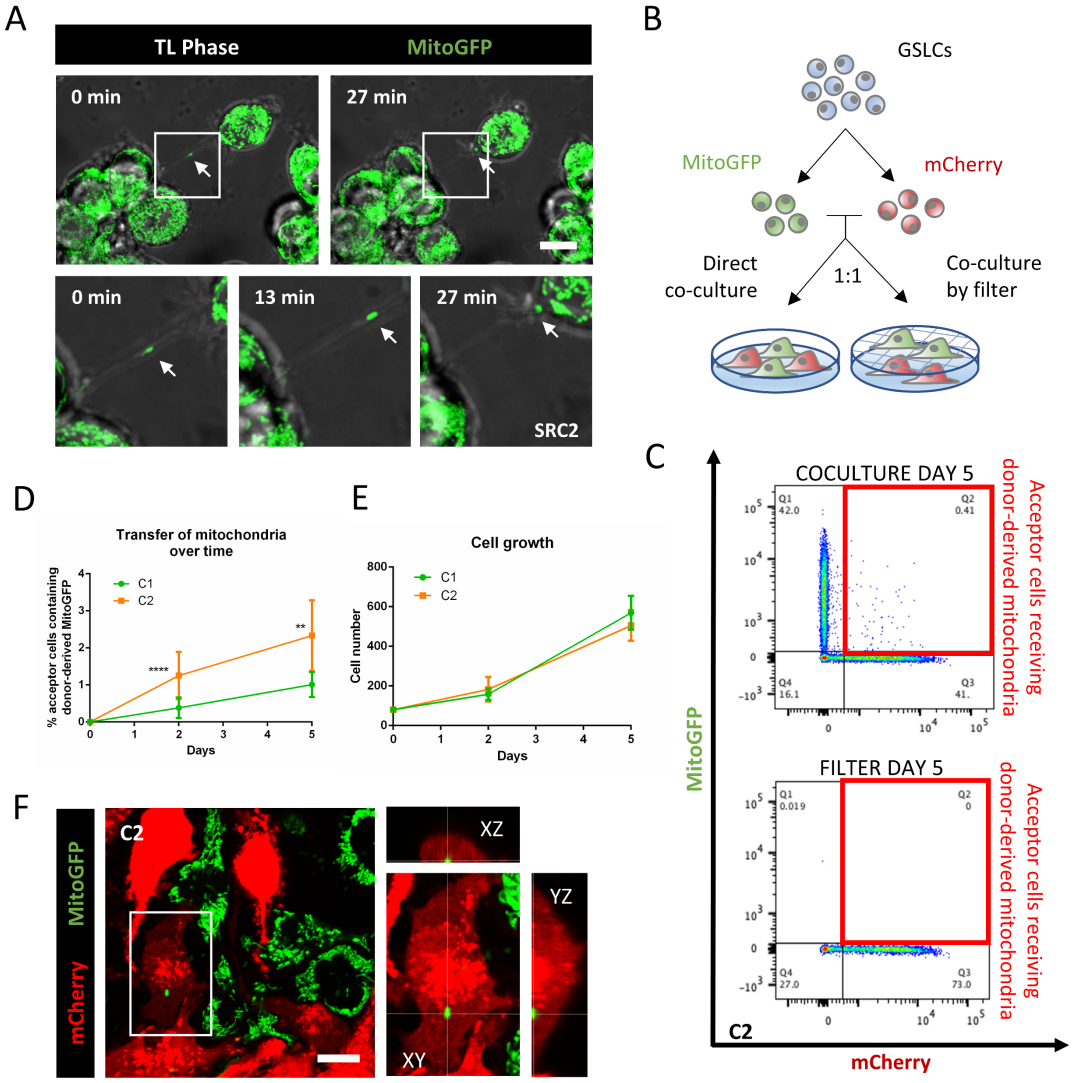

Figure Article 2. GSLCs transfer mitochondria through TNTs.

(A) C2 expressing MitoGFP are connected by TNTs containing mitochondria. Cells were seeded on laminin-coated dish and after 6 hours video were acquired using Bright field and laser 488 in a Spinning Disk microscope. Timeframes show the mitochondria moving along the connection and entering in one of the two connected cells. Each timeframe of the video is the result of the Z-projection of 18 slides (step size: 0.5 µm) (B) Schematic representation of the coculture experiment. Donor MitoGFP cells were co-cultured with acceptor mCherry cells at 1:1 ratio either by direct contact or through a 1 µm filter. (C) Representative flow cytometry plot of C2 after 5 days of coculture. Acceptor and donor cells respectively lie on the X and Y axis. Acceptor cells positive for MitoGFP signal are framed in the red boxes. (D) Quantification by flow cytometry of the mitochondria transfer over time in C1 and C2, respectively in green and orange. A minimum of 10000 events were analyzed after 2 or 5 days of coculture. C1 shows 0.38±0.27% and 1.01±0.33% of acceptor cells receiving mitochondria after 2 and 5 days, respectively (n=4). C2

shows 1.25±0.63% and 2.33±0.95% of acceptor cells receiving mitochondria after 2 and 5 days, respectively (n=5), significantly more than C1 ($p<0.0001$ (****) at day 2, $p=0.0085$ (**) at day 5). P-values were deduced from contrast comparing the two cell populations in a logistic regression model. Error bar = SD (E) Cell growth in co-culture experiment. 80000 GSLCs per well were plated at time 0 and counted after co-culture. For C1, 158000±28751 and 568866±85332 cells were counted after 2 and 5 days, respectively (n=3). For C2, 182900±61890 and 505260±77515 cells were counted after 2 and 5 days, respectively (n=5). Error bar = SD. ANOVA two-way test was performed and showed no significant difference between C1 and C2 at the two timepoint in analyse. (F) Representative image of co-culture assay in C2. Donor MitoGFP (in green) and acceptor mCherry cells (in red) were fixed after 5 days of co-culture, confocal images were acquired with 63x objective. In the magnification, the orthogonal view of an acceptor cell containing donor-derived mitochondria. Scale bar = 10 µm.

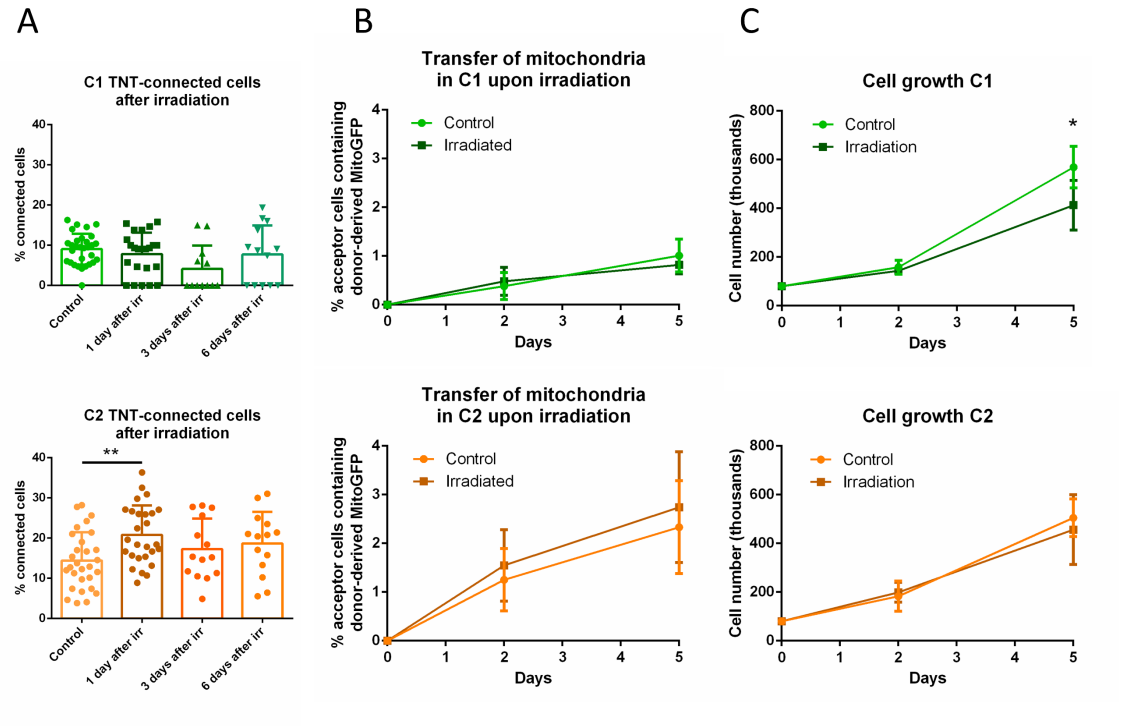

Figure Article 3. Effect of irradiation on GSLCs on TNT-based communication.

(A) Quantification of TNT-connected cells in C1 and C2 after irradiation, respectively in green and orange. GSLCs were irradiated 1 day before cell plating on laminin-coated surface, then fixed after 6h and stained with WGA. 2x2 tiles images were acquired with 60x objective and analysed by Icy software. The graphs represent means with SD. C1 were forming 7.8±5% (n=4, n cells=891), 4.1±6% (n=3, n cells=300) and 7.7±7% (n=3, n cell=313) of connecting cells after 1, 3 and 6 days from the irradiation, respectively. No statistical significant difference was observed compared to control (9.0±4%, n=5, n cells=1239). C2 were forming 20.8±7% (n=4, n cells =1368), 17.3±7% (n=3, n cell=552) and 18.7±8% (n=3, n cells=462) of connecting cells after 1, 3 and 6 days from the irradiation, respectively. A statistically significant increase was observed 1 day after irradiation compared to control (14.4±7%, n=4, n cells=1367, p=0.0073 (**)). Each dot represents an observation. P-values were deduced from contrast comparing the two cell populations in a logistic regression model. (B) Quantification of the mitochondria transfer by flow cytometry in both GSLCs over time in C1 and C2 upon irradiation, respectively in green and orange. Donor GSLC were irradiated 1 days before the co-culture, analysis was performed after 2 or 5 days (corresponding at 3 and 6 days from the irradiation). A minimum of 10000 events were analyzed per condition. In irradiated condition, C1 show 0.48±0.28% and 0.81±0.18% of acceptor cells receiving mitochondria after 2 and 5 days, respectively (n=4). No statistical significant difference was observed compared to control (day 2: 0.38±0.27%; day 5 1.01±0.33%; n=4). In irradiated condition,

C2 show 1.54±0.73% and 2.74±1.13% of acceptor cells receiving mitochondria after 2 and 5 days, respectively (n=5). No statistical significant difference was observed compared to control (day 2: 1.25±0.63%; day 5: 2.33±0.95%. n=5). P-values were deduced from contrast comparing the two cell populations in a logistic regression model. Graphs are means with SD. (C) Cell growth in irradiated co-culture experiment, as in fig 2E. For C1, 143970± 6653 and 413000±101930 cells were counted after 2 and 5 days, respectively, in the co-culture with irradiated cells (n=3). A significant reduction of cells was observed at day 5 compared to control condition (day 2: 158000±28751; day 5: 568866±85332, n=3). For C2, 199080±40341 and 456260±143521 cells were counted after 2 and 5 days, respectively, in the co-culture with irradiated cells (n=5). No significant difference was observed compared to control at the two timepoint in analyse (day 2: 182900±61890, day 5: 505260±77515, n=5). ANOVA two-way test was performed. P value < 0.05 (*), P values > 0.05 are not significant and not indicated on the figure.

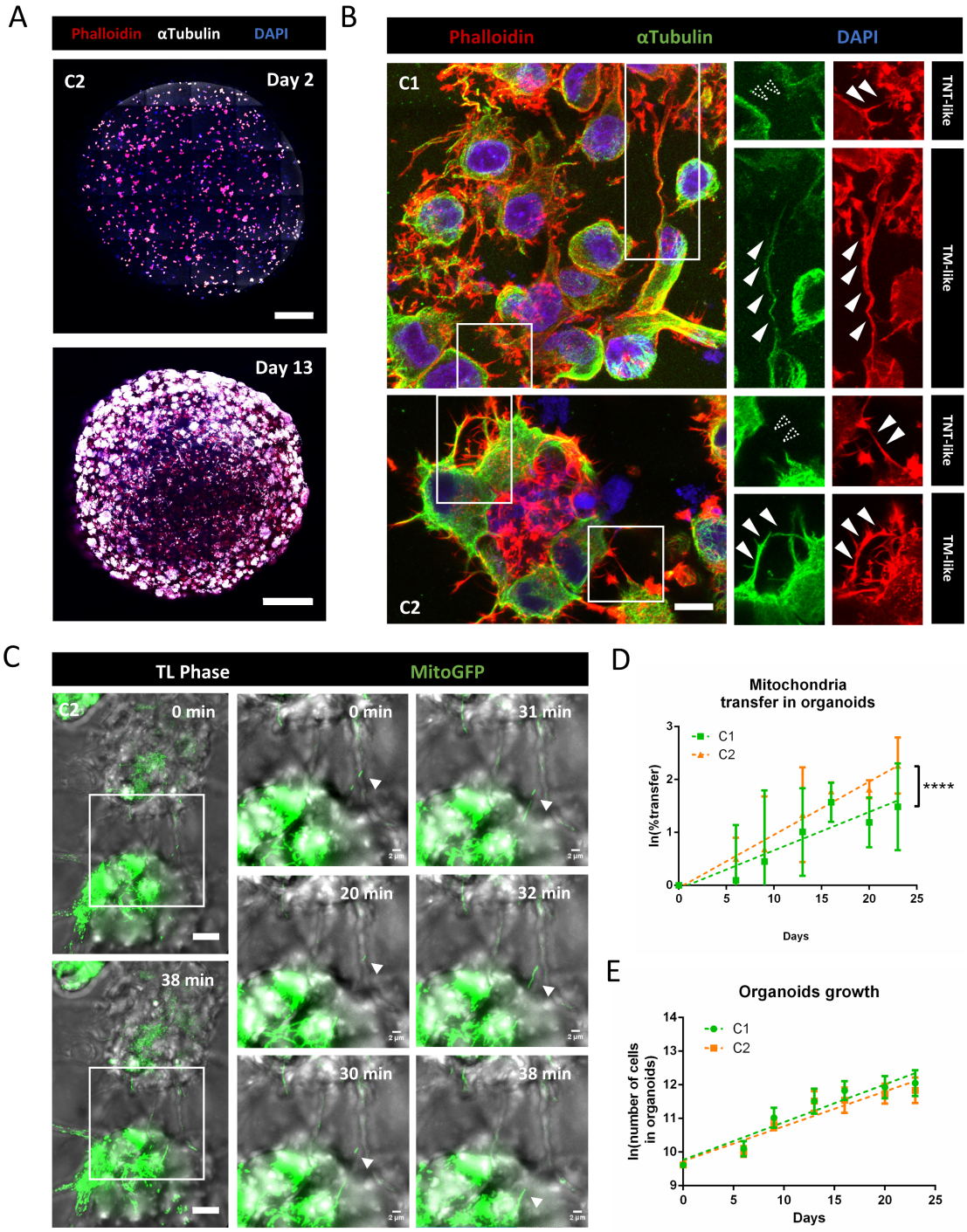

Figure Article 4. GSLCs in tumor organoids.

(A) Representative fluorescence images of the whole C2 tumor organoid at 2 and 13 days of growth using Pln-Apo 10X/0.45 objective confocal LSM700 inverted. The resulting images represent a max intensity projection of 5 and 31 sections (step size: 7 and 3.12µm), respectively, stained for anti-αTubulin (microtubules, white), Phalloidin (actin red) and nuclei (blue). Scale bars are 200 (top) and 500 µm (bottom). (B) Representative pictures of C1 and C2 tumor organoids at 9 and 6 days, respectively, stained for anti-αTubulin (microtubules, green), Phalloidin (actin

filaments, red), and nuclei (blue). Confocal images were acquired with 40X objective. Region of interest show either αTubulin-devoid connections, defined as TNT-like (<1 µm), or thick αTubulin-positive connections (>1 µm), named TM-like. Dashed arrowheads indicate absence of fluorescent signal at the connection level, white-filled arrowhead show positiveness to the signal. Both images are max intensity projections of 12 slices (step size: 0.38 µm). Scale bar = 10 µm. (C) TNT-like connection between C2 cells containing mitochondria in 6-days old tumor organoids. Timeframes result of the max projection of 62 slides (step size: 0.5µm) with a total physical thickness of 31µm, with 1 minute of interval time. White arrows point to the mitochondria movement inside the TNT at the different time points. Video were acquired using Bright field and laser 488 in a Spinning Disk microscope. (D) Quantification of the mitochondria transfer in tumor organoids over time in C1 and C2, respectively in green and orange. Organoids were prepared mixing donor and acceptor cells for each GSLC. Duplicates of a pool of 3 organoids were dissociated in a single cell suspension and fixed for flow cytometry analysis after 6, 9, 13, 16, 20 and 23 days of culture. All the cells in the suspension were analyzed to obtain the percentage of acceptor cells receiving mitochondria. C1: day 6 1.54±1.4%; day 9 2.80±2.9%; day 13 2.20±1.1%; day 16 5.07±2.06%; day 20 3.55±1.5%; day 23 3.05±0.84% (n=4). C2: day 6 1.72±0.7%; day 9 2.64±2.2%; day 13 4.96±4.35%; day 16 5.98±1.02%; day 20 5.57±0.03%; day 23 8.37±2.7% (n=3). Percentage of transfer was transformed into a logarithmic scale. Error bar = SD. P-values are deduced by comparing the slopes of the two cellular population in a logistic regression model as described in material and methods. P value < 0.0001 (****) (E) Cell number in tumor organoids. Duplicates of a pool of 3 organoids were dissociated in a single cell suspension C1: day 6 24800±5768; day 9 63150±18350; day 13 105850±43970; day 16 140450±33929; day 20 158600±60394 day 23 181800±78820 (n=4). C2: day 6 22600±3704; day 9 49700±8116; day 13 104200±33870; day 16 108580±42218; day 20 128800±34478; day 23 145080±47726 (n=4). The cell number was transformed into a logarithmic scale and slopes were compared by linear regression (dashed lines). No significant difference was observed between C1 and C2.

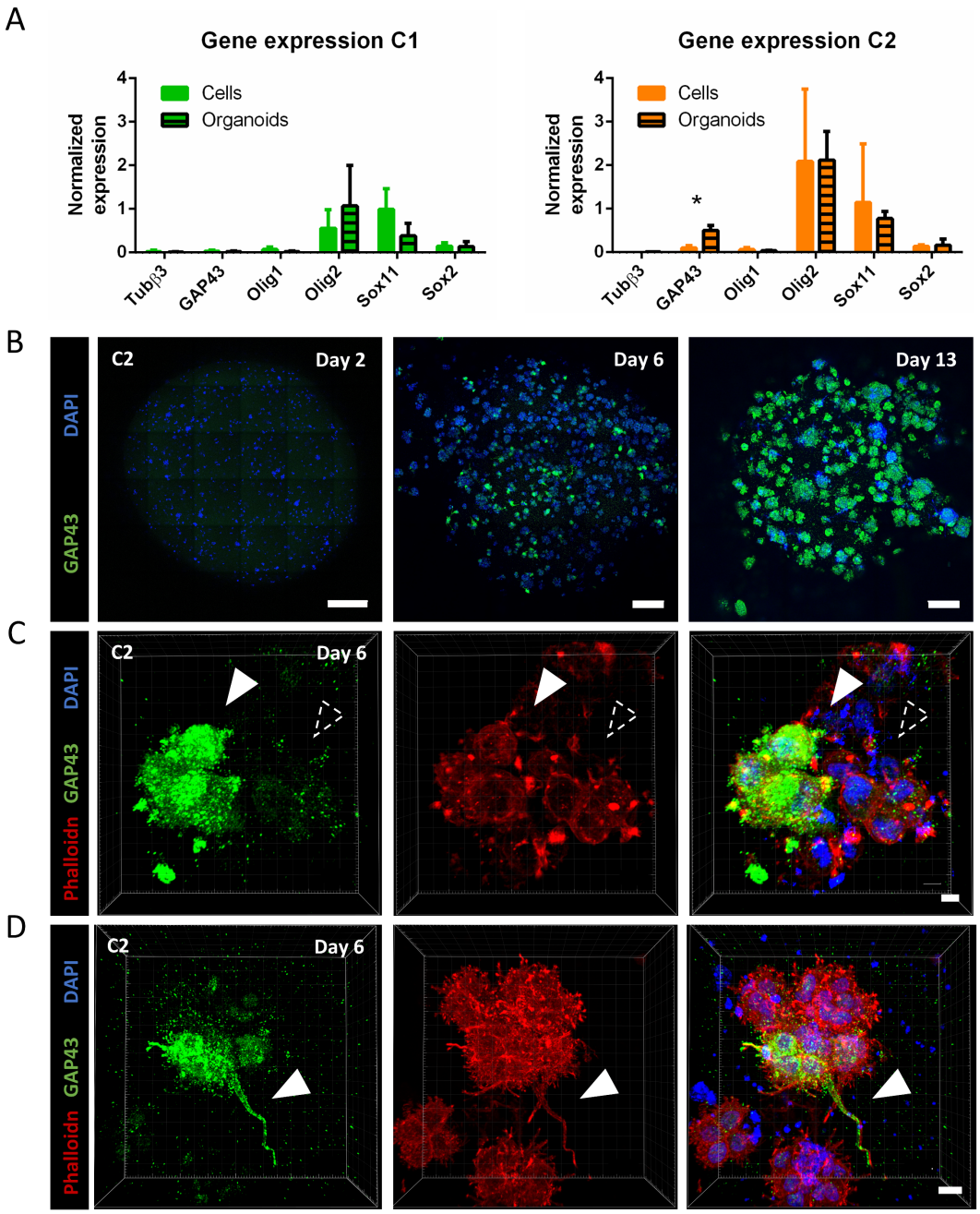

Figure Article 5. GAP43 expression and TM characterization in tumor organoids of GSLC cells.

(A) Expression of differentiation and progenitor/stem cells markers in C1 and C2 organoids, respectively in green and orange. The relative gene expressions were quantified by RT-qPCR after RNA extraction from 23-days-old organoids, normalized over the expression of HPRT. Note the 12-fold increased expression of GAP43 in C2 tumor organoids, and GFAP and CHI3L1 show no expression in both conditions and are not represented on the graph. The graphs represent means with SD of 3 and 4 independent experiments for C1 and C2 respectively, each point performed in triplicate. Holm-Sidak method was applied to determine statistical significance between cells and

organoids for each gene. P value < 0.05 (*), P values > 0.05 are not significant and not indicated on the figure. (B) GAP43 protein expression increases over time. 2, 6 and 13 days-old organoids were fixed and stained with anti-GAP43 (in green) and DAPI (in blue). Confocal images with 10x objective were acquired. Images result from the max intensity projection of 5, 20, 11 sections (step size: 7, 3.13, 3.13 µm), respectively. Scale bars: 500 µm, 200 µm, 200 µm (from left to right). (C) Heterogeneous expression of GAP43 in C2 tumor organoids. 6 days-old C2 organoids were fixed and stained with anti-GAP43 (in green), phalloidin (actin filaments, in red) and DAPI (in blue). Confocal images with 63x objective were acquired. 3D reconstruction of a 50-sections image (step size: 0.33 µm) was performed using Imaris Viewer software. White-filled arrowhead point to a cluster of cells expressing GAP43, alternatively a group of cells negative for its expression are indicated with a dashed arrowhead. Scale bar: 5 µm. (D) TM-like protrusion can express GAP43 in C2 organoids. 6 days-old C2 organoids were fixed and stained with anti-GAP43 (in green), phalloidin (actin filaments, in red) and DAPI (in blue). Confocal images with 63x objective were acquired. 3D reconstruction of a 77-sections image (step size: 0.77 µm) was perfomed using Imaris Viewer software. White-filled arrowheads point toward a TM-like extension expressing GAP43. Scale bar: 15 µm. 3D reconstructions were performed with Imaris Software.

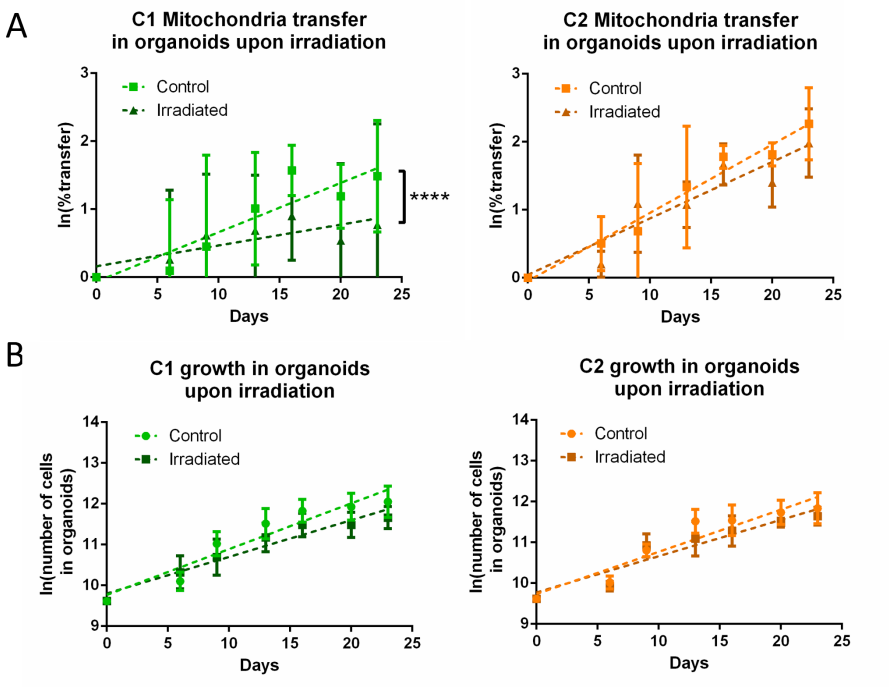

Figure Article 6. Effect of irradiation on tumor organoids.

(A) Quantification of the mitochondria transfer in tumor organoids upon irradiation in C1 and C2, respectively in green and orange. Organoids were prepared mixing donor and acceptor cells for each GSLC and irradiated at 5 days from their preparation. Experiment was performed as in Fig 4D. Control C1: day 6 1.54±1.4%; day 9 2.80±2.9%; day 13 2.20±1.1%; day 16 5.07±2.06%; day 20 3.55±1.5%; day 23 3.05±0.84%. Irradiated C1: day 6 1.90±1.6%; day 9 4.45±1.9%; day 13 2.50±1.7%; day 16 2.82±1.5%; day 20 2.39±1.61%; day 23 1.76±1.2% (n=4). Control C2: day 6 1.72±0.7%; day 9 2.64±2.2%; day 13 4.96±4.35%; day 16 5.98±1.02%; day 20 5.57±0.03%; day 23 8.37±2.7%. Irradiated C2: day 6 1.23±0.2%; day 9 3.50±2.3%; day 13 3.03±0.9%; day 16 5.46±1.5%; day 20 4.23±1.3%; day 23 7.21±1.7% (n=3). Percentage of transfer was transformed into a logarithmic scale. P-values are deduced by comparing the slopes of the two cellular population in a logistic regression model as described in material and methods. ($p<0.0001$, ****). (B) Effect of irradiation on cell number in tumor organoids. Irradiation was performed after 5 days from the organoid preparation. Duplicates of a pool of 3 organoids were dissociated in a single cell suspension and counted at each timepoint. Control C1: day 6 24800±5768; day 9 63150±18350; day 13 105850±43970; day 16 140450±33929; day 20 158600±60394 day 23 181800±78820. Irradiated C1: day 6 24767±14749; day 9 47100±18499; day 13 74700±28446; day 16 100050±32374; day 20 100700±32051; day 23 119000±29480 (n=4). Control C2: day 6 22600±3704; day 9 49700±8116; day 13 104200±33870; day 16 108580±42218; day 20 128800±34478; day 23 145080±47726. Irradiated C2: day 6 16667±6853; day 9 57150±16787; day

13 70250±29190; day 16 83400±29947; day 20 97725±10594; day 23 115600±23118 (n=4). The cell number was transformed into a logarithmic scale and slopes were compared by linear regression (dashed lines). No significant difference was observed between control and irradiated condition in both GSLCs. Error bar = SD.

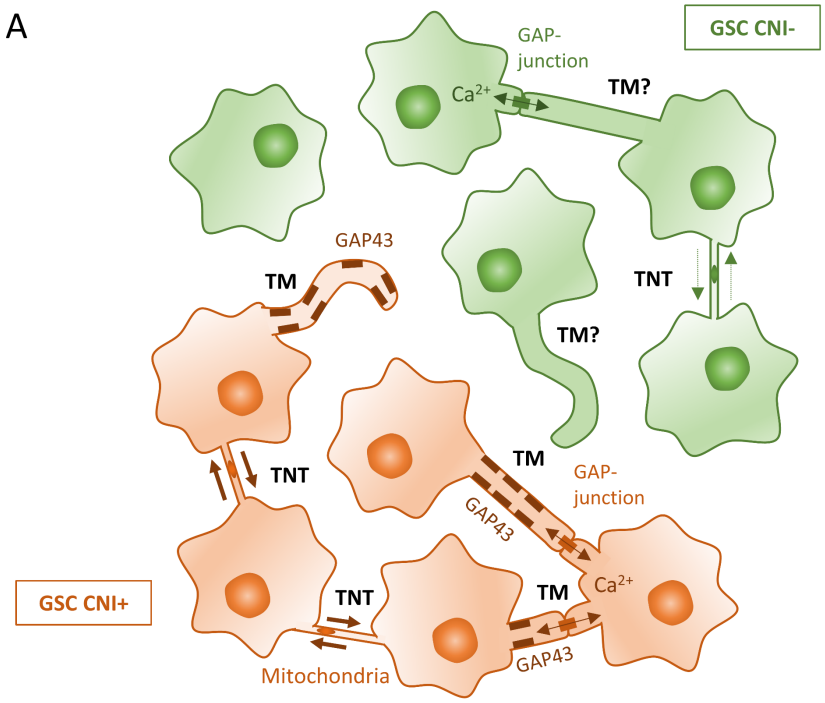

Figure Article 7. GSLC network. GSLCs interconnect through different types of cellular extensions.

TMs are thick (>1µm) protrusions that can either contact other cells through GAP-junctions, allowing the propagation of calcium flux, or be individual finger-like extensions not connecting remote cells. They can be positive for GAP43 (rectangles along the membranes of TM), neuronal Growth-Associated Protein. GSLCs also interconnect through TNTs, thinner (<1µm), open-ended connections which allow transfer of cellular cargos, such as mitochondria (ovals in TNTs). Tumoral heterogeneity is composed by areas with different metabolic ability, here classified by CNI parameter as - (less active, green) and + (more active, red). CNI+ form more TNT connections which allow mitochondria transfer.

Supplementary Figures

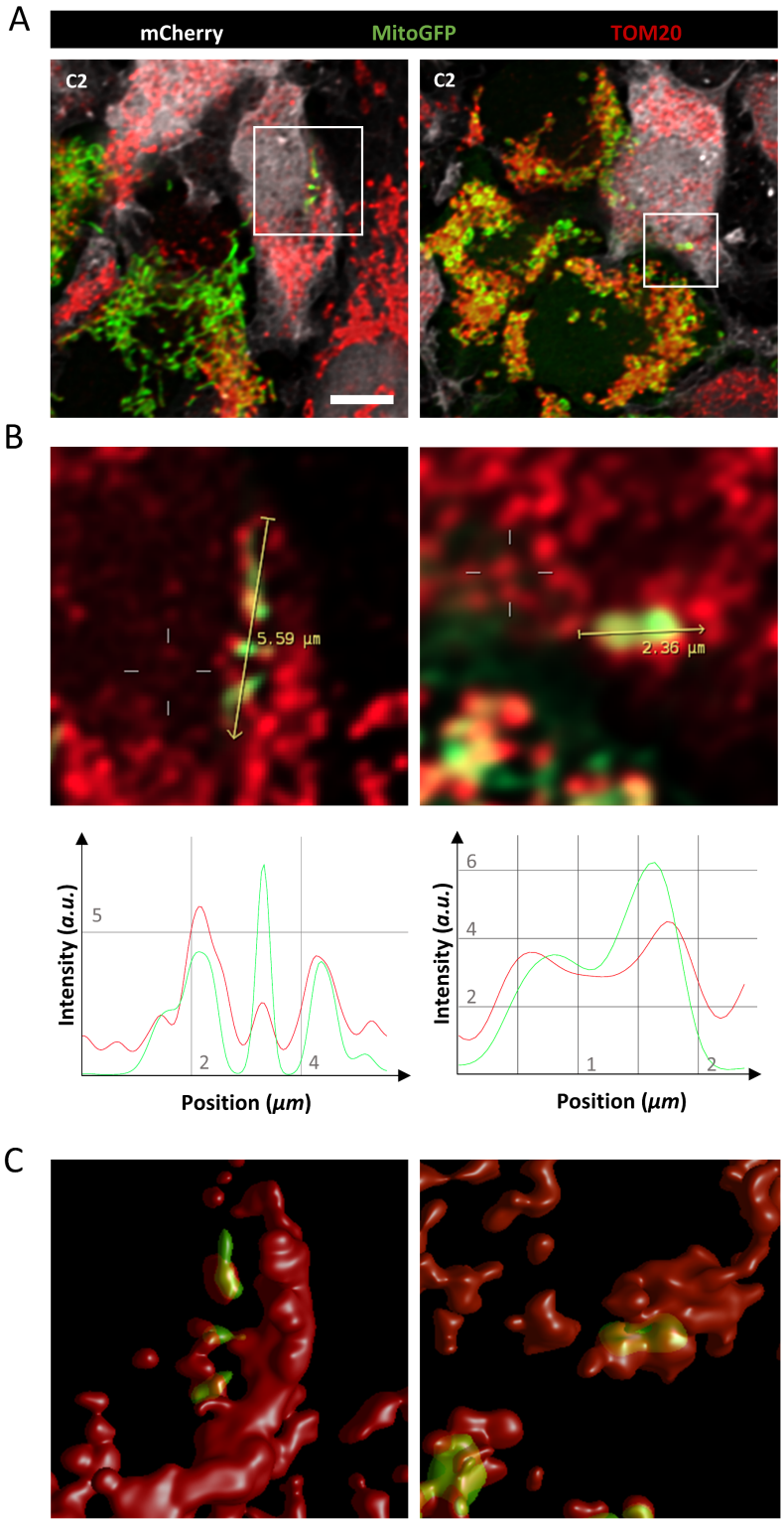

Supplementary Figure 1. MitoGFP signal in acceptor cells match with TOM20 mitochondrial marker staining.

(A) C2 MitoGFP (in green) and mCherry (in white) cells were co-cultured over 5 days on laminin-coated coverslips, then fixed and stained with anti-TOM20 (in red), mitochondrial marker. Confocal images were acquired with 63x objective and deconvolved with Huygens software. Acceptor cells containing donor-derived MitoGFP signal overlapping wit TOM20 staining were observed (z-stack=2; step size= 0.35 µm), Scale bar 5 µm. (B) A yellow arrow was drawn along the green mitochondria to obtain the intensity profile of MitoGFP and TOM20 signal. The two curves follow a similar trend. (C) The deconvolved 3-dimentional images of the area of the acceptor cells containing MitoGFP were reconstituted with Huygens Software. These images show volumes covered by MitoGFP and TOM20 signals and their overlap.

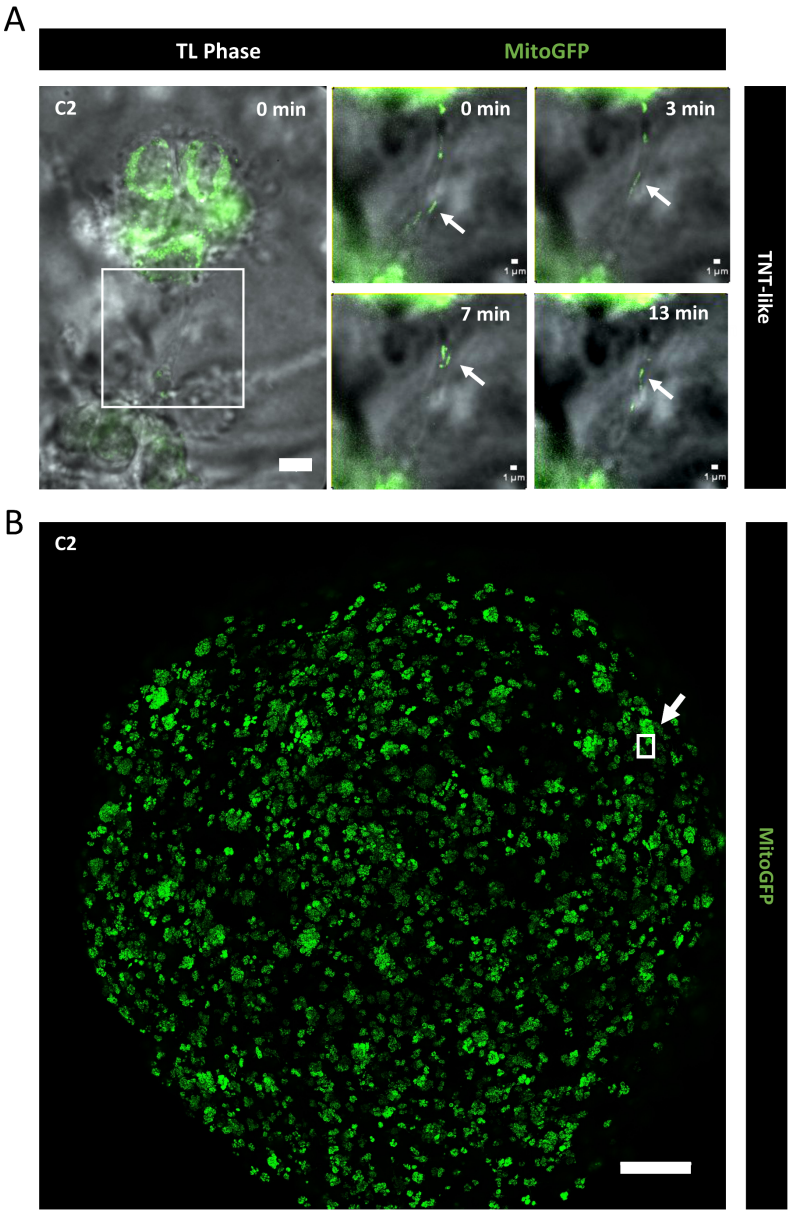

Supplementary Figure 2. Movement of mitochondria by live-imaging in C2-tumor organoids inside TNT-like connections.

(A) C2 MitoGFP tumor organoids were imaged at 7 days of culture, images composed of 25 z-stacks were acquired every 1 min for 13 min (step size 0.45 µm, total thickness ~12µm) acquired with transmitted light and green fluorescence (MitoGFP). Right panel show an overall vision of the TNT-like connection inside the tumor organoid a time 0 min. In the left panel are shown the areas magnified at different time points from 0 up time 13 min. White arrow points at mitochondrion inside the TNT-like connection. Scale bar: 10 µm. (B) 7 days-old C2 MitoGFP tumor organoids was fixed after the live-imaging and imaged by confocal microscopy. This image is the result of the z-projection of 11 stacks with 6 µm of step for a total thickness of 66 µm. The white frame with

arrow is representative of the size of area where the live-imaging video was acquired, not of the specific location. Scale bar: 400 µm.

Supplementary Video Legends

Supplementary Video 1. Movement of mitochondria along TNT-like connections in 2D-conditions.

C2 MitoGFP cells were plated on laminin-coated surface and imaged after 6h. 18-z-stacks images were acquired every 1 min for 27 min (step size: 0.47 µm) with merged transmitted light and green fluorescence (MitoGFP). The movie, resulting from the max z-projection of each time-frame, shows the transfer of mitochondria between two C2 cells expressing MitoGFP and connected by TNT-like connection in 2D culture. Scale bar 10 µm.

Supplementary Video 2. Transfer of mitochondria via TNT-like connections in tumor organoids.

C2 MitoGFP tumor organoids were imaged at 6 days of culture, images composed of 62 z-stacks were acquired every 1 min for 38 min (step size 0.45 µm, total thickness ~28 µm). On the left panel, video corresponding to the merge of time-frame images acquired with transmitted light and green fluorescence (MitoGFP). Only green fluorescence image is shown in the right panel, for better visualization. Videos are resulting from the max-z-projection. White and red arrows point at the movement of mitochondria inside TNT- and TM-like connections, respectively. Scale bar 10 µm.

Supplementary Video 3. Motion of mitochondria inside TNT-like connections in tumor organoids.

C2 MitoGFP tumor organoids were imaged at 7 days of culture, images composed of 25 z-stacks were acquired every 1 min for 13 min (step size 0.45 µm, total thickness ~12µm). Video corresponds to the merge of time-frame images acquired with transmitted light and green fluorescence (MitoGFP). White arrow points at mitochondrion inside the TNT-like connection. Scale bar 10 µm.

Material and Methods

Cell culture

The GBM samples were processed as described by (Avril et al., 2012). GSLCs were cultured in suspension in DMEM-F12 (Sigma D8437) supplemented with B27 (50x Gibco 17504-44), N2 (100x Gibco 17502-048) and 20 ng/ml of FGF-2 (Peprotech 100-18B) and EGF (Peprotech AF-100-15) at 37°C in 5% CO_2 humidified incubators. Fresh medium was added to the cell culture every 2-3 days. All GSC lines were used for the experiments in this medium at less than 25 passages. Absence of alteration upon culture passages on the stemness phenotype was monitored by RT-qPCR. Absence of mycoplasma contamination was verified with MycoAlert™ Mycoplasma Detection Kit (Lonza LT07-118). All methods were carried out in accordance with the approved guidelines of our institution.

Lentivirus preparation and transduction

Lentiviral particles have been produced using the cell line 293T cultured in Dulbecco's Modified Medium (ThermoFisher 31966-021) supplemented with 10% Fetal Bovine Serum (EuroBio CVFSVF00-01) and 1% Pen/Strep (100x Gibco 10378016) at 37°C in 5% CO_2 humidified incubators. Cells were plated at a 50-70% confluency the day before the transfection. Transfection mix was prepared in serum-free OptiMEM (ThermoFisher 51985-026) medium, using FuGENE HD Trasfection reagent protocol (Promega E2311). Plasmids coding for lentiviral components, pCMVR8,74 (Gag-Pol-Hiv1) and pMDG2 (VSV-G) vectors, and plasmid of interest were added in the transfection mix at a ratio of 4:1:4 µg, respectively. MitoGFP (pLV-CMV-mito-GFP) and mCherry (pLV-CMV-mCherry) plasmids encode respectively for a fragment of the subunit VIII of human cytochrome C oxidase fused with GFP, and for cytosolic mCherry under the Cytomegalovirus (CMV) promoter. After 48 hours the culture medium was collected for the concentration of the lentiviral particles using LentiX-Concentrator (TakaraBio 631231). GSLCs were infected and tested for the expression of the fluorescent marker by flow cytometry at different time points to monitor expression stability. Potential modification to stemness gene expression following the infection were monitored by RT-qPCR.

Tumor organoids preparation and culture

Tumor organoids were prepared accordingly to the protocol published in Hubert et al., 2016. GSLCs neurospheres were mechanically dissociated and counted. For the preparation of 100 organoids, 1,500,000 cells were centrifugated at 1200 rpm, supernatant was completely removed, and cells were homogeneously resuspended in 400 µL of complete Neurobasal medium (ThermoFisher 21103-049) supplemented with B27 (50x Gibco 17504-44), N2 (100x Gibco 17502-048), 1% Pen/Strep (100x Gibco 10378016), 2 mM L-Glutamine (100x Gibco 25030081), 20 ng/ml of FGF-2 (Peprotech 100-18B), 20 ng/ml EGF (Peprotech AF-100-15) and 1.6 mL of GelTrex (ThermoFischer A1413202). Single drops of 20 microliters of this solution were placed in sterile parafilm mould, obtained by pressing the parafilm between 2 PCR plates as indicated in Hubert et al., 2016. Drops were assuming a spherical, jellified shape and kept at 37°C for 1 hour before being washed in a Petri dish using the Neurobasal solution.

Tumor organoids were cultured at 37°C in 5% CO_2 humidified incubators in Neurobasal medium up to 23 days. Part of the cultured medium was removed and replaced with fresh one every 2-3 days.

TNT identification and counting

Tunneling nanotubes were identified accordingly to the protocol of Abounit et al., 2015. We experimentally assessed the ideal cell density for the observation of TNTs (40000 cells/cm^2 for both GSLCs). For GSLCs, the adhesion surface was previously coated with laminin 10 µg/mL (Sigma) for at least 2 hours. GSLCs were fixed after 6 hours, to avoid excessive cell flattening on the coated surface. 15 minutes fixation in solution 1 (2% PFA, 0.05% glutaraldehyde and 0.2 M HEPES in PBS) followed other 15 minutes in solution 2 (4% PFA and 0.2 M HEPES in PBS) were performed at 37°C in order to preserve TNTs integrity. Cells were washed with PBS and plasma membrane was labelled with fluorescent Wheat Germ Agglutinin (1:500 in PBS, Life Technologie W21405, W849,

W11261) for 20 min at RT. Nuclei ware stained with DAPI (1:5000 Sigma-Aldrich D9542) before mounting with home-made Mowiol.

Tiles confocal images of the whole volume of the cells were acquired with a Zeiss LSM 700 controlled by ZEN software. Optimal image stack was applied. Images were processed using ICY software to manually count the number of TNT-connected cells. Cells connected through thin, continuous, phalloidin-positive connections were counted as TNT-connected cells.

Immunofluorescence

Cell were seeded on glass coverslips at the TNT-density previously mentioned. Coverslips were coated with 10 µg/mL laminin (Sigma L2020). Cells were fixed with a solution of 4% PFA for 20 minutes at RT. After PBS washes, quenching and permeabilization steps were performed using 50 nM NH4Cl solution and 0.1-0.2% Triton-X100, respectively. 30 minutes of blocking was performed with a solution of 10% FBS. Primary antibodies were incubated diluted in the blocking solution for 1 hours. Anti-αTubulin (1:1000 Sigma-Aldrich T9026) and anti-GAP43 (1:500 Cell signalling 8945S) were used. Cells were washed in PBS and incubated for 45 minutes with secondary antibody anti-mouse and anti-rabbit Invitrogen Alexa 488, 564 or 647 antibodies (1:1000) or phalloidin-rhodamine to stain F-actin (1:500 R415 invitrogen) diluted in blocking solution. DAPI (1:5000 Sigma-Aldrich D9542) in PBS solution was applied for 5 minutes before washes and mounting with Mowiol.

Organoids were fixed with a solution of 4% PFA for 1 hour at 37°C. Subsequently organoids were washed with PBS-0.5% Tween and incubated in a solution of PBS + 10% FBS + 0.3% BSA (Sigma A9647) + 0.3% Triton-X100 0.3% containing primary antibody (mentioned above) overnight at 4°C. After washes with PBS-0.5% Tween, organoids were incubated in the same solution with the corresponding secondary antibody O/N at 4°C. Finally, organoids were washed with PBS-0.5% Tween and incubated with DAPI (1:1000 Sigma-Aldrich D9542) over 6h and finally mounted with a solution of 70% Glycerol.

Immunofluorescence staining were analysed on a Zeiss LSM 700 inverted confocal microscope (Carl Zeiss, Germany), with a Pln-Apo 10X/0.45 to image the entire organoid, 40X : EC Pln-Neo 40X/1.3 (NA = 1.3, working distance = 0.21mm) or Pln-Apo 63X/1.4 (NA = 1.4, working distance = 0.19mm) oil lens objective and a camera (AxioCam MRm; Carl Zeiss).

Time-lapse Microscopy

Time-lapse microscopy imaging in 2D- and 3D-conditions was performed on an inverted Spinning Disk microscope (Elipse Ti microscope system, Nikon Instruments, Melville, NY, USA) using 60 × 1.4NA CSU oil immersion objective lens using Bright field and Laser illumination 488. Pairs of images were captured in immediate succession with one of two cooled CCD cameras, which enabled time intervals between 20 and 30 s per z-stack. For live cell imaging, the 37 °C temperature was controlled with an Air Stream Stage Incubator, which also controlled humidity. In order to avoid the movement of tumor organoids during the acquisition ibidi µ-Dish 35 mm covered by coverslip allowing the culture medium covered the organoid during all the experiment.

Cells were incubated with 5% CO_2 during image acquisition. Image processing and movies were realized using MetaMorph, FIJI and Imaris software. 3D movies of transfer mitochondria were recorded using organoids between 1 day and 8 days old. The volume of the images corresponded to 20-40 µm thickness of the organoid.

Quantification of TNT-mediated transfer by flow cytometry

Transfer assays were performed accordingly to the protocol of Abounit et al., 2015. Stable GSLCs population expressing respectively MitoGFP were used as donor cells and mCherry as acceptor cells and mixed in a 1:1 ratio. For the 2D co-culture, cells were plated at the density previously mentioned (see TNT identification and counting). Cells were detached after 2 or 5 days of co-culture. To monitor the transfer by secretion in 2D co-culture, donor and acceptor cells were co-cultured separated by a 1 µm filter. Acceptor cells were similarly detached as previously mentioned and fixed for the flow cytometry analysis.

For tumor organoids, donor and acceptor cells were mixed 1:1 during the organoid preparation. At each timepoint, organoids were disaggregated using mechanical and chemical (StemPro Accutase, Thermofisher) dissociation. To monitor the transfer by secretion, organoids prepared of only acceptor or donor cells were cultured in the same culture medium separated by a 1 µm filter. For FACS analysis, cells were passed through a cell strainer to separate cell aggregates and fixed in 2% PFA. Flow cytometry data were acquired with a BD Symphony A5 flow cytometer.

Flow cytometry data were acquired with a BD Symphony A5 flow cytometer. GFP and mCherry fluorescence were analysed at 488 nm and 561 nm excitation wavelength, respectively. 10,000 events were acquired for each condition and data were analysed using FlowJo analysis software.

Irradiation

Irradiation was performed with X-Ray machine (Xstrahl LTD). 2 Gy irradiation were performed exposing the cells to X-rays for respectively 1 minute and 25 seconds (250 kV, 12 mA).

RT-qPCR

Total RNA extraction was performed using the RNeasy Mini Kit purchased from Qiagen. Reverse transcription was done using the Biorad iScript gDNA Clear cDNA Synthesis Kit. Oligonucleotides were designed using Prime PCR Look Up Tool (Bio-Rad), purchased from Eurofins Genomics, and sequences are presented in Supplementary Table 1. Quantitative PCR was then performed using the Bio-Rad iTaq™ universal SYBR® Green supermix and analysed using a CFX96TM real-time PCR detection system under the CFX Manager software (Bio-Rad). Gene expression was normalized to hypoxanthine-guanine phosphoribosyltransferase (HPRT).

Supplementary Table 1. Oligonucleotides used in qPCR

Gene	**Forward**	**Reverse**
HPRT	**5'-TAATTGGTGGAGATGATCTCTCAAC-3'**	**5'-TGCCTGACCAAGGAAAGC-3'**

GFAP	**5'-GGCAAAAGCACCAAAGACGG-3'**	**5'-GGCGGCGTTCCATTTACAAT-3'**
Olig1	**5'-AGGTAACCAGGCGTCTCACAGT-3'**	**5'-CGGTACTCCTGCGTGTTAATGA-3'**
Olig2	**5'- CAGAAGCGCTGATGGTCATA-3'**	**5'-TCGGCAGTTTTGGGTTATTC-3'**
Sox-2	**5'- AGACTAGGACTGAGAGAAAG-3'**	**5'- CCTCCTCCTCTGGCCGAT-3'**
TUBβ3	**5'-TCGTCCCGTCCGTGCGATTG-3'**	**5'-TTAGGGACGTGGTGTGGACG-3'**
Sox11	**5'-CTAGCATGCAGAGTGTAGTG-3'**	**5'-AGAAGCTGGTTAGATCGAAG-3'**
GAP43	**5'-GAACCTGAGGCTGACCAAG-3'**	**5'-AAGGGACTTCAGAGTGGAGC-3'**
CHI3L1	**5'-CTTTGAGACCCAAAGTTCCATG-3'**	**5'-ACGCTCTACGGCATGCTC-3'**

Statistical analysis

The statistical tests for percentage of connected cells and percentage of transfer were computed using either a logistic regression model computed using the 'glm' function of R software (https://www.R-project.org/.) or a mixed effect logistic regression model using the lmer (Bates et al., 2015) and lmerTest (Kuznetsova et al., 2017) R packages. For cell connection in 2D, a mixed effect logistic regression model was estimated, adjusted on the effect of cell type, timepoint and condition. This model was also adjusted on the second and third order interactions among these 3 covariates. A random effect corresponding to replication of the experiment was also added to the model in order to account for potential batch effect. For percentage of transfer, we estimated a mixed effect logistic regression model adjusted on the condition, the day and the number of organoids. Second order interactions among condition and day and among number of organoids and day were added to the model in order to normalize statistical tests on time-varying heterogeneity of the number of organoids. A random effect corresponding to replication of the experiment was also added to the model in order to account for potential batch effect. All statistical tests to compare groups (among either cell lines, timepoints or treatments) were deduced by computing contrasts of one the above mentioned logistic model. P-values were therefore adjusted using Tukey's method. To compare the gene expression measured by RT-qPCR, Holm-Sidak method was applied to determine statistical significance, with alpha=5. ANOVA two-way test was performed to compared cell number at different timepoints of the adherent culture. For the comparison of cell number in tumor organoids, the number of cells was transformed in logarithmic scale and slopes were compared.

Section IV: Discussion and Perspectives

Discussion

Context

The understanding of Glioblastoma (GBM), in its complexity and biological mechanisms, is a challenge still today, and this lack of knowledge has contributed to the failure of the various therapeutic attempts (Chinnaiyan et al., 2018; Y. Li et al., 2017). A diagnosis of GBM remains a death sentence in few months. Therefore, greater scientific and clinical efforts are needed to converge on the resolution of this dreadful disease. Luckily, GBM models of study are evolving and are increasingly directed towards the reconstitution in the laboratory of the original tumour complexity (Bian et al., 2018; Hubert et al., 2016; Jacob et al., 2020; Linkous et al., 2019). In fact, the main reason for GBM recurrence is to be attributed to the wide cellular heterogeneity, hence the difficulty in establishing a specific approach toward a single target. This heterogeneity is fuelled by the presence of cells with stem-like features, named GSCs, which hide from the treatment and keep the proliferation of the tumour alive after surgery (Prager et al., 2020). The detection and targeting of GSCs is complicated by the fact that their own population is also heterogeneous and their definition derives more from their characteristic abilities, such as tumorigenicity and self-renewal, rather than from the expression of specific markers (Lathia et al., 2015). In addition to this, GSCs have a strong ability to adapt to a changing environment including under the selective pressure implemented by the treatments and direct their progeny toward a therapy-resistant state (Prager et al., 2020). Unfortunately, the treatments themselves appear to favour these modifications (Dahan et al., 2014) and all together this promotes the establishment of a treatment resistant tumour phenotype. GSCs themselves often display multiple treatment-resistant characteristics as at metabolic level or in their genetic alterations and signaling pathways, which are still today matter of investigation (Hoang-Minh et al., 2018; Neftel et al., 2019; Patel et al., 2014). These features allow GSCs overcoming the medical care currently administrated to patients, hence surgery, radio and chemotherapy. Their peculiar intercellular communication seems to be one of the prominent features contributing to therapy-resistance. In the last five years, the work of the laboratory of Franck Winkler has

highlighted the presence of a physical cellular network between GSCs that facilitate cellular proliferation, cell invasion and treatment-resistance. This cellular teamwork is orchestrated by thick cellular extensions named Tumor Microtubes (TMs) that, through GAP-junctional proteins, allow the propagation and redistribution of intracellular calcium level (Osswald et al., 2015). Variations in the intracellular calcium concentration are associated to the intracellular damage induced by irradiation (Tombal et al., 2002). TMs may also not be directly connected to another cell body, but they can appear as individual protrusions extended into the microenvironment and driving cell invasion (Weil et al., 2017). TMs create a cellular network which involves also the surrounding healthy neurons (Venkataramani et al., 2019; Venkatesh et al., 2019). Their axons can dock on TMs, forming neurogliomal synapses mediated by the AMPA glutamate, and producing postsynaptic currents that promotes tumor growth (Venkataramani et al., 2019). This form of tumoral communication, appears to be quite unique as TMs provided a peculiar electrical and synaptic signaling between GSCs and with the surrounding neural circuits, not present in other tumors. Nevertheless, due to some similarities, the distinct nature of TMs and TNTs was not immediately evident and it has been wondered whether they were the same communicative structure or one the variant of the other. Indeed, they are both direct cell connections allowing the transmission of electrical signals. They both can contain Cx43 and are positive for the presence of various organelles along their length (Abounit & Zurzolo, 2012; Osswald et al., 2016). Albeit this initial confusion, the most recent evidences which I summarize here, suggests that the nature of TMs is likely neuritic and tailored towards synaptic communication (Jung et al., 2019), while TNTs are distinct open connections, found in a wide variety of cell types where they allow the transfer of large cellular cargos (Rustom et al., 2004; Sartori-Rupp et al., 2019). Furthermore, evidences of TNT-based communication exist in several cancer models and even in patient-derived tumoral tissue (as I reviewed in Pinto et al., 2020), thus arising the question as to whether TNTs may also exist in the context of GBM. TNTs are often described to be an adaptation to cellular stress like for presence of free radicals or harmful fibrillar aggregates and even pathogens (Abounit & Zurzolo, 2012; Gousset & Zurzolo, 2009; Jansens et al., 2020). Additionally, early developmental stages in multiple organism also appear to rely on this route for communication (Gerdes et al., 2013; Korenkova et al., 2020). The context of cancer brings together both the aspect of cellular stress, given by

its constant inflammation, proliferation and altered cellular processes, and the regression to cellular mechanisms typical of embryonic development, as cellular re-programming and stem cells differentiation. Cancer is therefore the ideal venue for the occurrence of TNTs. The understanding of the functioning, role and outcome of communication *via* TNTs in tumoral context is only at its dawn. So far, the study of TNTs in cancer have been sporadic, and often superficial, just providing evidence of their existence in different types of cancer; therefore it remains unclear whether a common pattern exists in the various forms of cancer. Nevertheless, the ability to interconnect and share material between cells composing the tumour, whether between tumour cells or in relation to the microenvironment, appear to be an advantage for tumour progression (Pinto et al., 2020). Mitochondria, mRNA, proteins, and in principle all cell components, can be donated from one cell to another, triggering by this process proliferation, invasion or defence against treatments. Alternatively, TNTs can be a way to discard harmful materials, as drugs, damaged organelles and free radicals. It is not clear whether the presence of the communication mediated by TNTs is, in any way, intrinsic to the alterations to which cancer cells are subject or triggered by specific local stress conditions or external agents, such as treatments. In conclusion, the possibility to form TNTs can be an advantage for some cells making them more aggressive and more apt to be positively selected by the tumoral environment and even to survive upon the administration of therapies. Thus, whether TNTs contribute to the tumoral networking observed in GBM, it remains an outstanding question.

After this premise, for the sake of convenience, I have organised my discussion into sub-chapters that allow me to address the discussion points of this work individually.

Presence of functional TNTs in GBM

To address the question of the presence and role of TNTs in Glioblastoma we needed to identify the presence of connections in GBM models and characterize their function. Various studies have defined cellular connections that presented different morphological features as TNTs, also contributing to an initial scepticism toward the existence of these structures (Gurke et al., 2008). Therefore, we addressed our question from a more

functional and quantitative, rather than structural point of view. The definition of TNT is an open membranous channel that allows the direct transfer of cellular cargos from cytoplasm to cytoplasm of two connected cells. In a previous work using U-251 GBM cell line, TNT-like connections were described to be containing ALS-associated aggregates (Ding et al., 2015), suggesting that these structures might be open for the exchange of cellular material. In another study, U-87 GBM cell line was displaying enhanced formation of TNT-like structures upon Cocaine treatment (Carone et al., 2015), although the role of these structures in transfer was not addressed. Considering these previous reports, I started characterizing the presence and functionality of TNTs in these two cellular models in addition to LN-18, another available GBM cell line. I applied a rigorous methodology previously established in our lab to perform TNT investigation (Abounit et al., 2015). According to strict criteria, I took into consideration only the connections floating above the dish surface for the TNT counting, in order to distinguish them from other adherent protrusions (Figure Cell Lines 1C). Additionally, I always performed a control for the transfer through secretion in the co-culture assay that was then removed for the quantification of the contact-mediated transfer (data not shown). I found that all the three cell lines could form TNT-like structures, with similar percentage of connected cells (Figure Cell Lines 1D), and could transfer vesicles, by contact-mediated mechanism, with equal capacity (Figure Cell Lines 1E). This quantitative data is consistent with the similar connection rate displayed by the three cell lines, indicating that the connections observed are likely functional TNTs, as also they were found to be containing DiD-labelled vesicles in U-87 cells (Figure Cell Lines 1F). This results suggest that TNT-mediated communication might occur in GBM, although, it worth noticing, that these immortalized cellular models, particularly U-87, although commonly used, fail in represent genotypic and phenotypic features of the original tumor and also lose tumorigenicity upon cellular passage (Jacobs et al., 2011; J. Lee et al., 2006; Zeng et al., 2018). Nonetheless this approach allowed me to set up the conditions for the study of TNTs in GBM, and to gather supportive data before moving toward a more relevant model.

In order to use a more physiological model, I moved to the study of primary patient-derived GSCs, obtained thanks to our participation in the MoGlimaging network, and the collaboration with the Equipe 11, headed by E. Moyal and C. Toulas, in the Oncopole

Center of Toulouse. We used two GSCs, named C1 and C2, originated from two distinct areas of the same tumor, specifically from the external and infiltrative zone (Figure Article 1A), often remaining after the surgery and target for the radio and chemotherapy. These cells demonstrated the criteria for the classification as cancer stem cells given their ability to generate tumor in immune-depressed mice and activation of stem cells signaling pathway, as survivin, implicated in the self-renewal (Dahan et al., 2014). We further characterized these cells for the expression of stemness and differentiation markers revealing a prolife typical of progenitor/stem cells, consistent with their pluripotency (Figure Article 1C). As GSCs are through to be at the origin of GBM relapse (Prager et al., 2020), we aimed to characterize TNT-mediated communication in these two cell populations. The possibility to work with two different populations, originated from the same tumor, allowed us to take into account the intratumoral heterogeneity in our study. In adherent culture, I observed thin, actin-rich connections between GSCs fitting the criteria of TNTs, as defined in the GBM cell line models (Figure Article 1D and E) and capable of transferring mitochondria *via* contact-mediated transfer as demonstrated with both live-cell imaging and co-culture FACS assay (Figure Article 2 and Supplementary Figure 1). I validated TNT-communicative abilities of C1 and C2 cells in a significant GBM model such as 3D tumor organoids prepared with the protocol published by the laboratory of Jeremy Rich in 2016 (Hubert et al., 2016). In this system, GSCs retain their tumorigenic potential, display histologic features of the original tumor, including single cell invasion, and present also regional heterogeneity (Hubert et al., 2016). C1 and C2 tumor organoids exhibited thin, actin-rich cell connections resembling those defined as TNTs in adherent culture. They were capable of transferring mitochondria as validated by both live-cell imaging and co-culture FACS assay (Figure Article 4C and D and Supplementary Figure 2). As I will discuss later, C1 and C2 cells exhibited TNTs with different functional abilities, in accordance with the heterogeneity of GSCs from the same tumor. Altogether, these observations, obtained from both 2D cell culture models and tumor organoids, strongly point toward the existence of TNTs as an active channel of communication in GBM, and in particular in GSCs despite the heterogeneous nature of their population within the same tumor.

Transfer of mitochondria

I started the project setting up the conditions for the study of the contact-mediated transfer in GBM cell lines using DiD-labelling, able to stain various membranous compartments inside the cells, that, although does not owe a specific significance in the pathophysiological context, allowed me the to monitor and quantify the transfer ability of the cells. In U-251, I tested the possibility of transferring mitochondria by contact-mediated mechanism and observed acceptor cells containing donor-derived mitochondria (Figure Cell Lines 2), suggesting that this transfer could occur by TNTs. For the investigation in the GSCs, we elected mitochondria as relevant cargo for the study of the TNT-mediated transfer. Indeed, mitochondria transfer have been described to impact on the metabolism of the recipient cells, increasing oxygen consumption and ATP production, providing energy for the elevated cellular proliferation displayed by cancer cells, that could also result enhanced (Caicedo et al., 2015). Increased migratory ability, angiogenesis, resistance to apoptosis and survival in response to therapies have also been described upon mitochondria transfer in various cancer and not-cancer cells (Hekmatshoar et al., 2018; Vignais et al., 2017). Moreover, GSCs cells have been described to be able to internalized isolated mitochondria derived from MSCs through a protocol defined MitoCeption (Nzigou Mombo et al., 2017) expected to modify cancer cells properties as described for breast cancer cell lines (Caicedo et al., 2015). Also, various work, including the one currently in progress in our lab (Civita et al., 2019; Zhang & Zhang, 2015, Saenz de Santa Maria et al., in preparation) described the exchange, *via* TNTs, of mitochondria between GBM cell lines and astrocytes. In GSCs, we monitored mitochondria transfer using both live-cell imaging, for the visualization, and co-culture FACS assay, for the quantification. The presence of this transfer was confirmed in both adherent culture as well as in tumor organoids (Figure Article 2 and Figure Article 4C and D). Moreover, no transfer was observed in the secretion controls (Figure Article 2C), suggesting that transfer required cell to cell contact and likely occurred through TNTs. To additionally confirm that the MitoGFP signal, observed by confocal microscopy in the acceptor cells, corresponded to real mitochondria I performed a co-staining with TOM20, marker of the outer mitochondrial membrane, and confirmed the overlapping of the two signals (Supplementary Figure 1). Although the percentage of transfer observed resulted

to be rather small, it was quite consistent among GBM cell lines (lower than 3% after 1 overnight of co-culture) and GSCs (lower than 3% after 5 days of co-culture), even considering the difference in the time of evaluation since GSCs were forming less TNTs (10-20%) compared to GBM cell lines (40%). Nevertheless, our aim was to evaluate that this transfer was possible, and even if apparently limited, it could become relevant in the tumoral context. Further studies are needed to evaluate the benefit that this transfer might provide to the receiving cells, as it will be later discussed in the "Perspective" section. It is important to mention that, beyond the relevance in the pathology of the transfer of mitochondria, the demonstration that this transfer can occur opens up to the possibility that this communication channel may be accessible for the passage of other cellular materials, as miRNA, proteins or other, also correlating with pro-oncogenic potential (Connor et al., 2015; Kolba et al., 2019a; Pinto et al., 2020).

Correlation between TNTs and therapy-resistant phenotype

The ability of cancer cells to establish intercellular connections could possibly correlate with a higher degree of tumor aggressiveness. For example, in both ovarian and breast cancers, highly malignant and metastatic cells are more prone to interconnect in tumor networks than their less aggressive counterparts (Ady et al., 2014; Connor et al., 2015). In GBM cell lines, we investigated whether the expression of MGMT, known chemoresistance marker, could correlate with different TNT-communicative abilities. In colon cancer, the acquisition of mutant KRAS upregulated TNT formation in recipient KRAS wildtype cancer cells (Desir et al., 2019). Neither LN-18 cells, expressing MGMT (data not shown), nor its induced expression in U-251TR cells (Figure Cell Lines 3B) correlated with different TNT frequency or percentage of transfer compared to the not-MGMT expressing cells (Figure Cell Lines 1D, 2C and D), suggesting that the expression of the resistance marker MGMT do not correlate with a variation in the TNT-mediated communication ability. However, a recent study reported that MGMT might be transferred through TNTs from MGMT-expressing GBM cells to MGMT-negative cells resulting in protection against cytotoxic therapy (Valdebenito et al., 2020).

Concerning the study of GSCs, our investigation, related to the presence and role of TNTs, was incorporated in the frame of our multidisciplinary network named MoGlimaging, which purpose is to share material and complement skills in order to improve our understanding of GBM treatment-resistance, predict the circumstances of the relapse, ameliorate the effect of the therapies and patients' quality-life. Thanks to this collaboration we obtained two GSCs, described in this manuscript, which area of origin of was previously characterized, at clinical level, in their metabolic activity by MRI spectroscopy in the frame of the clinical trial STEMRI (Identifier: NCT01872221), carried on in the Oncopole Center of Toulouse. This trial, and our consortium, aim to understand and possibly anticipate which are the features of the tumoral area and the cells at the origin of the relapse. The areas of origin of C1 and C2 cells, peripheral and infiltrative in both cases, were characterized for their CNI ratio, an index indicative of the tumoral proliferation over the ordinary neuronal activity. CNI >2 (CNI+) areas appears to be predictive of the relapse site, suggesting that the cells derived from this zone, in our case C2, could retain more elevated recurrence-initiating potential (Deviers et al., 2014; Laprie et al., 2008) than their counterpart with CNI <2 (CNI-), in our case C1. Of interest for our consortium is the characterization and comparison of CNI- and CNI+ regions and derived-cells in their biological features, as gene expression profile, migratory ability, radio-resistance, tumorigenicity in mice and also TNT-mediated communication, in order to profile the cells possibly driving GBM recurrence. C2 cells displayed more radio-resistance compared to C1, but not different invasive ability (data not shown, article in writing by the group in Toulouse). Interestingly, we observed higher TNT frequency and transfer ability in C2 cells compared to C1 (Figure Article 1F and 2C), in both adherent culture and tumor organoid model (Figure Article 2D and 4D). Despite our attempts it has been impossible to obtain a satisfactory quantification in the number of connections in the organoids, due to the complexity of the system and the difficulty in distinguishing the types of protrusion. Altogether, our data indicate that the incidence of TNT, and the consequent transfer, are more frequent in the more aggressive and putative recurrent-initiating cell population. Nevertheless, no general conclusion can here be made in respect of CNI parameter and the TNT-based communication, as we only analysed one tumor. Another couple of cell populations, corresponding to CNI- and CNI+ areas of another patient, are also in current investigation in our lab. Although no statistical difference was

observed in their TNT frequency preliminary data suggest that the transfer of mitochondria is more consistent in the CNI+ population compared to the CNI-. Beyond the CNI parameter, it worth noticing that, as both GSCs were obtained from the infiltrative borders of the tumor, target of the post-surgical treatment before the relapse, they are already *per se* an interesting subject for the study of the treatment-resistance phenotype. TNTs could be an intrinsic ability of GSCs exploited to contrast the effect of therapies. In general, more aggressive and therapy-resistant tumoral cells might better leverage this route of communication either to share beneficial, pro-tumoral materials or to get rid of therapy-damaged components or even drugs themselves, resulting in an evolutional advantage (Pinto et al., 2020).

Effect of treatments on TNT-mediated communication

TNTs are often described as response to cellular stress, and various treatments has been found to promote their formation, including chemotherapy with Doxorubicin (Desir et al., 2018; Matejka & Reindl, 2019; Ware et al., 2015; D. Zhu et al., 2005). I tested the effect of different concentrations of TMZ on TNT formation in U-251 and U-87 and found almost no variation except a tendency to an increased TNT connectivity after 24 hours from the administration of 50 µM of TMZ, although not statistically significant. Nevertheless, a recent report described an induced TNT formation in U-87 cells during the first day of 50 µM TMZ administration, this time significant (Valdebenito et al., 2020). The two findings are partially in concordance, since this latter work better proves the induction of TNTs that we retained to be only slightly relevant. The methodologies of TNT identification are different as in this work, they rather use live-cell imaging with an inferior magnification and resolution compared to the confocal microscopy I applied on fixed samples. Although more accurate, with our method I may have failed to capture significant variations in a wider field or the TNT induction could have been damped by the fixation step. This work (Valdebenito et al., 2020) also shows the induction of TNTs as a consequence of the irradiation in U-87. I have not deepened the study of U-87 cells due to the dubious validity of this cellular model (Allen et al., 2016; Zeng et al., 2018). Although our results were uncertain about a direct induction of TNTs, there seems to be a possibility that treatments

stimulate the formation of TNT in this cell line, albeit the relevance of this observation in pathophysiological terms remains doubtful.

Given the poor results obtained in response to TMZ, and the fact that the MoGliomaging consortium provided us a better characterization of the radioresistant phenotypes of the GSCs, we addressed the effect of irradiation on the TNT-based communication in this model. We decided to apply 2 Gy of irradiation, a dose that remain sub-toxic and allowed us to monitor modification in the cells without impacting on their viability, this is also the same dose daily administrated to the patients, effective as therapy in its regular administration (Dahan et al., 2014; Stupp, et al., 2005). Nonetheless, these results obtained are not easy to interpret: the irradiation appears to stimulate an acute TNT formation in C2 cells, as observed in the 2D adherent model (unfortunately we were unable to assess whether this was confirmed in the organoids due to technical limitations), and this could result in the slight tendency to greater mitochondria transfer observed in the 2D culture in the first few days after irradiation (Figure Article 3A and B). In the 3D model, which allowed us to evaluate the transfer of mitochondria for several weeks, the C2 cells do not show an induction of the transfer, but a resistant and constant functionality of this communicative route (Figure Article 6A). On the contrary, C1 cells, which in the 2D model did not vary significantly rather showed a tendency to a reduced presence of TNT as a result of irradiation (Figure Article 3A) and, in the 3D long-term model, they exhibited a reduction of this communication way (Figure Article 6A). Altogether, these data seem to suggest that the communication through TNTs is more active and resistant in C2 cells, compared to C1, consistently with the description of these as more resistant to treatment. In the second couple of CNI-/+ cells in analysis, preliminary data shows as well a tendency toward a more resistant mitochondria transfer upon irradiation in tumor organoids (data not shown), allowing us to speculate on different TNT-communicative abilities exhibited by CNI- and CNI+ cells. It's important to underline that this conclusion is drawn by taking together the results of the 2D and 3D model. Despite the differences of the two systems, both allow GSCs to retain their stemness (Hubert et al., 2016), in fact, adherent culture was performed on laminin-coated surface on which GSCs do not differentiate for the first week of culture (personal communication with Equipe 11), reason why I performed adherent co-culture assays for only 5 days and

longer co-culture in tumor organoids. Gene expression analysis, by RT-qPCR, of the cells cultured for 23 days in tumor organoids did not show a significant alteration of their progenitor/stem state, except for GAP-43, that will be discussed in the following paragraph (Figure Article 5A). Similarly, we compared the gene expression in 23-days-old organoids comparing control versus irradiated condition and we did not observe significant variations (data not shown), suggesting that the sub-toxic dose of irradiation applied was not inducing alteration or a selection of the cells composing the tumor organoid. Concerning the relevance of TNT-mediated communication in response to treatments, we could speculate on the possibility that maintaining and exploiting this route of communication may be an advantage for the most aggressive and resistant cells, as previously described.

Coexistence of TNTs and TMs

TMs have been described to have a major role in the intercommunication and treatment-resistance of GSCs in murine xenograft model (Osswald et al., 2015). As TNTs, TMs also can be cell-to-cell connections able to transmit electrical signal and present Cx43 staining (Abounit & Zurzolo, 2012), but they can also appear as single extensions, not connecting to another cell, driving the repopulation of surgically resected areas (Weil et al., 2017). Moreover, recent finding described a neuritic nature of these structures and their synaptic-like communication (Venkataramani et al., 2019; Venkatesh et al., 2019), pointing toward a distinct function for TMs in respect of TNTs, that instead allow the physical transfer of large cellular cargos for cytoplasm to cytoplasm. Several other cancers demonstrated the capability of a cellular interplay mediated by TNTs, but if this was the case also for GBM, or whether in this tumor the intercellular communication is exclusively orchestrated by TMs, still remain an outstanding question. In the work lead by the laboratory of F. Winkler, the tissue complexity of the *in vivo* condition and the limited resolution of the applicable imaging techniques prevented the visualization of thin, nanoscale structures as TNTs, leaving open the possibility that these could co-exist with TMs. As previously discussed, we directed the question on the presence of TNTs in GBM assessing for the presence of cell-to-cell connection displaying transferring ability in

various GBM models, discovering that this mean of communication was present and suggesting that TNT-based communication might exist in actual GBM tumors. C1 and C2 cells were found to express very low or even undetectable levels of GAP-43 (Figure Article 1C), principal driver of TM formation (Osswald et al., 2015), and in 2D adherent culture, we did not observe TM-like protrusions. Indeed here we identified only TNT-like connections negative for the presence of microtubules (Figure Article 1D), instead found in TMs (Osswald et al., 2015). Similarly, in the studies carried on in F. Winkler laboratory, GSCs able to grow TMs in murine xenograft failed in the formation of TMs in classical 2D culture (Weil et al., 2017), making necessary to address the co-existence of TNTs and TMs in 3D, tumoral representative, model. Indeed, when C1 and C2 cells were cultured in tumor organoids, in addition to the observation of thin, tubulin-negative, TNT-like connections, we also noticed thick, long and tubulin-positive cell extensions or connections resembling TMs (Figure Article 4B), some of which displayed positiveness for GAP-43 immunostaining (Figure Article 5D). In fact, as we assessed by RT-qPCR and immunofluorescence, culturing the cells in the tumor organoid model was inducing the expression of GAP-43, in C2 cells (Figure Article 5A and B). It is important to notice that similar induction of GAP-43 expression was not present in C1 cells (Figure Article 5A), although they still presented TM-like connections (Figure Article 4B). In tumor organoids, GSCs retain their tumorigenic, pluripotent potential and can give rise to cellular heterogeneity (Hubert et al., 2016) as we also confirmed this in our system observing that GAP-43 was heterogeneously expressed in the organoids (Figure Article 5C). Whether these structures observed were actual TMs, it should be assessed with functional assays for the visualization of an electrical transmission between the connected cells. However, tumor organoid model is relevant and might provide the conditions to recreate, in some extent, the tumoral complexity and cellular networking observed *in vivo* in murine xenograft. In light of these data, we can speculate that TNTs and TMs could co-exist in the same tumor and collaborate to GBM tumoral networking, providing complementary functions at the level of intercellular communication: TMs, as neurite-like component dedicated to the electrical/synaptic signal propagation (Jung et al., 2019), and TNTs, providing a route of the physical transport of cellular material. In relation to the microenvironment, TMs are the post-synaptic target of neuronal axons from which they receive pro-tumoral stimuli (Venkataramani et al., 2019), while TNTs have demonstrated

an interplay with astrocytes which exhibit, through the transfer of mitochondria, a protective role towards cancer cells (Civita et al., 2019; Zhang & Zhang, 2015). In conclusion, GBM seem to form a complex and advantageous intercellular network, where TNTs might contribute, together with TMs, to tumor progression and resistance to treatments.

Given these points of discussion, here the summary of our conclusions:

- TNT-based intercellular communication occurs in GBM as it has been demonstrated in various GBM cell lines as well as in patient-derived GSCs representative of the heterogeneity of the tumor and in GBM tumor organoids.
- TNTs are able to transfer mitochondria, and potentially other cargos, and can possibly provide a pro-tumoral thrust and an advantage to cancer cells.
- Compared to the other cell counterpart of the same tumor, more aggressive and therapy-resistance cells, that also represent the recurrence-driving population, are able to exploit more efficiently TNT-based communication and this network remains more active, if not even stimulated, in response to irradiation
- TNTs and TMs are distinct structures that can co-exist and cooperate in GBM networking, likely playing different and complementary roles act to promote tumor survival and progression

Perspectives

One general question about the future of this field, concerns the understanding of the role of TNTs in cancer. The biological impact of TNT-mediated communication and their functionality is still foggy, and whether distinct tumors types display similar mechanisms or, contrarily, they exploit differently the communication *via* TNTs, remains a relevant question. The implementation of "-omics" techniques in this field would bring a large number of useful information at this purpose. In fact, the methods currently in use, although necessary at the principle to develop a wider investigation, consist in the study

of a specific cargo, whose transfer is followed and a biological outcome is deduced. As we have already pointed out, many are the cellular cargoes that could trigger biological processes in the receiving cells. Some studies have implemented a more general approach in which they monitor the proteomic and transcriptomic changes in the cells receiving the transfer, allowing to deduce what are the elements received (proteins, miRNA) and the actual transcriptomic alterations triggered in these cells (Connor et al., 2015; Kolba et al., 2019a). The next step is the isolation of receiving cells that have undergone a change in their transcriptomic profile and investigate the alteration of their biological processes and behaviours, such as metabolism, migratory capacity and resistance to therapies (Caicedo et al., 2015; Feng et al., 2019; J. Lu et al., 2017). We could then further investigate the fate of these cells in the tumor landscape, whether the acquired abilities give an evolutionary advantage that favour their proliferation in the tumoral microenvironment, whether their migration can give rise to metastasis or whether they are the therapy-resistance cells responsible for a relapse.

All this can certainly be applied to the context of Glioblastoma, which desperately needs understanding in order to improve the duration and patients' quality of life. As follow-up of my project, it would be advisable to validate of the co-presence of TNTs and TMs, functional studies of TMs abilities should be performed in the tumor organoid model. For example, calcium imaging is based on loading of a chemical indicator, or its expression in the cells, and allows to detect by fluorescence imaging the intracellular calcium mobilization in TM-connected cells in live imaging as performed for TNTs and their mitochondria transfer. Alternatively, more magnified imaging technique have to be applied in the murine xenograft models, as the one in use of the laboratory of F. Winkler, in order to detect TNT-connections in this model. Another point concerns the investigation in the regard of a common behaviour, at TNTs level, between cells derived from CNI- or CNI+ areas. To fulfil this task, it is necessary to extend the investigation to a higher number of patients. Also, our study has raised the need to explore what biological consequences that TNTs bring in the communication between GSCs. We do not know whether the mitochondria transfer observed might be relevant and sufficient to impact on the metabolism of the receiving cells. In the practice, we should isolate the cells receiving the mitochondria transfer, by FACS sorting for example, and characterize these

in comparison to cells that have not received it. To address the issue of the metabolism, closely related to the exchange of mitochondria, SeaHorse assays should be carried out to detect changes in oxygen consumption, mitochondrial and glycolytic metabolism and ATP production. As mentioned above, the transfer of mitochondria *via* TNTs opens up the possibility of other cargoes being transferred through these connections, that could also promote a more aggressive phenotype in the receiving cells. It would be interesting to perform a single-cell-RNA sequencing of the cells receiving the transfer, to highlight which pathways are activated and identify in which direction the behaviour of these cells can evolve. Acquired migratory abilities could be monitored by assay in transwell or wound closure assay, or, since it would be advisable to remain a three-dimensional environment at least partially reconstituting the original tumoral environment, are to be considered migratory tests by incorporating the cells in Matrigel. Even more translational would be the use of these cells in murine xenograft and see if they can give rise to more aggressive tumors. This provides a relevant model also to show the acquisition of resistance to treatments, evaluating the life span of mice after irradiation. All this become particularly relevant when the initial partner of co-culture are different cells, as sensitive cells that receive the transfer from aggressive cells (for example C1 with C2) or co-culture GSCs-astrocytes, in order to assess whether the changes can also be transmitted to the other population.

Once evaluated the potential role of TNTs, it would be interesting to modulate their functionality in GBM models by using drugs or overexpress/downregulate drivers of TNT formation to test the consequence on the cells upon the induction/reduction of the TNT-based network. TNTs inhibition can be carried out using drugs directed against actin polymerization (Latrunculins, Cytochalasins) although these may have an impact on the homeostasis of the cell. Alternatively, TNT-networking could be up/downregulated acting on drivers, for example, the induced expression of CDC42, IRSp53 and VASP was downregulating TNT-communication in neuronal cell lines, while Eps8 overexpression would induce it (Delage et al., 2016) as also the overexpression of small GTPases Rab11a and Rab8a (S. Zhu et al., 2018). If the relevance of TNT communication would be confirmed by all this, they would become an important therapeutic target in order to dampen the tumoral thrust provided by their presence and functionality. Few drugs,

Tolytoxin and Cytarabine, have been described as able to specifically inhibit TNT formation in cell culture (Dilsizoglu Senol et al., 2019; Omsland et al., 2018), although they need to be tested in cancer mouse models. Our laboratory is setting up an automatic system for a high-content screening of potential drugs able to up/downregulate TNT-mediated communication, which could be next applied for pre-clinical studies. Conversely, TNTs have also been used as a route to diffuse therapeutics, like drugs (Desir et al., 2018) and nanoparticles (Formicola et al., 2019), aimed to affect predominantly the network of connected cancer cells. In future years the gained knowledge of TNT-based communication and their role in tumor progression could lead to the development of new, more effective therapies.

BIBLIOGRAPHY

Abounit, Saïda, Bousset, L., Loria, F., Zhu, S., de Chaumont, F., Pieri, L., Olivo-Marin, J.-C., Melki, R., & Zurzolo, C. (2016). Tunneling nanotubes spread fibrillar α-synuclein by intercellular trafficking of lysosomes. *The EMBO Journal*, *35*(19), 2120–2138. https://doi.org/10.15252/embj.201593411

Abounit, Saïda, Delage, E., & Zurzolo, C. (2015). Identification and Characterization of Tunneling Nanotubes for Intercellular Trafficking. *Current Protocols in Cell Biology*, *67*, 12.10.1-21. https://doi.org/10.1002/0471143030.cb1210s67

Abounit, Saida, Wu, J. W., Duff, K., Victoria, G. S., & Zurzolo, C. (2016). Tunneling nanotubes: A possible highway in the spreading of tau and other prion-like proteins in neurodegenerative diseases. *Prion*, *10*(5), 344–351. https://doi.org/10.1080/19336896.2016.1223003

Abounit, Saïda, & Zurzolo, C. (2012). Wiring through tunneling nanotubes – from electrical signals to organelle transfer. *J Cell Sci*, *125*(5), 1089–1098. https://doi.org/10.1242/jcs.083279

Aderetti, D. A., Hira, V. V. V., Molenaar, R. J., & van Noorden, C. J. F. (2018). The hypoxic peri-arteriolar glioma stem cell niche, an integrated concept of five types of niches in human glioblastoma. *Biochimica et Biophysica Acta (BBA) - Reviews on Cancer*, *1869*(2), 346–354. https://doi.org/10.1016/j.bbcan.2018.04.008

Ady, J. W., Desir, S., Thayanithy, V., Vogel, R. I., Moreira, A. L., Downey, R. J., Fong, Y., Manova-Todorova, K., Moore, M. A. S., & Lou, E. (2014). Intercellular communication in malignant pleural mesothelioma: Properties of tunneling nanotubes. *Frontiers in Physiology*, *5*, 400. https://doi.org/10.3389/fphys.2014.00400

Agnihotri, S., Burrell, K. E., Wolf, A., Jalali, S., Hawkins, C., Rutka, J. T., & Zadeh, G. (2013). Glioblastoma, a Brief Review of History, Molecular Genetics, Animal Models and Novel Therapeutic Strategies. *Archivum Immunologiae et Therapiae Experimentalis*, *61*(1), 25–41. https://doi.org/10.1007/s00005-012-0203-0

An, Z., Aksoy, O., Zheng, T., Fan, Q.-W., & Weiss, W. A. (2018). Epidermal growth factor receptor (EGFR) and EGFRvIII in glioblastoma (GBM): Signaling pathways and targeted therapies. *Oncogene*, *37*(12), 1561–1575. https://doi.org/10.1038/s41388-017-0045-7

Anido, J., Sáez-Borderías, A., Gonzàlez-Juncà, A., Rodón, L., Folch, G., Carmona, M. A., Prieto-Sánchez, R. M., Barba, I., Martínez-Sáez, E., Prudkin, L., Cuartas, I., Raventós, C., Martínez-Ricarte, F., Poca, M. A., García-Dorado, D., Lahn, M. M., Yingling, J. M., Rodón, J., Sahuquillo, J., … Seoane, J. (2010). TGF-β Receptor Inhibitors Target the CD44(high)/Id1(high) Glioma-Initiating Cell Population in Human Glioblastoma. *Cancer Cell*, *18*(6), 655–668. https://doi.org/10.1016/j.ccr.2010.10.023

Antanavičiūtė, I., Rysevaitė, K., Liutkevičius, V., Marandykina, A., Rimkutė, L., Sveikatienė, R., Uloza, V., & Skeberdis, V. A. (2014). Long-distance communication between laryngeal carcinoma cells. *PloS One*, *9*(6), e99196. https://doi.org/10.1371/journal.pone.0099196

Ariazi, J., Benowitz, A., De Biasi, V., Den Boer, M. L., Cherqui, S., Cui, H., Douillet, N., Eugenin, E. A., Favre, D., Goodman, S., Gousset, K., Hanein, D., Israel, D. I., Kimura, S., Kirkpatrick, R. B., Kuhn, N., Jeong, C., Lou, E., Mailliard, R., … Zurzolo, C. (2017). Tunneling Nanotubes and Gap Junctions-Their Role in Long-Range Intercellular Communication during Development, Health, and Disease Conditions. *Frontiers in Molecular Neuroscience*, *10*, 333. https://doi.org/10.3389/fnmol.2017.00333

Asencio-Barría, C., Defamie, N., Sáez, J. C., Mesnil, M., & Godoy, A. S. (2019). Direct Intercellular Communications and Cancer: A Snapshot of the Biological Roles of Connexins in Prostate Cancer. *Cancers*, *11*(9), Article 9. https://doi.org/10.3390/cancers11091370

Avril, T., Vauleon, E., Hamlat, A., Saikali, S., Etcheverry, A., Delmas, C., Diabira, S., Mosser, J., & Quillien, V. (2012). Human Glioblastoma Stem-Like Cells are More Sensitive to Allogeneic NK and T Cell-Mediated Killing Compared with Serum-Cultured Glioblastoma Cells. *Brain Pathology*, *22*(2), 159–174. https://doi.org/10.1111/j.1750-3639.2011.00515.x

Bao, S., Wu, Q., McLendon, R. E., Hao, Y., Shi, Q., Hjelmeland, A. B., Dewhirst, M. W., Bigner, D. D., & Rich, J. N. (2006). Glioma stem cells promote radioresistance by preferential activation of the DNA damage response. *Nature*, *444*(7120), 756–760. https://doi.org/10.1038/nature05236

Batash, R., Asna, N., Schaffer, P., Francis, N., & Schaffer, M. (2017). Glioblastoma Multiforme, Diagnosis and Treatment; Recent Literature Review. *Current Medicinal Chemistry*, *24*(27), 3002–3009. https://doi.org/10.2174/0929867324666170516123206

Bates, D., Mächler, M., Bolker, B., & Walker, S. (2015). Fitting Linear Mixed-Effects Models Using lme4. *Journal of Statistical Software*, *67*(1), 1–48. https://doi.org/10.18637/jss.v067.i01

Bhaduri, A., Di Lullo, E., Jung, D., Müller, S., Crouch, E. E., Espinosa, C. S., Ozawa, T., Alvarado, B., Spatazza, J., Cadwell, C. R., Wilkins, G., Velmeshev, D., Liu, S. J., Malatesta, M., Andrews, M. G., Mostajo-Radji, M. A., Huang, E. J., Nowakowski, T. J., Lim, D. A., … Kriegstein, A. R. (2020). Outer Radial Glia-like Cancer Stem Cells Contribute to Heterogeneity of Glioblastoma. *Cell Stem Cell*, *26*(1), 48-63.e6. https://doi.org/10.1016/j.stem.2019.11.015

Bian, S., Repic, M., Guo, Z., Kavirayani, A., Burkard, T., Bagley, J. A., Krauditsch, C., & Knoblich, J. A. (2018). Genetically engineered cerebral organoids model brain tumor formation. *Nature Methods*, *15*(8), 631–639. https://doi.org/10.1038/s41592-018-0070-7

Bonavia, R., Inda, M.-M., Cavenee, W., & Furnari, F. (2011). Heterogeneity Maintenance in Glioblastoma: A social network. *Cancer Research*, *71*(12), 4055–4060. https://doi.org/10.1158/0008-5472.CAN-11-0153

Bonnet, D., & Dick, J. E. (1997). Human acute myeloid leukemia is organized as a hierarchy that originates from a primitive hematopoietic cell. *Nature Medicine*, *3*(7), 730–737. https://doi.org/10.1038/nm0797-730

Braak, H., Alafuzoff, I., Arzberger, T., Kretzschmar, H., & Del Tredici, K. (2006). Staging of Alzheimer disease-associated neurofibrillary pathology using paraffin sections and immunocytochemistry. *Acta Neuropathologica*, *112*(4), 389–404. https://doi.org/10.1007/s00401-006-0127-z

Broekman, M. L., Maas, S. L. N., Abels, E. R., Mempel, T. R., Krichevsky, A. M., & Breakefield, X. O. (2018a). Multidimensional communication in the microenvirons of glioblastoma. *Nature Reviews. Neurology*, *14*(8), 482–495. https://doi.org/10.1038/s41582-018-0025-8

Broekman, M. L., Maas, S. L. N., Abels, E. R., Mempel, T. R., Krichevsky, A. M., & Breakefield, X. O. (2018b). Multidimensional communication in the microenvirons of glioblastoma. *Nature Reviews Neurology*, *14*(8), 482–495. https://doi.org/10.1038/s41582-018-0025-8

Buerki, R. A., & Lukas, R. V. (2016). Serum immuno-biomarkers in gliomas. *Neuroimmunology and Neuroinflammation*, *3*(9), 198. https://doi.org/10.20517/2347-8659.2016.41

Bush, N. A. O., Chang, S. M., & Berger, M. S. (2017). Current and future strategies for treatment of glioma. *Neurosurgical Review*, *40*(1), 1–14. https://doi.org/10.1007/s10143-016-0709-8

Butler, M., Pongor, L., Su, Y.-T., Xi, L., Raffeld, M., Quezado, M., Trepel, J., Aldape, K., Pommier, Y., & Wu, J. (2020). MGMT Status as a Clinical Biomarker in Glioblastoma. *Trends in Cancer*, *6*(5), 380–391. https://doi.org/10.1016/j.trecan.2020.02.010

Caicedo, A., Fritz, V., Brondello, J.-M., Ayala, M., Dennemont, I., Abdellaoui, N., de Fraipont, F., Moisan, A., Prouteau, C. A., Boukhaddaoui, H., Jorgensen, C., & Vignais, M.-L. (2015).

MitoCeption as a new tool to assess the effects of mesenchymal stem/stromal cell mitochondria on cancer cell metabolism and function. *Scientific Reports*, *5*. https://doi.org/10.1038/srep09073

Calabrese, C., Poppleton, H., Kocak, M., Hogg, T. L., Fuller, C., Hamner, B., Oh, E. Y., Gaber, M. W., Finklestein, D., Allen, M., Frank, A., Bayazitov, I. T., Zakharenko, S. S., Gajjar, A., Davidoff, A., & Gilbertson, R. J. (2007). A perivascular niche for brain tumor stem cells. *Cancer Cell*, *11*(1), 69–82. https://doi.org/10.1016/j.ccr.2006.11.020

Caneparo, L., Pantazis, P., Dempsey, W., & Fraser, S. E. (2011). Intercellular bridges in vertebrate gastrulation. *PloS One*, *6*(5), e20230. https://doi.org/10.1371/journal.pone.0020230

Carone, C., Genedani, S., Leo, G., Filaferro, M., Fuxe, K., & Agnati, L. F. (2015). In vitro effects of cocaine on tunneling nanotube formation and extracellular vesicle release in glioblastoma cell cultures. *Journal of Molecular Neuroscience: MN*, *55*(1), 42–50. https://doi.org/10.1007/s12031-014-0365-9

Castro-Castro, A., Marchesin, V., Monteiro, P., Lodillinsky, C., Rossé, C., & Chavrier, P. (2016). Cellular and Molecular Mechanisms of MT1-MMP-Dependent Cancer Cell Invasion. *Annual Review of Cell and Developmental Biology*, *32*(1), 555–576. https://doi.org/10.1146/annurev-cellbio-111315-125227

Chen, J., Li, Y., Yu, T.-S., McKay, R. M., Burns, D. K., Kernie, S. G., & Parada, L. F. (2012). A restricted cell population propagates glioblastoma growth after chemotherapy. *Nature*, *488*(7412), 522–526. https://doi.org/10.1038/nature11287

Chen, X., Guo, C., & Kong, J. (2012). Oxidative stress in neurodegenerative diseases. *Neural Regeneration Research*, *7*(5), 376–385. https://doi.org/10.3969/j.issn.1673-5374.2012.05.009

Cheng, L., Wu, Q., Guryanova, O. A., Huang, Z., Huang, Q., Rich, J. N., & Bao, S. (2011). Elevated invasive potential of glioblastoma stem cells. *Biochemical and Biophysical Research Communications*, *406*(4), 643–648. https://doi.org/10.1016/j.bbrc.2011.02.123

Chinnaiyan, P., Won, M., Wen, P. Y., Rojiani, A. M., Werner-Wasik, M., Shih, H. A., Ashby, L. S., Michael Yu, H.-H., Stieber, V. W., Malone, S. C., Fiveash, J. B., Mohile, N. A., Ahluwalia, M. S., Wendland, M. M., Stella, P. J., Kee, A. Y., & Mehta, M. P. (2018). A randomized phase II study of everolimus in combination with chemoradiation in newly diagnosed glioblastoma: Results of NRG Oncology RTOG 0913. *Neuro-Oncology*, *20*(5), 666–673. https://doi.org/10.1093/neuonc/nox209

Civita, P., M. Leite, D., & Pilkington, G. J. (2019). Pre-Clinical Drug Testing in 2D and 3D Human In Vitro Models of Glioblastoma Incorporating Non-Neoplastic Astrocytes: Tunneling Nano Tubules and Mitochondrial Transfer Modulates Cell Behavior and Therapeutic Respons. *International Journal of Molecular Sciences*, *20*(23), 6017. https://doi.org/10.3390/ijms20236017

Connor, Y., Tekleab, S., Nandakumar, S., Walls, C., Tekleab, Y., Husain, A., Gadish, O., Sabbisetti, V., Kaushik, S., Sehrawat, S., Kulkarni, A., Dvorak, H., Zetter, B., R. Edelman, E., & Sengupta, S. (2015). Physical nanoscale conduit-mediated communication between tumour cells and the endothelium modulates endothelial phenotype. *Nature Communications*, *6*, 8671. https://doi.org/10.1038/ncomms9671

Costanzo, M., Abounit, S., Marzo, L., Danckaert, A., Chamoun, Z., Roux, P., & Zurzolo, C. (2013). Transfer of polyglutamine aggregates in neuronal cells occurs in tunneling nanotubes. *Journal of Cell Science*, *126*(16), 3678–3685. https://doi.org/10.1242/jcs.126086

Crespo, I., Vital, A. L., Gonzalez-Tablas, M., Patino, M. del C., Otero, A., Lopes, M. C., de Oliveira, C., Domingues, P., Orfao, A., & Tabernero, M. D. (2015). Molecular and Genomic Alterations in Glioblastoma Multiforme. *The American Journal of Pathology*, *185*(7), 1820–1833. https://doi.org/10.1016/j.ajpath.2015.02.023

Crocetti, E., Trama, A., Stiller, C., Caldarella, A., Soffietti, R., Jaal, J., Weber, D. C., Ricardi, U., Slowinski, J., & Brandes, A. (2012). Epidemiology of glial and non-glial brain tumours in

Europe. *European Journal of Cancer*, *48*(10), 1532–1542. https://doi.org/10.1016/j.ejca.2011.12.013

Dahan, P., Martinez Gala, J., Delmas, C., Monferran, S., Malric, L., Zentkowski, D., Lubrano, V., Toulas, C., Cohen-Jonathan Moyal, E., & Lemarie, A. (2014). Ionizing radiations sustain glioblastoma cell dedifferentiation to a stem-like phenotype through survivin: Possible involvement in radioresistance. *Cell Death & Disease*, *5*, e1543. https://doi.org/10.1038/cddis.2014.509

Damodaran, N., Dilna, A., Kielkopf, C. S., Kagedal, K., Ollinger, K., & Nath, S. (2020). Amyloid-β induced membrane damage instigates tunneling nanotubes by exploiting PAK1 dependent actin remodulation. *BioRxiv*, 655340. https://doi.org/10.1101/655340

Danilchik, M., Williams, M., & Brown, E. (2013). Blastocoel-spanning filopodia in cleavage-stage Xenopus laevis: Potential roles in morphogen distribution and detection. *Developmental Biology*, *382*(1), 70–81. https://doi.org/10.1016/j.ydbio.2013.07.024

Darmanis, S., Sloan, S. A., Croote, D., Mignardi, M., Chernikova, S., Samghababi, P., Zhang, Y., Neff, N., Kowarsky, M., Caneda, C., Li, G., Chang, S. D., Connolly, I. D., Li, Y., Barres, B. A., Gephart, M. H., & Quake, S. R. (2017). Single-Cell RNA-Seq Analysis of Infiltrating Neoplastic Cells at the Migrating Front of Human Glioblastoma. *Cell Reports*, *21*(5), 1399–1410. https://doi.org/10.1016/j.celrep.2017.10.030

Davis, D. M., & Sowinski, S. (2008). Membrane nanotubes: Dynamic long-distance connections between animal cells. *Nature Reviews Molecular Cell Biology*, *9*(6), 431–436. https://doi.org/10.1038/nrm2399

de Boer, E., Harlaar, N. J., Taruttis, A., Nagengast, W. B., Rosenthal, E. L., Ntziachristos, V., & van Dam, G. M. (2015). Optical innovations in surgery. *The British Journal of Surgery*, *102*(2), e56-72. https://doi.org/10.1002/bjs.9713

Delage, E., Cervantes, D. C., Pénard, E., Schmitt, C., Syan, S., Disanza, A., Scita, G., & Zurzolo, C. (2016). Differential identity of Filopodia and Tunneling Nanotubes revealed by the opposite functions of actin regulatory complexes. *Scientific Reports*, *6*, 39632. https://doi.org/10.1038/srep39632

Desir, S., Dickson, E. L., Vogel, R. I., Thayanithy, V., Wong, P., Teoh, D., Geller, M. A., Steer, C. J., Subramanian, S., & Lou, E. (2016). Tunneling nanotube formation is stimulated by hypoxia in ovarian cancer cells. *Oncotarget*, *7*(28), 43150–43161. https://doi.org/10.18632/oncotarget.9504

Desir, S., O'Hare, P., Vogel, R. I., Sperduto, W., Sarkari, A., Dickson, E. L., Wong, P., Nelson, A. C., Fong, Y., Steer, C. J., Subramanian, S., & Lou, E. (2018). Chemotherapy-Induced Tunneling Nanotubes Mediate Intercellular Drug Efflux in Pancreatic Cancer. *Scientific Reports*, *8*(1), 9484. https://doi.org/10.1038/s41598-018-27649-x

Desir, S., Wong, P., Turbyville, T., Chen, D., Shetty, M., Clark, C., Zhai, E., Romin, Y., Manova-Todorova, K., Starr, T. K., Nissley, D. V., Steer, C. J., Subramanian, S., & Lou, E. (2019). Intercellular Transfer of Oncogenic KRAS via Tunneling Nanotubes Introduces Intracellular Mutational Heterogeneity in Colon Cancer Cells. *Cancers*, *11*(7). https://doi.org/10.3390/cancers11070892

Deviers, A., Ken, S., Filleron, T., Rowland, B., Laruelo, A., Catalaa, I., Lubrano, V., Celsis, P., Berry, I., Mogicato, G., Cohen-Jonathan Moyal, E., & Laprie, A. (2014). Evaluation of the Lactate-to-N-Acetyl-aspartate Ratio Defined With Magnetic Resonance Spectroscopic Imaging Before Radiation Therapy as a New Predictive Marker of the Site of Relapse in Patients With Glioblastoma Multiforme. *International Journal of Radiation Oncology*Biology*Physics*, *90*(2), 385–393. https://doi.org/10.1016/j.ijrobp.2014.06.009

Diksin, M., Smith, S. J., & Rahman, R. (2017). The Molecular and Phenotypic Basis of the Glioma Invasive Perivascular Niche. *International Journal of Molecular Sciences*, *18*(11). https://doi.org/10.3390/ijms18112342

Dilsizoglu Senol, A., Pepe, A., Grudina, C., Sassoon, N., Reiko, U., Bousset, L., Melki, R., Piel, J., Gugger, M., & Zurzolo, C. (2019). Effect of tolytoxin on tunneling nanotube formation and function. *Scientific Reports*, *9*. https://doi.org/10.1038/s41598-019-42161-6

Ding, X., Ma, M., Teng, J., Teng, R. K. F., Zhou, S., Yin, J., Fonkem, E., Huang, J. H., Wu, E., & Wang, X. (2015). Exposure to ALS-FTD-CSF generates TDP-43 aggregates in glioblastoma cells through exosomes and TNTs-like structure. *Oncotarget*, *6*(27), 24178–24191. https://doi.org/10.18632/oncotarget.4680

Dong, L.-F., Kovarova, J., Bajzikova, M., Bezawork-Geleta, A., Svec, D., Endaya, B., Sachaphibulkij, K., Coelho, A. R., Sebkova, N., Ruzickova, A., Tan, A. S., Kluckova, K., Judasova, K., Zamecnikova, K., Rychtarcikova, Z., Gopalan, V., Andera, L., Sobol, M., Yan, B., … Neuzil, J. (2017). Horizontal transfer of whole mitochondria restores tumorigenic potential in mitochondrial DNA-deficient cancer cells. *ELife*, *6*. https://doi.org/10.7554/eLife.22187

Errede, M., Mangieri, D., Longo, G., Girolamo, F., de Trizio, I., Vimercati, A., Serio, G., Frei, K., Perris, R., & Virgintino, D. (2018). Tunneling nanotubes evoke pericyte/endothelial communication during normal and tumoral angiogenesis. *Fluids and Barriers of the CNS*, *15*. https://doi.org/10.1186/s12987-018-0114-5

Eugenin, E. A., Gaskill, P. J., & Berman, J. W. (2009). Tunneling nanotubes (TNT) are induced by HIV-infection of macrophages. *Cellular Immunology*, *254*(2), 142–148. https://doi.org/10.1016/j.cellimm.2008.08.005

Feng, Y., Zhu, R., Shen, J., Wu, J., Lu, W., Zhang, J., Zhang, J., & Liu, K. (2019). Human Bone Marrow Mesenchymal Stem Cells Rescue Endothelial Cells Experiencing Chemotherapy Stress by Mitochondrial Transfer Via Tunneling Nanotubes. *Stem Cells and Development*, *28*(10), 674–682. https://doi.org/10.1089/scd.2018.0248

Ferrari, R., Martin, G., Tagit, O., Guichard, A., Cambi, A., Voituriez, R., Vassilopoulos, S., & Chavrier, P. (2019). MT1-MMP directs force-producing proteolytic contacts that drive tumor cell invasion. *Nature Communications*, *10*(1), 4886. https://doi.org/10.1038/s41467-019-12930-y

Flynn, K. C. (2013). The cytoskeleton and neurite initiation. *Bioarchitecture*, *3*(4), 86–109. https://doi.org/10.4161/bioa.26259

Formicola, B., D'Aloia, A., Dal Magro, R., Stucchi, S., Rigolio, R., Ceriani, M., & Re, F. (2019). Differential Exchange of Multifunctional Liposomes Between Glioblastoma Cells and Healthy Astrocytes via Tunneling Nanotubes. *Frontiers in Bioengineering and Biotechnology*, *7*. https://doi.org/10.3389/fbioe.2019.00403

Fykerud, T. A., Knudsen, L. M., Totland, M. Z., Sørensen, V., Dahal-Koirala, S., Lothe, R. A., Brech, A., & Leithe, E. (2016). Mitotic cells form actin-based bridges with adjacent cells to provide intercellular communication during rounding. *Cell Cycle (Georgetown, Tex.)*, *15*(21), 2943–2957. https://doi.org/10.1080/15384101.2016.1231280

Gallop, J. L. (2019). Filopodia and their links with membrane traffic and cell adhesion. *Seminars in Cell & Developmental Biology*. https://doi.org/10.1016/j.semcdb.2019.11.017

Galluzzi, L., & Kroemer, G. (2018). Potent immunosuppressive effects of the oncometabolite R-2-hydroxyglutarate. *OncoImmunology*, *7*(12), e1528815. https://doi.org/10.1080/2162402X.2018.1528815

Garnier, D., Renoult, O., Alves-Guerra, M.-C., Paris, F., & Pecqueur, C. (2019). Glioblastoma Stem-Like Cells, Metabolic Strategy to Kill a Challenging Target. *Frontiers in Oncology*, *9*. https://doi.org/10.3389/fonc.2019.00118

Gerdes, H.-H., Rustom, A., & Wang, X. (2013). Tunneling nanotubes, an emerging intercellular communication route in development. *Mechanisms of Development*, *130*(6), 381–387. https://doi.org/10.1016/j.mod.2012.11.006

González-Méndez, L., Gradilla, A.-C., & Guerrero, I. (2019). The cytoneme connection: Direct long-distance signal transfer during development. *Development (Cambridge, England)*, *146*(9), Article 9. https://doi.org/10.1242/dev.174607

Gousset, K., Schiff, E., Langevin, C., Marijanovic, Z., Caputo, A., Browman, D. T., Chenouard, N., de Chaumont, F., Martino, A., Enninga, J., Olivo-Marin, J.-C., Männel, D., & Zurzolo, C. (2009). Prions hijack tunnelling nanotubes for intercellular spread. *Nature Cell Biology*, *11*(3), 328–336. https://doi.org/10.1038/ncb1841

Gousset, K., & Zurzolo, C. (2009). Tunnelling nanotubes: A highway for prion spreading? *Prion*, *3*(2), 94–98. https://doi.org/10.4161/pri.3.2.8917

Greaves, M., & Maley, C. C. (2012). Clonal evolution in cancer. *Nature*, *481*(7381), 306–313. https://doi.org/10.1038/nature10762

Griessinger, E., Moschoi, R., Biondani, G., & Peyron, J.-F. (2017). Mitochondrial Transfer in the Leukemia Microenvironment. *Trends in Cancer*, *3*(12), 828–839. https://doi.org/10.1016/j.trecan.2017.10.003

Guan, X., Hasan, M. N., Maniar, S., Jia, W., & Sun, D. (2018). Reactive Astrocytes in Glioblastoma Multiforme. *Molecular Neurobiology*, *55*(8), 6927–6938. https://doi.org/10.1007/s12035-018-0880-8

Guo, J., Yao, C., Chen, H., Zhuang, D., Tang, W., Ren, G., Wang, Y., Wu, J., Huang, F., & Zhou, L. (2012). The relationship between Cho/NAA and glioma metabolism: Implementation for margin delineation of cerebral gliomas. *Acta Neurochirurgica*, *154*(8), 1361–1370. https://doi.org/10.1007/s00701-012-1418-x

Gupta, K., & Burns, T. C. (2018). Radiation-Induced Alterations in the Recurrent Glioblastoma Microenvironment: Therapeutic Implications. *Frontiers in Oncology*, *8*. https://doi.org/10.3389/fonc.2018.00503

Gurke, S., Barroso, J. F. V., & Gerdes, H.-H. (2008). The art of cellular communication: Tunneling nanotubes bridge the divide. *Histochemistry and Cell Biology*, *129*(5), 539–550. https://doi.org/10.1007/s00418-008-0412-0

Hambardzumyan, D., Gutmann, D. H., & Kettenmann, H. (2016). The role of microglia and macrophages in glioma maintenance and progression. *Nature Neuroscience*, *19*(1), 20–27. https://doi.org/10.1038/nn.4185

Hanif, F., Muzaffar, K., Perveen, K., Malhi, S. M., & Simjee, S. U. (2017). Glioblastoma Multiforme: A Review of its Epidemiology and Pathogenesis through Clinical Presentation and Treatment. *Asian Pacific Journal of Cancer Prevention : APJCP*, *18*(1), 3–9. https://doi.org/10.22034/APJCP.2017.18.1.3

Hanna, S. J., McCoy-Simandle, K., Leung, E., Genna, A., Condeelis, J., & Cox, D. (2019). Tunneling nanotubes, a novel mode of tumor cell-macrophage communication in tumor cell invasion. *Journal of Cell Science*, *132*(3). https://doi.org/10.1242/jcs.223321

Hase, K., Kimura, S., Takatsu, H., Ohmae, M., Kawano, S., Kitamura, H., Ito, M., Watarai, H., Hazelett, C. C., Yeaman, C., & Ohno, H. (2009). M-Sec promotes membrane nanotube formation by interacting with Ral and the exocyst complex. *Nature Cell Biology*, *11*(12), 1427–1432. https://doi.org/10.1038/ncb1990

Hashimoto, M., Bhuyan, F., Hiyoshi, M., Noyori, O., Nasser, H., Miyazaki, M., Saito, T., Kondoh, Y., Osada, H., Kimura, S., Hase, K., Ohno, H., & Suzu, S. (2016). Potential Role of the Formation of Tunneling Nanotubes in HIV-1 Spread in Macrophages. *The Journal of Immunology*, *196*(4), 1832–1841. https://doi.org/10.4049/jimmunol.1500845

Hayakawa, K., Esposito, E., Wang, X., Terasaki, Y., Liu, Y., Xing, C., Ji, X., & Lo, E. H. (2016). Transfer of mitochondria from astrocytes to neurons after stroke. *Nature*, *535*(7613), 551–555. https://doi.org/10.1038/nature18928

Hekmatshoar, Y., Nakhle, J., Galloni, M., & Vignais, M.-L. (2018). The role of metabolism and tunneling nanotube-mediated intercellular mitochondria exchange in cancer drug resistance. *The Biochemical Journal*, *475*(14), 2305–2328. https://doi.org/10.1042/BCJ20170712

Hoang-Minh, L. B., Siebzehnrubl, F. A., Yang, C., Suzuki-Hatano, S., Dajac, K., Loche, T., Andrews, N., Schmoll Massari, M., Patel, J., Amin, K., Vuong, A., Jimenez-Pascual, A., Kubilis, P.,

Garrett, T. J., Moneypenny, C., Pacak, C. A., Huang, J., Sayour, E. J., Mitchell, D. A., … Deleyrolle, L. P. (2018). Infiltrative and drug-resistant slow-cycling cells support metabolic heterogeneity in glioblastoma. *The EMBO Journal*, *37*(23), e98772. https://doi.org/10.15252/embj.201798772

Hodges, L. C., Smith, J. L., Garrett, A., & Tate, S. (1992). Prevalence of glioblastoma multiforme in subjects with prior therapeutic radiation. *The Journal of Neuroscience Nursing: Journal of the American Association of Neuroscience Nurses*, *24*(2), 79–83. https://doi.org/10.1097/01376517-199204000-00005

Horská, A., & Barker, P. B. (2010). Imaging of Brain Tumors: MR Spectroscopy and Metabolic Imaging. *Neuroimaging Clinics of North America*, *20*(3), 293–310. https://doi.org/10.1016/j.nic.2010.04.003

Hua, K., & Ferland, R. J. (2018). Primary cilia proteins: Ciliary and extraciliary sites and functions. *Cellular and Molecular Life Sciences : CMLS*, *75*(9), 1521–1540. https://doi.org/10.1007/s00018-017-2740-5

Hubert, C. G., Rivera, M., Spangler, L. C., Wu, Q., Mack, S. C., Prager, B. C., Couce, M., McLendon, R. E., Sloan, A. E., & Rich, J. N. (2016). A Three-Dimensional Organoid Culture System Derived from Human Glioblastomas Recapitulates the Hypoxic Gradients and Cancer Stem Cell Heterogeneity of Tumors Found In Vivo. *Cancer Research*, *76*(8), 2465–2477. https://doi.org/10.1158/0008-5472.CAN-15-2402

Inda, M.-M., Bonavia, R., Mukasa, A., Narita, Y., Sah, D. W. Y., Vandenberg, S., Brennan, C., Johns, T. G., Bachoo, R., Hadwiger, P., Tan, P., DePinho, R. A., Cavenee, W., & Furnari, F. (2010). Tumor heterogeneity is an active process maintained by a mutant EGFR-induced cytokine circuit in glioblastoma. *Genes & Development*, *24*(16), 1731–1745. https://doi.org/10.1101/gad.1890510

Inda, M.-M., Bonavia, R., & Seoane, J. (2014). Glioblastoma Multiforme: A Look Inside Its Heterogeneous Nature. *Cancers*, *6*(1), 226–239. https://doi.org/10.3390/cancers6010226

Innocenti, M. (2018). New insights into the formation and the function of lamellipodia and ruffles in mesenchymal cell migration. *Cell Adhesion & Migration*, *12*(5), 401–416. https://doi.org/10.1080/19336918.2018.1448352

Jacob, F., Salinas, R. D., Zhang, D. Y., Nguyen, P. T. T., Schnoll, J. G., Wong, S. Z. H., Thokala, R., Sheikh, S., Saxena, D., Prokop, S., Liu, D.-A., Qian, X., Petrov, D., Lucas, T., Chen, H. I., Dorsey, J. F., Christian, K. M., Binder, Z. A., Nasrallah, M., … Song, H. (2020). A Patient-Derived Glioblastoma Organoid Model and Biobank Recapitulates Inter- and Intra-tumoral Heterogeneity. *Cell*, *180*(1), 188-204.e22. https://doi.org/10.1016/j.cell.2019.11.036

Jacobs, V. L., Valdes, P. A., Hickey, W. F., & De Leo, J. A. (2011). Current review of in vivo GBM rodent models: Emphasis on the CNS-1 tumour model. *ASN NEURO*, *3*(3). https://doi.org/10.1042/AN20110014

Jansens, R. J. J., Tishchenko, A., & Favoreel, H. W. (2020). Bridging the Gap: Virus Long-Distance Spread via Tunneling Nanotubes. *Journal of Virology*, *94*(8). https://doi.org/10.1128/JVI.02120-19

Jansens, R. J. J., Van den Broeck, W., De Pelsmaeker, S., Lamote, J. A. S., Van Waesberghe, C., Couck, L., & Favoreel, H. W. (2017). Pseudorabies Virus US3-Induced Tunneling Nanotubes Contain Stabilized Microtubules, Interact with Neighboring Cells via Cadherins, and Allow Intercellular Molecular Communication. *Journal of Virology*, *91*(19), e00749-17, e00749-17. https://doi.org/10.1128/JVI.00749-17

Jhaveri, N., Chen, T. C., & Hofman, F. M. (2016). Tumor vasculature and glioma stem cells: Contributions to glioma progression. *Cancer Letters*, *380*(2), 545–551. https://doi.org/10.1016/j.canlet.2014.12.028

Johnson, B. E., Mazor, T., Hong, C., Barnes, M., Aihara, K., McLean, C. Y., Fouse, S. D., Yamamoto, S., Ueda, H., Tatsuno, K., Asthana, S., Jalbert, L. E., Nelson, S. J., Bollen, A. W., Gustafson, W. C., Charron, E., Weiss, W. A., Smirnov, I. V., Song, J. S., … Costello, J. F. (2014). Mutational Analysis Reveals the Origin and Therapy-driven Evolution of Recurrent Glioma. *Science (New York, N.Y.)*, *343*(6167), 189–193. https://doi.org/10.1126/science.1239947

Jung, E., Alfonso, J., Osswald, M., Monyer, H., Wick, W., & Winkler, F. (2019). Emerging intersections between neuroscience and glioma biology. *Nature Neuroscience*, *22*(12), 1951–1960. https://doi.org/10.1038/s41593-019-0540-y

Jung, E., Osswald, M., Blaes, J., Wiestler, B., Sahm, F., Schmenger, T., Solecki, G., Deumelandt, K., Kurz, F. T., Xie, R., Weil, S., Heil, O., Thomé, C., Gömmel, M., Syed, M., Häring, P., Huber, P. E., Heiland, S., Platten, M., … Winkler, F. (2017). Tweety-Homolog 1 Drives Brain Colonization of Gliomas. *Journal of Neuroscience*, *37*(29), 6837–6850. https://doi.org/10.1523/JNEUROSCI.3532-16.2017

Kim, S.-S., Pirollo, K. F., & Chang, E. H. (2015). Isolation and Culturing of Glioma Cancer Stem Cells. *Current Protocols in Cell Biology / Editorial Board, Juan S. Bonifacino ... [et Al.]*, *67*, 23.10.1-23.10.10. https://doi.org/10.1002/0471143030.cb2310s67

King, T. C. (2007). 3—Tissue Homeostasis, Damage, and Repair. In T. C. King (Ed.), *Elsevier's Integrated Pathology* (pp. 59–88). Mosby. https://doi.org/10.1016/B978-0-323-04328-1.50009-7

Klezovitch, O., & Vasioukhin, V. (2015). Cadherin signaling: Keeping cells in touch. *F1000Research*, *4*(F1000 Faculty Rev). https://doi.org/10.12688/f1000research.6445.1

Kolba, M. D., Dudka, W., Zaręba-Kozioł, M., Kominek, A., Ronchi, P., Turos, L., Chroscicki, P., Wlodarczyk, J., Schwab, Y., Klejman, A., Cysewski, D., Srpan, K., Davis, D. M., & Piwocka, K. (2019a). Tunneling nanotube-mediated intercellular vesicle and protein transfer in the stroma-provided imatinib resistance in chronic myeloid leukemia cells. *Cell Death & Disease*, *10*(11), 1–16. https://doi.org/10.1038/s41419-019-2045-8

Kolba, M. D., Dudka, W., Zaręba-Kozioł, M., Kominek, A., Ronchi, P., Turos, L., Chroscicki, P., Wlodarczyk, J., Schwab, Y., Klejman, A., Cysewski, D., Srpan, K., Davis, D. M., & Piwocka, K. (2019b). Tunneling nanotube-mediated intercellular vesicle and protein transfer in the stroma-provided imatinib resistance in chronic myeloid leukemia cells. *Cell Death & Disease*, *10*(11), 1–16. https://doi.org/10.1038/s41419-019-2045-8

Korenkova, O., Pepe, A., & Zurzolo, C. (2020). Fine intercellular connections in development: TNTs, cytonemes, or intercellular bridges? *Cell Stress*, *4*(2), 30–43. https://doi.org/10.15698/cst2020.02.212

Kornberg, T. B., & Roy, S. (2014). Cytonemes as specialized signaling filopodia. *Development*, *141*(4), 729–736. https://doi.org/10.1242/dev.086223

Kretschmer, A., Zhang, F., Somasekharan, S. P., Tse, C., Leachman, L., Gleave, A., Li, B., Asmaro, I., Huang, T., Kotula, L., Sorensen, P. H., & Gleave, M. E. (2019). Stress-induced tunneling nanotubes support treatment adaptation in prostate cancer. *Scientific Reports*, *9*. https://doi.org/10.1038/s41598-019-44346-5

Kuznetsova, A., Brockhoff, P. B., & Christensen, R. H. B. (2017). lmerTest Package: Tests in Linear Mixed Effects Models. *Journal of Statistical Software*, *82*(1), 1–26. https://doi.org/10.18637/jss.v082.i13

Lan, X., Jörg, D. J., Cavalli, F. M. G., Richards, L. M., Nguyen, L. V., Vanner, R. J., Guilhamon, P., Lee, L., Kushida, M. M., Pellacani, D., Park, N. I., Coutinho, F. J., Whetstone, H., Selvadurai, H. J., Che, C., Luu, B., Carles, A., Moksa, M., Rastegar, N., … Dirks, P. B. (2017). Fate mapping of human glioblastoma reveals an invariant stem cell hierarchy. *Nature*, *549*(7671), 227–232. https://doi.org/10.1038/nature23666

Laprie, A., Catalaa, I., Cassol, E., McKnight, T. R., Berchery, D., Marre, D., Bachaud, J.-M., Berry, I., & Moyal, E. C.-J. (2008). Proton Magnetic Resonance Spectroscopic Imaging in Newly

Diagnosed Glioblastoma: Predictive Value for the Site of Postradiotherapy Relapse in a Prospective Longitudinal Study. *International Journal of Radiation Oncology*Biology*Physics*, *70*(3), 773–781. https://doi.org/10.1016/j.ijrobp.2007.10.039

Latario, C. J., Schoenfeld, L. W., Howarth, C. L., Pickrell, L. E., Begum, F., Fischer, D. A., Grbovic-Huezo, O., Leach, S. D., Sanchez, Y., Smith, K. D., & Higgs, H. N. (2020). Tumor microtubes connect pancreatic cancer cells in an Arp2/3 complex-dependent manner. *Molecular Biology of the Cell*, *31*(12), 1259–1272. https://doi.org/10.1091/mbc.E19-11-0605

Lathia, J. D., Gallagher, J., Heddleston, J. M., Wang, J., Eyler, C. E., MacSwords, J., Wu, Q., Vasanji, A., McLendon, R. E., Hjelmeland, A. B., & Rich, J. N. (2010). Integrin alpha 6 regulates glioblastoma stem cells. *Cell Stem Cell*, *6*(5), 421–432. https://doi.org/10.1016/j.stem.2010.02.018

Lathia, J. D., Mack, S. C., Mulkearns-Hubert, E. E., Valentim, C. L. L., & Rich, J. N. (2015). Cancer stem cells in glioblastoma. *Genes & Development*, *29*(12), 1203–1217. https://doi.org/10.1101/gad.261982.115

Lathia, J. D., Mattson, M. P., & Cheng, A. (2008). Notch: From Neural Development to Neurological Disorders. *Journal of Neurochemistry*, *107*(6), 1471–1481. https://doi.org/10.1111/j.1471-4159.2008.05715.x

Laurindo, F. R. M., Liberman, M., Fernandes, D. C., & Leite, P. F. (2018). Chapter 8 - Endothelium-Dependent Vasodilation: Nitric Oxide and Other Mediators. In P. L. Da Luz, P. Libby, A. C. P. Chagas, & F. R. M. Laurindo (Eds.), *Endothelium and Cardiovascular Diseases* (pp. 97–113). Academic Press. https://doi.org/10.1016/B978-0-12-812348-5.00008-8

Lee, C. Y. (2017). Strategies of temozolomide in future glioblastoma treatment. *OncoTargets and Therapy*, *10*, 265–270. https://doi.org/10.2147/OTT.S120662

Lee, G., Auffinger, B., Guo, D., Hasan, T., Deheeger, M., Tobias, A. L., Kim, J. Y., Atashi, F., Zhang, L., Lesniak, M. S., James, C. D., & Ahmed, A. U. (2016). Dedifferentiation of Glioma Cells to Glioma Stem-like Cells By Therapeutic Stress-induced HIF Signaling in the Recurrent GBM Model. *Molecular Cancer Therapeutics*, *15*(12), 3064–3076. https://doi.org/10.1158/1535-7163.MCT-15-0675

Lee, J., Kotliarova, S., Kotliarov, Y., Li, A., Su, Q., Donin, N. M., Pastorino, S., Purow, B. W., Christopher, N., Zhang, W., Park, J. K., & Fine, H. A. (2006). Tumor stem cells derived from glioblastomas cultured in bFGF and EGF more closely mirror the phenotype and genotype of primary tumors than do serum-cultured cell lines. *Cancer Cell*, *9*(5), 391–403. https://doi.org/10.1016/j.ccr.2006.03.030

Li, Q.-J., Cai, J.-Q., & Liu, C.-Y. (2016). Evolving Molecular Genetics of Glioblastoma. *Chinese Medical Journal*, *129*(4), 464–471. https://doi.org/10.4103/0366-6999.176065

Li, Y., Ali, S., Clarke, J., & Cha, S. (2017). Bevacizumab in Recurrent Glioma: Patterns of Treatment Failure and Implications. *Brain Tumor Research and Treatment*, *5*(1), 1–9. https://doi.org/10.14791/btrt.2017.5.1.1

Linkous, A., Balamatsias, D., Snuderl, M., Edwards, L., Miyaguchi, K., Milner, T., Reich, B., Cohen-Gould, L., Storaska, A., Nakayama, Y., Schenkein, E., Singhania, R., Cirigliano, S., Magdeldin, T., Lin, Y., Nanjangud, G., Chadalavada, K., Pisapia, D., Liston, C., & Fine, H. A. (2019). Modeling Patient-Derived Glioblastoma with Cerebral Organoids. *Cell Reports*, *26*(12), 3203-3211.e5. https://doi.org/10.1016/j.celrep.2019.02.063

Liu, G., Yuan, X., Zeng, Z., Tunici, P., Ng, H., Abdulkadir, I. R., Lu, L., Irvin, D., Black, K. L., & Yu, J. S. (2006). Analysis of gene expression and chemoresistance of CD133+ cancer stem cells in glioblastoma. *Molecular Cancer*, *5*(1), 67. https://doi.org/10.1186/1476-4598-5-67

Loria, F., Vargas, J. Y., Bousset, L., Syan, S., Salles, A., Melki, R., & Zurzolo, C. (2017). α-Synuclein transfer between neurons and astrocytes indicates that astrocytes play a role in degradation rather than in spreading. *Acta Neuropathologica*, *134*(5), 789–808. https://doi.org/10.1007/s00401-017-1746-2

Lou, E., Fujisawa, S., Morozov, A., Barlas, A., Romin, Y., Dogan, Y., Gholami, S., Moreira, A. L., Manova-Todorova, K., & Moore, M. A. S. (2012). Tunneling Nanotubes Provide a Unique Conduit for Intercellular Transfer of Cellular Contents in Human Malignant Pleural Mesothelioma. *PLoS ONE*, *7*(3). https://doi.org/10.1371/journal.pone.0033093

Louis, D. N., Perry, A., Reifenberger, G., von Deimling, A., Figarella-Branger, D., Cavenee, W. K., Ohgaki, H., Wiestler, O. D., Kleihues, P., & Ellison, D. W. (2016). The 2016 World Health Organization Classification of Tumors of the Central Nervous System: A summary. *Acta Neuropathologica*, *131*(6), 803–820. https://doi.org/10.1007/s00401-016-1545-1

Lu, J. J., Yang, W. M., Li, F., Zhu, W., & Chen, Z. (2019). Tunneling Nanotubes Mediated microRNA-155 Intercellular Transportation Promotes Bladder Cancer Cells' Invasive and Proliferative Capacity. *International Journal of Nanomedicine*, *14*, 9731–9743. https://doi.org/10.2147/IJN.S217277

Lu, J., Zheng, X., Li, F., Yu, Y., Chen, Z., Liu, Z., Wang, Z., Xu, H., & Yang, W. (2017). Tunneling nanotubes promote intercellular mitochondria transfer followed by increased invasiveness in bladder cancer cells. *Oncotarget*, *8*(9), 15539–15552. https://doi.org/10.18632/oncotarget.14695

Lurtz, M. M., & Louis, C. F. (2007). Intracellular calcium regulation of connexin43. *American Journal of Physiology. Cell Physiology*, *293*(6), C1806-1813. https://doi.org/10.1152/ajpcell.00630.2006

Malta, T. M., de Souza, C. F., Sabedot, T. S., Silva, T. C., Mosella, M. S., Kalkanis, S. N., Snyder, J., Castro, A. V. B., & Noushmehr, H. (2018). Glioma CpG island methylator phenotype (G-CIMP): Biological and clinical implications. *Neuro-Oncology*, *20*(5), 608–620. https://doi.org/10.1093/neuonc/nox183

Marin-Valencia, I., Yang, C., Mashimo, T., Cho, S., Baek, H., Yang, X.-L., Rajagopalan, K. N., Maddie, M., Vemireddy, V., Zhao, Z., Cai, L., Good, L., Tu, B. P., Hatanpaa, K. J., Mickey, B. E., Matés, J. M., Pascual, J. M., Maher, E. A., Malloy, C. R., … Bachoo, R. M. (2012). Analysis of tumor metabolism reveals mitochondrial glucose oxidation in genetically diverse human glioblastomas in the mouse brain in vivo. *Cell Metabolism*, *15*(6), 827–837. https://doi.org/10.1016/j.cmet.2012.05.001

Marlein, C. R., Piddock, R. E., Mistry, J. J., Zaitseva, L., Hellmich, C., Horton, R. H., Zhou, Z., Auger, M. J., Bowles, K. M., & Rushworth, S. A. (2019). CD38-Driven Mitochondrial Trafficking Promotes Bioenergetic Plasticity in Multiple Myeloma. *Cancer Research*, *79*(9), 2285–2297. https://doi.org/10.1158/0008-5472.CAN-18-0773

Marlein, C. R., Zaitseva, L., Piddock, R. E., Robinson, S. D., Edwards, D. R., Shafat, M. S., Zhou, Z., Lawes, M., Bowles, K. M., & Rushworth, S. A. (2017). NADPH oxidase-2 derived superoxide drives mitochondrial transfer from bone marrow stromal cells to leukemic blasts. *Blood*, *130*(14), 1649–1660. https://doi.org/10.1182/blood-2017-03-772939

Matejka, N., & Reindl, J. (2019). Perspectives of cellular communication through tunneling nanotubes in cancer cells and the connection to radiation effects. *Radiation Oncology (London, England)*, *14*. https://doi.org/10.1186/s13014-019-1416-8

McGranahan, N., & Swanton, C. (2017). Clonal Heterogeneity and Tumor Evolution: Past, Present, and the Future. *Cell*, *168*(4), 613–628. https://doi.org/10.1016/j.cell.2017.01.018

McKinney, M. C., Stark, D. A., Teddy, J., & Kulesa, P. M. (2011). Neural crest cell communication involves an exchange of cytoplasmic material through cellular bridges revealed by photoconversion of KikGR. *Developmental Dynamics : An Official Publication of the American Association of Anatomists*, *240*(6), 1391–1401. https://doi.org/10.1002/dvdy.22612

Miller, J., Fraser, S. E., & McClay, D. (1995). Dynamics of thin filopodia during sea urchin gastrulation. *Development (Cambridge, England)*, *121*(8), 2501–2511.

Moschoi, R., Imbert, V., Nebout, M., Chiche, J., Mary, D., Prebet, T., Saland, E., Castellano, R., Pouyet, L., Collette, Y., Vey, N., Chabannon, C., Recher, C., Sarry, J.-E., Alcor, D., Peyron, J.-F., & Griessinger, E. (2016). Protective mitochondrial transfer from bone marrow stromal cells to acute myeloid leukemic cells during chemotherapy. *Blood*, *128*(2), 253–264. https://doi.org/10.1182/blood-2015-07-655860

Neftel, C., Laffy, J., Filbin, M. G., Hara, T., Shore, M. E., Rahme, G. J., Richman, A. R., Silverbush, D., Shaw, M. L., Hebert, C. M., Dewitt, J., Gritsch, S., Perez, E. M., Gonzalez Castro, L. N., Lan, X., Druck, N., Rodman, C., Dionne, D., Kaplan, A., … Suvà, M. L. (2019). An Integrative Model of Cellular States, Plasticity, and Genetics for Glioblastoma. *Cell*, *178*(4), 835-849.e21. https://doi.org/10.1016/j.cell.2019.06.024

Nichols, C. A., Gibson, W. J., Brown, M. S., Kosmicki, J. A., Busanovich, J. P., Wei, H., Urbanski, L. M., Curimjee, N., Berger, A. C., Gao, G. F., Cherniack, A. D., Dhe-Paganon, S., Paolella, B. R., & Beroukhim, R. (2020). Loss of heterozygosity of essential genes represents a widespread class of potential cancer vulnerabilities. *Nature Communications*, *11*(1), 2517. https://doi.org/10.1038/s41467-020-16399-y

Nzigou Mombo, B., Gerbal-Chaloin, S., Bokus, A., Daujat-Chavanieu, M., Jorgensen, C., Hugnot, J.-P., & Vignais, M.-L. (2017). MitoCeption: Transferring Isolated Human MSC Mitochondria to Glioblastoma Stem Cells. *Journal of Visualized Experiments : JoVE*, *120*. https://doi.org/10.3791/55245

Ohgaki, H., & Kleihues, P. (2007). Genetic Pathways to Primary and Secondary Glioblastoma. *The American Journal of Pathology*, *170*(5), 1445–1453. https://doi.org/10.2353/ajpath.2007.070011

Ohno, H., Hase, K., & Kimura, S. (2010). M-Sec. *Communicative & Integrative Biology*, *3*(3), 231–233.

Olar, A., Wani, K. M., Diefes, K., Heathcock, L. E., van Thuijl, H. F., Gilbert, M. R., Armstrong, T. S., Sulman, E. P., Cahill, D. P., Vera-Bolanos, E., Yuan, Y., Reijneveld, J. C., Ylstra, B., Wesseling, P., & Aldape, K. D. (2015). IDH mutation status and role of WHO grade and mitotic index in overall survival in grade II–III diffuse gliomas. *Acta Neuropathologica*, *129*(4), 585–596. https://doi.org/10.1007/s00401-015-1398-z

Omsland, M., Pise-Masison, C., Fujikawa, D., Galli, V., Fenizia, C., Parks, R. W., Gjertsen, B. T., Franchini, G., & Andresen, V. (2018). Inhibition of Tunneling Nanotube (TNT) Formation and Human T-cell Leukemia Virus Type 1 (HTLV-1) Transmission by Cytarabine. *Scientific Reports*, *8*(1), 11118. https://doi.org/10.1038/s41598-018-29391-w

Onfelt, B., Nedvetzki, S., Benninger, R. K. P., Purbhoo, M. A., Sowinski, S., Hume, A. N., Seabra, M. C., Neil, M. A. A., French, P. M. W., & Davis, D. M. (2006). Structurally distinct membrane nanotubes between human macrophages support long-distance vesicular traffic or surfing of bacteria. *Journal of Immunology (Baltimore, Md.: 1950)*, *177*(12), 8476–8483. https://doi.org/10.4049/jimmunol.177.12.8476

Osswald, M., Jung, E., Sahm, F., Solecki, G., Venkataramani, V., Blaes, J., Weil, S., Horstmann, H., Wiestler, B., Syed, M., Huang, L., Ratliff, M., Karimian Jazi, K., Kurz, F. T., Schmenger, T., Lemke, D., Gömmel, M., Pauli, M., Liao, Y., … Winkler, F. (2015). Brain tumour cells interconnect to a functional and resistant network. *Nature*, *528*(7580), 93–98. https://doi.org/10.1038/nature16071

Osswald, M., Jung, E., Wick, W., & Winkler, F. (2019). Tunneling nanotube-like structures in brain tumors. *CANCER REPORTS*, *2*(6), e1181. https://doi.org/10.1002/cnr2.1181

Osswald, M., Solecki, G., Wick, W., & Winkler, F. (2016). A malignant cellular network in gliomas: Potential clinical implications. *Neuro-Oncology*, *18*(4), 479–485. https://doi.org/10.1093/neuonc/now014

Osuka, S., & Van Meir, E. G. (n.d.). Overcoming therapeutic resistance in glioblastoma: The way forward. *The Journal of Clinical Investigation*, *127*(2), 415–426. https://doi.org/10.1172/JCI89587

Parker, N. R., Khong, P., Parkinson, J. F., Howell, V. M., & Wheeler, H. R. (2015). Molecular heterogeneity in glioblastoma: Potential clinical implications. *Frontiers in Oncology*, *5*, 55. https://doi.org/10.3389/fonc.2015.00055

Pasquier, J., Guerrouahen, B. S., Al Thawadi, H., Ghiabi, P., Maleki, M., Abu-Kaoud, N., Jacob, A., Mirshahi, M., Galas, L., Rafii, S., Le Foll, F., & Rafii, A. (2013). Preferential transfer of mitochondria from endothelial to cancer cells through tunneling nanotubes modulates chemoresistance. *Journal of Translational Medicine*, *11*, 94. https://doi.org/10.1186/1479-5876-11-94

Patel, A. P., Tirosh, I., Trombetta, J. J., Shalek, A. K., Gillespie, S. M., Wakimoto, H., Cahill, D. P., Nahed, B. V., Curry, W. T., Martuza, R. L., Louis, D. N., Rozenblatt-Rosen, O., Suvà, M. L., Regev, A., & Bernstein, B. E. (2014). Single-cell RNA-seq highlights intratumoral heterogeneity in primary glioblastoma. *Science (New York, N.Y.)*, *344*(6190), 1396–1401. https://doi.org/10.1126/science.1254257

Perry, A., & Wesseling, P. (2016). Chapter 5—Histologic classification of gliomas. In M. S. Berger & M. Weller (Eds.), *Handbook of Clinical Neurology* (Vol. 134, pp. 71–95). Elsevier. https://doi.org/10.1016/B978-0-12-802997-8.00005-0

Pinto, G., Brou, C., & Zurzolo, C. (2020). Tunneling Nanotubes: The Fuel of Tumor Progression? *Trends in Cancer*, Oct;6(10):874-888. https://doi.org/10.1016/j.trecan.2020.04.012

Prager, B. C., Bhargava, S., Mahadev, V., Hubert, C. G., & Rich, J. N. (2020). Glioblastoma Stem Cells: Driving Resilience through Chaos. *Trends in Cancer*, *6*(3), 223–235. https://doi.org/10.1016/j.trecan.2020.01.009

Prasetyanti, P. R., & Medema, J. P. (2017). Intra-tumor heterogeneity from a cancer stem cell perspective. *Molecular Cancer*, *16*. https://doi.org/10.1186/s12943-017-0600-4

Pyrgaki, C., Trainor, P., Hadjantonakis, A.-K., & Niswander, L. (2010). Dynamic imaging of mammalian neural tube closure. *Developmental Biology*, *344*(2), 941–947. https://doi.org/10.1016/j.ydbio.2010.06.010

Q, P., Xj, Y., Hm, W., Xt, D., W, W., Y, L., & Jm, L. (2012, January). *Chemoresistance to temozolomide in human glioma cell line U251 is associated with increased activity of O6-methylguanine-DNA methyltransferase and can be overcome by metronomic temozolomide regimen*. Cell Biochemistry and Biophysics; Cell Biochem Biophys. https://doi.org/10.1007/s12013-011-9280-7

Rabé, M., Dumont, S., Álvarez-Arenas, A., Janati, H., Belmonte-Beitia, J., Calvo, G. F., Thibault-Carpentier, C., Séry, Q., Chauvin, C., Joalland, N., Briand, F., Blandin, S., Scotet, E., Pecqueur, C., Clairambault, J., Oliver, L., Perez-Garcia, V., Nadaradjane, A., Cartron, P.-F., … Vallette, F. M. (2020). Identification of a transient state during the acquisition of temozolomide resistance in glioblastoma. *Cell Death & Disease*, *11*(1), 1–14. https://doi.org/10.1038/s41419-019-2200-2

Rajakulendran, N., Rowland, K. J., Selvadurai, H. J., Ahmadi, M., Park, N. I., Naumenko, S., Dolma, S., Ward, R. J., So, M., Lee, L., MacLeod, G., Pasiliao, C., Brandon, C., Clarke, I. D., Cusimano, M. D., Bernstein, M., Batada, N., Angers, S., & Dirks, P. B. (2019). Wnt and Notch signaling govern self-renewal and differentiation in a subset of human glioblastoma stem cells. *Genes & Development*, *33*(9–10), 498–510. https://doi.org/10.1101/gad.321968.118

Ranzinger, J., Rustom, A., Abel, M., Leyh, J., Kihm, L., Witkowski, M., Scheurich, P., Zeier, M., & Schwenger, V. (2011). Nanotube action between human mesothelial cells reveals novel aspects of inflammatory responses. *PloS One*, *6*(12), e29537. https://doi.org/10.1371/journal.pone.0029537

Reichert, D., Scheinpflug, J., Karbanová, J., Freund, D., Bornhäuser, M., & Corbeil, D. (2016). Tunneling nanotubes mediate the transfer of stem cell marker CD133 between hematopoietic progenitor cells. *Experimental Hematology*, *44*(11), 1092-1112.e2. https://doi.org/10.1016/j.exphem.2016.07.006

Reya, T., Morrison, S. J., Clarke, M. F., & Weissman, I. L. (2001). Stem cells, cancer, and cancer stem cells. *Nature*, *414*(6859), 105–111. https://doi.org/10.1038/35102167

Rustom, A., Saffrich, R., Markovic, I., Walther, P., & Gerdes, H.-H. (2004). Nanotubular highways for intercellular organelle transport. *Science (New York, N.Y.)*, *303*(5660), 1007–1010. https://doi.org/10.1126/science.1093133

Sabelström, H., Quigley, D. A., Fenster, T., Foster, D. J., Fuchshuber, C. A. M., Saxena, S., Yuan, E., Li, N., Paterno, F., Phillips, J. J., James, C. D., Norling, B., Berger, M. S., & Persson, A. I. (2019). High density is a property of slow-cycling and treatment-resistant human glioblastoma cells. *Experimental Cell Research*, *378*(1), 76–86. https://doi.org/10.1016/j.yexcr.2019.03.003

Sáenz-de-Santa-María, I., Bernardo-Castiñeira, C., Enciso, E., García-Moreno, I., Chiara, J. L., Suarez, C., & Chiara, M.-D. (2017). Control of long-distance cell-to-cell communication and autophagosome transfer in squamous cell carcinoma via tunneling nanotubes. *Oncotarget*, *8*(13), 20939–20960. https://doi.org/10.18632/oncotarget.15467

Sartori-Rupp, A., Cordero Cervantes, D., Pepe, A., Gousset, K., Delage, E., Corroyer-Dulmont, S., Schmitt, C., Krijnse-Locker, J., & Zurzolo, C. (2019). Correlative cryo-electron microscopy reveals the structure of TNTs in neuronal cells. *Nature Communications*, *10*(1), 342. https://doi.org/10.1038/s41467-018-08178-7

Schachtner, H., Calaminus, S. D. J., Thomas, S. G., & Machesky, L. M. (2013). Podosomes in adhesion, migration, mechanosensing and matrix remodeling. *Cytoskeleton (Hoboken, N.J.)*, *70*(10), 572–589. https://doi.org/10.1002/cm.21119

Schiffer, D., Annovazzi, L., Casalone, C., Corona, C., & Mellai, M. (2018). Glioblastoma: Microenvironment and Niche Concept. *Cancers*, *11*(1). https://doi.org/10.3390/cancers11010005

Schiffer, D., Mellai, M., Annovazzi, L., & Cassoni, C. C. and P. (2015). Tumor Microenvironment—Perivascular and Perinecrotic Niches. *Molecular Considerations and Evolving Surgical Management Issues in the Treatment of Patients with a Brain Tumor*. https://doi.org/10.5772/58962

Schumacher, T., Bunse, L., Pusch, S., Sahm, F., Wiestler, B., Quandt, J., Menn, O., Osswald, M., Oezen, I., Ott, M., Keil, M., Balß, J., Rauschenbach, K., Grabowska, A. K., Vogler, I., Diekmann, J., Trautwein, N., Eichmüller, S. B., Okun, J., … Platten, M. (2014). A vaccine targeting mutant IDH1 induces antitumour immunity. *Nature*, *512*(7514), 324–327. https://doi.org/10.1038/nature13387

Sharma, A., & Shiras, A. (2016). Cancer stem cell-vascular endothelial cell interactions in glioblastoma. *Biochemical and Biophysical Research Communications*, *473*(3), 688–692. https://doi.org/10.1016/j.bbrc.2015.12.022

Sharma, P., Hu-Lieskovan, S., Wargo, J. A., & Ribas, A. (2017). Primary, Adaptive and Acquired Resistance to Cancer Immunotherapy. *Cell*, *168*(4), 707–723. https://doi.org/10.1016/j.cell.2017.01.017

Sherer, N. M., Lehmann, M. J., Jimenez-Soto, L. F., Horensavitz, C., Pypaert, M., & Mothes, W. (2007). Retroviruses can establish filopodial bridges for efficient cell-to-cell transmission. *Nature Cell Biology*, *9*(3), 310–315. https://doi.org/10.1038/ncb1544

Shukla, G., Alexander, G. S., Bakas, S., Nikam, R., Talekar, K., Palmer, J. D., & Shi, W. (2017). Advanced magnetic resonance imaging in glioblastoma: A review. *Chinese Clinical Oncology*, *6*(4), 40–40. https://doi.org/10.21037/cco.2017.06.28

Singh, S. K., Clarke, I. D., Terasaki, M., Bonn, V. E., Hawkins, C., Squire, J., & Dirks, P. B. (2003). Identification of a cancer stem cell in human brain tumors. *Cancer Research*, *63*(18), 5821–5828.

Son, M. J., Woolard, K., Nam, D.-H., Lee, J., & Fine, H. A. (2009). SSEA-1 is an enrichment marker for tumor-initiating cells in human glioblastoma. *Cell Stem Cell*, *4*(5), 440–452. https://doi.org/10.1016/j.stem.2009.03.003

Sosa, V., Moliné, T., Somoza, R., Paciucci, R., Kondoh, H., & LLeonart, M. E. (2013). Oxidative stress and cancer: An overview. *Ageing Research Reviews*, *12*(1), 376–390. https://doi.org/10.1016/j.arr.2012.10.004

Souriant, S., Balboa, L., Dupont, M., Pingris, K., Kviatcovsky, D., Cougoule, C., Lastrucci, C., Bah, A., Gasser, R., Poincloux, R., Raynaud-Messina, B., Al Saati, T., Inwentarz, S., Poggi, S., Moraña, E. J., González-Montaner, P., Corti, M., Lagane, B., Vergne, I., … Vérollet, C. (2019). Tuberculosis Exacerbates HIV-1 Infection through IL-10/STAT3-Dependent Tunneling Nanotube Formation in Macrophages. *Cell Reports*, *26*(13), 3586-3599.e7. https://doi.org/10.1016/j.celrep.2019.02.091

Sowinski, S., Jolly, C., Berninghausen, O., Purbhoo, M. A., Chauveau, A., Köhler, K., Oddos, S., Eissmann, P., Brodsky, F. M., Hopkins, C., Onfelt, B., Sattentau, Q., & Davis, D. M. (2008). Membrane nanotubes physically connect T cells over long distances presenting a novel route for HIV-1 transmission. *Nature Cell Biology*, *10*(2), 211–219. https://doi.org/10.1038/ncb1682

Spees, J. L., Olson, S. D., Whitney, M. J., & Prockop, D. J. (2006). Mitochondrial transfer between cells can rescue aerobic respiration. *Proceedings of the National Academy of Sciences of the United States of America*, *103*(5), 1283–1288. https://doi.org/10.1073/pnas.0510511103

Ståhl, A., Johansson, K., Mossberg, M., Kahn, R., & Karpman, D. (2019). Exosomes and microvesicles in normal physiology, pathophysiology, and renal diseases. *Pediatric Nephrology (Berlin, Germany)*, *34*(1), 11–30. https://doi.org/10.1007/s00467-017-3816-z

Stritzelberger, J., Distel, L., Buslei, R., Fietkau, R., & Putz, F. (2018). Acquired temozolomide resistance in human glioblastoma cell line U251 is caused by mismatch repair deficiency and can be overcome by lomustine. *Clinical & Translational Oncology: Official Publication of the Federation of Spanish Oncology Societies and of the National Cancer Institute of Mexico*, *20*(4), 508–516. https://doi.org/10.1007/s12094-017-1743-x

Stupp, R., Hegi, M. E., Mason, W. P., van den Bent, M. J., Taphoorn, M. J. B., Janzer, R. C., Ludwin, S. K., Allgeier, A., Fisher, B., Belanger, K., Hau, P., Brandes, A. A., Gijtenbeek, J., Marosi, C., Vecht, C. J., Mokhtari, K., Wesseling, P., Villa, S., Eisenhauer, E., … National Cancer Institute of Canada Clinical Trials Group. (2009). Effects of radiotherapy with concomitant and adjuvant temozolomide versus radiotherapy alone on survival in glioblastoma in a randomised phase III study: 5-year analysis of the EORTC-NCIC trial. *The Lancet. Oncology*, *10*(5), 459–466. https://doi.org/10.1016/S1470-2045(09)70025-7

Stupp, R., Mason, W. P., van den Bent, M. J., Weller, M., Fisher, B., Taphoorn, M. J. B., Belanger, K., Brandes, A. A., Marosi, C., Bogdahn, U., Curschmann, J., Janzer, R. C., Ludwin, S. K., Gorlia, T., Allgeier, A., Lacombe, D., Cairncross, J. G., Eisenhauer, E., & Mirimanoff, R. O. (2005). Radiotherapy plus Concomitant and Adjuvant Temozolomide for Glioblastoma. *New England Journal of Medicine*, *352*(10), 987–996. https://doi.org/10.1056/NEJMoa043330

Stupp, R., Mason, W. P., van den Bent, M. J., Weller, M., Fisher, B., Taphoorn, M. J. B., Belanger, K., Brandes, A. A., Marosi, C., Bogdahn, U., Curschmann, J., Janzer, R. C., Ludwin, S. K., Gorlia, T., Allgeier, A., Lacombe, D., Cairncross, J. G., Eisenhauer, E., Mirimanoff, R. O., … National Cancer Institute of Canada Clinical Trials Group. (2005). Radiotherapy plus concomitant and adjuvant temozolomide for glioblastoma. *The New England Journal of Medicine*, *352*(10), 987–996. https://doi.org/10.1056/NEJMoa043330

Sun, Y., Kong, W., Falk, A., Hu, J., Zhou, L., Pollard, S., & Smith, A. (2009). CD133 (Prominin) Negative Human Neural Stem Cells Are Clonogenic and Tripotent. *PLoS ONE*, *4*(5). https://doi.org/10.1371/journal.pone.0005498

Suvà, M. L., Rheinbay, E., Gillespie, S. M., Patel, A. P., Wakimoto, H., Rabkin, S. D., Riggi, N., Chi, A. S., Cahill, D. P., Nahed, B. V., Curry, W. T., Martuza, R. L., Rivera, M. N., Rossetti, N., Kasif, S., Beik, S., Kadri, S., Tirosh, I., Wortman, I., … Bernstein, B. E. (2014).

Reconstructing and reprogramming the tumor-propagating potential of glioblastoma stem-like cells. *Cell*, *157*(3), 580–594. https://doi.org/10.1016/j.cell.2014.02.030

Tan, A. S., Baty, J. W., Dong, L.-F., Bezawork-Geleta, A., Endaya, B., Goodwin, J., Bajzikova, M., Kovarova, J., Peterka, M., Yan, B., Pesdar, E. A., Sobol, M., Filimonenko, A., Stuart, S., Vondrusova, M., Kluckova, K., Sachaphibulkij, K., Rohlena, J., Hozak, P., … Berridge, M. V. (2015). Mitochondrial genome acquisition restores respiratory function and tumorigenic potential of cancer cells without mitochondrial DNA. *Cell Metabolism*, *21*(1), 81–94. https://doi.org/10.1016/j.cmet.2014.12.003

Teddy, J. M., & Kulesa, P. M. (2004). In vivo evidence for short- and long-range cell communication in cranial neural crest cells. *Development (Cambridge, England)*, *131*(24), 6141–6151. https://doi.org/10.1242/dev.01534

Thakkar, J. P., Dolecek, T. A., Horbinski, C., Ostrom, Q. T., Lightner, D. D., Barnholtz-Sloan, J. S., & Villano, J. L. (2014). Epidemiologic and Molecular Prognostic Review of Glioblastoma. *Cancer Epidemiology, Biomarkers & Prevention : A Publication of the American Association for Cancer Research, Cosponsored by the American Society of Preventive Oncology*, *23*(10), 1985–1996. https://doi.org/10.1158/1055-9965.EPI-14-0275

Thayanithy, V., Dickson, E. L., Steer, C., Subramanian, S., & Lou, E. (2014). Tumor-stromal cross talk: Direct cell-to-cell transfer of oncogenic microRNAs via tunneling nanotubes. *Translational Research: The Journal of Laboratory and Clinical Medicine*, *164*(5), 359–365. https://doi.org/10.1016/j.trsl.2014.05.011

Tilney, L. G., Tilney, M. S., & DeRosier, D. J. (1992). Actin Filaments, Stereocilia, and Hair Cells: How Cells Count and Measure. *Annual Review of Cell Biology*, *8*(1), 257–274. https://doi.org/10.1146/annurev.cb.08.110192.001353

Tombal, B., Denmeade, S. R., Gillis, J.-M., & Isaacs, J. T. (2002). A supramicromolar elevation of intracellular free calcium ([Ca 2+] i) is consistently required to induce the execution phase of apoptosis. *Cell Death & Differentiation*, *9*(5), 561–573. https://doi.org/10.1038/sj.cdd.4400999

Ung, N., & Yang, I. (2015). Nanotechnology to augment immunotherapy for the treatment of glioblastoma multiforme. *Journal of Neuro-Oncology*, *123*(3), 473–481. https://doi.org/10.1007/s11060-015-1814-1

Valdebenito, S., Audia, A., Bhat, K. P. L., Okafo, G., & Eugenin, E. A. (2020). Tunneling Nanotubes Mediate Adaptation of Glioblastoma Cells to Temozolomide and Ionizing Radiation Treatment. *IScience*, *23*(9), 101450. https://doi.org/10.1016/j.isci.2020.101450

Vargas, J. Y., Grudina, C., & Zurzolo, C. (2019). The prion-like spreading of α-synuclein: From in vitro to in vivo models of Parkinson's disease. *Ageing Research Reviews*, *50*, 89–101. https://doi.org/10.1016/j.arr.2019.01.012

Vargas, J. Y., Loria, F., Wu, Y.-J., Córdova, G., Nonaka, T., Bellow, S., Syan, S., Hasegawa, M., van Woerden, G. M., Trollet, C., & Zurzolo, C. (2019). The Wnt/Ca2+ pathway is involved in interneuronal communication mediated by tunneling nanotubes. *The EMBO Journal*, *38*(23), e101230. https://doi.org/10.15252/embj.2018101230

Veillat, V., Spuul, P., Daubon, T., Egaña, I., Kramer, Ij., & Génot, E. (2015). Podosomes: Multipurpose organelles? *The International Journal of Biochemistry & Cell Biology*, *65*, 52–60. https://doi.org/10.1016/j.biocel.2015.05.020

Venkataramani, V., Tanev, D. I., Strahle, C., Studier-Fischer, A., Fankhauser, L., Kessler, T., Körber, C., Kardorff, M., Ratliff, M., Xie, R., Horstmann, H., Messer, M., Paik, S. P., Knabbe, J., Sahm, F., Kurz, F. T., Acikgöz, A. A., Herrmannsdörfer, F., Agarwal, A., … Kuner, T. (2019). Glutamatergic synaptic input to glioma cells drives brain tumour progression. *Nature*, *573*(7775), 532–538. https://doi.org/10.1038/s41586-019-1564-x

Venkatesh, H. S., Johung, T. B., Caretti, V., Noll, A., Tang, Y., Nagaraja, S., Gibson, E. M., Mount, C. W., Polepalli, J., Mitra, S. S., Woo, P. J., Malenka, R. C., Vogel, H., Bredel, M., Mallick,

P., & Monje, M. (2015). Neuronal Activity Promotes Glioma Growth through Neuroligin-3 Secretion. *Cell*, *161*(4), 803–816. https://doi.org/10.1016/j.cell.2015.04.012

Venkatesh, H. S., Morishita, W., Geraghty, A. C., Silverbush, D., Gillespie, S. M., Arzt, M., Tam, L. T., Espenel, C., Ponnuswami, A., Ni, L., Woo, P. J., Taylor, K. R., Agarwal, A., Regev, A., Brang, D., Vogel, H., Hervey-Jumper, S., Bergles, D. E., Suvà, M. L., … Monje, M. (2019). Electrical and synaptic integration of glioma into neural circuits. *Nature*, *573*(7775), 539–545. https://doi.org/10.1038/s41586-019-1563-y

Venkatesh, H. S., Tam, L. T., Woo, P. J., Lennon, J., Nagaraja, S., Gillespie, S. M., Ni, J., Duveau, D. Y., Morris, P. J., Zhao, J. J., Thomas, C. J., & Monje, M. (2017). Targeting neuronal activity-regulated neuroligin-3 dependency in high-grade glioma. *Nature*, *549*(7673), 533–537. https://doi.org/10.1038/nature24014

Verhaak, R. G. W., Hoadley, K. A., Purdom, E., Wang, V., Qi, Y., Wilkerson, M. D., Miller, C. R., Ding, L., Golub, T., Mesirov, J. P., Alexe, G., Lawrence, M., O'Kelly, M., Tamayo, P., Weir, B. A., Gabrie, S., Winckler, W., Gupta, S., Jakkula, L., … Hayes, D. N. (2010). An integrated genomic analysis identifies clinically relevant subtypes of glioblastoma characterized by abnormalities in PDGFRA, IDH1, EGFR and NF1. *Cancer Cell*, *17*(1), 98. https://doi.org/10.1016/j.ccr.2009.12.020

Victoria, G. S., Arkhipenko, A., Zhu, S., Syan, S., & Zurzolo, C. (2016). Astrocyte-to-neuron intercellular prion transfer is mediated by cell-cell contact. *Scientific Reports*, *6*, 20762. https://doi.org/10.1038/srep20762

Victoria, G. S., & Zurzolo, C. (2015). Trafficking and degradation pathways in pathogenic conversion of prions and prion-like proteins in neurodegenerative diseases. *Virus Research*, *207*, 146–154. https://doi.org/10.1016/j.virusres.2015.01.019

Victoria, G. S., & Zurzolo, C. (2017). The spread of prion-like proteins by lysosomes and tunneling nanotubes: Implications for neurodegenerative diseases. *The Journal of Cell Biology*, *216*(9), 2633–2644. https://doi.org/10.1083/jcb.201701047

Vignais, M.-L., Caicedo, A., Brondello, J.-M., & Jorgensen, C. (2017). Cell Connections by Tunneling Nanotubes: Effects of Mitochondrial Trafficking on Target Cell Metabolism, Homeostasis, and Response to Therapy. *Stem Cells International*, *2017*, 6917941. https://doi.org/10.1155/2017/6917941

Vlashi, E., Lagadec, C., Vergnes, L., Matsutani, T., Masui, K., Poulou, M., Popescu, R., Della Donna, L., Evers, P., Dekmezian, C., Reue, K., Christofk, H., Mischel, P. S., & Pajonk, F. (2011). Metabolic state of glioma stem cells and nontumorigenic cells. *Proceedings of the National Academy of Sciences of the United States of America*, *108*(38), 16062–16067. https://doi.org/10.1073/pnas.1106704108

Walsh, J. H., Karnes, W. E., Cuttitta, F., & Walker, A. (1991). Autocrine growth factors and solid tumor malignancy. *Western Journal of Medicine*, *155*(2), 152–163.

Wang, J., Liu, X., Qiu, Y., Shi, Y., Cai, J., Wang, B., Wei, X., Ke, Q., Sui, X., Wang, Y., Huang, Y., Li, H., Wang, T., Lin, R., Liu, Q., & Xiang, A. P. (2018). Cell adhesion-mediated mitochondria transfer contributes to mesenchymal stem cell-induced chemoresistance on T cell acute lymphoblastic leukemia cells. *Journal of Hematology & Oncology*, *11*. https://doi.org/10.1186/s13045-018-0554-z

Wang, X., & Gerdes, H.-H. (2015). Transfer of mitochondria via tunneling nanotubes rescues apoptotic PC12 cells. *Cell Death and Differentiation*, *22*(7), 1181–1191. https://doi.org/10.1038/cdd.2014.211

Wang, Xiang, Veruki, M. L., Bukoreshtliev, N. V., Hartveit, E., & Gerdes, H.-H. (2010). Animal cells connected by nanotubes can be electrically coupled through interposed gap-junction channels. *Proceedings of the National Academy of Sciences of the United States of America*, *107*(40), 17194–17199. https://doi.org/10.1073/pnas.1006785107

Wang, Xiaoqing, Yu, X., Xie, C., Tan, Z., Tian, Q., Zhu, D., Liu, M., & Guan, Y. (2016). Rescue of Brain Function Using Tunneling Nanotubes Between Neural Stem Cells and Brain

Microvascular Endothelial Cells. *Molecular Neurobiology*, *53*(4), 2480–2488. https://doi.org/10.1007/s12035-015-9225-z

Wang, Y., Cui, J., Sun, X., & Zhang, Y. (2011). Tunneling-nanotube development in astrocytes depends on p53 activation. *Cell Death and Differentiation*, *18*(4), 732–742. https://doi.org/10.1038/cdd.2010.147

Ware, M. J., Tinger, S., Colbert, K. L., Corr, S. J., Rees, P., Koshkina, N., Curley, S., Summers, H. D., & Godin, B. (2015). Radiofrequency treatment alters cancer cell phenotype. *Scientific Reports*, *5*, 12083. https://doi.org/10.1038/srep12083

Weber, P. A., Chang, H.-C., Spaeth, K. E., Nitsche, J. M., & Nicholson, B. J. (2004). The permeability of gap junction channels to probes of different size is dependent on connexin composition and permeant-pore affinities. *Biophysical Journal*, *87*(2), 958–973. https://doi.org/10.1529/biophysj.103.036350

Weil, S., Osswald, M., Solecki, G., Grosch, J., Jung, E., Lemke, D., Ratliff, M., Hänggi, D., Wick, W., & Winkler, F. (2017). Tumor microtubes convey resistance to surgical lesions and chemotherapy in gliomas. *Neuro-Oncology*, *19*(10), 1316–1326. https://doi.org/10.1093/neuonc/nox070

Wesseling, P., & Capper, D. (2018). WHO 2016 Classification of gliomas. *Neuropathology and Applied Neurobiology*, *44*(2), 139–150. https://doi.org/10.1111/nan.12432

Xu, W., Santini, P. A., Sullivan, J. S., He, B., Shan, M., Ball, S. C., Dyer, W. B., Ketas, T. J., Chadburn, A., Cohen-Gould, L., Knowles, D. M., Chiu, A., Sanders, R. W., Chen, K., & Cerutti, A. (2009). HIV-1 evades virus-specific IgG2 and IgA responses by targeting systemic and intestinal B cells via long-range intercellular conduits. *Nature Immunology*, *10*(9), 1008–1017. https://doi.org/10.1038/ni.1753

Yuan, Y., Jiang, Y.-C., Sun, C.-K., & Chen, Q.-M. (2016). Role of the tumor microenvironment in tumor progression and the clinical applications (Review). *Oncology Reports*, *35*(5), 2499–2515. https://doi.org/10.3892/or.2016.4660

Zeng, Y., Wang, X., Wang, J., Yi, R., Long, H., Zhou, M., Luo, Q., Zhai, Z., Song, Y., & Qi, S. (2018). The Tumorgenicity of Glioblastoma Cell Line U87MG Decreased During Serial In Vitro Passage. *Cellular and Molecular Neurobiology*, *38*(6), 1245–1252. https://doi.org/10.1007/s10571-018-0592-7

Zhang, L., & Zhang, Y. (2015). Tunneling nanotubes between rat primary astrocytes and C6 glioma cells alter proliferation potential of glioma cells. *Neuroscience Bulletin*, *31*(3), 371–378. https://doi.org/10.1007/s12264-014-1522-4

Zhu, D., Tan, K. S., Zhang, X., Sun, A. Y., Sun, G. Y., & Lee, J. C.-M. (2005). Hydrogen peroxide alters membrane and cytoskeleton properties and increases intercellular connections in astrocytes. *Journal of Cell Science*, *118*(Pt 16), 3695–3703. https://doi.org/10.1242/jcs.02507

Zhu, S., Abounit, S., Korth, C., & Zurzolo, C. (2017). Transfer of disrupted-in-schizophrenia 1 aggregates between neuronal-like cells occurs in tunnelling nanotubes and is promoted by dopamine. *Open Biology*, *7*(3), Article 3. https://doi.org/10.1098/rsob.160328

Zhu, S., Bhat, S., Syan, S., Kuchitsu, Y., Fukuda, M., & Zurzolo, C. (2018). Rab11a-Rab8a cascade regulates the formation of tunneling nanotubes through vesicle recycling. *Journal of Cell Science*, *131*(19), Article 19. https://doi.org/10.1242/jcs.215889

Zhu, S., Victoria, G. S., Marzo, L., Ghosh, R., & Zurzolo, C. (2015). Prion aggregates transfer through tunneling nanotubes in endocytic vesicles. *Prion*, *9*(2), 125–135. https://doi.org/10.1080/19336896.2015.1025189

Zong, H., Verhaak, R. G., & Canoll, P. (2012). The cellular origin for malignant glioma and prospects for clinical advancements. *Expert Review of Molecular Diagnostics*, *12*(4), 383–394. https://doi.org/10.1586/erm.12.30

Annexe

CellPress REVIEWS

Review

Tunneling Nanotubes: The Fuel of Tumor Progression?

Giulia Pinto,[1,2] Christel Brou,[1,3] and Chiara Zurzolo[1,3,*]

Tunneling nanotubes (TNTs) are thin membrane tubes connecting remote cells and allowing the transfer of cellular content. TNTs have been reported in several cancer *in vitro, ex vivo*, and *in vivo* models. Cancer cells exploit TNT-like connections to exchange material between themselves or with the tumoral microenvironment. Cells acquire new abilities (e.g., enhanced metabolic plasticity, migratory phenotypes, angiogenic ability, and therapy resistance) via these exchanges, contributing to cancer aggressiveness. Here, we review the morphological and functional features of TNT-like structures and their impact on cancer progression and resistance to therapies. Finally, we discuss the case of glioblastoma (GBM), in which a functional and resistant network between cancer cells in an *in vivo* model has been described for the first time.

Highlights

TNTs are physical membranous channels of communication between cells.

TNTs transfer mitochondria, nucleic acids, lysosomes, autophagosomes, protein-containing vesicles, and drugs.

Different types of TNT-like structure have been shown in several cancer cell lines, murine xenograft models, and in tumor sections from patients

TNT-mediated transfer of material can promote invasiveness, angiogenic ability, proliferation, metabolism plasticity, and therapy resistance

In gliomas, a functional network, comprising different types of intercellular connection, including TNTs, drives a more aggressive phenotype

Cancer and Intercellular Communication

Cancer is among the leading causes of mortality worldwide, responsible for 1 in 6 deaths, according to the World Health Organization. Over the past decades, many therapeutic strategies have proven their effectiveness and the overall cancer death rate has been reduced by 27% [1]. Several features of cancer cells make these pathologies very aggressive and difficult to cure, such as their uncontrollable proliferative capacity and their ability to obtain nourishment through neoformed blood vessels, to infiltrate healthy tissues forming metastasis, to evade the immune system, and, finally, to adapt to clinical treatments. In this context, intercellular communication, particularly, cell-to-cell transfer of cellular material, can contribute to each of the aforementioned characteristics, including treatment resistance. Over the past 20 years, numerous studies have shown that exosomes and exovesicles are able to carry malignant content (e.g., proteins and nucleic acids), likely helping the recipient cells to express genes supporting proliferation, colonization, and immune evasion, or to recover from damage provoked by treatment [2,3]. Recent work highlighted a new communication mechanism implemented by tumor cells, tunneling nanotubes (TNTs), which are physical channels providing cytoplasmic continuity between distant cells (Figure 1A). TNTs are thin, actin-based membrane tubes that, by contrast to other cellular protrusions, listed in Table 1, are open-ended at their extremities [4,5]. They allow the transfer of various-sized cargoes (Figure 1), such as small molecules (e.g., Ca^{2+} ions), macromolecules (proteins, nucleic acids, etc.), and even organelles (vesicles, mitochondria, lysosomes, autophagosomes, etc.) [6]. Several cells can be connected by TNTs, possibly leading to the formation of a functional cellular network [7].

TNTs were first identified in 2004 by Rustom and colleagues in cultures of pheochromocytoma PC12 cells [4]. Later, several other publications reported the presence of 'TNT-like structures' (heterogenous intercellular connections, defined on the basis of their morphology) in many other cell types in *in vitro* cultures, including astrocytes [8], immune cells [9], as well as in tumor cancer cell lines, where their occurrence was often correlated with more aggressive tumor phenotypes [10,11]. Beyond tumors, TNT-like structures have been observed in early developmental stages in various organisms [12] as well as in relation to stress-induced responses, such as oxidative stress [8,13], allowing the discharge of cellular waste or dangerous materials. Similarly,

[1]Unité de Trafic Membranaire et Pathogenèse, Institut Pasteur, UMR3691 CNRS, 28 rue du Docteur Roux, F-75015 Paris, France
[2]Sorbonne Université, ED394 - Physiologie, Physiopathologie et Thérapeutique, F-75005 Paris, France
[3]These authors contributed equally to this work

*Correspondence: chiara.zurzolo@pasteur.fr (C. Zurzolo).

 https://doi.org/10.1016/j.trecan.2020.04.012
© 2020 Elsevier Inc. All rights reserved.

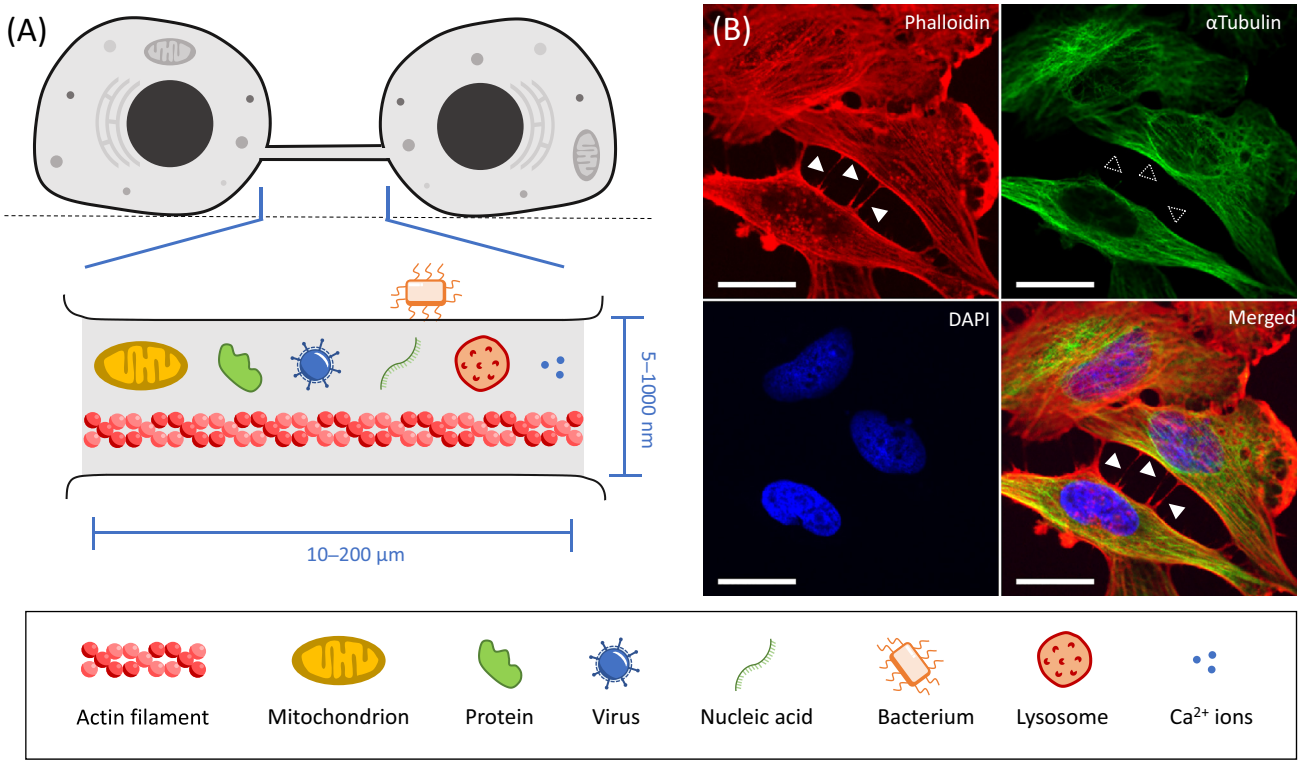

Figure 1. Tunneling Nanotubes (TNTs) in Cell Culture. (A) Schematic of two cells connected by a TNT in cell culture. The connection floats above the adhesion surface (dashed line). The lower part shows a magnification of the TNT and possible cargoes traveling along it. The range of TNT diameters and lengths is indicated. (B) Representative fluorescence images of TNTs between cells in culture. U-251 glioblastoma cells were plated at a density of 20 k cells/cm^2 for 24 h, fixed with PFA 4%, and permeabilized in 0.2% Triton-X100. Actin filaments (in red), microtubules (in green), and nuclei (in blue) were stained with phalloidin-rhodamine (1/500 Invitrogen R415), anti-αTubulin (1/1000 Sigma-Aldrich T9026), and DAPI (Sigma-Aldrich D9542), respectively. White-filled arrowheads point to TNTs positive for actin staining. Dashed arrowheads indicate the absence of tubulin staining. Confocal images acquired with Spinning Disk Yokogawa CSU-X1. Scale bars 20 µm.

they can be used as a route for the dissemination of pathogens, such as HIV [14,15], bacteria [9], and prions and amyloid fibrils in the case of neurodegenerative diseases [16–21]. Although TNT-like structures have been clearly identified as physical and functional entities in solid tumors [22–26], the existence of these connections in whole healthy organs or tissues is still a matter of debate. Here, we review studies on TNTs and their heterogeneity in cancers and their possible role in tumor progression and development of treatment resistance, with a particular focus on GBM.

Detection of TNT-like Structures *In Vitro* and *In Vivo* in Cancer

The first identification of TNTs occurred in PC12 cells, which are derived from a rare rat tumor of adrenal gland tissue [4]. Subsequently, many other cancer cell lines have been shown to form membranous connections bridging distant cells, as summarized in Table 1. Of importance for this review, TNT-like structures were also observed in primary cells directly obtained from patients, for example, from squamous cell carcinoma [24,25], mesothelioma [10,22], and different forms of leukemia [27–29]. Cancer cells can form heterotypic connections with cells of the tumor microenvironment (TME), including mesenchymal [30], endothelial [11], and immune cells [31]. Crosstalk with the TME has a significant role in sustaining cancer progression, providing nutrients or buffering metabolic stress [32], and interaction with immune cells can contribute to overcoming immunosurveillance [33]. While it is possible to identify TNT-like structures between

Table 1. Types of Cellular Projection

Name	Description	Actin/microtubule content	Membrane fusion with target cell?	Function	Refs
Cilia	Large protuberances emerging from cell body	Actin and microtubules	No	Environment sensing, coordination of signaling pathways	[83]
Stereocilia	Thin specialized cell protrusions on apical surface	Actin	No	Cellular polarity, transduction of mechanic stimuli	[84]
Lamellipodia and ruffles	Dynamic veil-shaped cell protrusions	Actin	No	Leading edge in cell migration	[85]
Filopodia	Finger-like, dynamic, thin membrane protrusions	Actin	No	Cell adhesion, environment sensing	[86]
Cytonemes/specialized filopodia	Finger-like, dynamic, thin membrane protrusions extending to target cell	Actin	No	Morphogen delivery by direct contact with target cells	[87]
Mitotic bridges	Thin bridges between daughter cells after mitosis	Actin	Yes	Reminiscent of cellular division, can share material	[88]
Neurites	Large extensions from cell body of neurons	Actin and microtubules	No	Neurotransmitter release/reception and propagation of action potential	[89]
Tumor microtubes	Thick membrane extensions containing GAP junctions, either connecting two cells or finger-like protrusions	Actin and microtubules	Yes/No	Transmission of intercellular ion fluxes, cell invasion, formation of neuron–glioma synapses	[67,72,73,90]
TNTs	Thin membrane connections, open-ended	Actin, sometimes microtubules	Yes	Exchange of cellular cargo between cells	[6]
Invadopodia	Finger-like membrane protrusions	Actin	No	Matrix degradation	[91]
Podosomes	Dynamic membrane-bound microdomains	Actin	No	Adhesion, mechanosensing, and matrix degradation	[92]

the same or different cell types in cell cultures using light microscopy [34], their identification in a more complex context, such as animal models or tumor resections, is still challenging. This is because no specific marker for these structures has been identified yet, and the optical resolution of classical microscopy does not allow for the morphological characterization of these connections in a tissue environment [5,12]. Therefore, the heterogeneity and lack of structural characterization of TNTs represent major problems for their investigation. Given their morphological heterogeneity and poor molecular and structural characterization, the intercellular connections observed to date have been named differently in different studies (nanoscale conduit [11], tunneling nanotubes [22], intercellular bridges [12] ,or membranous tunneling tubes [24]). This has raised both confusion and skepticism in the field [35], and calls out for both more rigorous definition and more accurate technical approaches to study them. We propose that 'TNT' should only refer to the connections that fulfill the following characteristics: (i) continuous membrane connections with the plasma membrane of the connected cells; (ii) nonadherent to substratum; (iii) containing actin; (iv) proven cargo transport; and (v) open-ended (Table 1). By contrast, we refer to 'TNT-like' connections when one or more of these properties is not fulfilled or has not been assessed.

The first documentation of TNT-like structures *ex vivo* in solid tumors was provided by the laboratory of Emil Lou in 2012, which described mitochondria-containing connections in tissue sections of a mesothelioma resected from a patient [22]. These observations were followed by others, showing various intercellular connections in squamous cell carcinoma [24,25], ovarian

Table 2. Tumor Cell Models Used for the Study of TNT-Mediated Communication *In Vitro*

Tumor model	Cargo	TNT function	TNT regulators[a]	Year of publication	Refs
Rat pheochromocytoma cell lines	Lysosomes, soluble and membrane markers	n.d.	n.d.	2004	[4]
HeLa (cervical cancer)	Calcium	n.d.	M-Sec	2009	[46]
Mesothelioma cell lines and primary human mesothelioma cells	Golgi vesicles, mitochondria, fluorescent proteins	n.d.	Low serum (+), hyperglycemic (+), acidic medium (+), EMT-inducing cytokines (+), metformin (–), everolimus (–), latrunculin A (–)	2012	[22]
Ovarian and breast cancer cell lines	Cytoplasmic content, mitochondria	Mitochondria transfer from stromal cells promotes chemoresistance	n.d.	2013	[30]
Osteosarcoma and ovarian cancer cell lines	miRNA	Spreading of genetic and oncogenic material between tumoral–tumoral and tumoral–stromal cells	Low serum and hyperglycemic medium (+)	2014	[23]
Mesothelioma cell lines	n.d.	TNT correlates with more aggressive phenotype and expression of genes related to invasion and metastasis	Low serum and hyperglycemic medium (+), migrastatin (–)	2014	[10]
Head and neck squamous cell carcinoma primary cells	Mitochondria and nucleic acids	Electrical coupling	n.d.	2014	[24]
Primary rat astrocytes and glioma cell line	Mitochondria	Support in glioma cell proliferation	H_2O_2 (+), latrunculin A (–)	2015	[13]
Metastatic breast cancer cell lines	miRNA	Transfer of miRNA alters phenotype of receiving endothelial cells. TNT correlates with more aggressive phenotype	Docetaxel (–), latrunculin A (–), cytochalasin D (–)	2015	[11]
Pancreatic adenocarcinoma cell lines	Electron-dense particles	n.d.	Radiofrequency treatment (+)	2015	[56]
Rat pheochromocytoma cell lines	Mitochondria	Rescued UV-treated apoptotic cells	Cytochalasin B (–)	2015	[60]
Ovarian cancer cell lines (different chemoresistances)	Mitochondria	Adaptation mechanism to hypoxia in chemoresistant cells	Hypoxia (+)	2016	[42]
Head and neck squamous cell carcinoma cell lines	Lysosomes, mitochondria, autophagosomes	n.d.	MMP2, FAK	2017	[25]
Bladder cancer cell lines	Mitochondria	Mitochondria transfer promotes invasiveness	n.d.	2017	[37]
Acute myeloid leukemia primary cells	Mitochondria	Mitochondria transfer from bone marrow supports cancer cell metabolism and promotes stress-adaptative response	NOX2	2017	[28]
Pancreatic adenocarcinoma and ovarian cancer cell lines	Doxorubicin	Redistribution of drug	Doxorubicin (+)	2018	[26]
Acute lymphoblastic leukemia cell lines and human primary T leukemic cells	Mitochondria	Mitochondria transfer promotion of chemoresistance	Cytochalasin D (–), MTX (-)	2018	[27]
Colon cancer cell lines	n.d.	Transfer of oncogenic protein (mutated KRAS) and activation of Erk pathway in acceptor cells	KRAS	2019	[45]
Breast cancer cell lines	Membrane and/or vesicles	Transfer between macrophages and tumor cells inducing invasiveness	M-Sec	2019	[31]

(continued on next page)

Table 2. (continued)

Tumor model	Cargo	TNT function	TNT regulators[a]	Year of publication	Refs
Prostate cancer cell lines	Lysosomes, mitochondria, stress-induced chaperones	Adaptation mechanism therapeutic stress	Chemotherapy by androgen receptor blockade (+), low serum, hyperglycemic, acidic medium (+), hypoxia (+), cytochalasin D (–)	2019	[43]
Chronic myeloid leukemia cell lines	Protein-containing vesicles	Protein transfer from stromal cells provides protection to leukemic cells	n.d.	2019	[38]
Patient bone marrow cells and multiple myeloma-derived cell lines	Mitochondria	Mitochondria transfer from bone marrow supports cancer cell metabolism and promotes stress-adaptative response	CD38, Chemotherapy by bortezomid (+), cytochalasin B (–)	2019	[29]
Bladder cancer cell lines	miRNA	Induction of invasive and proliferative phenotype	n.d.	2019	[53]
GBM cancer cell line	Functionalized liposomes	Delivery of nanoparticles	n.d.	2019	[76]

[a](+), induced; (–), inhibited; n.d., not described.

[23] and pancreatic cancer [26], and human glioblastoma (GBM) cells engrafted into mice models [36] (Table 2). Little is known about the structural and functional features of these connections *in vivo*. In some cases, however, the presence of mitochondria and possibly other cargoes inside them supports the hypothesis that these structures are open-ended and, thus, are canonical TNTs and allow the transfer of cargoes.

Morphology and Structure of TNTs

Despite the lack of a specific marker, TNTs can be identified in cell culture by fluorescent labeling of the plasma membrane and cytoskeleton components, observed by using light microscopy (Figure 1B). However, specific fixation protocols are needed to preserve their delicate and fragile nature [34], and functional assays have to be performed in addition to morphological studies to fulfill the definition of TNTs (see earlier). TNTs exhibit high variability in their morphology, in terms of length, thickness, and cytoskeleton content, specifically regarding the presence/absence of microtubules [34]. Nevertheless, they always appear as actin-based connections and their presence and functionality can be affected by inhibitors of actin polymerization (e.g., latrunculin or cytochalasin) (Table 2). In cancer cellular models, the observed connections can range from tens to several hundreds of microns [10,11,25]. In some tumor tissues, exceptional connections >500 μm have been observed [24,36]. Although in most *in vitro* studies, the diameter of the connections in tissues was on the nanoscale (<1 μm), microscale connections (>1 μm) [24,36] were also present. However, these long and thick connections fit best with the definition of tumor microtubes rather than of TNTs (Table 1). At present, we do not know whether TNTs display different morphologies *in vitro* or *in vivo* or whether nanoscale connections are detectable in the complexity of the tissue. The thickness of TNTs also correlates with their cytoskeleton content, with protrusions containing microtubules having larger diameters [9]. However, some cancers appear to present both types of connection: those containing only actin and those with both actin and microtubules [11,25].

A few studies have addressed the ultrastructure of TNTs in cancer models with the use of electron microscopy [37,38]. A deeper structural analysis of TNTs, using a combination of cryo-fluorescence microscopy with cryo-electron microscopy, was conducted recently. This study used a catecholaminergic differentiated (CAD) cell line, established from a brain tumor in a transgenic mouse, and SH-SY5Y cells, isolated from a patient with neuroblastoma [5]. By using

experimental conditions set up to better preserve TNT structure, this study showed that, in these two types of neuronal cell line, TNTs can comprise multiple individual tubes (named iTNTs) held together by N-cadherin-positive structures and often open-ended at their tips [5]. Nonetheless, whether iTNTs exist in different cell types and tumors and/or *in vivo* remain open questions.

Functional Approaches

The distinguishing characteristic of TNTs with respect to other cellular extensions (e.g., filopodia or mitotic bridges; Table 1) is their ability to transfer cellular material. Some research has provided qualitative evidence of cargoes inside TNT-like structures observed in different cancers [22,37], without proving that actual transfer had occurred and without excluding cell division as the mechanism by which the cellular material was shared. To exclude the latter, membrane vesicles or organelles, such as mitochondria or lysosomes, can be labeled in a population of cells defined as donors. This population is then co-cultured with an acceptor population (differently labeled) to further detect and quantify the cargoes transferred in the acceptors by fluorescence microscopy (in fixed or live condition) or flow cytometry [34]. The co-culture has to be performed placing the two populations in direct physical contact at an appropriate cell density that favors the formation and detection of TNTs. To evaluate secretion as a possible mechanism of transfer, the two populations can be separated by a filter that allows the transfer of secreted material, or they can be grown in different dishes and the acceptor population challenged with the supernatant from donor cells [34]. The weakness of this approach is that it only allows the direct transfer (cell contact mediated) of the labeled cargo to be determined. It does not consider other materials that could be transported through the same connections, including those that could be shared in the opposite direction. To overcome this limit, other approaches, such as mass spectrometry [38] and transcriptomic analysis [11], have been recently applied to detect alterations at the proteome and transcriptome levels. In these examples, the acceptor population acquired protumoral features correlated with the transfer of proteins or miRNA involved in cell survival, drug response, or cellular reprogramming. All these approaches show how TNTs might be differently exploited in various types of cancer (Table 2). However, we still do not know whether the variability observed at the TNT level in the various studies and in the various cancers corresponds to different roles for TNTs in the cancers or just to the different questions addressed.

Few approaches have studied the dynamics and transfer ability of these structures *in vivo*. Using multiphoton microscopy, connections between human tumor cells were detected in mouse xenografts [36] (Table 3), while the transfer between human and murine cells was quantified by amplification of species-specific DNA sequences or detection of labeled material by flow cytometry [11,28,29]. Although powerful and of interest, these approaches make it possible to monitor the transfer without specifically identifying its mechanism, in particular without excluding the secretion mechanism.

In conclusion, due to the limitations of the *in vivo* models (e.g., TNT preservation and observation), the field needs to pursue the study of these fragile structures in cellular models that are representative as much as possible of the tumoral tissue (e.g., patient-derived cells); this would enable researchers to address more easily specific questions on the mechanism and content of the transfer and its impact on the receiving cells. In parallel, new tissular models recapitulating the tumoral context as tumor-derived organoid cultures need to be implemented in the field. Finally, additional efforts need to be made to overcome the technical limitations of the *in vivo* study of TNTs to finally unravel their role in physiopathological contexts beyond their morphological diversities.

Tumoral Context Might Favor TNT Connectivity

Since their discovery, TNTs have been described as a mechanism of adaptive response to cellular stress. Interestingly, several cancer-related environmental conditions have been shown to

Table 3. Evidence of TNT-like Communication in Tissue

Cancer	Model	Labeling	Year of publication	Refs
Malignant pleural mesothelioma and lung adenocarcinoma	Patient tissue	Mitochondria	2012	[22]
Ovarian cancer	Patient tissue	Mitochondria	2014	[23]
Osteosarcoma	Murine orthotopic model of osteosarcoma	Mitochondria	2014	[23]
Head and neck squamous cell carcinoma	Patient tissue	F-actin, mitochondria	2014	[24]
Glioma	Mouse tumor xenograft from primary stem cells	Cytosolic GFP expression	2015	[36]
Head and neck squamous cell carcinoma	Patient tissue	Actin, tubulin	2017	[25]
	Mouse tumor xenograft from cell line	Actin, tubulin	2017	[25]
Acute myeloid leukemia	Mouse tumor xenograft from human leukemic cells	Mitochondria	2017	[28]
Glioma	Mouse tumor xenograft from primary stem cells	Cytosolic GFP expression	2017	[67]
Pancreatic adenocarcinoma	Patient tissue	Mitochondria	2018	[26]
Developing human telencephalon and human GBM	Patient tissue	Collagen IV	2018	[54]
Multiple myeloma	Mouse tumor xenograft from cell line	Mitochondria	2019	[29]

stimulate their formation. Reactive oxygen species (ROS), known to be intensively produced by cancer cells [39], have been shown to induce TNT formation in different contexts, including cancer [8,13,20,29,40] (Table 1). Moreover, treatments such as chemo and radiotherapy induce ROS production [41]. Hypoxia, typical of the denser tumor regions, has been found to be a TNT inducer in ovarian [42] and prostate cancers [43]. Interestingly, other conditions mimicking the TME *in vitro* stimulate TNT-mediated communication, such as acidic pH, hyperglycemia, serum deprivation [22,43], and exposure to tumor necrosis factor (TNF)-α normally produced during inflammation [44]. Finally, different signaling pathways that are often dysregulated in cancer have been shown to be involved in TNT formation, such as PI3K/Akt/mTOR [37,40,42,43], K-RAS [45] ,and p53 [13,40]. These signaling cascades could activate downstream proteins, such as M-Sec in the case of immune cells [46], which are involved in actin remodeling and polymerization and have been shown to induce TNT formation [47]. Altogether, these findings suggest that the tumor context, globally experienced as a stress by cells, provides the conditions that favor TNT formation and communication. In turn, we can speculate that this route for intercellular communication allowing cells to share material may result in a beneficial effect for the connected cancer cells, as described in the following sections.

Roles of TNT in Cancer Progression

The ability of cancer cells to interconnect among themselves is correlated with more aggressive cancer phenotypes. For example, in ovarian and breast cancers, highly malignant and metastatic cells are more prone to interconnect in tumor networks than their less aggressive counterparts [10,11]. Also, in gliomas, where for the first time tumors have been described as a functional intercommunicating network, there is a correlation between extended interconnectivity and the most aggressive grades of tumors and their poorer therapeutic outcome in response to radiotherapy [36]. However, the mechanisms of treatment resistance have not been fully elucidated yet. Different cancers could be applying different strategies to protect themselves from the

therapeutic attempts and eventually a unique mechanism may be determined. Here, we review the possible roles of TNT-like connections in different types of cancer and how they affect cancer progression. We then focus on the specific example of GBM.

TNT-Mediated Transfer Can Promote Aggressive Features

TNTs appear to drive the acquisition of aggressive features in the receiving cells through the transfer of different cellular materials. As we will see, cells may use TNTs as a route to remove dangerous material (Figure 2A,C). Another possibility is that the uptake of cellular material, such as miRNA, mitochondria, or other sets of proteins, might drive phenotypic modifications of the recipient cells (Figure 2A,B).

In breast cancer, TNT-mediated contacts from cells of the TME, such as macrophages, appear to drive the acquisition of an invasive phenotype in the cancer cells [31]. Although it is not clear how

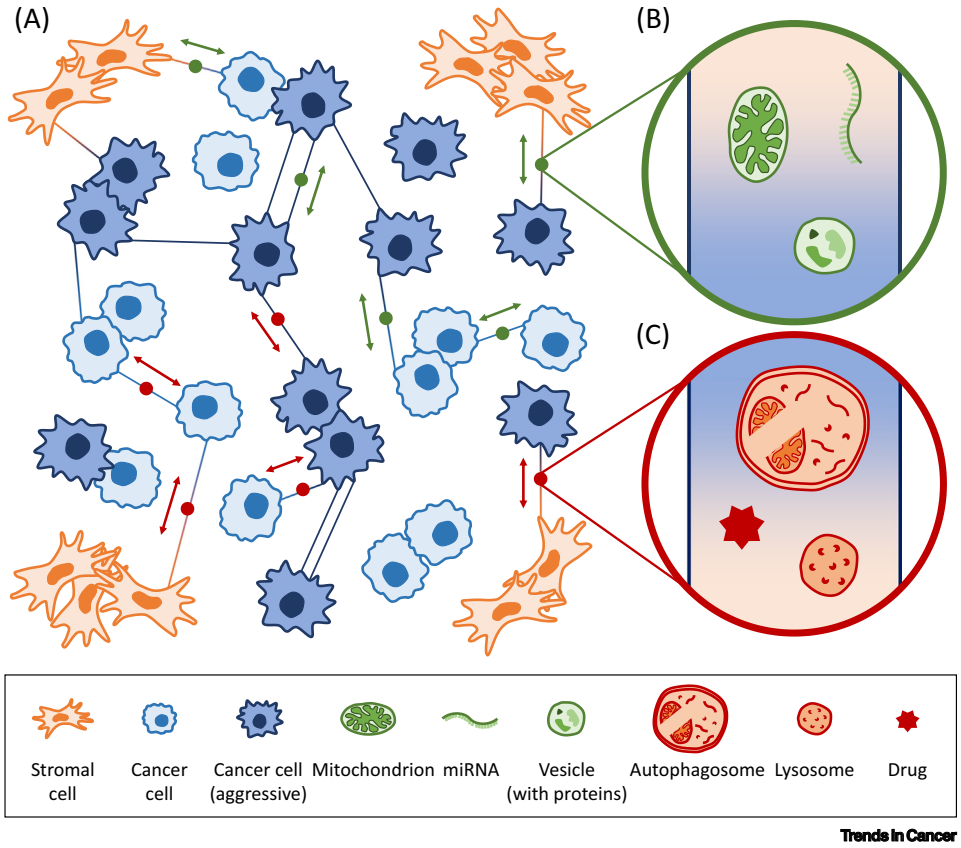

Figure 2. Schematic of a Tunneling Nanotube (TNT)-Based Network in Cancer. (A) Cancer cells with different states of aggressiveness coexist and interact via TNTs. Aggressive cancer cells (dark blue) display higher interconnection rates than their less aggressive counterparts (light blue). Cancer cells are surrounded by stromal cells (red) to which they also communicate through TNTs. The homotypic or heterotypic connections between these cell types can be used to share oncogenic content (green circle) or to remove material to degrade (red circle). (B) Magnification of oncogenic cargoes traveling along the connection providing protumoral features in the receiving cell and healthy lysosomes. Acquisition of mitochondria can promote chemoresistance and invasiveness and provide metabolic help in stress-induced conditions. Transfer of miRNA can drive modifications in the phenotype of recipient cells, leading to a more aggressive phenotype. Moreover, cellular vesicle content can impact the proteomic profile of the receiving cells and change their ability to respond to treatments. (C) Different materials discarded by a cell through TNTs. Organelles used for degradation, such as autophagosomes and lysosomes, might be transferred via TNTs as a clearing mechanism. TNTs could also be used as a route for the redistribution of drugs, which would otherwise be toxic in high concentration.

this contact could induce this phenotypic switch, mitochondria appear to be good candidates for transferred cargo that could induce invasiveness. In fact, breast cancer cells have been shown to be able to receive mitochondria from mesenchymal cells (MSCs) through TNT-like structures [30]. Furthermore, the uptake of isolated mitochondria derived from MSCs, by a protocol defined as MitoCeption, was able to induce migratory ability and cellular proliferation [48]. Many studies have shown TNT-mediated mitochondria transfer to be possible [24,25,30,49]; however, the possibility that mitochondria could be transferred through the supernatant should be considered, given that research has suggested that the mitochondria could be released and taken up by neighboring cells [50]. Transfer of mitochondria has also been found to restore tumorigenic potential in cells devoid of mitochondrial DNA [51,52], although these studies did not address the mechanism of mitochondrial transfer. Furthermore, TNT-mediated traffic of mitochondria was correlated with increased invasiveness in bladder cancer [37]. Here, different cancer cell lines in co-culture could exchange functional mitochondria with each other, possibly stimulating the migratory capacity of the acceptor cells, as assessed by *in vitro* assays. Furthermore, their ability to form larger tumors with a higher vascularization index was stimulated when implanted in nude mice. In a second study, additional evidence suggested that the acquisition of these protumor properties is due to TNT-mediated transfer of miRNA from the most aggressive to the least aggressive cells, leading to the activation of the Deptor-mTOR signaling pathway, an important downstream mediator of cancer cell proliferation and motility [53].

Endothelial cells (ECs) have a critical role in physiological and tumoral vascularization and their angiogenic potential might be regulated by TNT-mediated interactions. TNT-like connections sprouting from ECs or pericytes have been identified in sections of developing human cerebral cortex and human GBM, two contexts in which the process of vascularization is intensively active [54]. Moreover, ECs experiencing chemotherapy stress are able to receive mitochondria from MSCs via TNT connections and this transfer could rescue the damaged cells, promoting cell proliferation and restoring migratory and angiogenic abilities [55]. Furthermore, elegant work by Connor and colleagues [11] showed that TNT-mediated transfer from metastatic cancer cells to ECs can induce an alteration of the miRNA profile of the receiving cells. This work showed for the first time TNTs as a route for the dissemination of oncogenic material that resulted in reprogramming of the ECs. Altogether, the current evidence suggests that TNT-mediated transfer of mitochondria and mRNA stimulates invasiveness, proliferation, and angiogenic ability.

TNTs Can Support Therapy Resistance

Intercellular communication through TNT-like structures and resistance to therapies appear to be tightly correlated. As for the other cancer features that might be driven by contact-mediated transfer of cargoes, TNT-like structures may provide a way for distributing harmful substances and cellular wastes, or sharing defensive tools against treatment, such as mitochondria, miRNA, and specific factors (Figure 2). TNT-mediated communication appears to be stimulated by radiotherapy, which causes free radical production, known to be a TNT inducer [41], and by radiofrequency treatment [56], and chemotherapy [43]. A recent study in prostatic cancer showed that chemotherapeutic blockage of the androgen receptor, which induces metabolic stress, enhanced TNT-like structure formation [43]. Disrupting these connections by cytochalasin D sensitized prostatic cancer cells to treatment-induced cell death, suggesting that the presence of this stress-induced network favors cancer cell survival upon treatment. In this study, lysosomes, mitochondria, and stress-induced chaperones were observed inside the TNT-like structures. Therefore, it is possible that transferring these cellular components benefits stressed cells. Conversely, TNT-like structures could be used as a way to remove damaged organelles or autophagosomes [25] and possibly other dangerous substances, such as ROS, produced in response to treatments, or the drugs themselves (Figure 2C). Transfer of a soluble drug via

TNT-like structures has also been observed in both pancreatic and ovarian cancer cellular models [26]. Here, multidrug-resistant cell lines use TNT-like connections to redistribute doxorubicin from chemoresistant toward chemosensitive cells, leading to cell death of the latter and enrichment of the therapy-resistant population. Although the possibility of using TNT-like structures as a drug outflow pathway must be considered, there are currently no quantitative data supporting the actual relevance of this mechanism *in vivo*. Also, this work raises questions over the specificity of the transferred materials through TNTs, and whether this occurs through an active or passive mechanism of redistribution.

As mentioned earlier, TNT-based networking allows the exchange of 'defensive tools' against treatment (Figure 2A). The transfer of mitochondria has been shown to modulate the response to treatments in a beneficial manner for the recipient cells [49,57,58], impacting their cellular metabolism [48,58], rescuing their aerobic respiration [59], and providing metabolic support against treatment-related stress [58]. This was first observed in PC12 cells, where delivery of healthy mitochondria through TNT-like structures from untreated to UV-injured cells protected the latter from apoptosis [60]. This rescue mechanism is also applied by MSCs to chemotherapy-treated ECs [55]. Both MSCs and ECs have been found to transfer mitochondria to cancer cells of different origins, resulting in an improved resistance to doxorubicin in the cells that received the transfer [30]. This mechanism appears to be critical in different forms of leukemia. Leukemic cells, engrafted in murine bone marrow, were able to obtain and receive mitochondria from stromal cells with an impact on cancer cell metabolism [27,28,58], cell proliferation [58,61], and chemoresistance [27]. The disruption of this transfer increased the sensitivity of the cancer cells to various chemotherapies [27]. This suggests that MSCs have a protective role toward tumor cells by eliminating the damaged mitochondria they receive, thereby stabilizing the homeostasis of the cancer population, and possibly providing metabolic support. Moreover, chemotherapy-induced ROS production can enhance mitochondria transfer [28], again suggesting mitochondrial transfer as a mechanism for adaptation to treatment. Interestingly, the inhibition of CD38, previously described to promote mitochondrial release from astrocytes [50], could prevent the contact-mediated mitochondria transfer from MSCs to leukemic cells, resulting in increased apoptosis of the leukemic cells and improved mouse survival [29]. This opens the possibility of specifically targeting mitochondria transfer at the clinical level. Following this evidence, others have assessed the communication between stroma and leukemic cancer cells. Mass spectrometry was used to reveal the transfer of specific factors, such as stress-induced chaperones, together with cellular vesicles, with a potential role in survival and adaptation [38]. Other cargoes, such as miRNA, can be transferred between cells, leading to the acquisition of therapy resistance. Thayanithy and collaborators [23] showed that the transfer of miR-19 and miR-199a occurred in heterotypic connections between different cancer cell lines of the same tumor: osteosarcoma and ovarian cancer, respectively. Specifically, miR-199a appears to be differentially expressed in chemosensitive and chemoresistant cells, suggesting that the transfer of this particular miRNA drives treatment-resistant features in the receiving cells. Thus, TNTs could be a beneficial feature for cancer cells, and the ability to exploit this efficient route of communication may be positively selected during treatment.

GBM: An 'Exemplary' or 'Peculiar' Case of TNT-Like Network?

Among the deadliest types of cancer, GBM stands out for its aggressiveness and resilience in response to treatment. GBM is the most undifferentiated and invasive cancer within the gliomas and is classified as a grade IV tumor. Surgery followed by chemo and radiotherapy is insufficient to eradicate completely cancer cells from the brain, although the mean survival of patients increases from less than 1 year to ~15 months [62,63]. Currently, no treatment is effective in preventing cancer relapse and the reasons for therapy failure are poorly understood. Some

studies correlate the occurrence of relapse with elevated intratumoral heterogeneity: distinct molecular profiles coexist and exhibit differential therapeutic responses [64]. In particular, GBM stem cells (GSCs) have been found to be the most resistant to treatments and likely are at the origin of relapses [65]. Moreover, treatments can positively modulate tumor heterogeneity by inducing cellular plasticity and transdifferentiation [66].

As outlined earlier, during the past few years, various studies have supported the possibility that intercellular communication through cell–cell connections are a critical mechanism for treatment failure and tumor relapse. GBM is the first case where a functional and resistant network among cancer cells has been described in an *in vivo* model [36]. Specifically, GSCs from patients with different grades of glioma were implanted in nude mouse brains, where they developed a multicellular and communicative network. In this study, Winkler and collaborators demonstrated that highly interconnected tumors, which corresponded to higher malignant grades of the original tumor, were more resistant to irradiation [36]. Cancer cells were able to propagate ion fluxes by long and thick membrane protrusions, containing both actin and microtubules, which the authors termed 'tumor microtubes' (TMs) (Table 1). Moreover, the same authors suggested that TMs are essential for driving the repopulation of a surgically resected area in GBM mouse models [67] (Figure 3). The formation of TMs appears to be dependent on the expression of connexin 43 (Cx43), a monomeric component of GAP junctions, and growth-associated protein 43 (GAP-43), a crucial protein for neurite formation, regeneration, and plasticity [36]. When Cx43 or GAP-43 were knocked down, the number of TMs decreased and the sensitivity to radiotherapy increased. Cx43 is a known regulator of the intracellular concentration of Ca^{2+} [68] and it has been also described to have a critical but controversial role in GBM progression, acting both as tumor suppressor and tumor inducer, promoting growth, cell migration, and resistance to apoptosis [69]. Interestingly, Gerdes and colleagues [70] reported earlier that a subset of TNTs observed in kidney-derived cells contained Cx43 forming a hemi-connexon or a GAP junction at their tip. It was also proposed that GAP junctions could mediate the transfer of electrical signals in electrically coupled TNTs [6]. Nonetheless, the presence of GAP junctions along TNT connections would not allow the transfer of any cargo of a size superior to their pore size (1 kDa) [71], such as organelles or macromolecules. In the case of TMs, the authors did not report the transfer of conventional TNT cargoes, such as mitochondria or vesicles, within their lumen, although they did observe nuclei traveling along these connections from a healthy cell to a cell damaged by the treatment [36]. In addition, TMs display neurite-like features, because they have been described to be postsynaptic targets for the surrounding neurons. Indeed, axons can dock onto TMs and generate synchronized calcium transients in glioma networks via AMPA receptors [72,73], Furthermore, depolarization of the postsynaptic glioma cells promoted TM-dependent proliferation [73] and invasion [72].

Overall, the nature of TMs and the mechanisms at stake in this cellular network still need to be unraveled. As for their morphological appearance and physical properties, TMs are very different from TNTs because they are not open-ended, they are much thicker (1.7 μm on average), more stable in time [74], and contain both actin and microtubules, thus resembling more of a neuritic extension than TNTs [75] (Table 1). Nevertheless, direct cell–cell communication appears to have a key role in the resistance to treatment in GBM and growing evidence suggests that the transfer of cargo mediated by open connections contributes to tumor progression, as shown previously in other cancer forms. A few *in vitro* studies suggest that GBM cells are capable of transferring cellular material through thinner TNT-like structures. U-87 and U-251 cell lines, common GBM cellular models, can form TNT-like structures [76–78] (Figure 1), and their formation can be increased in response to external stimuli, such as protein aggregate uptake or cocaine administration [77,78]. Moreover, preliminary studies show that communication between

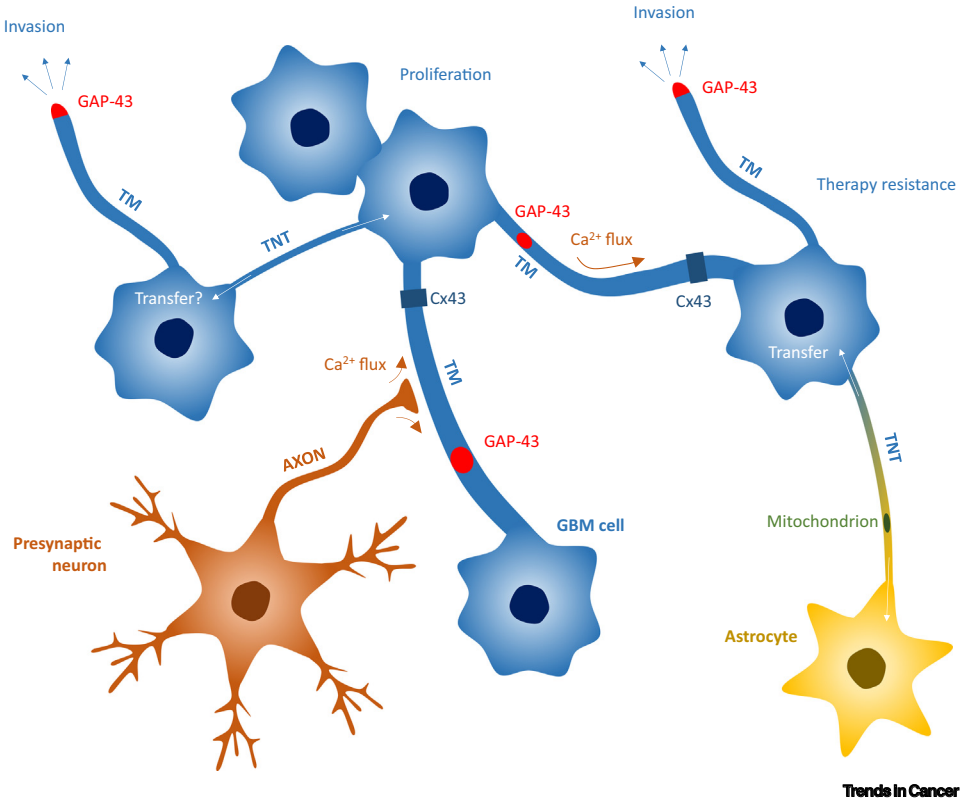

Figure 3. Schematic of a Glioblastoma (GBM) Network and Different Types of Intercellular Connection. GBM cells (blue) interconnect forming a functional network comprising different types of connection. Thick (>1 μm) protrusions (tumor microtubes; TMs) connect GBM cells and contain both Connexin 43 (Cx43) and growth-associated protein 43 (GAP-43), which regulate Ca^{2+} flux along the network. Thinner (<1 μm) TNT-like connections are present between GBM cells and may allow the transfer of material. GBM cells also form TMs that do not contact other cells and are able to drive cell invasion in a GAP-43-dependent manner. Presynaptic neurons (orange) extend axons that appose onto TMs and regulate the Ca^{2+} flux along the GBM network, promoting cell invasion and cell proliferation. Astrocytes (yellow) of the tumoral brain environment can communicate with GBM cells through TNT-like connections and transfer mitochondria to the tumoral cells, eventually affecting the behavior (e.g., proliferation and response to treatments) of the receiving cells.

Outstanding Questions

Are TNT-like structures a common feature in all cancers?

Does the structural diversity observed in TNT-like structures *in vitro* and *in vivo* correspond to different roles in cell–cell communication?

What other cellular materials are transferred through TNTs beyond those detected by specific labeling?

What are the molecular mechanisms that drive phenotypic modification following transfer of cellular content?

astrocytes and glioma cells, known to facilitate cancer progression [79], can occur through TNT-like structures [13,76] and the transfer of mitochondria appears to modulate GBM cell abilities in favor of a more proliferative [13] and drug-resistant state [80]. However, the study of intercellular exchange of material needs to be elevated in more complex and representative tumor models. The fact that GBM cells were able to form a network in mice xenografts, but failed in forming connections when cultured *in vitro* [67], suggests that TMs exist only in the *in vivo* condition. It is possible that GBM networks comprise several types of connection that vary in size and properties: open-ended TNTs, synaptic-like connections ,and/or thick GAP junction-linked protrusions, such as TMs (Figure 3).

Concluding Remarks and Future Perspectives

Over the past decade, growing evidence has supported the existence and importance of intercellular communication based on TNT-like connections in various tumors. Several cancer cell types have been shown to grow such connections and communicate through them in culture, and similar structures have been found in tumor sections [22], proving their existence in real tumors. Different studies have described TNT-like structures with diverse morphologies and characteristics; therefore, the ability to transfer cellular material has been used to define them functionally rather than structurally.

Cancer is one of the few contexts where TNTs have been functionally described, whereby the transfer of cellular cargoes has been shown to have an impact on the behavior of the recipient cells and lead to further development of the disease. However, fundamental questions remain regarding the structural diversity of the different protrusions, as well as the molecular determinants and the signaling pathways that would stimulate their growth in cancer cells compared with noncancer cells.

Until now, the outcome of the transfer has been more often addressed as impacting predetermined features. For example, studies have investigated whether the unilateral transfer of a specific tagged cargo affected the migratory capacity or angiogenesis of the recipient cells. The observation of a specific cargo transfer does not necessarily implicate a role for that specific cargo, since other material, not detected because it is nonlabeled, could be transported through the connections and lead to changes in the partner cells. Few studies have addressed the question globally, designing experiments to study the alteration induced by the transfer in the receiving cells at the transcriptomic [11] or proteomic [38] level. Even less work, if any, has addressed the changes under the assumption that bilateral transfer could occur and modify the fate of each one of the two connected cells. Moreover, the mechanisms by which the transfer of cargoes mediated by TNTs impacts the migratory or angiogenic ability of the cell remain largely unknown. In the case of resistance to treatments, the acquisition of cargoes, such as mitochondria and miRNA, could be the direct cause of enhanced regrowth potential [51,52] or transcriptomic reprogramming [23], respectively, leading to the establishment of a more resistant phenotype. In other cases, the treatment itself appears to induce TNT-mediated communication, which probably acts as the mechanism in response to the induced stress [29,55], protecting the cells from the induced damage. Overall, the ability of certain cancer cells to exploit TNTs as mechanisms of communication might be positively selected during treatment, favoring such cells to become the majority (see Outstanding Questions).

To address the complexity of the real pathology and also the diversity of TNT-like connections, the use of models representative of the tumor environment is required. Many of the studies reported here were carried out in cell lines *in vitro.* Only more recent work has addressed the study of TNT-like structures with the use of patient-derived xenografts in mice. Based on current knowledge, it appears that blocking TNT-like connectivity could be a promising strategy to fight cancer, eventually hindering cancer progression and sensitizing tumor cells toward treatments. A couple of drugs have been described as being able to specifically inhibit TNT formation in cell culture [81,82], but these need to be tested in cancer mouse models. Conversely, TNTs have also been used as a route to diffuse therapeutics, such as drugs [26] and nanoparticles [76], affecting predominantly the network of connected cancer cells. Certainly, a deeper understanding of TNT-based communication is critical for a better comprehension of cancer progression and treatment resistance, and, in future years, this knowledge could lead to the development of new, more effective therapies.

Acknowledgments

This work was funded by grants from HTE (HTE201502) and Institut National du Cancer (PLBIO18-103) to C.Z., and Fondation ARC pour la Recherche sur le Cancer to G.P. (DOC20190508549). G.P. is supported by HTE and Fondation ARC. We also thank Inés Sáenz-de-Santa-María Fernández, Maura Samarani, and Diego Cordero Cervantes for critical reading.

References

1. Siegel, R.L. *et al.* (2019) Cancer statistics, 2019. *CA Cancer J. Clin.* 69, 7–34
2. Ruivo, C.F. *et al.* (2017) The biology of cancer exosomes: insights and new perspectives. *Cancer Res.* 77, 6480–6488
3. Sheehan, C. and D'Souza-Schorey, C. (2019) Tumor-derived extracellular vesicles: molecular parcels that enable regulation of the immune response in cancer. *J. Cell Sci.* 132, jcs235085
4. Rustom, A. *et al.* (2004) Nanotubular highways for intercellular organelle transport. *Science* 303, 1007–1010
5. Sartori-Rupp, A. *et al.* (2019) Correlative cryo-electron microscopy reveals the structure of TNTs in neuronal cells. *Nat. Commun.* 10, 342
6. Abounit, S. and Zurzolo, C. (2012) Wiring through tunneling nanotubes – from electrical signals to organelle transfer. *J. Cell Sci.* 125, 1089–1098

7. Ariazi, J. *et al.* (2017) Tunneling nanotubes and gap junctions-their role in long-range intercellular communication during development, health, and disease conditions. *Front. Mol. Neurosci.* 10, 333
8. Zhu, D. *et al.* (2005) Hydrogen peroxide alters membrane and cytoskeleton properties and increases intercellular connections in astrocytes. *J. Cell Sci.* 118, 3695–3703
9. Onfelt, B. *et al.* (2006) Structurally distinct membrane nanotubes between human macrophages support long-distance vesicular traffic or surfing of bacteria. *J. Immunol.* 177, 8476–8483
10. Ady, J.W. *et al.* (2014) Intercellular communication in malignant pleural mesothelioma: properties of tunneling nanotubes. *Front. Physiol.* 5, 400
11. Connor, Y. *et al.* (2015) Physical nanoscale conduit-mediated communication between tumour cells and the endothelium modulates endothelial phenotype. *Nat. Commun.* 6, 8671
12. Korenkova, O. *et al.* (2020) Fine intercellular connections in development: TNTs, cytonemes, or intercellular bridges? *Cell Stress* 4, 30–43
13. Zhang, L. and Zhang, Y. (2015) Tunneling nanotubes between rat primary astrocytes and C6 glioma cells alter proliferation potential of glioma cells. *Neurosci. Bull.* 31, 371–378
14. Sowinski, S. *et al.* (2008) Membrane nanotubes physically connect T cells over long distances presenting a novel route for HIV-1 transmission. *Nat. Cell Biol.* 10, 211–219
15. Souriant, S. *et al.* (2019) Tuberculosis exacerbates HIV-1 infection through IL-10/STAT3-dependent tunneling nanotube formation in macrophages. *Cell Rep.* 26, 3586–3599
16. Gousset, K. and Zurzolo, C. (2009) Tunnelling nanotubes: a highway for prion spreading? *Prion* 3, 94–98
17. Zhu, S. *et al.* (2015) Prion aggregates transfer through tunneling nanotubes in endocytic vesicles. *Prion* 9, 125–135
18. Abounit, S. *et al.* (2016) Tunneling nanotubes: a possible highway in the spreading of tau and other prion-like proteins in neurodegenerative diseases. *Prion* 10, 344–351
19. Abounit, S. *et al.* (2016) Tunneling nanotubes spread fibrillar α-synuclein by intercellular trafficking of lysosomes. *EMBO J.* 35, 2120–2138
20. Victoria, G.S. and Zurzolo, C. (2017) The spread of prion-like proteins by lysosomes and tunneling nanotubes: implications for neurodegenerative diseases. *J. Cell Biol.* 216, 2633–2644
21. Gousset, K. *et al.* (2009) Prions hijack tunnelling nanotubes for intercellular spread. *Nat. Cell Biol.* 11, 328–336
22. Lou, E. *et al.* (2012) Tunneling nanotubes provide a unique conduit for intercellular transfer of cellular contents in human malignant pleural mesothelioma. *PLoS ONE* 7, e33093
23. Thayanithy, V. *et al.* (2014) Tumor-stromal cross talk: direct cell-to-cell transfer of oncogenic microRNAs via tunneling nanotubes. *Transl. Res.* 164, 359–365
24. Antanavičiūtė, I. *et al.* (2014) Long-distance communication between laryngeal carcinoma cells. *PLoS ONE* 9, e99196
25. Sáenz-de-Santa-María, I. *et al.* (2017) Control of long-distance cell-to-cell communication and autophagosome transfer in squamous cell carcinoma via tunneling nanotubes. *Oncotarget* 8, 20939–20960
26. Desir, S. *et al.* (2018) Chemotherapy-induced tunneling nanotubes mediate intercellular drug efflux in pancreatic cancer. *Sci. Rep.* 8, 9484
27. Wang, J. *et al.* (2018) Cell adhesion-mediated mitochondria transfer contributes to mesenchymal stem cell-induced chemoresistance on T cell acute lymphoblastic leukemia cells. *J. Hematol. Oncol.* 11, 11
28. Marlein, C.R. *et al.* (2017) NADPH oxidase-2 derived superoxide drives mitochondrial transfer from bone marrow stromal cells to leukemic blasts. *Blood* 130, 1649–1660
29. Marlein, C.R. *et al.* (2019) CD38-driven mitochondrial trafficking promotes bioenergetic plasticity in multiple myeloma. *Cancer Res.* 79, 2285–2297
30. Pasquier, J. *et al.* (2013) Preferential transfer of mitochondria from endothelial to cancer cells through tunneling nanotubes modulates chemoresistance. *J. Transl. Med.* 11, 94
31. Hanna, S.J. *et al.* (2019) Tunneling nanotubes, a novel mode of tumor cell-macrophage communication in tumor cell invasion. *J. Cell Sci.* 132, jcs223321
32. Yuan, Y. *et al.* (2016) Role of the tumor microenvironment in tumor progression and the clinical applications (Review). *Oncol. Rep.* 35, 2499–2515
33. Sharma, P. *et al.* (2017) Primary, adaptive and acquired resistance to cancer immunotherapy. *Cell* 168, 707–723
34. Abounit, S. *et al.* (2015) Identification and characterization of tunneling nanotubes for intercellular trafficking. *Curr. Protoc. Cell Biol.* 67, 12.10.1–12.10.21
35. Gurke, S. *et al.* (2008) The art of cellular communication: tunneling nanotubes bridge the divide. *Histochem. Cell Biol.* 129, 539–550
36. Osswald, M. *et al.* (2015) Brain tumour cells interconnect to a functional and resistant network. *Nature* 528, 93–98
37. Lu, J. *et al.* (2017) Tunneling nanotubes promote intercellular mitochondria transfer followed by increased invasiveness in bladder cancer cells. *Oncotarget* 8, 15539–15552
38. Kolba, M.D. *et al.* (2019) Tunneling nanotube-mediated intercellular vesicle and protein transfer in the stroma-provided imatinib resistance in chronic myeloid leukemia cells. *Cell Death Dis.* 10, 1–16
39. Sosa, V. *et al.* (2013) Oxidative stress and cancer: an overview. *Ageing Res. Rev.* 12, 376–390
40. Wang, Y. *et al.* (2011) Tunneling-nanotube development in astrocytes depends on p53 activation. *Cell Death Differ.* 18, 732–742
41. Matejka, N. and Reindl, J. (2019) Perspectives of cellular communication through tunneling nanotubes in cancer cells and the connection to radiation effects. *Radiat. Oncol.* 14, 218
42. Desir, S. *et al.* (2016) Tunneling nanotube formation is stimulated by hypoxia in ovarian cancer cells. *Oncotarget* 7, 43150–43161
43. Kretschmer, A. *et al.* (2019) Stress-induced tunneling nanotubes support treatment adaptation in prostate cancer. *Sci. Rep.* 9, 7826
44. Ranzinger, J. *et al.* (2011) Nanotube action between human mesothelial cells reveals novel aspects of inflammatory responses. *PLoS ONE* 6, e29537
45. Desir, S. *et al.* (2019) Intercellular transfer of oncogenic KRAS via tunneling nanotubes introduces intracellular mutational heterogeneity in colon cancer cells. *Cancers (Basel)* 11, 892
46. Hase, K. *et al.* (2009) M-Sec promotes membrane nanotube formation by interacting with Ral and the exocyst complex. *Nat. Cell Biol.* 11, 1427–1432
47. Ohno, H. *et al.* (2010) M-Sec. *Commun. Integr. Biol.* 3, 231–233
48. Caicedo, A. *et al.* (2015) MitoCeption as a new tool to assess the effects of mesenchymal stem/stromal cell mitochondria on cancer cell metabolism and function. *Sci. Rep.* 5, 9073
49. Hekmatshoar, Y. *et al.* (2018) The role of metabolism and tunneling nanotube-mediated intercellular mitochondria exchange in cancer drug resistance. *Biochem. J.* 475, 2305–2328
50. Hayakawa, K. *et al.* (2016) Transfer of mitochondria from astrocytes to neurons after stroke. *Nature* 535, 551–555
51. Tan, A.S. *et al.* (2015) Mitochondrial genome acquisition restores respiratory function and tumorigenic potential of cancer cells without mitochondrial DNA. *Cell Metab.* 21, 81–94
52. Dong, L.-F. *et al.* (2017) Horizontal transfer of whole mitochondria restores tumorigenic potential in mitochondrial DNA-deficient cancer cells. *Elife* 6, e22187
53. Lu, J.J. *et al.* (2019) Tunneling nanotubes mediated microRNA-155 intercellular transportation Promotes bladder cancer cells' invasive and proliferative capacity. *Int. J. Nanomedicine* 14, 9731–9743
54. Errede, M. *et al.* (2018) Tunneling nanotubes evoke pericyte/endothelial communication during normal and tumoral angiogenesis. *Fluids Barriers CNS* 15, 28
55. Feng, Y. *et al.* (2019) Human bone marrow mesenchymal stem cells rescue endothelial cells experiencing chemotherapy stress by mitochondrial transfer via tunneling nanotubes. *Stem Cells Dev.* 28, 674–682
56. Ware, M.J. *et al.* (2015) Radiofrequency treatment alters cancer cell phenotype. *Sci. Rep.* 5, 12083
57. Vignais, M.-L. *et al.* (2017) Cell connections by tunneling nanotubes: effects of mitochondrial trafficking on target cell metabolism, homeostasis, and response to therapy. *Stem Cells Int.* 2017, 6917941

58. Moschoi, R. *et al.* (2016) Protective mitochondrial transfer from bone marrow stromal cells to acute myeloid leukemic cells during chemotherapy. *Blood* 128, 253–264
59. Spees, J.L. *et al.* (2006) Mitochondrial transfer between cells can rescue aerobic respiration. *Proc. Natl. Acad. Sci. U. S. A.* 103, 1283–1288
60. Wang, X. and Gerdes, H.-H. (2015) Transfer of mitochondria via tunneling nanotubes rescues apoptotic PC12 cells. *Cell Death Differ.* 22, 1181–1191
61. Griessinger, E. *et al.* (2017) Mitochondrial transfer in the leukemia microenvironment. *Trends Cancer* 3, 828–839
62. Batash, R. *et al.* (2017) Glioblastoma multiforme, diagnosis and treatment; recent literature review. *Curr. Med. Chem.* 24, 3002–3009
63. Stupp, R. *et al.* (2005) Radiotherapy plus concomitant and adjuvant temozolomide for glioblastoma. *N. Engl. J. Med.* 352, 987–996
64. Lathia, J.D. *et al.* (2015) Cancer stem cells in glioblastoma. *Genes Dev.* 29, 1203–1217
65. Chen, L. *et al.* (2015) Glioblastoma recurrence patterns near neural stem cell regions. *Radiother. Oncol.* 116, 294–300
66. Dahan, P. *et al.* (2014) Ionizing radiations sustain glioblastoma cell dedifferentiation to a stem-like phenotype through survivin: possible involvement in radioresistance. *Cell Death Dis.* 5, e1543
67. Weil, S. *et al.* (2017) Tumor microtubes convey resistance to surgical lesions and chemotherapy in gliomas. *Neuro-oncology* 19, 1316–1326
68. Lurtz, M.M. and Louis, C.F. (2007) Intracellular calcium regulation of connexin43. *Am. J. Physiol. Cell Physiol.* 293, C1806–C1813
69. Sin, W.-C. *et al.* (2012) Opposing roles of connexin43 in glioma progression. *Biochim. Biophys. Acta* 1818, 2058–2067
70. Wang, X. *et al.* (2010) Animal cells connected by nanotubes can be electrically coupled through interposed gap-junction channels. *Proc. Natl. Acad. Sci. U. S. A.* 107, 17194–17199
71. Weber, P.A. *et al.* (2004) The permeability of gap junction channels to probes of different size is dependent on connexin composition and permeant-pore affinities. *Biophys. J.* 87, 958–973
72. Venkataramani, V. *et al.* (2019) Glutamatergic synaptic input to glioma cells drives brain tumour progression. *Nature* 573, 532–538
73. Venkatesh, H.S. *et al.* (2019) Electrical and synaptic integration of glioma into neural circuits. *Nature* 573, 539–545
74. Osswald, M. *et al.* (2019) Tunneling nanotube-like structures in brain tumors. *Cancer Rep.* 2, e1181
75. Jung, E. *et al.* (2019) Emerging intersections between neuroscience and glioma biology. *Nat. Neurosci.* 22, 1951–1960
76. Formicola, B. *et al.* (2019) Differential exchange of multifunctional liposomes between glioblastoma cells and healthy astrocytes via tunneling nanotubes. *Front. Bioeng. Biotechnol.* 7, 403
77. Carone, C. *et al.* (2015) In vitro effects of cocaine on tunneling nanotube formation and extracellular vesicle release in glioblastoma cell cultures. *J. Mol. Neurosci.* 55, 42–50
78. Ding, X. *et al.* (2015) Exposure to ALS-FTD-CSF generates TDP-43 aggregates in glioblastoma cells through exosomes and TNTs-like structure. *Oncotarget* 6, 24178–24191
79. Guan, X. *et al.* (2018) Reactive astrocytes in glioblastoma multiforme. *Mol. Neurobiol.* 55, 6927–6938
80. Civita, P. *et al.* (2019) Pre-clinical drug testing in 2D and 3D human in vitro models of glioblastoma incorporating non-neoplastic astrocytes: tunneling nano tubules and mitochondrial transfer modulates cell behavior and therapeutic response. *Int. J. Mol. Sci.* 20, 6017
81. Dilsizoglu Senol, A. *et al.* (2019) Effect of tolytoxin on tunneling nanotube formation and function. *Sci. Rep.* 9, 5741
82. Hashimoto, M. *et al.* (2016) Potential role of the formation of tunneling nanotubes in HIV-1 spread in macrophages. *J. Immunol.* 196, 1832–1841
83. Hua, K. and Ferland, R.J. (2018) Primary cilia proteins: ciliary and extraciliary sites and functions. *Cell. Mol. Life Sci.* 75, 1521–1540
84. Tilney, L.G. *et al.* (1992) Actin filaments, stereocilia, and hair cells: how cells count and measure. *Annu. Rev. Cell Biol.* 8, 257–274
85. Innocenti, M. (2018) New insights into the formation and the function of lamellipodia and ruffles in mesenchymal cell migration. *Cell Adhes. Migr.* 12, 401–416
86. Gallop, J.L. (2019) Filopodia and their links with membrane traffic and cell adhesion. *Semin. Cell Dev. Biol.* 102, 81–89
87. Kornberg, T.B. and Roy, S. (2014) Cytonemes as specialized signaling filopodia. *Development* 141, 729–736
88. Fykerud, T.A. *et al.* (2016) Mitotic cells form actin-based bridges with adjacent cells to provide intercellular communication during rounding. *Cell Cycle* 15, 2943–2957
89. Flynn, K.C. (2013) The cytoskeleton and neurite initiation. *Bioarchitecture* 3, 86–109
90. Osswald, M. *et al.* (2016) A malignant cellular network in gliomas: potential clinical implications. *Neuro-Oncology* 18, 479–485
91. Castro-Castro, A. *et al.* (2016) Cellular and molecular mechanisms of MT1-MMP-dependent cancer cell invasion. *Annu. Rev. Cell Dev. Biol.* 32, 555–576
92. Veillat, V. *et al.* (2015) Podosomes: multipurpose organelles? *Int. J. Biochem. Cell Biol.* 65, 52–60

Résumé

Le glioblastome (GBM) est un cancer du cerveau très agressif dont la rechute après les thérapies est provoquée par des cellules souches appelées GSC. La communication intercellulaire joue un rôle dans la résistance aux thérapies, car les GSC peuvent s'interconnecter par des extensions épaisses, les Tumor Microtubes (TM), qui favorisent la transmission de courant à travers des GAP-junctions. Les Tunneling Nanotubes (TNT) sont de minces canaux de communication ouverts entre cellules permettant le transfert bilatéral de matériel cellulaire. Ils ont également été décrits dans plusieurs cancers associés à un phénotype plus malin.

L'objectif de mon projet était de déterminer si des TNT existaient dans divers modèles de GBM et s'ils contribuaient à la communication cellulaire et à la résistance aux thérapies. J'ai utilisé trois lignées cellulaires et deux GSC provenant d'un même patient. Toutes ces cellules étaient capables de former des TNT transférant vésicules ou mitochondries en culture adhérente. Les deux GSC ont montré différentes capacités de communication par TNT, tant dans des conditions de contrôle que d'irradiation, en accord avec l'hétérogénéité de la tumeur d'origine. En cultivant les GSC dans des organoïdes tumoraux, un modèle tridimensionnel représentatif de plusieurs caractéristiques tumorales, j'ai démontré la présence de TNT fonctionnels, ainsi que de connexions ressemblant aux TM. En conclusion, je propose que les TNT existent dans le GBM, où ils permettent le transfert de matériel cellulaire et qu'avec les TM, ils sont impliqués dans la résistance aux thérapies et la rechute du GBM.

Summary

Glioblastoma (GBM) is a very aggressive brain cancer that relapses after therapy and is caused by stem cells called GSCs. Intercellular communication plays a role in resistance to therapy, as the GSCs can interconnect through thick extensions, named Tumor Microtubes (TM), which promote the transmission of current through GAP-junctions. Tunneling Nanotubes (TNTs) are thin open communication channels between cells allowing the bilateral transfer of cellular material. They have also been described in several cancers and associated with a more malignant phenotype.

The aim of my project was to determine whether TNTs exist in various GBM models and whether they contribute to cellular communication and resistance to therapy. I used three cell lines and two GSCs from the same patient. All of these cells were capable of forming TNTs transferring vesicles or mitochondria in adherent culture. The two GSCs showed different TNT communication capabilities under both control and irradiation conditions, in accordance with the heterogeneity of the original tumour. By cultivating the GSCs in tumour organoids, a three-dimensional model representative of several tumour characteristics, I demonstrated the presence of functional TNT, as well as TM-like connections. In conclusion, I propose that TNTs exist in the GBM, where they allow the transfer of cellular material and that together with TMs, they are involved in resistance to therapies and relapse of the GBM.